

Charles University in Prague

1st Faculty of Medicine

Study Program: Molecular and Cellular Biology, Genetics and Virology

Field of Study: Department of Pediatric and Inherited Metabolic Disorders



CHARLES UNIVERSITY
First Faculty of Medicine

Kendrah KIDD

**Identifikace a charakterizace dědičně podmíněných
onemocnění ledvin**

**Identification and Characterization of Individuals
with Inherited Kidney Disease**

Dissertation

Final Thesis Supervisor: prof. Ing. Stanislav Kmoch, CSc.

Consultants: prof. Anthony J. Bleyer, MD., MSc. and Mgr. Martina Živná,
PhD.

Prague 2024


Declaration:

I declare that I have prepared the final thesis independently and that I have properly presented it and cited all used sources and literature. At the same time, I declare that work it has not been used to obtain another or the same title.

I agree to the permanent storage of the electronic version of my work in the database system of the inter-university project Theses.cz for the purpose of continuous control similarities of qualification papers.

In Prague, 02.04.2024

Kendrah KIDD, MSc

A handwritten signature in black ink that reads "Kendrah Kidd". The signature is written in a cursive style with a clear, legible font.

Signature

Identification Record

KIDD, Kendrah. *Identifikace a charakterizace dědičně podmíněných onemocnění ledvin. [Identification and Characterization of Inherited Kidney Disease]*. Praha, 2024. 160p., 1 app. Dissertation (PhD). Charles University, 1st Faculty of Medicine, Department of Pediatric and Inherited Metabolic Disorders. Supervisor Kmoč, Stanislav. Consultants Bleyer, Anthony J. and Živná, Martina.

ACKNOWLEDGEMENTS

First and foremost, I am extremely grateful to my Supervising Tutor, prof. Ing. Stanislav Kmoch, Csc and my Consultants prof. Anthony J. Bleyer, MD, MS and Mgr. Martina Živná, PhD for their expert guidance, continuous support, and patience during my PhD study. Thanks to their established team science approach to better understand families with rare inherited kidney disease, I was able to pursue this opportunity and I have gained so much from their immense knowledge and experience.

Special thanks to prof. Barry Freedman, MD at Wake Forest University School of Medicine for your continued support while I pursued a PhD through Charles University and continued my position in the Section of Nephrology.

To my colleagues at Charles University, Kateřina Hodaňová, Petr Vyleťal, Veronika Barešová, Alena Vrbacká, Tereza Kmočová, Klára Svojšová, Helena Trešlová, Hana Hartmannová, Marie Zikanová, and Viktor Straneky, thank your expertise, thoughtful discussion, and teamwork. Eva Oliveriusová thank you for your attention and help with shipments to your team.

Thank you to my colleagues on the Wake Forest Rare Inherited Kidney Disease Team, Abby Taylor, Lauren Martin, and Vicki Robins, for your collegiality, discussions, and commitment to finding answers for families. Carl Langefeld, Adrienne Williams, and Hannah Ainsworth thank you for helping me to curate and strengthen the registry and statistical discussions. Kim Hairston thank you for your encouragement and help with administrative aspects for my PhD.

To my husband, Chris Ward, I am eternally grateful for believing in me. To my children Ellis, Rory, and Osmund (*in memory*), you inspire me daily.

Thank you to my friends Jane Maccubbin, Shacana Mertson, and April New Schultz.

Thank you to prof. Anna Greka, MD, PhD, the Greka Lab, and Broad Clinical Labs at The Broad Institute of Harvard and MIT, I am grateful for your collaboration and your confidence in my work.

To my colleagues world-wide, thank you for your collaboration and interest to identify and better understand families with rare inherited kidney disease.

I am especially grateful to individuals and families with inherited kidney disease who continually participate in our research efforts.

FUNDING

This work was supported by the following institutional programs, grants, and foundations:

Charles University in Prague (UNCE 204064, PROGRES-Q26/LF1, SVV 260367/2017, UNCE/MED/007 and Cooperation)

Ministry of Health of the Czech Republic (NV17-29786A, NV19-08-00137)

Ministry of Education of the Czech Republic (LQ1604 NPU, LTAUSA19068)

Ministry of Education, Youth and Sports of the Czech Republic (NU21-07-00033)

National Centre for New Methods of Diagnosis, Monitoring, Treatment and Prevention of Genetic Diseases (TN02000132)

National Institute for Treatment of Metabolic and Cardiovascular Diseases (CarDia: LX22NPO5104)

National Institute of Diabetes and Digestive and Kidney Diseases (NIDDK-R21 DK106584)

Black-Brogan Foundation

Slim Health Foundation

Sequencing and genotyping were kindly provided by the National Centre for Medical Genomics (LM2015091, LM2018132, LM2023067).

REDCap is supported through National Center for Advancing Translational Sciences Wake Forest Clinical and Translational Science Award (UL1TR001420).

Table of Contents

1.	Introduction and Commented Results	1
1.1	Inherited Kidney Disease	5
1.2	Autosomal Dominant Tubulointerstitial Kidney Disease (ADTKD) due to <i>UMOD</i> Pathogenic Variants	9
1.3	ADTKD due to <i>REN</i> Pathogenic Variants	16
1.4	ADTKD due to <i>MUC1</i> Pathogenic Variants	21
1.5	Rare Inherited Kidney Disease Registry	34
1.6	Genetic, Biologic, and Clinical Factors Associated with ADTKD Prognosis	44
1.7	Rare Inherited Kidney Disease Genes and Novel ADTKD Gene Discovery	50
1.8	Summary and Future Research	55
2.	References	57
3.	Summary and Conclusions	70
4.	Results	75
4.1	Bleyer, Kidd et al. 2020 <i>Outcomes of patient self-referral for the diagnosis of several rare inherited kidney diseases.</i>	75
4.2	Kidd et al. 2020 <i>Genetic and Clinical Predictors of Age of ESKD in Individuals with Autosomal Dominant Tubulointerstitial Kidney Disease Due to UMOD Mutations.</i>	84
4.3	Živná, Kidd et al. 2020 <i>An International Cohort Study of Autosomal Dominant Tubulointerstitial Kidney Disease due to REN Mutations Identifies Distinct Clinical Subtypes.</i>	99
4.4	Olinger, Hofmann, Kidd et al. 2020 <i>Clinical and genetic spectra of autosomal dominant tubulointerstitial kidney disease due to mutations in UMOD and MUC1.</i>	116
4.5	Kmochová, Kidd et al. 2023 <i>Autosomal dominant ApoA4 mutations present as tubulointerstitial kidney disease with medullary amyloidosis.</i>	132

5.	List of Publications, Awards, Grants and Presentations	146
5.1	Publications	146
5.2	Awards	150
5.3	Grants	150
5.4	Presentations	150

Abstrakt

Úvod: Selhání ledvin (ESKD) je spojeno s vysokou morbiditou a mortalitou. Příčina ESKD je často neznámá. Asi 10 % případů ESKD je podmíněna geneticky. Autosomálně dominantní tubulointersticiální onemocnění ledvin (ADTKD) je charakterizováno chronickým onemocněním ledvin (CKD) vedoucím k ESKD ve věku okolo 45 let bez proteinurie a hematurie. Nejčastější genetickou příčinou ADTKD jsou patogenní varianty *UMOD*, *MUC1* a *REN*, asi 15% případů má neznámou genetickou příčinu. **Cíle:** (1) Zvýšení povědomí o ADTKD mezi klinickými nefrology. (2) Správná genetická klasifikace ADTKD a identifikace nových genů a jejich variant podmiňujících ADTKD. (3) Rozšíření znalostí patogenetických mechanismů ADTKD. (4) Prohloubení znalostí klinické charakterizace ADTKD a identifikace faktorů ovlivňujících progresi ADTKD. (5) Identifikace nových patogenních variant *MUC1* v rodinách s ADTKD a vyloučenou prevalentní variantou duplikace cytosinu ve VNTR *MUC1*. **Metody:** V rámci práce studentka vyvinula interaktivní databázi umožňující přímý kontakt s pacienty, lékaři a výzkumníky. Studentka zavedla laboratorní protokoly pro izolaci DNA a odběr a odesílání vzorků na příslušné genetické testování. Významně se podílela na interpretaci identifikovaných genetických variant. Dále vytvořila patientské dotazníky pro zlepšení znalosti klinických charakteristik ADTKD. **Výsledky:** Od roku 2018 jsme rozšířili náš ADTKD registr o 238 nových rodin na celkový počet 1100. Patogenní varianty *UMOD*, *MUC1* a *REN* jsme identifikovali u 126, 297 resp. 115 případů. Nalezli jsme patogenní varianty *APOA4* jako nové genetické příčiny ADTKD. Identifikovali jsme faktory spojené s progresí ADTKD, což jsou typ patogenní varianty, dna, věk ESKD u rodičů a pohlaví. Definovali jsme odlišné klinické podtypy ADTKD-*REN*. **Závěr:** Zvýšili jsem schopnost nefrologů rozpoznat ADTKD a tím zlepšili správnost určení diagnózy ve skupině CKD. Dále jsme rozšířili spektrum genetických příčin ADTKD a identifikovali faktory ovlivňující progresi ADTKD.

Abstract

Background: End-stage kidney disease (ESKD) is associated with high morbidity and mortality, with the cause of ESKD unknown in many cases. At least 10% of patients have a genetic cause of ESKD, with many undiagnosed. Autosomal dominant tubulointerstitial kidney disease (ADTKD) is characterized by a bland urinary sediment and chronic kidney disease (CKD) leading to ESKD at a mean age of 45y. The most common genetic causes of ADTKD are pathogenic variants in *UMOD*, *MUC1*, and *REN*, with an unknown cause in 15%. **Specific Aims:** (1) To better understand ADTKD prevalence by expanding outreach. (2) To classify ADTKD families genetically and identify new genetic causes. (3) To expand existing knowledge of ADTKD pathophysiology. (4) To better characterize ADTKD clinically and identify factors associated with progression. (5) To identify novel *MUC1* pathogenic variants in undiagnosed ADTKD families. **Methods:** I developed an interactive computer database that allowed direct contact with participants, clinicians, and researchers. I oversaw and instituted laboratory protocols to collect samples, isolate DNA, and send for appropriate genetic testing. I assisted in interpretation of genetic variants. I created patient surveys to assess ADTKD clinical characteristics. **Results:** Since 2018, we recruited 238 new families, increasing our total number of families to 1100. We identified *UMOD*, *MUC1*, and *REN* pathogenic variants in 126, 297, and 115 individuals. We identified *APOA4* as a new genetic cause of ADTKD. We identified an *in vitro* score, gout, parental age of ESKD, and gender as factors associated with ADTKD progression. We identified distinct subtypes of ADTKD-*REN*. **Conclusion:** We significantly increased our knowledge of the prevalence, characteristics, and genetic causes of ADTKD. Future work will focus on identification of new therapies, based on our clinical, genetic, and pathophysiologic findings.

Identification and Characterization of Inherited Kidney Disease

1. Introduction and Commented Results

Chronic kidney disease (CKD) is characterized by kidney structural or functional abnormalities, with a worldwide prevalence of 9%-13% [Kovesdy 2022]. Patients with CKD (CKD) often progress to end-stage kidney disease (ESKD). Understanding the causes of CKD is of paramount importance in identifying potential therapies to reverse this common condition. It is estimated that at least 10% of individuals with advanced CKD have an inherited form of kidney disease. Historically, inherited conditions such as autosomal dominant polycystic kidney disease and Alport syndrome were recognizable due to obvious and pathognomonic clinical findings on ultrasound or with kidney biopsy. However, there are many forms of inherited kidney disease (IKD) that have been undiagnosed or undefined due to mundane clinical characteristics and inability to perform genetic testing. Over the last two decades, with expansion of knowledge in genetics and its application, the genetic basis of many kidney diseases has been identified. Conditions once thought to be rare are now more commonly identified, and potential therapies are being developed. However, there remain many genetic conditions for which the genetic cause has not been identified [Devuyst et al. 2014, Vivante et al. 2016, Levin et al. 2017].

Autosomal dominant tubulointerstitial kidney disease (ADTKD) is an example of an IKD that was poorly understood until genetic research led to an increasing understanding of its clinical presentation, prevalence, and pathophysiology. ADTKD is characterized by CKD leading to ESKD at a variable age, between 22 and 80 years, with a mean age of approximately 45 years. ADTKD is characterized by a bland urinary sediment, with no blood or protein in the urine. While kidney biopsies are extremely useful in the diagnosis of

glomerular diseases, pathologic findings in ADKD are nonspecific, with tubular cell pathologic changes and interstitial fibrosis being most commonly found. Thus, ADTKD is a condition that is difficult to diagnose or distinguish clinically.

In 2002, pathogenic variants in the *UMOD* gene were identified as the genetic cause of ADTKD, allowing further characterization of this disorder and the ability to diagnose this condition [Hart et al. 2002]. Prior to 2002, less than 50 families had been diagnosed worldwide with this condition. Since genetic identification of *UMOD*, and subsequently *REN*, *MUC1*, and *SEC61A1* as genetic causes of ADTKD, we now know that there are thousands of families suffering from these conditions [Živná et al. 2009, Kirby et al. 2013, Bolar et al. 2016]. While the major causes of ADTKD have been identified, in approximately 15% of cases the genetic cause of ADTKD remains unknown [**see results, paper 4.1 Bleyer, Kidd et al. 2020**].

The long-term goal of the Rare IKD Team of Charles University and Wake Forest School of Medicine (RIKD Team) team is to identify the genetic basis of disease in individuals with IKD, to better characterize clinical and genetic predictors of disease, improve understanding of clinical progression, and to expand existing knowledge of disease pathophysiology. The team utilizes a team science approach based upon the research framework outlined in Figure 1.

Referred families with IKD are contacted by The Wake Forest group, who collect clinical and family history data and organize sample collections for genetic testing and biobanking. First, clinical characterization is performed to determine if the participants and their families suffer from ADTKD. After a clinical diagnosis of possible ADTKD is made, samples are tested for mutations in genes known to cause ADTKD, including *UMOD*, *REN*,

MUC1 and *SEC61A1*. In the RIKD family registry, mutations in these genes are found to cause kidney disease in about 65% of participating families, with 15% of cases still with an unidentified etiology. If directed gene testing is negative, whole exome or whole genome sequencing may follow to attempt to identify a causative gene in the family [Figure 1].

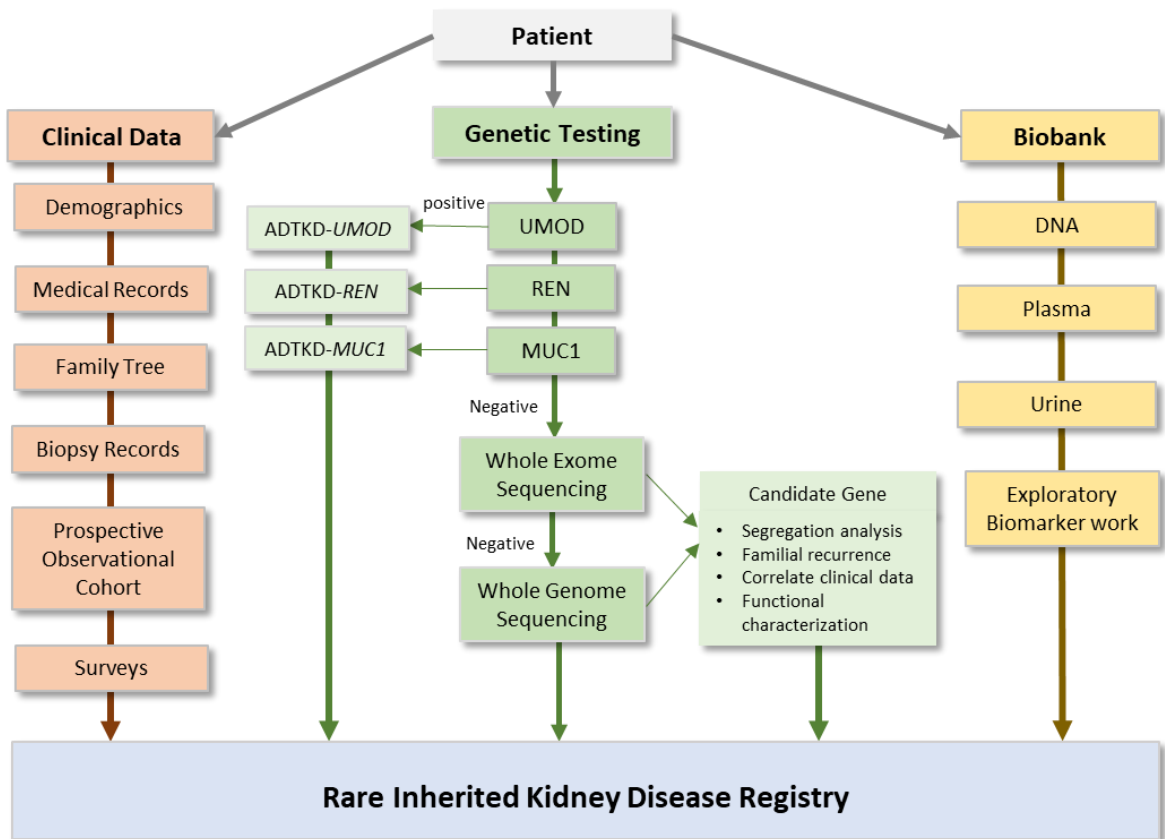


Figure 1. Rare IKD (RIKD) Team Research Framework. Patients enter the research study and their clinical, genetic and biobank data are integrated and stored in the rare inherited kidney disease (RIKD) registry.

To better understand ADTKD, our team has established collaborations with medical professionals and researchers in the Czech Republic, United States, European Union, United Kingdom, Australia, Canada, and South America establishing the world’s largest registry of over 1,100 families with ADTKD. Our collaborative work has expanded the knowledge of

ADTKD and characterization of patients with ADTKD [Bleyer et al. 2014, Gast et al. 2018, Cormican et al. 2019, Cormican et al. 2020, Elhassan et al. 2023, **see results, papers 4.1 Bleyer, Kidd et al. 2020, 4.2 Kidd et al. 2020, 4.3 Živná, Kidd et al. 2020, 4.4 Olinger, Hofmann, Kidd et al. 2020**].

I joined the RIKD team of Wake Forest as a research scientist in 2012. At the start of my thesis in 2018, the RIKD Team had been referred approximately 862 families with IKD. As ADTKD is poorly diagnosed, poorly characterized clinically and pathophysiologically, and all genetic causes have not been identified, the specific aims of my doctoral study included:

1. To more accurately determine the prevalence of ADTKD by expanding outreach to families with this condition.
2. To classify families with ADTKD genetically and to identify new genetic causes of ADTKD.
3. To expand existing knowledge of ADTKD pathophysiology
4. To better characterize ADTKD clinically and identify factors associated with CKD progression.
5. To identify novel *MUC1* mutations in suspected ADTKD-*MUC1* families who tested negative for the cytosine duplication that commonly causes ADTKD-*MUC1*.

In the following text I will discuss the current knowledge of the field and will relate it to the results of my work. I have authored five papers, and I am first author for two of them.

1.1 Inherited Kidney Disease

Chronic Kidney Disease

Chronic kidney disease (CKD) is defined as kidney structure or function abnormalities present for three or more months with health implications. CKD has been recognized as a global public health burden associated with poor quality of life, increased hospitalization, mortality and economic cost [Eckardt et al. 2013, Hill et al. 2016, Levin et al. 2017, Kovesdy 2022]. Global mean estimates of CKD estimate approximately 14% of adults 30-39 years and 34% of individuals over 70 years having CKD. The endpoint of CKD progression is ESKD. Once ESKD is reached, patients no longer have enough kidney function to maintain life and would die shortly without renal replacement therapy (RRT). RRT options include hemodialysis, peritoneal dialysis, or kidney transplantation. While hemodialysis and peritoneal dialysis are life-saving for patients with ESKD, they require patients to receive dialysis three days a week or daily. Both hemodialysis and peritoneal dialysis are associated with poor quality of life, and patients receiving hemodialysis or peritoneal dialysis have a shorter life expectancy than patients with cancer. Kidney transplantation is a superior option but is associated with shortened survival due to accelerated vascular disease and increased cancer risk due to immunosuppression. In addition, the mean graft survival for a cadaveric kidney is only 10-12 years. Thus, CKD is a common problem associated with poor survival and decreased quality of life [Eckardt et al. 2013, Hill et al. 2016, Kovesdy 2022].

It is estimated that 10% of families that exhibit early-onset CKD have a monogenic disorder. These disorders have a remarkably high penetrance, resulting in a more rapid loss of kidney function over time compared to other causes of kidney disease [Vivante et al. 2016,

Levin et al. 2017]. Identification of causative genes for IKD is important for the following reasons: 1) It provides families and their healthcare providers with a cause for the IKD that has been present in their family, often for generations. 2) It allows physicians and researchers to better characterize the clinical phenotype. 3) Genetic testing can be performed to identify family members with disease and also identify unaffected family members who may be able to serve potential kidney donors to other family members. 4) A genetic diagnosis prevents unnecessary diagnostic procedures that may carry risk (e.g. percutaneous kidney biopsy). 5). More rigorous monitoring of CKD progression can be performed in genetically affected individuals. 6) Identification of the genetic cause of kidney disease guides research into the genetics, cell biology, pathology, and clinical manifestations of disease. 7) Identification of the genetic cause of kidney disease is the first step in identifying a potential treatment.

IKD Gene Discovery

Adult or autosomal dominant polycystic kidney disease (ADPKD) was reported to be inherited in a 1957 study of 284 probands with polycystic kidneys often leading to ESKD [Dalgaard 1957]. In 1985, the PKD1 locus was the first IKD locus mapped, the loci positioned at chromosome 16 [Reeders et al. 1985]. Nine years later, the polycystin 1 (*PKD1*) gene was sequenced and mutations causing ADPKD were identified in four families [The European Polycystic Kidney Disease Consortium 1994].

In 1990, the first IKD gene-disease association was identified in families with X-linked Alport Syndrome. Families with Alport Syndrome present clinically with progressive CKD and presence of hearing loss. Mutations in the *COL4A5* gene encoding alpha 5(IV) collagen chain, mapped to Xq22.3, segregated within three large families [Barker et al. 1990]. Four years later, *COL4A3* and *COL4A4* were reported as causative for autosomal

recessive Alport Syndrome. These genes are both located at 2p36.3 and encode alpha 3(IV) and alpha 4(IV) collagen chains, respectively. Two families were described with homozygous mutations in *COL4A3* and two families with homozygous mutations in *COL4A4*. These findings supported the idea that individual chains of alpha (IV) collagen are important for the structural integrity of the glomerular basement membrane, and disruptions can lead to disease [Mochizuki et al. 1994].

Rare IKD

ADPKD is the most common form of IKD, affecting an estimated 600,000 people in the US [Nobakht et al. 2020]. Rare diseases are defined by population frequency, with definitions varying between countries and organizations. In the US, a disease is considered rare if it is present in less than 200,000 individuals. Alport Syndrome is a rare disease, affecting an estimated 30,000-60,000 people in the US [Watson et al. 2023]. The vast majority of IKDs are rare diseases.

Autosomal Dominant Tubulointerstitial Kidney Disease

Smith and Graham described medullary cysts found in an 8-year-old girl who suffered from anemia, elevated blood urea nitrogen, and CKD without proteinuria or hematuria. Pathology findings of her kidney described for the first-time medullary cysts along with interstitial fibrosis and tubular atrophy. Neither parent was clinically affected, and no siblings were noted [Smith and Graham 1945].

In 1960, Goldman et al. described medullary cystic kidney disease in the proband of a large family. They were able to identify 60 affected family members through five generations. Of these 60 family members, 14 had died from kidney disease and three had CKD. The family findings were consistent with autosomal dominant inheritance. Clinical

findings included anemia, salt wasting, a bland urinary sediment (no blood or protein in the urine) and CKD. Review of kidney pathology reports revealed medullary cysts, interstitial fibrosis, dilated tubules and irregularities of the basement membrane. No extrarenal characteristics were reported [Goldman et al. 1960].

Eight cases referred of medullary cystic disease and familial juvenile nephronophthisis were reviewed in 1967. The inheritance patterns varied among the families. All affected individuals suffered from slowly progressive CKD, anemia, polyuria, and the absence of proteinuria or hematuria. Kidney biopsies revealed interstitial fibrosis, tubular dilation and atrophy. Chronic idiopathic tubulointerstitial nephropathy was suggested as a more descriptive encompassing name, or simply nephronophthisis [Mongeau et al. 1967].

Massari et al. in 1980, described a large family with autosomal dominant inheritance of kidney disease with hyperuricemia and gout, absence of proteinuria and hematuria. Nine patients presented with CKD and an additional three presented with hyperuricemia only. Review of available kidney biopsies showed tubular atrophy, wrinkling, and thickening of basement membrane and interstitial fibrosis but no medullary cysts [Massari et al. 1980].

Linkage studies in large, well phenotyped families with medullary cystic kidney disease and/or familial juvenile hyperuricemic nephropathy allowed researchers to map the disease, revealing genetic heterogeneity with at least three different loci identified at 1q21, 1q41, and 16p12.3 [Christodoulou et al. 1998, Scolari et al. 1999, Stibůrková 2000, Hodanová et al. 2005]. These locations were later identified to be the following causative genes *MUC1*, *REN*, and *UMOD* [Kirby et al. 2013, Živná et al. 2009, Hart et al. 2002].

In 2015, a consensus report was written to address the varied and sometimes misleading names given to this disease group over decades of studying these families. The following nomenclature was suggested: inheritance-phenotype-gene. This group of diseases has since been known as autosomal dominant tubulointerstitial kidney disease (ADTKD). ADTKD features include: 1) autosomal dominant inheritance, 2) progressive CKD with ESKD between 3rd – 7th decades of life, 3) bland urinary sediment. Biopsy findings tend to be nonspecific showing 1) tubular atrophy 2) interstitial fibrosis, 3) thickening of basement membranes, 4) tubule dilation. Additional phenotypes associated are addressed by gene specific subtypes, as gout seen more often in patients with *UMOD* mutations [Eckhardt et al. 2015].

1.2 ADTKD due to *UMOD* Pathogenic Variants

Cilindrina, Tamm Horsfall Protein and Uromodulin

In 1873, Dr. Carlo Rovida described a cylindrical urinary protein termed “cilindrina” produced by the renal tubular cells that led to the formation of hyaline casts [Thielemans et al. 2023]. Drs. Tamm and Horsfall identified a urinary mucoprotein that inhibited viral hemagglutination in 1950, naming it Tamm Horsfall protein (THP). Further, they found THP to be the most common protein in human urine. THP is produced exclusively by the thick ascending limb of the kidney [Tamm and Horsfall 1950, Tamm and Horsfall 1952]. In 1986, Drs. Muchmore and Decker identified a urinary glycoprotein with immunosuppressive properties that binds and modulates interleukin-1, naming the protein uromodulin (*UMOD*) [Muchmore and Decker 1986]. Pennica et al. determined through protein analysis in 1987 that *UMOD* was found in human urine regardless of gender or pregnancy and presented evidence that THP and *UMOD* were identical proteins [Pennica et al. 1987].

***UMOD* Gene**

The cDNA sequence of *UMOD* was published in 1987. The gene is composed of 11 exons, which synthesize a 640 amino acid peptide sequence containing a very high number of cysteine residues (48), which constitute 7.5% of amino acids in the protein. *UMOD* contains epidermal growth factor (EGF)-like domains coded within the protein [Pennica et al. 1987]. In 1993, *UMOD* was mapped to chromosome 16p12.3-16p13.11, which extends over 20kb region [Pook et al. 1993].

UMOD Structure

UMOD encodes a signal peptide, four EGF-like domains, a cysteine rich domain (domain of 8 cysteine residues (D8C)), and a zona pellucida domain used in polymerization. The 24-amino acid signal peptide guides the precursor *UMOD* to the endoplasmic reticulum (ER), where the signal peptide is cleaved, resulting in a 616 amino acid mature peptide. Post-translational modifications that include formation of 24 disulfide bridges, eight glycosylation sites, and a glycosyl phosphatidyl inositol (GPI) anchor used to tether the protein to the cell membrane. *UMOD* is transported to the apical surface of thick ascending cells, where it is cleaved by the protease hepsin and enters the tubular lumen [Brunati et al. 2015]. It then polymerizes via the ZP domain to form a filamentous matrix [Mary et al. 2022]. *UMOD* is then excreted in the urine.

UMOD Function

UMOD has been implicated in a variety of physiological functions. Due to its filamentous properties in the tubular lumen, the role of *UMOD* in water reabsorption affecting urine concentration have been studied, as well as protective effects against urinary tract infection and kidney stone formation. Data also suggest that *UMOD* may regulate

potassium, sodium, calcium, and magnesium transport [Devuyst et al. 2017, Mary et al. 2022].

***UMOD* Pathogenic Variants as a Cause of ADTKD**

In 1999, Scolari et al. mapped a four generation Italian kindred with autosomal dominant medullary cystic kidney disease type 2 (ADMCKD2) to chromosome 16p.12. This study utilized the phenotype of autosomal dominant inheritance, defective urine concentration, normal to small kidneys with or without medullary cysts, kidney biopsy findings of tubular-interstitial fibrosis, tubular atrophy or thickening of the tubular basement membrane. Seven candidate genes in the region were discussed, including uromodulin/THP [Scolari et al. 1999].

In 2000, Stibůrková et al. mapped three Czech families with familial juvenile hyperuricemic nephropathy (FJHN) to chromosome 16p11.2. The FJHN phenotype was described with autosomal dominant inheritance, CKD, presence of gout, and progression to ESKD during middle age. Additionally, patients presented with reduced fractional excretion of uric acid, ultrasound findings of small kidneys with increased echogenicity with or without medullary cysts, and kidney biopsy findings of tubulointerstitial nephropathy. Two candidate genes were discussed, one of which was *UMOD* [Stibůrková et al. 2000].

UMOD was identified as the causative gene for ADMCKD2 and FJHN in 2002 when the Wake Forest team published a study of four families (one with ADMCKD2 and three with FJHN). A p.H177-R185_deletion and three missense pathogenic variants (p.Gly103Cys, p.Cys148Try, and p.Cys217Arg) segregated within the respective families in all clinically affected individuals. It was noted that the common phenotype among the four families was CKD of tubulointerstitial origin, with variable presentation of hyperuricemia

or medullary cysts. Identifying that both ADMCKD2 and FJHN resulted from pathogenic variants in *UMOD*, a new disease name, *UMOD* associated kidney disease (UAKD), was suggested [Hart et al. 2002].

Within a year of publication, 24 families were published with IKD due to *UMOD* mutations [Rampoldi et al. 2003, Dahan et al. 2003, Wolf et al. 2003, Bleyer et al. 2003, Turner et al. 2003]. In 2018 and 2019, *UMOD* was reported in two large cohort studies as the third most common genetic cause of IKD identified after ADPKD and Alport Syndrome [Gast et al, 2018; Groopman et al. 2019]. The number of patients and families identified with *UMOD* mutations in our registry [described in Chapter 1.5] continues to grow since its discovery in 2002, as seen in Figure 2.

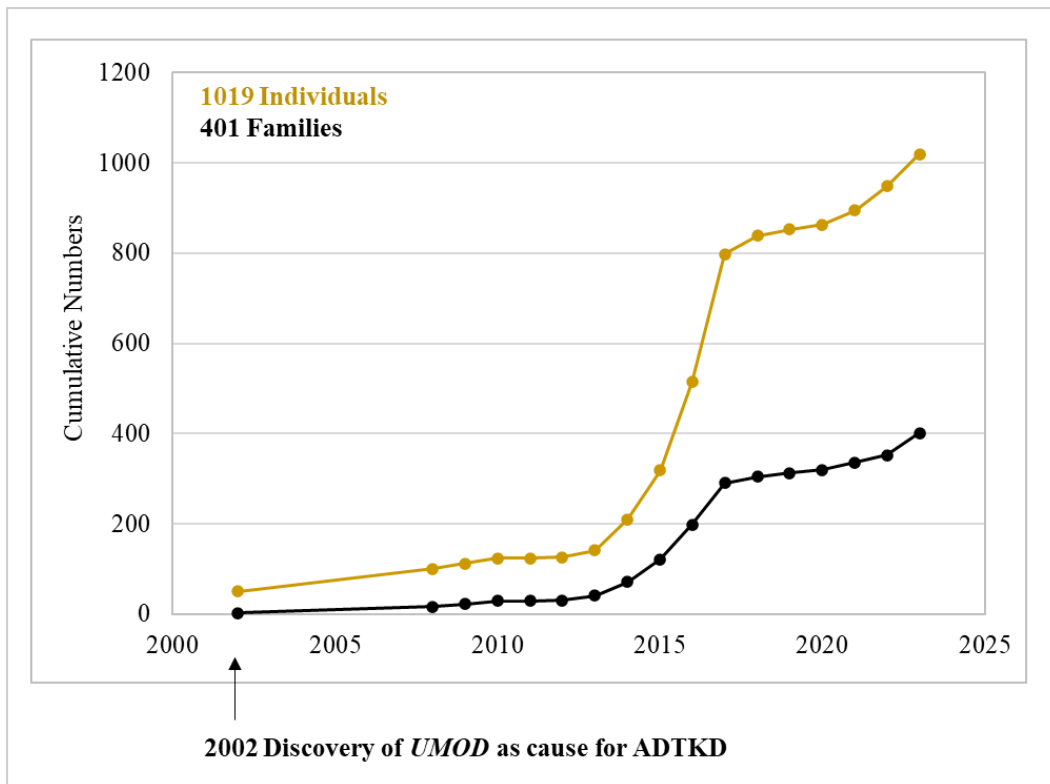


Figure 2. Growth of RIKD ADTKD-*UMOD* Registry from 2002-2023.

***UMOD* Pathogenic Variants**

In 2020, I assembled and analyzed the data on the largest international cohort of ADTKD-*UMOD* patients that has been studied, describing 125 unique *UMOD* mutations in 722 genotyped patients from investigators in 13 countries. Of the evaluated *UMOD* mutations 120 (96%) were missense, 4 (3%) were in-frame deletions and 1 (1%) was a deletion-inversion. Fifty-nine (46%) mutations involved a cysteine residue. Thirty-three (71%) of the 48 cysteine residues in *UMOD* were altered in 201 (28%) patients. All the altered cysteine residues were encoded by exons 3 and 4. 124 (99%) mutations were also located within exons 3 and 4 [see results, paper 4.2 Kidd et al. 2020].

I maintain a registry of known *UMOD* mutations for the RIKD team, currently reporting 165 unique mutations, 160 of which cluster to exons 3 and 4 [Figure 3]. The registry is available for public use (<https://redcap.link/UMOD.mutations>) and I have created a survey tool for input of new mutations. I have also created a figure including all available *UMOD* pathogenic variants that is available for download website [Figure 4].

***UMOD* Single Nucleotide Polymorphism Factors of CKD**

A genome-wide association study (GWAS) of CKD identified three loci of interest located in the *UMOD* promoter. The rs4293393-A-G minor allele G, present in 19% of the general population, was found to reduce the amount of uromodulin produced and was also associated with a reduction in CKD risk [Köttgen et al. 2010]. The rs12917707-G-T minor allele T, present in 13% of the general population, was found to reduce CKD risk. Individuals with this allele had a higher estimated glomerular filtration rate (eGFR), a calculation used to estimate kidney function. The rs13333226 minor allele G variant, present in 23% of the

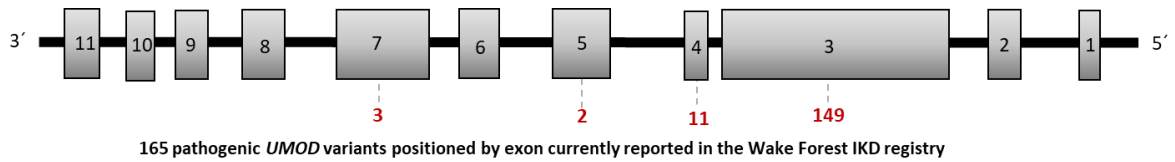


Figure 3. Genetic map of *UMOD*. *UMOD* is composed of 11 exons with number of pathogenic variants reported in the Wake Forest Rare IKD Registry as cause for ADTKD-*UMOD* annotated by exon. Clustering is seen in exons 3 and 4.

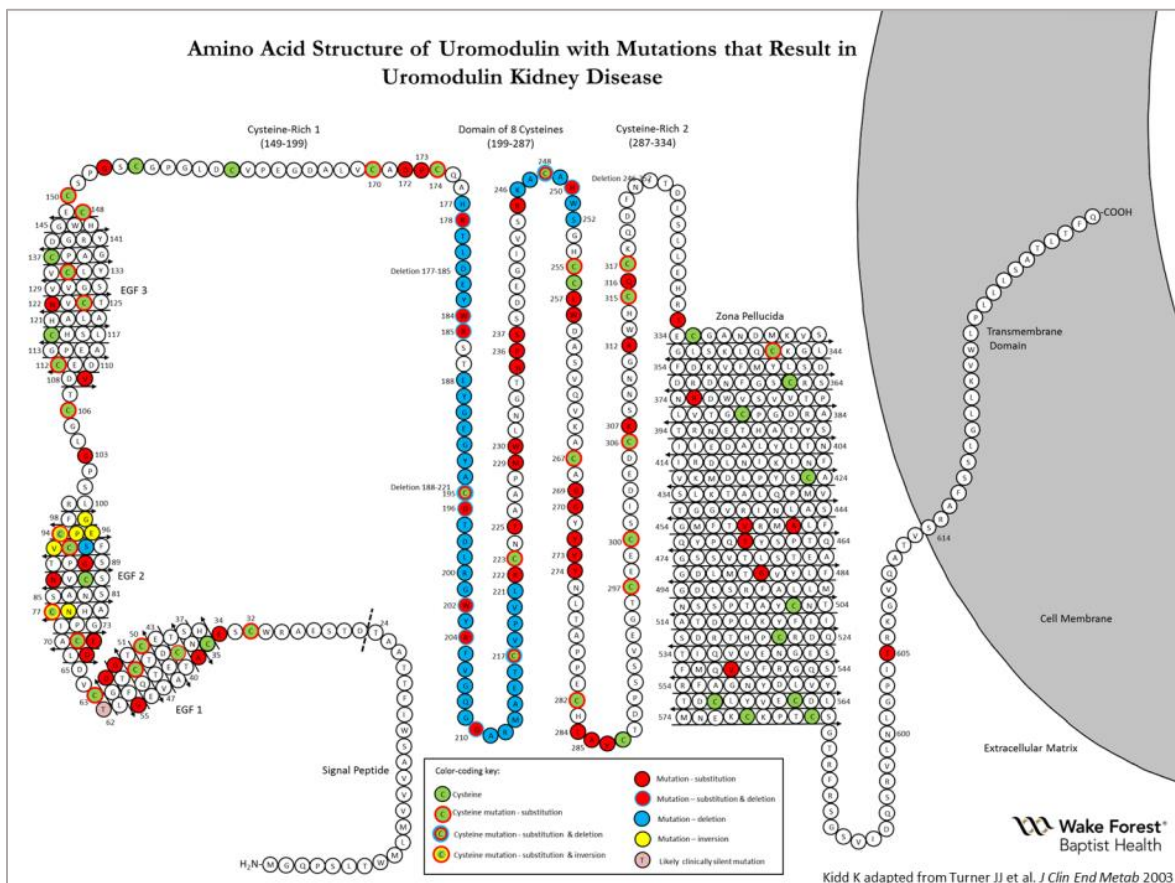


Figure 4. Annotated *UMOD* Map. This is an annotated map of *UMOD* showing each amino acid. Cysteines are green. Pathogenic variants (labeled as mutations) are color coded: red missense, blue deletion, and yellow deletion-insertion. This map is available for download at <https://redcap.link/UMOD.mutations>.

general population, was found to have a decreased risk of hypertension and cardiovascular event [Rampoldi et al. 2011].

Effects of Mutant UMOD

The first immunohistochemistry reports of UMOD in kidney biopsies revealed mutant UMOD (mUMOD) forms intracellular aggregates within tubular epithelial cells [Dahan et al. 2003, Rampoldi et al. 2003, Bleyer et al. 2005]. Immunofluorescence microscopy further showed accumulation of mUMOD in the endoplasmic reticulum (ER) [Vylet'al et al. 2006]. This evidence indicates *UMOD* mutations affect protein folding and trafficking, leading to intracellular accumulation [Figure 5]. This abnormal deposition leads to either absent or strongly reduced UMOD secretion in the urine of patients with ADTKD-*UMOD* [Rampoldi et al. 2003, Bleyer et al. 2004, Vylet'al et al. 2006].

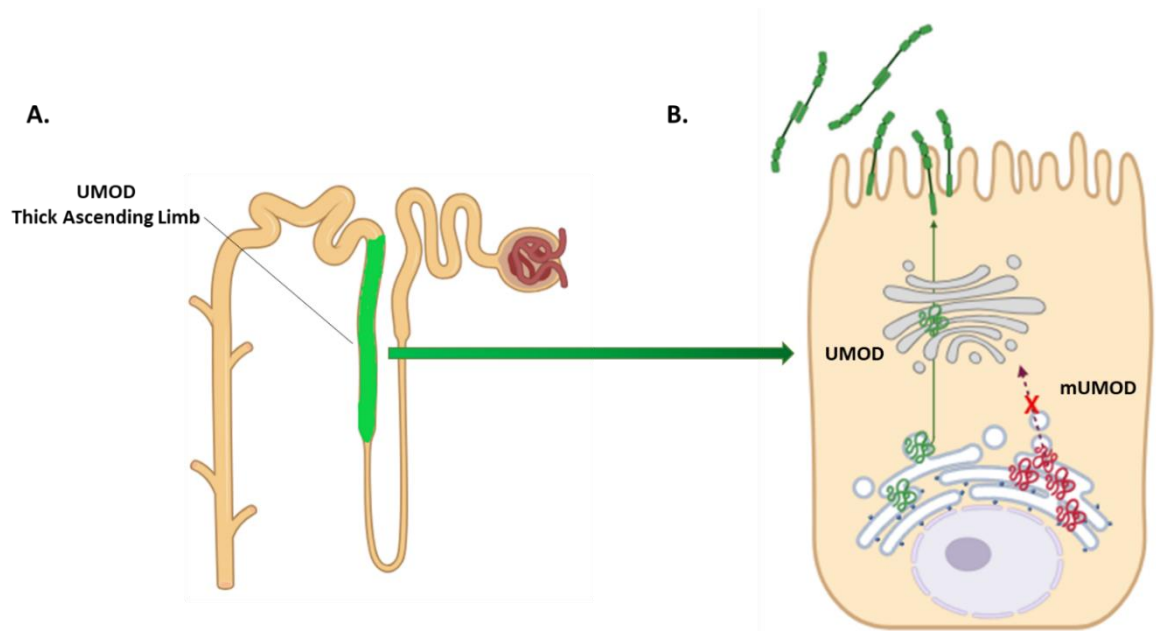


Figure 5. UMOD expression in the nephron. A) UMOD is expressed in the thick ascending limb of the Loop of Henle (green). B) Typical UMOD processing in the cell (green arrows). Mutant UMOD (mUMOD) accumulation within the endoplasmic reticulum in ADTKD-*UMOD* (burgundy arrows with red “X”).

Further work demonstrated that thick ascending limb cells do not undergo apoptosis in response to accumulation of mUMOD within the ER, instead inducing the unfolded protein response (UPR). The UPR is induced to decrease protein load within the ER by lowering the amount of protein entering the ER for post-translational modification while boosting ER folding capacity and ERAD [Schaeffer et al. 2017]. Understanding the pathophysiologic processes leading to aberrant mUMOD accumulation within the cell and the signaling pathways induced by its presence are useful for identifying therapeutic targets [Dvela-Levitt et al. 2019].

1.3 ADTKD due to *REN* Pathogenic Variants

Renin Angiotensin Aldosterone System

Renin (REN) was one of the first hormones discovered in 1898 when Tigerstedt and Bergmann identified a substance in renal extracts affecting arterial pressure. The investigators named this substance “renin” [Basso and Terragno 2001]. REN is expressed in the juxtaglomerular cells of the kidney and is a major component of the renin-angiotensin-aldosterone system (RAAS), an extensively studied system that regulates blood pressure and electrolyte balance [Galen et al. 1984, Basso and Terragno 2001].

***REN* Gene**

REN was mapped to chromosome 1 in 1984 [Chirgwin et al. 1984]. The *REN* gene encodes 10 exons translating into 406 amino acids, containing trypsin and pepsin-sensitive domains to cleave for its activation [Morris et al. 1984].

REN Structure

The REN peptide is composed of a 23 amino acid signal peptide (SP, “pre-” domain), 43 amino acid prosegment (“pro-” domain), and 340 amino acid mature REN, which contains two glycosylation sites and three cysteine-cysteine disulfide bridges. Preprorenin describes the full peptide sequence, including the SP, which guides preprorenin to the ER for post-translational modifications, where the SP is cleaved.

Prorenin is composed of the prosegment plus the mature REN sequence. The prosegment of prorenin acts as a plug to block substrates from entering the catalytic site of renin. Prorenin is guided from the ER to Golgi for post-translational modification via ER-Golgi intermediate compartment vesicles (ERGIC), which monitor for misfolding or other aberrations. Prorenin leaves the Golgi apparatus after processing, entering one of two pathways depending upon cellular signals. The constitutive pathway stores prorenin in clear vesicles until it is secreted into the circulation. Prorenin may also enter the regulatory pathway, where protogranules are released containing prorenin and proteases. These proteases cleave the prosegment to release active, mature REN, which is then secreted into the circulation [Morris and Smith 1991, Sielecki et al. 1989, Schweda et al. 2007].

REN Function

REN functions within the RAAS in a vitally important enzymatic role. REN is an aspartyl protease with a single specific substrate, angiotensinogen. Upon hypotensive conditions, prorenin undergoes proteolysis into its active form, REN. This initiates a cascade involving the conversion of angiotensinogen to angiotensin I, further proteolyzed by angiotensin-converting enzyme (ACE) into angiotensin II, which is a potent vasoconstrictor. Angiotensin II also stimulates aldosterone release from the kidneys, which signals

reabsorption of sodium and water, raising blood volume and pressure [Persson 2003, Schweda et al. 2007]

***REN* Pathogenic Variants as a Cause of IKD and ADTKD**

In 2005, homozygous and compound heterozygous pathogenic variants in RAAS genes *REN*, *AGT*, *AGTR1* and *ACE* were identified as genetic causes of autosomal recessive renal tubular dysgenesis (RTD), a rare and fatal disease, in 11 fetuses from six families. Prenatal oligohydramnios and fetal anuria are the first clinical signs of RTD. Affected individuals frequently survive only a few days after birth or are stillborn. Kidney pathology shows absent or few distinct proximal tubules. This was the first report of a monogenic disease associated with the RAAS, emphasizing the system's critical involvement in the kidney and kidney development [Gribouval et al. 2005].

A family with FJHN was mapped to a novel locus at chromosome 1q41, adding to the genetic heterogeneity of ADMCKD/FJHN/UAKD in 2005. This large family presented with anemia, hyperuricemia, slowly progressive CKD leading to ESKD between 55 and 68 years. Ultrasound revealed small, echogenic kidneys. Patients did not have proteinuria, hematuria, or gout [Hodanová et al. 2005].

In 2009, *REN* was identified as the second gene-disease association for FJHN/ADMCK2 in three unrelated families by the RIKD Team of Wake Forest and Charles University. Two heterozygous pathogenic variants were identified within the SP of preprorenin: p.Leu16del in two families and p.Leu16Arg in another family. Families presented with autosomal dominant inheritance, childhood anemia, hyperuricemia, and progressive CKD leading to ESKD between 43-68 years of age. Kidney biopsies showed tubulointerstitial fibrosis and tubular atrophy. The proximal tubules were irregular and

dystrophic [Živná et al. 2009]. Of note, one of the families identified with a *REN* pathogenic variant was described by Hodanová et al. 2005.

***REN* Pathogenic Variants**

Eleven *REN* pathogenic variants have been published as homozygous or compound heterozygous causes for RTD. Of these variants, five altered splicing, three resulted in an early truncation, two were missense, and one was an in-frame duplication [Gribouval et al. 2012].

Schaeffer et al. published a pathogenic variant p.Leu381Pro in mature *REN* as a cause for *ADTKD-REN*, the first non-SP *REN* pathogenic variant identified as causing disease [Schaeffer et al. 2019]. In 2020, Živná, Kidd et al. published a large international cohort of 111 *ADTKD-REN* patients, describing 15 unique heterozygous mutations. I participated in the recruitment of the international cohort, analysis of data and creation of the manuscript. Fourteen (94%) of the pathogenic variants were missense, and one was an in-frame deletion. Eight of the pathogenic variants (50%) were positioned within the SP of preprorenin, three (19%) were positioned within the prosegment of prorenin, and four (31%) were positioned within mature *REN* [Figure 6, see results, paper 4.3 Živná, Kidd et al. 2020].

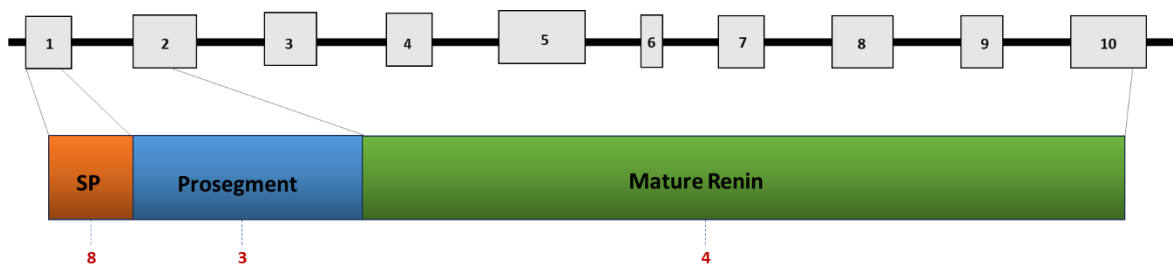


Figure 6. Genetic map of *REN*. *REN* is composed of 10 exons encoding signal peptide (SP), prosegment, and mature renin. Number of pathogenic variants reported in the Wake Forest RIKD Registry as cause for *ADTKD-REN* annotated by protein segment.

Effects of Mutant REN

REN is required for embryonic renal development, and the absence of REN, due to biallelic pathogenic variants results in early death and incomplete kidney development [Gribouval et al. 2012].

Heterozygous pathogenic variants within the SP of *ADTKD-REN* reduce the production of REN in juxtaglomerular cells. This decreased production leads to low REN and aldosterone levels and mild hyperkalemia. When the SP is altered, the preprorenin is unable to be translocated to the ER for processing, leading to the overall reduction in REN observed. The unprocessed aberrant preprorenin accumulates intracellularly, activating the UPR and triggering apoptosis and inflammation [Figure 7] [Živná et al. 2009]. Mutant prorenin and mature REN alter intracellular transport and folding of REN by distinct mechanisms, as detailed in the manuscript Chapter 1.6 [Figure 7] [Schaeffer et al. 2019, see results, paper 4.3 Živná, Kidd et al. 2020].

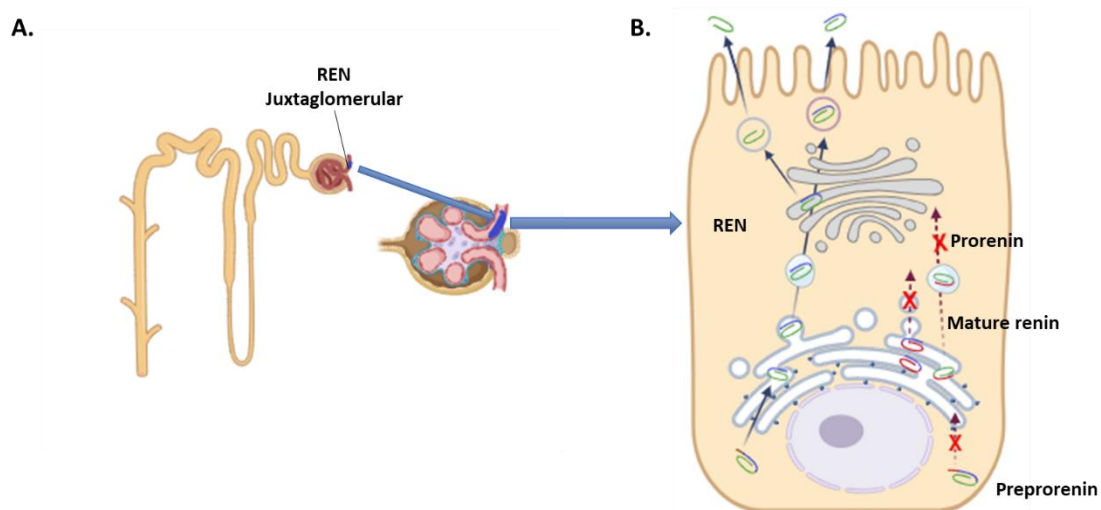


Figure 7. REN expression in the nephron. A) REN is expressed in the juxtaglomerular cells (purple). B) Typical REN processing in the cell (blue arrows). Pathogenic variants in each segment of REN (shown in red) accumulate in different parts of the cell in *ADTKD-REN* (burgundy arrows with red “X”).

Treatment with Fludrocortisone

9 α -fluorohydrocortisone, known as fludrocortisone acetate, was identified as a treatment for aldosterone deficiency in adrenal insufficiency (Addison's disease) in 1955 [Witten et al. 1955]. In 2010, a 10-year-old girl with ADTKD-REN caused by the SP pathogenic variant p.Cys20Arg underwent fludrocortisone treatment to ameliorate clinical symptoms of hyporeninemic hypoaldosteronism. The treatment was successful, resulting in an increase in blood pressure, lowering of serum potassium, and appropriate sodium retention [Bleyer et al. 2010]. In 2020, data from nine patients administered fludrocortisone showed no adverse effects. Studies showed a decrease in serum potassium values, increase in serum bicarbonate levels, and an increase in blood pressure [see results, paper 4.3 Živná, Kidd et al. 2020]. Fludrocortisone treatment improves blood pressure and may decrease production of both REN and mutated REN, which could result in improvements in kidney function over time.

1.4 ADTKD due to *MUC1* Pathogenic Variants

MUC1 Background

Mucin proteins are categorized by their function and structure as heavily glycosylated proteins. These proteins contain variable number of tandem repeat (VNTR) regions, with a high proline, threonine, and serine content. Currently, 22 mucins have been identified and are classified as either membrane-bound or secreted gel-forming [Pajic et al. 2022].

Mucin-1 (MUC1) was first identified in 1981 as a mammary gland milk mucin [Taylor-Papadimitriou et al. 1981]. Other names for MUC1 have included polymorphic

epithelial mucin, peanut-lectin binding urinary mucin and epithelial membrane antigen. Nomenclature guidance in 1990 proposed using “Mucin” for protein and “*MUC*” for the gene, followed by a number chronologically assigned to each mucin cloned [Gendler et al. 1991]. MUC1 is expressed throughout the body as a membrane-bound mucin and is expressed in epithelial tissues such as the oral mucosa, lung, breast, colon, and kidney [Patton et al. 1995]. In the kidney, MUC1 is expressed in the thick ascending limb of the loop of Henle, distal convoluted tubule, and collecting duct [Živná, Kidd et al. 2022].

***MUC1* Gene**

The cDNA for *MUC1* was sequenced and described in 1987 and localized to chromosome 1q21 in 1990[Gendler et al. 1987, Gendler et al. 1990]. *MUC1* encodes seven exons and includes an 82% guanine-cytosine (GC) rich VNTR region, which varies from 2 to 125 repeats, resulting in considerable heterogeneity in peptide sequence length [Lancaster et al. 1990, Gendler et al. 1991].

MUC1 Structure

MUC1 contains several distinct domains: signal peptide, extracellular VNTR, SEA domain, hydrophobic transmembrane domain, and a C-terminus cytoplasmic tail [Gendler et al. 2001, Kirby et al. 2013]. The polymorphic nature of the VNTR was first described in 1987 analysis of urine samples from a single family, showing each family member having two distinct lengths of MUC1 [Swallow et al. 1987]. The proline residues provide a rigidity to the structure, while threonine and serine residue provide glycosylation sites [Cascio and Finn 2016]. The polymorphic nature of the VNTR suggests the length is not critical for function. The VNTR acts as a scaffold for heavy glycosylation regulated by tissue-specific

factors [Gendler et al. 1987]. At the SEA domain, the extracellular glycosylated VNTR cleaves from the transmembrane domain. The MUC1 SEA domain utilizes mechanical pressure to induce this proteolysis, perhaps in response to pressure on the epithelial tissue where it is expressed [Macao et al. 2005].

MUC1 Function

MUC1 functions as a protective barrier to epithelial tissue due to its heavily glycosylated extracellular VNTR domain. It is involved in lubrication, maintenance of cell hydration and entrapment of potentially harmful particles, cellular debris, or viral pathogens. The SEA domain may help to regulate cell shedding, rupture and response to pressure and stimuli [Gendler et al. 1991, Hanisch and Müller 2000, Chen et al. 2021].

In cancer biology, aberrant changes in glycosylation in MUC1 have been well described. The cytoplasmic tail of MUC1 can be phosphorylated, with its role in cell signal cascades leading to tumor formation and metastasis being studied extensively [Hanisch and Müller 2000, Rahn et al. 2004, Cascio and Finn 2016].

***MUC1* Pathogenic Variants as a Cause of ADTKD**

The first linkage for a form of ADMCKD was to chromosome 1q21 in 1998, with this form of ADMCKD subsequently known as ADMCKD1. DNA linkage mapping was performed in two large Cypriot families comprising of 89 individuals, 25 (28%) of which were clinically affected. Further genetic findings revealed the two families shared the same disease haplotype, indicating a common ancestor [Christodoulou et al. 1998]. One of these families, 4901 was phenotyped by Stavrou et al., characterizing 44 family members and identifying 23 as clinically affected, 13 still living and able to provide samples for genetic

testing. Clinically affected family members presented with CKD progressing to ESKD at an average age of 62 years, without proteinuria or hematuria. Hypertension and hyperuricemia occurred at a similar level of eGFR as other individuals with non-genetic forms of CKD [Stavrou et al. 1998].

In 2001, six ADMCKD Finnish families were identified and underwent linkage analysis, with five of the families mapped to 1q21. Clinical findings include autosomal dominant inheritance, slowly worsening CKD to ESKD between ages 25 years to 55 years and hypertension. None of the families linked to 1q21 had hyperuricemia or gout reported [Auranen et al. 2001].

A large Native American family was identified with ADMCKD1 and linked to 1q21 in 2004. Diagnosis of the disease had been missed by more than 10 nephrologists and was only suspected when a pre-transplant kidney biopsy of an asymptomatic daughter (planning for living-related kidney donation) revealed tubulointerstitial fibrosis. Clinical information was obtained for 18 clinically affected family members, and DNA samples were collected on 50 family members. Linkage analysis was performed for 34 individuals. Clinical findings included CKD with progression to ESKD between ages 35 and 66 years. Urinalysis showed no hematuria, and proteinuria present in two of the clinically affected patients. Four individuals had medullary cysts. Kidney biopsy findings included glomerular sclerosis, tubular atrophy, tubulointerstitial fibrosis. It was noted that lack of severe symptoms in ADMCKD can lead to under- or late diagnosis for patients [Kiser et al. 2004].

The causal gene at 1q21 was identified in 2013 in the landmark paper by Kirby et al., which included members of the RIKD Team of Charles University and Wake Forest School of Medicine. The investigation described a pathogenic variant in the *MUC1* gene, which

had not been identified by massively parallel sequencing (MPS) due to its presence in the GC-rich VNTR region of *MUC1*. Six large diverse families clinically diagnosed with ADMCKD1 underwent linkage analysis to identify they shared the genetic loci 1q21. The families did not share a haplotype, indicating each family harbored an independently arising pathogenic variant at 1q21. Evaluation of coding and non-coding regions was unremarkable, leading to dedicated genetic analysis of the VNTR regions. The *MUC1* VNTR is difficult to assess due to its 80-82% GC content. A single cytosine duplication within a heptanucleotide cytosine tract was identified. All six families carried this +C duplication, with each family having a different VNTR size and different location of the +C duplication within the VNTR [Kirby et al. 2013]. Of note, one of the families was the Native American family described previously [Kiser et al. 2004].

Genetic Testing for *MUC1*

Due to the difficulty in sequencing the VNTR, The Broad Institute of Harvard and MIT working together with the RIKD team, developed a probe extension assay to test for the +C duplication within the VNTR. Utilizing the restriction enzyme MwoI, which cleaves the *MUC1* wild type allele, while +C duplication destroys restriction site and mutated allele remains intact. Restriction cleavage is followed by PCR amplification of intact repeat unit using nested flanking PCR primers (in 60-bp repeat). Interrogation of +C duplication is performed by mass spectrometry probe extension assay. In an evaluation of the original 62 clinically affected and 79 asymptomatic individuals evaluated through linkage analysis and VNTR sequencing, results of the probe extension assay aligned perfectly with the initial VNTR sequencing results. Twenty-one other smaller families presenting with ADMCKD

and negative for *UMOD* and *REN* pathogenic variants underwent *MUC1* analysis, with 13 being found to have a +C duplication within their VNTR [Kirby et al. 2013].

The Wake Forest RIKD Team became the *MUC1* VNTR testing coordinating center for The Broad Institute Biological Sample Platform, a research testing center. Coordinating testing for IKD patients enrolled into the Wake Forest RIKD research study and for any other IKD researchers (collaborators) interested in having their patients tested for the *MUC1* +C duplication. Our coordination with collaborators led to identification of the +C duplication in the Cypriot families linked to 1q21 by Christodoulo et al. Upon joining the Wake Forest team in 2012, I became the genetic testing coordinator for *MUC1* analysis – sharing sample requirements with collaborators, receiving samples, organizing testing queues, preparation of each sample according to The Broad Institute’s protocol, shipping batches of samples for analysis; then upon completion of analysis, review results and disseminate to each team. The Broad Institute only accepts samples for *MUC1* testing prepared and shipped from our team.

In 2016, our team worked with The Broad Institute to develop a clinically validated mass spectrometry assay to identify the *MUC1* +C duplication [Blumenstiel et al. 2016]. This remains the only clinically validated *MUC1* test. The Wake Forest team is still the coordinating center for all samples that undergo *MUC1* analysis, and these results are documented in our registry [**described in Chapter 1.5**]. The number of patients and families identified with *MUC1* pathogenic variants continues to grow since its discovery in 2013, as seen in Figure 8. We have tested a total of 2519 individuals and identified 930 individuals and 330 families with ADTKD-*MUC1*.

Identification of Novel *MUC1* Pathogenic Variants

The +C duplication leads to a frameshift for the rest of the *MUC1* gene, altering the peptide sequence to an early truncating neopeptide (MUC1-fs). To study patient biopsies for abnormal MUC1 aggregation, an antibody for MUC1-fs was developed [Kirby et al. 2013]. Due to MUC1 expression in epithelial tissue, biopsy staining does not have to be limited to kidney tissue but can also be performed on breast tissue, skin, and sebaceous glands [Živná, Kidd et al. 2018].

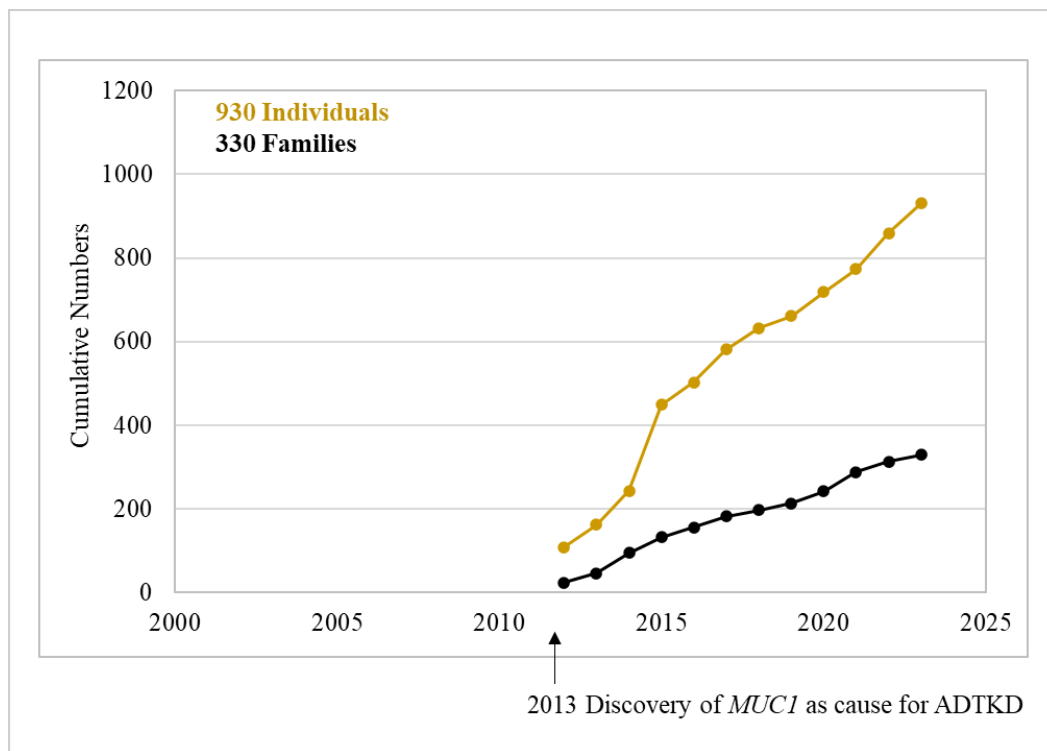


Figure 8. Growth of ADTKD-*MUC1* Registry from 2013-2023.

Despite many families being identified with pathogenic variants in *UMOD*, *MUC1* and *REN* there were still families presenting with ADTKD who tested negative for *UMOD*, *REN* and +C duplication in VNTR of *MUC1* using the probe extension assay but positive

for MUC1-fs in kidney biopsy. The RIKD team developed a hypothesis that the production of the specific MUC1-fs protein is critical and required for *ADTKD-MUC1*. Due to primary structure of VNTR, this MUC1-fs protein is synthesized by all *MUC1* where is in VNTR either insertion of $(3n+1)$ nucleotides or deletion of $(3n-1)$ nucleotides than the only +C duplication. Of note, the Broad assay could only identify the +C duplication. While other pathogenic variants could not be identified genetically, the frameshift protein could still be detected by staining tissues for MUC1-fs.

I worked with Mgr. Martina Živná to develop a protocol to identify the MUC1-fs protein, both in available tissue biopsies and in urine shipped from distant sites. Patients were instructed to collect 1st morning urines, cooled via ice bath, and shipped with an ice pack overnight to Wake Forest. We then fix and stain the slides for shipping to the Charles University. The urinary cell slides were then stained for normal MUC1 and MUC1-fs in *ADTKD-MUC1* patients and control patients including *ADTKD-UMOD* and evaluated. Sensitivity for MUC1-fs immunostaining of urinary cell slides was found to be 94% compared to 95% in kidney biopsies. Specificity was found to be 88% for MUC1-fs immunostaining of urinary cell slides vs. 82% in available kidney biopsies [Živná, Kidd et al. 2018]. Urinary cell slides were then evaluated for 17 families presenting with *ADTKD* but negative for *UMOD* pathogenic variants and *MUC1* +C duplication. Six families were positive for MUC1-fs staining. These families then underwent Illumina sequencing and five novel *MUC1* VNTR pathogenic variants were identified: a +A insertion, +G insertion, +16 base pair duplication, -C deletion +AT insertion, and another +C duplication found after a four-cytosine sequence. Eleven families with *ADTKD* remained without a causal gene

identified, indicating genetic heterogeneity beyond the currently known ADTKD genes [Živná, Kidd et al. 2018].

We then studied plasma wild-type MUC1 (MUC1-wt) levels as a method to screen for ADTKD-*MUC1*. We utilized the commercially available CA15-3 assay that has been used to monitor plasma MUC1 levels in breast cancer [Klee et al. 2004]. We hypothesized that patients with ADTKD-*MUC1* would have serum MUC1 levels that were approximate half those of unaffected individuals, due to the loss of production of MUC1-wt from the affected allele. Eighty-five ADTKD-*MUC1* patients, 6850 non-CKD reference population values, and 249 control patients (135 ADTKD-*UMOD* and 114 genetically unaffected family members) were assessed for CA15-3 values. Patients with a *MUC1* pathogenic variant had CA15-3 levels 40% lower than patients with *UMOD* pathogenic variants, genetically unaffected family members and non-CKD controls. While there was considerable overlap of values, 22% of ADTKD-*MUC1* patients had a CA15-3 level less than 5 U/mL compared to none in controls and 1% of the reference population. CA15-3 values over 20 U/mL were found in 1% of ADTKD-*MUC1* patients, 18% of controls and 25% of the reference population [Vylet' al, Kidd et al. 2021]. While follow-up genetic testing should be employed, CA15-3 provides a way to stratify patients for novel *MUC1* evaluation, using a value of 5U/mL or less for inclusion and a value of 20U/mL for exclusion intermediate values can be evaluated further with family history review and/or availability of urinary cell smear or biopsy for MUC1-fs staining.

Expansion of *MUC1* Sequencing

A large Dutch family with ADTKD was negative for pathogenic variants in *UMOD* and *MUC1* +C duplication. Whole-exome sequencing was employed, filtering for

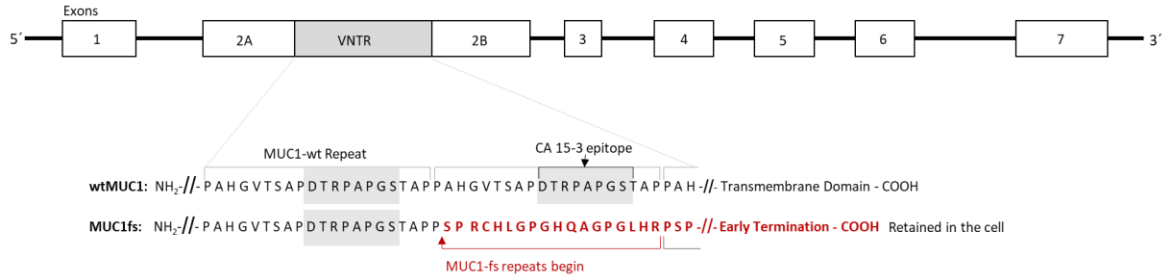


Figure 9. MUC1 Gene Map. *MUC1* is composed of seven exons with a variable number of tandem repeats (VNTR) that may have 2-125 repeats. Schematic for MUC1-wt VNTR sequence compared to resultant MUC1-fs. CA 15-3 epitope is also labeled. All pathogenic MUC1 variants in the RIKD registry result in the same MUC1-fs.

CKD genes including *UMOD*, *MUC1*, and *REN*. A novel *MUC1* pathogenic variant was identified before the VNTR, c.326_350dup, the 25 base-pair duplication creating the same +1 frameshift, resulting in MUC1-fs (Figure 9). The pathogenic variant segregated with four affected family members. Kidney biopsy evaluation of MUC1-fs revealed positive staining and showed interstitial fibrosis and granular staining [de Haan et al. 2023].

When I reviewed a large whole-exome sequencing cohort published in 2019, I identified a patient that had been found to have a *MUC1* p.Ala135fs (NM_001204285.2:c.401dup, ClinVarID: 591327), a variant of unknown significance (VUS) [Table S6 Groopman et al. 2019]. Our team spoke with the corresponding author on the status of *MUC1* analysis and found out that further *MUC1* genetic testing had not been pursued. With the patient's permission, we were able to collect a sample and perform genetic testing, revealing the presence of the +C duplication [data not published]. We hypothesize this particular *MUC1* +C duplication occurs at the beginning of the VNTR, as whole-exome sequencing does not pick up the entirety of the *MUC1* VNTR [Bleyer et al. 2019].

For the large number of families with ADTKD without a genetic diagnosis, sequencing the *MUC1* VNTR for rare variants is crucial. For families with ADTKD that test negative for *UMOD*, *REN* and the *MUC1* +C duplication, our team has developed a real-time single-molecule sequencing workflow using PacBio technology. We have already successfully identified an additional 10 families with novel *MUC1* variation [manuscript in progress]. Prioritizing families for the PacBio workflow can be done by applying our MUC1-*fs* and CA15-3 screening techniques [Živná, Kidd et al. 2018, Vylet’al, Kidd et al. 2021].

***MUC1* Single Nucleotide Polymorphism**

Alternate splice forms of *MUC1* were reported by Gendler et al. in 1991, describing a site within intron 1/exon2 that resulted in one form having an additional 27 base pairs (9 amino acids). This insertion does not affect the reading frame [Gendler et al. 1991]. This site has been designated as the SNP rs4072037-C-T. A study in dry eye patients revealed this to be a codominant trait for MUC1 production. The C allele (40% frequency) is associated the peptide sequence that includes nine additional amino acids, and the T allele (60% frequency) is associated with the shorter sequence length [Imbert et al. 2008]. The rs4072037 TT was identified as a risk allele for gastric cancer [Saeki et al. 2011]. A GWAS in CKD identified the rs4072037 TT as a risk allele for kidney function decline [Xu et al. 2018]. A study of ectopic pregnancy identified the T allele as a risk allele for ectopic pregnancy [Pujol Gualdo et al. 2023]. Further, a study in patients with sarcoidosis measuring plasma MUC1 levels, showed that patients with the rs4072037 CC genotype produced a significantly higher amount of MUC1 compared to those with the TT genotype, with heterozygous individuals being intermediate [Janssen et al. 2005]. We have also observed this in plasma CA15-3 (MUC1-wt) in patients with ADTKD-*MUC1* and ADTKD-*UMOD*.

Patients with ADTKD-*MUC1* produce significantly less MUC1 overall [Vylet' al, Kidd et al. 2021].

MUC1-fs Pathophysiology

MUC1 3n+1 pathogenic variants cause a frameshift affecting the remaining VNTR sequence. The self-terminating mutant MUC1-fs truncates the peptide and results in loss of the SEA, transmembrane and cytosolic domains. This creates a new protein that the human body has never interacted with before. Staining of ADTKD-*MUC1* patient kidney tissue with an antibody specific to MUC1-fs revealed intracellular localization to the distal tubule and collecting duct [Kirby et al. 2013]. Immunostaining with the MUC1-fs antibody in non-kidney tissue from patients with ADTKD-MUC1 also revealed intracellular deposition. While the MUC1-fs deposits intracellularly in all tissues producing MUC1 in affected individuals, it is notable that disease only occurs in the kidney and patients do not have an increased risk for cancer [Bleyer et al. 2014, Živná, Kidd et al. 2018]. Staining of ADTKD-*MUC1* patient urinary cells with MUC1-wt and MUC1-fs antibodies show that MUC1-wt is localized to the cell surface, showing even coverage compared to MUC1-fs forming intracellular aggregates [Figure 10] [Živná, Kidd et al. 2018].

Further Investigations to Understand MUC1-fs Pathophysiology

Dvela-Levitt et al. showed that in patient cells, patient derived organoids, and a knock-in mouse model, MUC1-fs accumulation occurs exclusively in the ER-Golgi intermediate compartment (ERGIC) [Figure 10]. MUC1-fs accumulation activates the ATF6 branch of the UPR but is unable to clear the MUC1-fs protein [Dvela-Levitt et al.

2019]. The constant slow accumulation of MUC1-fs leads to intracellular stress, accelerated apoptosis, tubular cell death, nephron dropout, and slow progression of CKD.

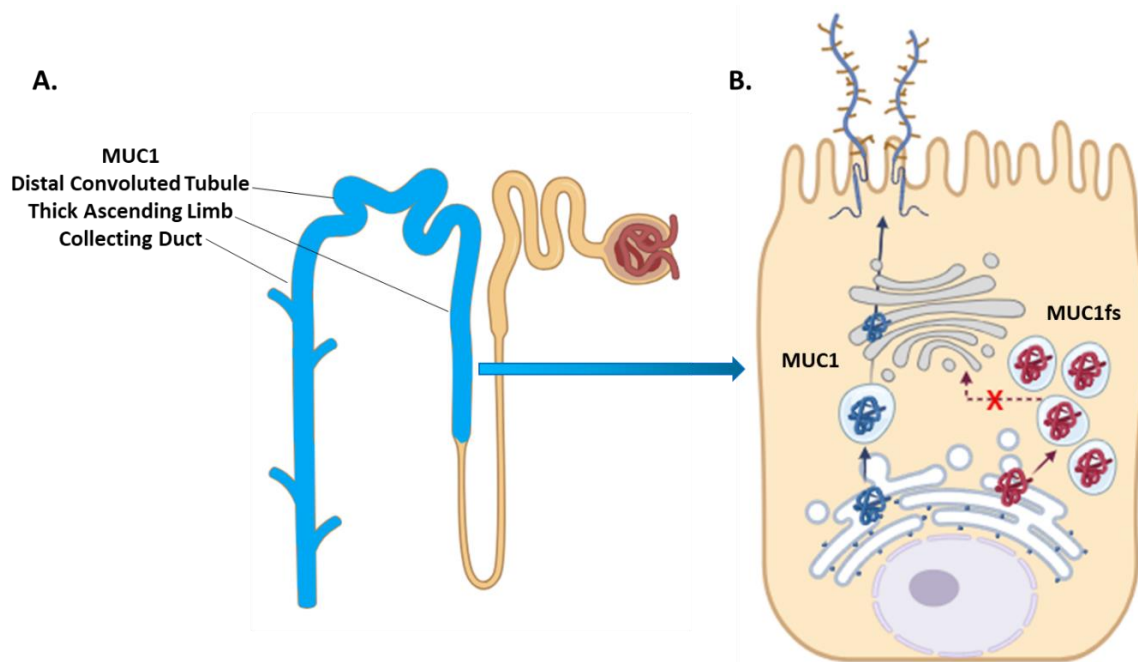


Figure 10. MUC1 expression in the nephron. A) MUC1 is expressed in the distal convoluted tubule, thick ascending limb, and collecting duct (blue). B) Typical MUC1 processing in the cell (blue arrows). MUC1 frameshift (MUC1-fs) accumulation in endoplasmic reticulum Golgi intermediate compartment (ERGIC) vesicles in ADTKD-*MUC1* (burgundy arrows with red “X”).

Understanding the processes leading to aberrant intracellular MUC1-fs accumulation and the signaling pathways induced by its presence are essential for identifying therapeutic targets. Dvela-Levitt et al. identified a compound designated BRD4780 as a potential treatment. BRD4780 is a small molecule that binds to TMED9, releasing the MUC1-fs and allowing it to enter lysosomal degradation. A modified compound is currently undergoing animal studies, with an exciting potential as a future therapy in ADTKD-*MUC1* patients [Dvela-Levitt et al. 2019].

1.5 Rare Inherited Kidney Disease Registry

In 1981 a five-year prospective study of an Australian family with autosomal dominant familial urate nephropathy was published. The index case presented with ESKD, a strong family history of gout and CKD. Family history was traced back five generations with a review of 33 family members. Two deceased family members were known to have kidney disease, one having gout. Eight living family members were followed over a five-year period, showing decline in kidney function over time. Serum uric acid measurements revealed hyperuricemia in asymptomatic family members. Histological findings from five kidney biopsies revealed tubular atrophy, interstitial fibrosis, and obstructive tubular lesions even in asymptomatic family members. The mean age of ESKD was 36 years [Richmond et al. 1981]. Once *UMOD* genetic testing was available, the family was found to have a *UMOD* in-frame deletion, p.Lys246-Ser252del.

Establishment of a Rare IKD Registry

The Wake Forest RIKD registry was established in 1996 when the first family with IKD was referred to Anthony J. Bleyer, MD, MS, who leads the Wake Forest component of the RIKD. Information about the family was collected including pedigree, demographics, medical records on affected individuals, samples collected, and genetic testing results. This family would later be published in the seminal paper describing *UMOD* pathogenic variants in uromodulin as for a cause of ADTKD [Hart et al. 2002]. Over time, the registry has grown to include over 1100 family referrals.

Identifying families with rare disease requires outreach, education, and communication. Physicians need to have access to information about the rare disease,

including presentation, genetic testing available, and treatment plan. Patients are eager to learn the cause of IKD that may have affected their family for many generations.

Recruitment for the IKD Registry utilizes a multifaceted approach of publications, reviews, presentations at national meetings, invited lectures, providing information for other medical and rare disease platforms, and creation of an email list to referring physicians to share IKD updates. The Internet has become an increasingly useful method for patients with a rare disease to find the rare clinical research team interested in their condition. [see results, paper 4.1 Bleyer, Kidd et al. 2020].

I have maintained the websites that allow patients to find our registry:

<https://www.wakehealth.edu/condition/m/mucin-1-kidney-disease>

<https://www.wakehealth.edu/condition/u/uromodulin-kidney-disease>.

IKD Registry Framework

Our team utilizes the research framework outlined in Figure 1. From the beginning, we have accepted patients into the study without physician referral, realizing that many physicians have little interest in identifying the cause of disease. Patients are also referred by their academic or non-academic healthcare providers. Patients then are asked to provide their consent to participate in the study, which has been approved by the institutional review boards of Wake Forest University School of Medicine and First Faculty of Medicine, Charles University. Patients provide many types of information: contact information, demographics, family history, pedigrees, laboratory measurements records, biopsy and ultrasound reports, any prior genetic testing reports, as well as coordinating to provide samples for DNA isolation, plasma and urine to store in the biobank.

Genetic testing begins with single gene testing for the common ADTKD genes *MUC1*, *UMOD* and/or *REN*. *MUC1* analysis is provided by the Broad Institute of Harvard

and MIT [Blumenstiel et al. 2016], and *UMOD* and *REN* testing are performed by the Kmoch team of First Faculty of Medicine, Charles University [see results, paper 4.2 Kidd et al. 2020, paper 4.3 Živná, Kidd et al. 2020]. Families negative for pathogenic variants in these ADTKD genes undergo whole exome or whole genome sequencing to evaluate for pathogenic variants in other known IKD genes, as well as novel gene candidates. If a candidate gene is identified, the exomes of other families with unknown causes of IKD are analyzed for similar findings. Further efforts to determine if a candidate gene is causal include expansion of pedigrees. In addition, skin biopsies, fibroblast culture, immunostaining of renal and non-renal tissues, and collection of samples for mRNA are performed. The team also utilizes platforms such as GeneMatcher to see if other teams have patients with pathogenic variants in the candidate gene, match phenotypes and are amenable to collaboration [Bolar et al. 2016, Hartmannová et al., 2016 Cochran et al. 2018, Zikánová et al. 2018, Buglioni et al. 2021, Sikora et al. 2022, see results, paper 4.5 Kmochová, Kidd et al. 2023].

The laboratory at Wake Forest has received and processed over 6000 samples since 1996, over 5200 of which are DNA samples for genetic testing [Figure 11]. In 2015 I worked with our team and external collaborators to establish a protocol for processing, aliquoting, and storing plasma and urine for studying potential biomarkers of disease. I supervise and maintain the Wake Forest IKD Biobank, which is the largest ADTKD biobank in the world. We have 1451 plasma and 1353 urine samples from 939 IKD patients, as well as unaffected family members that can be used as healthy controls.

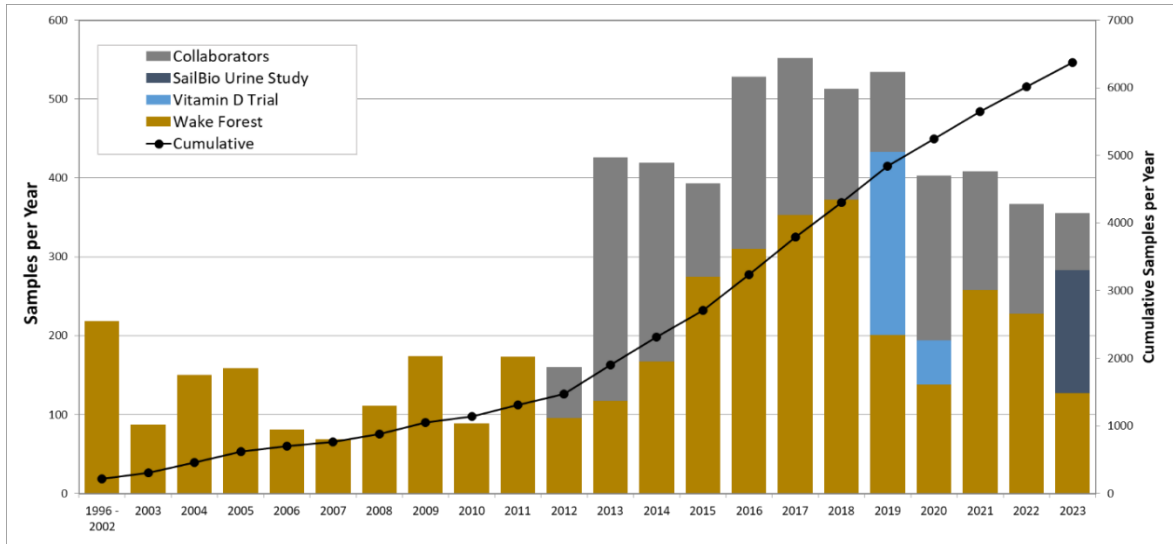


Figure 11. Samples collected and processed by the Wake Forest laboratory. Sample collection began in 1996. Each year shows the total samples collected divided by sample type: Collaborator samples are DNA samples for MUC1 genetic testing, Wake Forest samples are DNA as well as urine and plasma for biobanking, the Vitamin D Trial and Urine Study were clinical trials coordinated and run by Wake Forest. Cumulative is the total samples collected and processed.

Growth of the ADTKD Registry

Identification of patients with ADTKD has increased 35% since I began my PhD programme in 2018 [Table 1]. The ADTKD registry currently has information on 1019 ADTKD-*UMOD* patients, 930 ADTKD-*MUC1* patients, and 130 ADTKD-*REN* patients. Table 2 shows the sizes of the WF-RIKD cohort and collaborator cohorts currently in the ADTKD registry. Figures 2 and 8 show growth of numbers of ADTKD-*UMOD* and ADTKD-*MUC1* cohorts, showing steady growth since the identification of each causative gene. As ADTKD is a rare condition, data from each patient increases our knowledge about this condition and increases statistical power for clinical characterization or future clinical trials. For example, future clinical trials may require a kidney biopsy before and after a potential therapy. For this reason, we have collected over 100 kidney biopsies on patients with ADTKD to better understand the pathologic changes and help to design a biopsy

component for a future trial [see results, papers 4.2 Kidd et al. 2020, 4.3 Živná, Kidd et al. 2020, 4.4 Olinger, Hofmann, Kidd et al. 2020].

Table 1. Identification of Individuals with ADTKD from 2018 to 2023

ADTKD-		2018	2023	Increase (n)	Increase (%)
<i>UMOD</i>	Individuals	893	1019	+126	14%
	Families	305	401	+96	32%
<i>MUC1</i>	Individuals	633	930	+297	47%
	Families	197	330	+133	68%
<i>REN</i>	Individuals	15	130	+115	>100%
	Families	7	37	+30	>100%
<i>TOTAL</i>	Individuals	1541	2079	+538	35%
	Families	509	768	+259	51%

Table 2. Current ADTKD Wake Forest and Collaborator Cohorts in the RIKD Registry

ADTKD		WF cohort	Collab cohort	Total
<i>UMOD</i>	Individuals	647	372	1019
	Families	245	156	401
<i>MUC1</i>	Individuals	449	481	930
	Families	150	180	330
<i>REN</i>	Individuals	28	102	130
	Families	14	23	37
<i>TOTAL</i>	Individuals	1124	955	2079
	Families	409	359	768

Building the REDCap RIKD Registry

Research Electronic Data Capture (REDCap) is a secure, dynamic virtual data collection and management database platform sponsored by the National Institute of Health

(NIH) available at no cost to REDCap consortium institutions teams. REDCap provides a wide range of tools for tailoring to allow flexibility in design, including branching logic, calculated fields, longitudinal data capture capability, research arms, study calendar building, e-consent, file uploading, and survey functions that can be used to meet the specific needs of the project. The research team can enter data into the project, and patients can complete surveys, sharing valuable insight and data directly to their study record. External collaborators can be provided access to de-identified study data, and teams can specify which data is accessible to every user to ensure data protection for their patients. Datasets are easily generated to contain any variable within the project and utilizing Boolean logic set filters to include or exclude specific data. Data is then exported into a variety of file types for direct use by statistical programs (SPSS, SAS, STATA, R) [Harris et al. 2009]. The platform is hosted by over 5,800 consortium institutions including the First Faculty of Medicine and Wake Forest University School of Medicine.

In 2015, I developed the Wake Forest IKD REDCap Project, which currently houses 1,444 variables and 9,640 records. Each patient in the study has a unique record in the REDCap project, including each family member reported in a pedigree. This record synthesizes a variety of data types, including patient's clinical, genetic, and biobank data (see Figure 1). The Rare IKD project is designed to capture cross-sectional information, such as demographics or disease status, as well as longitudinal data such as medical records or samples collected over time. I oversee data entry of our study coordinators and laboratory technicians at Wake Forest to maintain consistency and accuracy. We can then generate robust datasets including any combination of stored data for analysis [Figure 12] [see

results, papers 4.1 Bleyer, Kidd et al. 2020, 4.2 Kidd et al. 2020, 4.3 Živná, Kidd et al. 2020, 4.4 Olinger, Hofmann, Kidd et al. 2020, 4.5 Kmochová, Kidd et al. 2023].

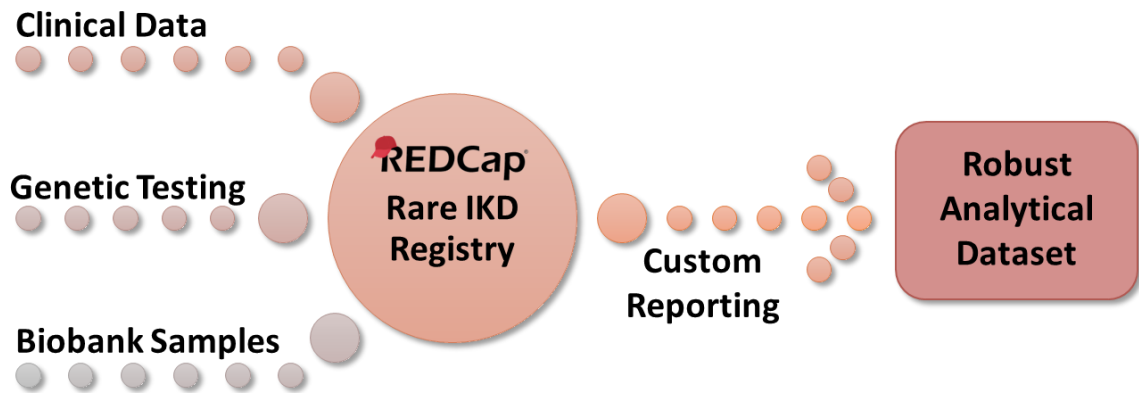


Figure 12. Data flow in the Rare IKD REDCap registry. The REDCap registry collects and integrates many types of data that can be used to create datasets for aggregate summaries for progress reports, curating the data for integrity, as well statistical analysis and modeling.

In addition, I wrote four sub-study protocols for institutional approval and developed the REDCap projects. The goal of these initiatives is to gain a better understanding of the factors that influence patients IKD progression and how ADTKD impacts other aspects of health in a subset of patients genotyped with *ADTKD-UMOD* or *ADTKD-MUC1*. These studies are survey-based and designed to collect information directly from patients enrolled in our study. (1) The IKD Health Survey is an extensive online self-reporting survey for patients covering clinical and environmental factors [study ongoing]. (2) The Quality of Life in Patients with ADTKD study examined quality of life in our patients with ADTKD and the impact of genetic diagnosis [Bleyer, Kidd et al. 2019]. (3) The Women’s Health Outcomes in ADTKD study showed that mothers with ADTKD do well with pregnancy, and their babies have excellent outcomes [Bleyer, Kidd et al. 2023]. (4) The COVID-19 Outcomes in ADTKD showed that patients with *ADTKD-MUC1* are at a markedly increased

risk of death from COVID-19 [manuscript in progress, **see presentation 5.4 Kidd et al. 2022**]. (5) The 21 Study: A Prospective Longitudinal Natural History Study of Patients with ADTKD is following patients over time and evaluating their progressive loss of kidney function [study ongoing, **see presentation 5.4 Kidd et al. 2021, 2022**].

Lessons from the IKD Registry

A retrospective analysis of the IKD registry published in 2020 was pivotal in being the first study of a rare disease registry to investigate individuals with a rare disease and their journey from referral to diagnosis. The study reviewed 665 referrals for ADTKD evaluation and their outcomes. 275 participants underwent genetic testing and had an outcome. Healthcare providers (HCP) from academic institutions provided 41% of referrals, non-academic HCP provided 33% of referrals, and direct family referrals provided 27% of referrals. All study participants who contacted us without a referral from their provider found us through Internet searches. In contrast, HCPs were more likely to contact us due to personally knowing Dr. Bleyer and his work in the field. Thirty-six percent of referrals were from families with four or more affected family members [**see results, paper 4.1 Bleyer, Kidd et al. 2020**].

172 families (62%) and 567 family members were genetically diagnosed with ADTKD. Of those diagnosed with ADTKD, 42 (25%) were families and 116 (21%) were family members who were direct family referrals. Notably patients who were self-referred had the same probability of being diagnosed with ADTKD as referrals from physicians. [**see results, paper 4.1 Bleyer, Kidd et al. 2020**].

Evaluating demographics of referrals from HCPs compared to direct family referrals, revealed what is known as the digital divide. 99% of the direct family referrals that resulted

in enrollment and genetic testing samples were from white households. Furthermore, the median income of families in zip codes based on direct family referrals was \$77,316, which was much higher than the 2010 US median household income of \$49,445 [United States Census Bureau 2011]. There were no direct family referrals from African American families and few from non-English speaking countries. Factors that contribute to the digital divide and limit access to healthcare information via the internet include the availability of affordable internet services, access to internet-connected devices, and a lack of familiarity with how to use the internet to access health care information and answer questions about kidney disease in their family [see results, paper 4.1 Bleyer, Kidd et al. 2020]. These are challenges faced by our registry and other rare disease researchers. We are working to discover ways to increase outreach and education to all populations in order to diagnose families and expand our understanding of these diseases.

Large Scale Genotyping for IKD

Currently, more than 350 genes have been identified as causes of IKD. A seminal study published in 2019 by Groopman et al. described the results of 3,315 individuals with CKD who underwent whole exome sequencing. 307 (9.1%) individuals were found to have a pathogenic variant in 66 different genes associated with monogenic CKD. The most common causes of CKD were variants causing ADPKD (*PKD1* or *PKD2* (31%) and Alport Syndrome *COL4A3*, *COL4A4*, or *COL4A5* (31%). Pathogenic variants in *UMOD* were identified in nine patients (3%), and a *SEC61A1* pathogenic variant identified in one patient. Table S6 listed one patient with a variant of uncertain significance (VUS) in *REN*, one with a VUS in *UMOD*, and two were identified with VUS in *MUC1*. Unfortunately, no additional family or clinical information is given for these cases [Groopman et al. 2019]. A letter to the

editor was written regarding inclusion of *MUC1* in analysis, as whole-exome sequencing does not fully sequence and capture *MUC1* pathogenic variants within the VNTR [Bleyer et al. 2019].

Commercial genetic testing companies have developed broad gene panels, giving nephrologists the ability to order testing for their clinic patients instead of stepwise single gene testing, which can be time consuming and expensive and require physicians to follow a genetic testing strategy based on clinical characteristics and genes associated with these particular phenotypes. The Natera Renasight™ panel analyzes 380 IKD genes utilizing next-generation sequencing including ADTKD genes *UMOD*, *REN*, and *SEC61A1*. Results of their first 1,007 panels identified 220 (21%) patients with a monogenic cause for CKD in 48 genes. The most prevalent findings were pathogenic or likely pathogenic variants for ADPKD *PKD1* or *PKD2* (44%) and Alport Syndrome *COL4A3*, *COL4A4*, or *COL4A5* (23%). Two patients with *UMOD* pathogenic variants were identified (1%), and none with pathogenic or likely pathogenic variants in *REN* or *SEC61A1*. It is noted in the discussion that whole exome and next-generation sequencing do not capture *MUC1* pathogenic variants, as they occur within VNTR regions and are not properly sequenced [Bleyer et al. 2022].

While these are powerful methods and studies to add to our understanding of IKD, and patients with pathogenic or likely pathogenic variants find the genetic cause of their disease, families are often not further referred to research groups that are working to better understand, characterize and develop curative treatment for their family's rare IKD [see results, papers 4.2 Kidd et al. 2020, 4.3 Živná, Kidd et al. 2020, 4.4 Olinger, Hofmann, Kidd et al. 2020].

Additionally, families that have negative results or VUS are often considered to have had a complete evaluation and are not further referred for more advanced genetic testing to find the cause of their IKD. Specifically, *MUC1* genetic testing, which is not part of IKD gene panels due to the requirement of specialized genetic testing, is often not performed [see results, paper 4.5 Kmochová, Kidd et al. 2023].

1.6 Genetic, Biologic, and Clinical Factors Associated with ADTKD Prognosis

There is significant variation in clinical presentation and disease progression within all types of IKD. The development of methods that leverage genetic, clinical, and pathophysiological characteristics to better understand patient outcomes and stratify patients for clinical trials could be extremely beneficial. The two most well-known approaches attempting to correlate genotype with phenotype and pathology are found in the study of ADPKD and Alport Syndrome. The Predicting Renal Outcomes in Polycystic Kidney Disease (PROKD) study developed a predictive model of age of ESKD by integrating clinical and pathogenic variant data. Investigators studying Alport Syndrome have used a similar approach by integrating pathogenic variant type, position, with clinical and pathology data [Elliott et al. 2023]. Using this as a foundation, we have begun work to better understand the impact of pathogenic variant and clinical data on patient outcomes in ADTKD.

Clinical Characterization of ADTKD

ADTKD is a slowly progressive kidney disease, with marked intra and inter-familial variance in disease progression [Figure 13]. Often individuals are asymptomatic until past age 20 years, when decreased kidney function may be detected in individuals who undergo

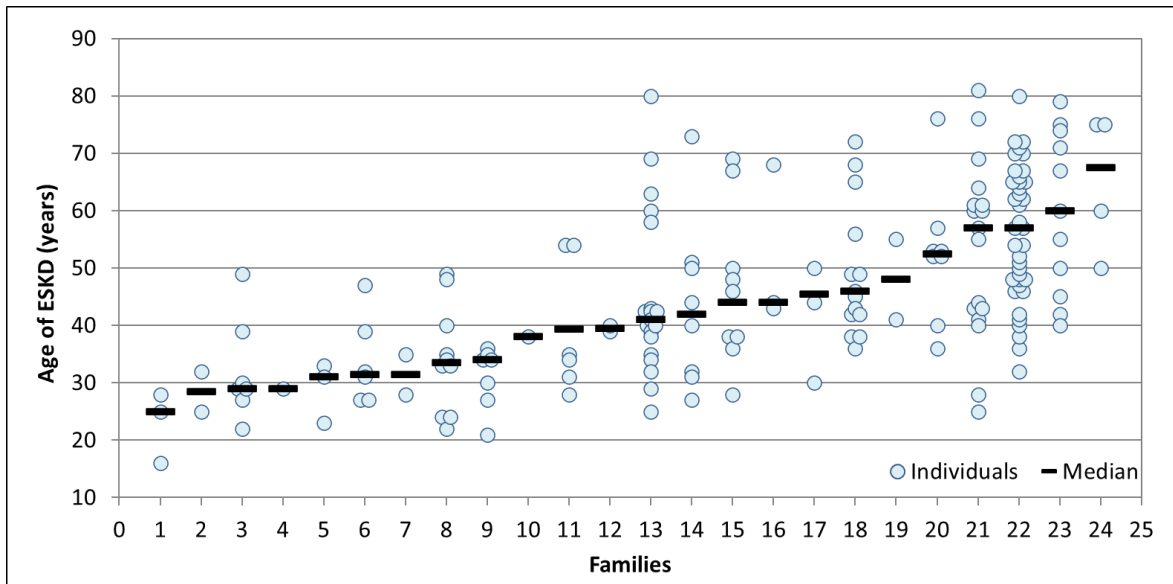


Figure 13. Variable rate of progression to end stage kidney disease (ESKD) in families with ADTKD. Each column represents a family. Each circle represents a family member’s age of ESKD. The black line is the median age of ESKD for the family. Families are arranged by earliest to latest median age of ESKD.

routine bloodwork. Patients have a bland urinary sediment and may or may not have hyperuricemia [Bleyer et al. 2021]. The decline in kidney function may be gradual, occurring over 20 to 50 years. According to our registry data, the rate of decline is often not linear, and patients may experience several years of decline, followed by stable kidney function for several years. The reasons for this variable rate of change are unknown. The median age for ESKD is 45 years of age, ranging from 20 to 80 years [Živná, Kidd et al. 2022, see results, papers 4.2 Kidd et al. 2020, 4.4 Olinger, Hofmann, Kidd et al. 2020].

Clinical Predictors in ADTKD-*UMOD*

In 2020, Kidd et al. and Olinger et al. published the two largest cohorts of ADTKD-*UMOD* patients. Clinical data evaluated included: gender, weight, height, smoking status, gout presence and age of 1st gout attack, age of ESKD (if reached) or last age without having reached ESKD, family mean age of ESKD, and affected parent age of ESKD. Body mass

index, smoking status, and presence of gout were found non-significant in predicting decline to ESKD. The best clinical predictors of rapid loss of kidney function was the age of first gout attack ($P= 0.000053$), male gender ($P=0.0028$), familial age of ESKD ($P=0.009$) and age of parent reaching ESKD ($P=0.0045$), especially if the mother was the affected parent ($P=0.0017$) [see results, papers 4.2 Kidd et al. 2020, 4.4 Olinger, Hofmann, Kidd et al.].

Clinical Predictors in ADTKD-*MUC1*

Individuals with ADTKD-*MUC1* have an earlier age of ESKD compared to ADTKD-*UMOD* (36 years vs 46 years, $P<0.0001$). Gout was only present in 26% of ADTKD-*MUC1* patients, with the age of onset significantly later than that seen with ADTKD-*UMOD* (45 years vs 27 years) [see results, paper 4.4 Olinger, Hofmann, Kidd et al. 2020]. ADTKD-*MUC1* remains difficult to diagnose unless a doctor is knowledgeable about the condition, or a family knows how to use the right search terms on the Internet to locate a group that studies ADTKD and can coordinate genetic testing. ADTKD-*MUC1* diagnosis is difficult because the only clinical characteristics are CKD, a bland urine sediment and family history. This leads to under-diagnosis and under-representation as a cause of IKD.

The clinically available laboratory test CA15-3, which measures wild-type MUC1 in the blood, is helpful for screening potential ADTKD-*MUC1* families when the value is less than 5 U/mL [Vylet' al, Kidd et al. 2021]. However, it was not found to be significantly associated with decline in kidney function (data not published).

Score Derived to Prioritize Genetic Testing in ADTKD Index Cases

A clinical score was developed utilizing the presence of family history, age of gout onset, serum uric acid, histological changes (if biopsy is available) and absence of

proteinuria, hematuria, diabetes or uncontrolled hypertension, and renal cysts/enlarged kidneys. A score greater than 5 indicates the patient should be genetically tested for *UMOD* pathogenic variants, and less than 5 genetically tested for *MUC1* pathogenic variants. This score can be useful for clinicians to determine what genetic testing is most appropriate for a patient, reduce the cost of unjustified genetic testing, improve diagnostic rates, and enhance clinical management of patients [see results, paper 4.4 Olinger, Hofmann, Kidd et.al. 2020].

Genetic Predictors in ADTKD-*UMOD*

The 2020 ADTKD-*UMOD* cohort study evaluated 125 unique *UMOD* pathogenic variants to determine if variability of CKD progression to ESKD observed within ADTKD-*UMOD* patients was associated with characteristics of the variant. All pathogenic variants were evaluated for position and domain location, and missense pathogenic variants were evaluated based upon original versus resultant amino acid and biochemical property of original versus resultant amino acid. Unfortunately, no association was found between the type of *UMOD* pathogenic variant and the age of ESKD [see results, paper 4.2 Kidd et al. 2020].

As the rs4293393 G allele (allele frequency 19%) had been found in prior studies to lower *UMOD* production by approximately 50% and be protective against progression of CKD [Trudu et al. 2017], we hypothesized that families with the rs4293393 G allele immediately preceding their mutant *UMOD* gene would produce less mutant *UMOD* and have a later age of onset of ESKD. Based on population allele frequencies, approximately 19% of the families should have had the rs4293393 G allele in the mutant *UMOD* promoter. Instead, only 12% of families in our cohort had the minor G allele in phase with m*UMOD*

vs the expected 19% ($P=0.0037$), suggesting a protective effect. However, as Hardy Weinberg equilibrium had not been preserved, and we could not carry out a Mendelian randomization analysis [see results, paper 4.2 Kidd et al. 2020].

As part of this investigation, we attempted to correlate *n in vitro* and clinical findings. Schaffer and colleagues had noted that transport and glycosylation of mUMOD varied by mutation type. With milder mutations, more mature glycosylated UMOD was secreted and less mUMOD was retained in the endoplasmic reticulum. These authors created a score from 1 to 4, with 1 having the most mature UMOD secreted and least mUMOD retained intracellularly, and a score of 4 having the most mUMOD retained within the ER and the least mature UMOD secreted. In our statistical analysis, we were able to show that a lower *in vitro* score correlated with a later age of onset of ESKD. We have applied the findings of this study to characterize new variants, assess whether they are benign, and help to predict the mean age of ESKD for individuals affected with *de novo* pathogenic variants. Use of the *in vitro* score may also be helpful in stratifying patients in future clinical trials [see results, paper 4.2 Kidd et al. 2020].

Other investigators have now begun to correlate age of ESKD with structural models, also using the *in vitro* score that we studied [Johannesen et al. 2022, abstract Kwon et al. Unraveling the conformational dynamics of UMOD protein variants in autosomal dominant tubule interstitial kidney disease: Insights from molecular dynamics simulations. 2024. *Biophys Journal* 123(8).].

Genetic, Clinical and Pathophysiology Predictors in ADTKD-REN

Živná, Kidd et al. published the largest cohort of patients with ADTKD-REN, describing 111 patients and 15 heterozygous pathogenic variants. This landmark study identified three distinct subtypes of ADTKD-REN that are genetically, clinically, and pathophysiologically distinct based upon the location of the variant.

Pathogenic variants in the signal peptide affected the ability of prorenin to translocate into the ER for post-translational modification. Patients with these variants are more severely affected with clinical presentation at age 20 years. Affected individuals have a high likelihood of anemia as a child (91%) and reach ESKD at an average age of 53 years [see results, paper 4.3 Živná, Kidd et al. 2020].

Prosegment REN mutations accumulate in the ER-Golgi intermediate compartments (ERGIC) and lead to reduced prorenin and REN levels. Patients with prorenin pathogenic variants have an intermediate phenotype, with clinical presentation around age 22. Of affected individuals 69% had childhood anemia and 65% developed gout. The mean age of ESKD was 51 years [see results, paper 4.3 Živná, Kidd et al. 2020].

REN pathogenic variants in the mature REN allow prorenin to enter the ER, but the mutated protein is misfolded and accumulates within the ER, in a similar manner to ADTKD-UMOD [see results, paper 4.3 Živná, Kidd et al. 2020]. Patients with these variants present similarly to ADTKD-UMOD patients. Gout is common (occurring in 64%) and affected individuals do not suffer from anemia during childhood. ESKD in patients with mature REN pathogenic variants occurs at a mean age of 64 years, significantly older than in individuals with other REN pathogenic variants, and at an older age than ADTKD-UMOD

patients, who reach ESKD at an average of 45 years [see results, papers 4.2 Kidd et al. 2020, 4.3 Živná, Kidd et al. 2020, 4.4 Olinger, Hofmann, Kidd et al. 2020].

Similar to the PROPKD score in ADTKD and clinical prognostic scoring for Alport syndrome, the ADTKD-*REN* subtype (pathogenic variant in signal peptide, prorenin, or mature renin) informs on prognosis, which is useful in counseling patients [see results, paper 4.3 Živná, Kidd et al. 2020, Elliott et al. 2023].

1.7 Rare Inherited Kidney Disease Genes and Novel ADTKD Gene Discovery

The genetic heterogeneity of MCKD, now ADTKD, was explored in the literature prior to gene-disease discovery [Kroiss et al. 2000, Hildebrandt and Otto 2000]. While this thesis has examined the most common ADTKD causative genes, *UMOD*, *MUC1*, and *REN*, rare ADTKD genes have been identified and novel genes remain to be discovered.

ADTKD-*SEC61A1*

In 2016, Bolar et al., including our RIKD team, identified *SEC61A1* as a cause for ADTKD in two families presenting with CKD, congenital anemia, and presence of intrauterine growth delay or neutropenia. Ultrasound and kidney biopsy showed small kidneys with cysts, tubular atrophy, and secondary glomerular sclerosis [Bolar et al. 2016].

SEC61A1 is a subunit alpha of the *SEC61* transport complex, also known as the translocon. The translocon is an ER transmembrane channel pore that transports proteins into the ER for post-translational modification, moving misfolded protein into the cytosol for ER-associated protein degradation (ERAD), and playing a role in cellular calcium homeostasis. *SEC61A1* forms the constriction ring and plug for the translocon, which opens and closes the channel protein [Bolar et al. 2016].

Whole exome sequencing identified two heterozygous missense *SEC61A1* variants, p.Thr185Ala and p.Val67Gly. Immunofluorescence microscopy of patient kidney biopsies showed mutant SEC61A1 mislocalized in the Golgi, indicating this protein is recognized as misfolded and not able to reach its physiological localization membrane of ER [Bolar et al. 2016].

Groopman et al. identified another family with a *SEC61A1* p.Ile428Met pathogenic variant in their whole-exome sequencing cohort study [Groopman et al. 2019]. A *de novo* case was also reported in 2020 with patients with a p.Thr185Ala pathogenic variant presenting with CKD, hyperuricemia, anemia and lymphopenia [Espino-Hernandez et al. 2020].

Three other families with immunodeficiency disorders and affected with *SEC61A1* have been reported in the literature [Schubert et al. 2018, Van Nieuwenhove et al. 2020]. One of these families suffered from hyperuricemia (a possible sign of renal transport abnormality), with the other two families having no evidence of kidney involvement [Van Nieuwenhove et al. 2020]. Two of the immunodeficiency pathogenic variants, p.Val85Asp and p.Gln92Arg, are involved with the formation of the translocon pore, and the other, p.Glu318Ter, is a loss of function variant that is only partially penetrant in the family [Schubert et al. 2018, Van Nieuwenhove et al. 2020]. Colocalization experiments of the two missense mutations performed in patient fibroblasts show localization of the mutant SEC61A1 to the ER and Golgi. Calcium flux measurements were altered in patient cells, indicating a destabilization of calcium homeostasis, or “leakiness” of the translocon [Van Nieuwenhove et al. 2020].

The *SEC61A1* p.Arg236Cys variant was reported in a family with autosomal dominant polycystic liver. The proband presented with liver cysts and hyperuricemia, while the parent had atypical PKD and CKD. Colocalization studies showed this mutation did not colocalize to the ER and Golgi but was degraded by the proteasome instead [Schlevogt et al. 2023].

Due to the rarity of this disease the phenotypic variability is of great interest, and a *SEC61A1* cohort study should be performed in the future.

Mitochondrial Tubulointerstitial Kidney Disease

A small family with four affected family members was referred, with a family history of progressive CKD, without proteinuria or hematuria. The pedigree was indicative of autosomal dominant inheritance. Genetic testing was performed, and the family was negative for *UMOD* and *MUC1* pathogenic variants. Kidney biopsy showed nonspecific, chronic tubulointerstitial nephropathy. However renal mitochondria were described as “dysmorphic mega-mitochondria”. Next-generation sequencing revealed a mitochondria pathogenic variant in the *MT-TF* gene, which codes for mitochondrial phenylalanine transfer RNA. This variant was identified in all four family members [Buglioni et al. 2020]. Pathogenic variants in *MT-TF* have been reported as a cause for IKD in 14 families [Tzen et al., 2001, Connor et al. 2017, Buglioni et al. 2020, Popp et al. 2022, Viering et al. 2022].

We have reviewed our registry for unresolved families that have potential mitochondrial inheritance patterns to perform sequencing and analysis for mitochondrial pathogenic variants.

***APOA4* - a Novel Cause for ADTKD**

A large family was referred to Wake Forest in 2015 presenting with autosomal dominant inheritance and slowly progressive CKD without proteinuria or hematuria. The proband's percutaneous kidney biopsy pathology revealed typical ADTKD findings – tubulointerstitial fibrosis, sclerotic glomeruli, tubular atrophy, along with vascular sclerosis. The proband tested negative for pathogenic variants in *UMOD* and *MUC1*. Kidney biopsies, urinary cell smears and plasma CA15-3 levels of clinically affected family members indicated a *MUC1* pathogenic variant was not present [see results, paper 4.5 Kmochová, Kidd et al. 2023].

Whole-genome sequencing was performed on five clinically affected family members, revealing a shared region at chromosome 11q23.2 containing only one candidate gene, *APOA4*. *APOA4* encodes apolipoprotein A-IV (ApoA4). ApoA4 is expressed in the small intestine and synthesized in response to dietary fat intake. It is incorporated into chylomicrons and enters the circulatory system, where ApoA4 dissociates from the chylomicron and can circulate as a monomer or homodimer [Weinburg et al. 1990, Duverger et al. 1993]. It is filtered through the glomerulus, reabsorbed, and degraded in the proximal and distal tubules [Lingenhel et al. 2006]. Thirteen cases of sporadic ApoA4 amyloidosis have been reported in the literature. Patients presenting with CKD, minimal proteinuria and no hematuria. In all cases, ApoA4 deposits were identified in the medulla of the kidney [see results, paper 4.5 Kmochová, Kidd et al. 2023].

Analysis of *APOA4* revealed a heterozygous p.Leu66Val variant. Utilizing Sanger sequencing to perform segregation analysis of 19 family members, 10 individuals were found to have the p.Leu66Val variant, supporting its pathogenicity. Two genetically affected

female family members retained normal kidney function. The nine genetically unaffected individuals were asymptomatic. Evaluation of our IKD whole exome and whole genome sequencing database identified two additional families with p.Leu66Val variants and two families with a heterozygous missense variant, p.Asp33Asn. A total of 48 individuals were identified with an *APOA4* pathogenic variant [see results, paper 4.5 Kmochová, Kidd et al. 2023].

Clinical characterization revealed that the plasma lipid profile was similar for genetically affected and unaffected family members, and premature atherosclerosis was not present. The mean age of ESKD for patients with the p.Leu66Val pathogenic variant was 58.2 ± 11.1 years and 66.7 ± 10.2 years for patients with the p.Asp33Asn pathogenic variant. The mean age of ESKD was higher than for other forms of ADTKD (e.g. mean age of ESKD of 45 for ADTKD-*UMOD* and 43 for ADTKD-*MUC1*). Four of the 48 genetically affected patients with a pathogenic variant in *APOA4* had a kidney biopsy specimen that included medullary tissue. In all four individuals, ApoA4 amyloid deposits were identified in the medullary tissue, as observed in sporadic cases. Mass spectrometric analysis of medullary amyloid from three patients revealed that the mutant ApoA4 was the predominant protein in the amyloid deposits [see results, paper 4.5 Kmochová, Kidd et al. 2023].

This discovery identified a gene-disease association for *APOA4* as another genetic cause for ADTKD. Patients have clinical findings consistent with other forms of ADTKD and should be genetically tested for *UMOD*, *MUC1*, and if negative *APOA4*. Genetic testing for these families would preclude the need to perform percutaneous kidney biopsies, which often do not include medullary tissue for amyloidosis identification [see results, paper 4.5 Kmochová, Kidd et al. 2023].

ADTKD-Unknown

Currently 15% of our referrals that have a suspected ADTKD diagnosis are negative for pathogenic variants in *UMOD*, *MUC1*, *REN*, *SEC61A1*, and now *APOA4* [see **results, paper 4.1 Bleyer, Kidd et al. 2020**]. Based upon our current successful framework, we are hopeful to resolve more of these families. Additional work is ongoing to analyze our whole-exome and whole-genome database to review VUS and phenotype in other known IKD genes, evaluate novel candidate genes, perform variant interpretation, as well as recruit additional family members for segregation analysis, coordinate additional samples for functional evaluation and outreach to colleagues for collaboration.

1.8 Summary and Future Research

Our team's research framework has provided a foundation for genotyping workflow to assess new families in parallel for *MUC1*, *UMOD*, and *REN* pathogenic variants. Since 2018, we have been able to increase recruitment in our patient registry 31% (14% *UMOD*, 47% *MUC1*, >100% *REN*). This increase helps us to perform more robust natural history studies, understand disease prevalence and will help provide patients for future clinical trials.

Identification of novel genes not only gives families a cause for the disease that has affected their family for generations, but also gives physicians and researchers a better understanding of the genetic heterogeneity of tubulointerstitial kidney disease. Studying the pathophysiology of the disease expands our understanding of how these pathogenic variants lead to development of CKD and ESKD. In the cases of pathogenic variants in *UMOD*, *REN* or *MUC1* the pathogenetic mechanism that leads to ESKD is intracellular accumulation of misfolded mutated proteins. These misfolded proteins activate the endoplasmic reticulum

(ER) stress and unfolded protein response (UPR). Renal epithelial tubular cells have high protein turnover, metabolic activity and limited regenerative capacities. Sustained ER stress and UPR initiate processes leading to deterioration of kidney function and development of ADTKD. UMOD, MUC1, and REN are glycoproteins abundantly expressed in kidney, and their biosynthesis depends on proper function of the translocon (SEC61A). ADTKD-*APOA4* has a separate pathogenetic mechanism. This understanding opens the possibility of targeted, specific curative treatments based on disease pathophysiology. Table 3 summarizes our current knowledge of ADTKD.

Table 3. ADTKD Characteristics and Associated Genes

ADTKD Shared Clinical Characteristics				
Autosomal dominant inheritance				
Chronic kidney disease leading to end stage kidney disease in the 3 rd through 7 th decade of life				
Bland urinary sediment (minimal proteinuria and no hematuria)				
Renal ultrasound show normal or small kidneys, may be echogenic with or without cysts				
Kidney biopsy often nonspecific show tubulointerstitial fibrosis, tubular atrophy, thickening of basement membrane				
ADTKD Gene-Disease Association and Differential Clinical Characteristics				
Gene	Protein	Disease name	Differential Characteristics	Year Identified
<i>UMOD</i>	Uromodulin	ADTKD- <i>UMOD</i>	Gout in some families prior to <i>CKD</i>	2002, Hart et al.
<i>REN</i>	Renin	ADTKD- <i>REN</i>	Anemia in childhood, gout, mild hypotension, mild hyperkalemia	2009, Zivna et al.
<i>MUC1</i>	Mucin-1	ADTKD- <i>MUC1</i>	No other associated symptoms	2013, Kirby et al.
<i>SEC61A1</i>	SEC61A1	ADTKD- <i>SEC61A1</i>	Neutropenia, growth delay	2016, Bolar et al.
<i>APOA4</i>	ApoA4	ADTKD- <i>APOA4</i>	Medullary amyloidosis	2023, Kmochova et al.

In respect to clinical trial development, we have already participated in the 1st two clinical trials for ADTKD-*MUC1*, one studying the effect of Vitamin-D on MUC1 production (2019-2020, manuscript in preparation), and the other a non-interventional specimen collection study to validate our specimen collection and processing protocol for a

federally regulated trial. with Wake Forest being the only site coordinating patients across the USA (2022-2023, data unpublished). We are also currently performing a prospective observational study of ADTKD-*UMOD* and ADTKD-*MUC1* patients with CKD prior ESKD. This study currently has 209 enrolled, providing labs every 3-4 months with a paired health survey and a baseline biobanked sample (plasma and urine). We are already in contact with companies interested in developing a curative treatment for ADTKD. Having a large, well phenotyped “clinical trial ready” patient cohort will help to garner interest in our registry population and move ADTKD more quickly towards a future clinical trial.

ADTKD-*Unknown* families comprise approximately 15% of the RIKD registry. To further pursue identification of genetic diagnosis these undiagnosed families, we will use *MUC1*-fs screening, PacBio sequencing, whole genome sequencing, RNA seq, analysis of copy number variations and retrospective evaluation of our existing WES data [Figure 1].

2. References

Auranen M, Ala-Mello S, Turunen JA, Järvelä I. Further evidence for linkage of autosomal-dominant medullary cystic kidney disease on chromosome 1q21. *Kidney Int.* 2001 Oct;60(4):1225-32.

Barker DF, Hostikka SL, Zhou J, Chow LT, Oliphant AR, Gerken SC, Gregory MC, Skolnick MH, Atkin CL, Tryggvason K. Identification of mutations in the COL4A5 collagen gene in Alport syndrome. *Science.* 1990 Jun 8;248(4960):1224-7.

Basso N, Terragno NA. History about the discovery of the renin-angiotensin system. *Hypertension.* 2001 Dec 1;38(6):1246-9.

Bleyer AJ, Hart TC, Shihabi Z, Robins V, Hoyer JR. Mutations in the uromodulin gene decrease urinary excretion of Tamm-Horsfall protein. *Kidney Int.* 2004 Sep;66(3):974-7.

Bleyer AJ, Hart TC, Willingham MC, Iskandar SS, Gorry MC, Trachtman H. Clinicopathologic findings in medullary cystic kidney disease type 2. *Pediatr Nephrol*. 2005 Jun;20(6):824-7.

Bleyer AJ, Kidd K, Johnson E, Robins V, Martin L, Taylor A, Pinder AJ, Bowline I, Frankova V, Živná M, Taylor KB, Kim N, Baek JJ, Hartmannová H, Hodaňová K, Vylet'al P, Votruba M, Kmoch S. Quality of life in patients with autosomal dominant tubulointerstitial kidney disease. *Clin Nephrol*. 2019 Dec;92(6):302-311.

Bleyer AJ, Kidd KO, Williams AH, Johnson E, Robins V, Martin L, Taylor A, Kim A, Bowline I, Connaughton DM, Langefeld CD, Zivna M, Kmoch S. Maternal health and pregnancy outcomes in autosomal dominant tubulointerstitial kidney disease. *Obstet Med*. 2023 Sep;16(3):162-169.

Bleyer AJ, Kmoch S, Antignac C, Robins V, Kidd K, Kelsoe JR, Hladik G, Klemmer P, Knohl SJ, Scheinman SJ, Vo N, Santi A, Harris A, Canaday O, Weller N, Hulick PJ, Vogel K, Rahbari-Oskoui FF, Tuazon J, Deltas C, Somers D, Megarbane A, Kimmel PL, Sperati CJ, Orr-Urtreger A, Ben-Shachar S, Waugh DA, McGinn S, Bleyer AJ Jr, Hodanová K, Vylet'al P, Živná M, Hart TC, Hart PS. Variable clinical presentation of an MUC1 mutation causing medullary cystic kidney disease type 1. *Clin J Am Soc Nephrol*. 2014 Mar;9(3):527-35.

Bleyer AJ, Kmoch S, Greka A. Diagnostic Utility of Exome Sequencing for Kidney Disease. *N Engl J Med*. 2019 May 23;380(21):2080.

Bleyer AJ, Trachtman H, Sandhu J, Gorry MC, Hart TC. Renal manifestations of a mutation in the uromodulin (Tamm Horsfall protein) gene. *Am J Kidney Dis*. 2003 Aug;42(2):E20-6.

Bleyer AJ, Westemeyer M, Xie J, Bloom MS, Brossart K, Eckel JJ, Jones F, Molnar MZ, Kotzker W, Anand P, Kmoch S, Xue Y, Strom S, Punj S, Demko ZP, Tabriziani H, Billings PR, McKanna T. Genetic Etiologies for Chronic Kidney Disease Revealed through Next-Generation Renal Gene Panel. *Am J Nephrol*. 2022;53(4):297-306.

Bleyer AJ, Wolf MT, Kidd KO, Zivna M, Kmoch S. Autosomal dominant tubulointerstitial kidney disease: more than just HNF1β. *Pediatr Nephrol*. 2022 May;37(5):933-946.

Bleyer AJ, Zivná M, Hulková H, Hodanová K, Vyletal P, Sikora J, Zivný J, Sovová J, Hart TC, Adams JN, Elleder M, Kapp K, Haws R, Cornell LD, Kmoch S, Hart PS. Clinical and molecular characterization of a family with a dominant renin gene mutation and response to treatment with fludrocortisone. *Clin Nephrol*. 2010 Dec;74(6):411-22.

Blumenstiel B, DeFelice M, Birsoy O, Bleyer AJ, Kmoch S, Carter TA, Gnirke A, Kidd K, Rehm HL, Ronco L, Lander ES, Gabriel S, Lennon NJ. Development and Validation of a Mass Spectrometry-Based Assay for the Molecular Diagnosis of Mucin-1 Kidney Disease. *J Mol Diagn*. 2016 Jul;18(4):566-71.

Bolar NA, Golzio C, Živná M, Hayot G, Van Hemelrijk C, Schepers D, Vandeweyer G, Hoischen A, Huyghe JR, Raes A, Matthys E, Sys E, Azou M, Gubler MC, Praet M, Van Camp G, McFadden K, Padiaditakis I, Přistoupilová A, Hodaňová K, Vyleťal P, Hartmannová H, Stránecký V, Hůlková H, Barešová V, Jedličková I, Sovová J, Hnízda A, Kidd K, Bleyer AJ, Spong RS, Vande Walle J, Mortier G, Brunner H, Van Laer L, Kmoch S, Katsanis N, Loeys BL. Heterozygous Loss-of-Function SEC61A1 Mutations Cause Autosomal-Dominant Tubulo-Interstitial and Glomerulocystic Kidney Disease with Anemia. *Am J Hum Genet.* 2016 Jul 7;99(1):174-87.

Brunati M, Perucca S, Han L, Cattaneo A, Consolato F, Andolfo A, Schaeffer C, Olinger E, Peng J, Santambrogio S, Perrier R, Li S, Bokhove M, Bachi A, Hummler E, Devuyst O, Wu Q, Jovine L, Rampoldi L. The serine protease hepsin mediates urinary secretion and polymerisation of Zona Pellucida domain protein uromodulin. *Elife.* 2015 Dec 17;4:e08887.

Buglioni A, Hasadsri L, Nasr SH, Hogan MC, Moyer AM, Siddique K, Kidd K, Kmoch S, Hodaňová K, Bleyer AJ, Alexander MP. Mitochondriopathy Manifesting as Inherited Tubulointerstitial Nephropathy Without Symptomatic Other Organ Involvement. *Kidney Int Rep.* 2021 Jun 12;6(9):2514-2518.

Cascio S, Finn OJ. Intra- and Extra-Cellular Events Related to Altered Glycosylation of MUC1 Promote Chronic Inflammation, Tumor Progression, Invasion, and Metastasis. *Biomolecules.* 2016; 6(39).

Chen W, Zhang Z, Zhang S, Zhu P, Ko JK, Yung KK. MUC1: Structure, Function, and Clinic Application in Epithelial Cancers. *Int J Mol Sci.* 2021 Jun 18;22(12):6567.

Chirgwin JM, Schaefer IM, Rotwein PS, Piccini N, Gross KW, Naylor SL. Human renin gene is on chromosome 1. *Somat Cell Mol Genet.* 1984 Jul;10(4):415-21.

Christodoulou K, Tsingis M, Stavrou C, Eleftheriou A, Papapavlou P, Patsalis PC, Ioannou P, Pierides A, Constantinou Deltas C. Chromosome 1 localization of a gene for autosomal dominant medullary cystic kidney disease. *Hum Mol Genet.* 1998 May;7(5):905-11.

Cochran B, Kovačiková T, Hodaňová K, Živná M, Hnízda A, Niehaus AG, Bonnacaze A, Balasubraminiam G, Ceballos-Picot I, Hawfield A, Kidd K, Kmoch S, Bleyer AJ. Chronic tubulointerstitial kidney disease in untreated adenine phosphoribosyl transferase (APRT) deficiency: A case report. *Clin Nephrol.* 2018 Oct;90(4):296-301.

Connor TM, Hoer S, Mallett A, Gale DP, Gomez-Duran A, Posse V, Antrobus R, Moreno P, Sciacovelli M, Frezza C, Duff J, Sheerin NS, Sayer JA, Ashcroft M, Wiesener MS, Hudson G, Gustafsson CM, Chinnery PF, Maxwell PH. Mutations in mitochondrial DNA causing tubulointerstitial kidney disease. *PLoS Genet.* 2017 Mar 7;13(3):e1006620.

Cormican S, Connaughton DM, Kennedy C, Murray S, Živná M, Kmoch S, Fennelly NK, O'Kelly P, Benson KA, Conlon ET, Cavalleri G, Foley C, Doyle B, Dorman A, Little MA,

Lavin P, Kidd K, Bleyer AJ, Conlon PJ. Autosomal dominant tubulointerstitial kidney disease (ADTKD) in Ireland. *Ren Fail*. 2019 Nov;41(1):832-841.

Cormican S, Kennedy C, Connaughton DM, O'Kelly P, Murray S, Živná M, Kmoch S, Fennelly NK, Benson KA, Conlon ET, Cavalleri GL, Foley C, Doyle B, Dorman A, Little MA, Lavin P, Kidd K, Bleyer AJ, Conlon PJ. Renal transplant outcomes in patients with autosomal dominant tubulointerstitial kidney disease. *Clin Transplant*. 2020 Feb;34(2):e13783.

Dahan K, Devuyt O, Smaers M, Vertommen D, Loute G, Poux JM, Viron B, Jacquot C, Gagnadoux MF, Chauveau D, Büchler M, Cochat P, Cosyns JP, Mougenot B, Rider MH, Antignac C, Verellen-Dumoulin C, Pirson Y. A cluster of mutations in the UMOD gene causes familial juvenile hyperuricemic nephropathy with abnormal expression of uromodulin. *J Am Soc Nephrol*. 2003 Nov;14(11):2883-93.

Dalgaard OZ. Bilateral polycystic disease of the kidneys; a follow-up of two hundred and eighty-four patients and their families. *Acta Med Scand Suppl*. 1957;328:1-255.

de Haan A, van Eerde AM, Eijgelsheim M, Rump P, van der Zwaag B, Hennekam E, Živná M, Kmoch S, Bleyer AJ, Kidd K, Vogt L, Knoers NVAM, de Borst MH. Novel MUC1 variant identified by massively parallel sequencing explains interstitial kidney disease in a large Dutch family. *Kidney Int*. 2023 May;103(5):986-989.

Devuyt O, Knoers NV, Remuzzi G, Schaefer F; Board of the Working Group for Inherited Kidney Diseases of the European Renal Association and European Dialysis and Transplant Association. Rare inherited kidney diseases: challenges, opportunities, and perspectives. *Lancet*. 2014 May 24;383(9931):1844-59.

Devuyt O, Olinger E, Rampoldi L. Uromodulin: from physiology to rare and complex kidney disorders. *Nat Rev Nephrol*. 2017 Sep;13(9):525-544.

Duverger N, Ghalim N, Ailhaud G, Steinmetz A, Fruchart JC, Castro G. Characterization of apoA-IV-containing lipoprotein particles isolated from human plasma and interstitial fluid. *Arterioscler Thromb*. 1993 Jan;13(1):126-32.

Dvela-Levitt M, Kost-Alimova M, Emani M, Kohnert E, Thompson R, Sidhom EH, Rivadeneira A, Sahakian N, Roignot J, Papagregoriou G, Montesinos MS, Clark AR, McKinney D, Gutierrez J, Roth M, Ronco L, Elonga E, Carter TA, Gnirke A, Melanson M, Hartland K, Wieder N, Hsu JC, Deltas C, Hughey R, Bleyer AJ, Kmoch S, Živná M, Barešova V, Kota S, Schlondorff J, Heiman M, Alper SL, Wagner F, Weins A, Golub TR, Lander ES, Greka A. Small Molecule Targets TMED9 and Promotes Lysosomal Degradation to Reverse Proteinopathy. *Cell*. 2019 Jul 25;178(3):521-535.e23.

Eckardt KU, Alper SL, Antignac C, Bleyer AJ, Chauveau D, Dahan K, Deltas C, Hosking A, Kmoch S, Rampoldi L, Wiesener M, Wolf MT, Devuyt O; Kidney Disease: Improving

Global Outcomes. Autosomal dominant tubulointerstitial kidney disease: diagnosis, classification, and management--A KDIGO consensus report. *Kidney Int.* 2015 Oct;88(4):676-83.

Eckardt KU, Coresh J, Devuyst O, Johnson RJ, Köttgen A, Levey AS, Levin A. Evolving importance of kidney disease: from subspecialty to global health burden. *Lancet.* 2013 Jul 13;382(9887):158-69.

Elhassan EAE, Murray SL, Connaughton DM, Kennedy C, Cormican S, Cowhig C, Stapleton C, Little MA, Kidd K, Bleyer AJ, Živná M, Kmoch S, Fennelly NK, Doyle B, Dorman A, Griffin MD, Casserly L, Harris PC, Hildebrandt F, Cavalleri GL, Benson KA, Conlon PJ. The utility of a genetic kidney disease clinic employing a broad range of genomic testing platforms: experience of the Irish Kidney Gene Project. *J Nephrol.* 2022 Jul;35(6):1655-1665.

Elliott MD, Rasouly HM, Gharavi AG. Genetics of Kidney Disease: The Unexpected Role of Rare Disorders. *Annu Rev Med.* 2023 Jan 27;74:353-367.

Espino-Hernández M, Palma Milla C, Vara-Martín J, González-Granado LI. De novo SEC61A1 mutation in autosomal dominant tubulo-interstitial kidney disease: Phenotype expansion and review of literature. *J Paediatr Child Health.* 2021 Aug;57(8):1305-1307.

The European Polycystic Kidney Disease Consortium. The polycystic kidney disease 1 gene encodes a 14 kb transcript and lies within a duplicated region on chromosome 16. *Cell.* 1994 Jun 17;77(6):881-94. Erratum in: *Cell* 1995 Jun 30;81(7): following 1170. Erratum in: *Cell.* 1994 Aug 26;78(4):725.

Galen FX, Devaux C, Houot AM, Menard J, Corvol P, Corvol MT, Gubler MC, Mounier F, Camilleri JP. Renin biosynthesis by human tumoral juxtaglomerular cells. Evidences for a renin precursor. *J Clin Invest.* 1984 Apr;73(4):1144-55.

Gast C, Marinaki A, Arenas-Hernandez M, Campbell S, Seaby EG, Pengelly RJ, Gale DP, Connor TM, Bunyan DJ, Hodaňová K, Živná M, Kmoch S, Ennis S, Venkat-Raman G. Autosomal dominant tubulointerstitial kidney disease-UMOD is the most frequent non polycystic genetic kidney disease. *BMC Nephrol.* 2018 Oct 30;19(1):301.

Gendler SJ. MUC1, the renaissance molecule. *J Mammary Gland Biol Neoplasia.* 2001 Jul;6(3):339-53.

Gendler SJ, Burchell JM, Duhig T, Lamport D, White R, Parker M, Taylor-Papadimitriou J. Cloning of partial cDNA encoding differentiation and tumor-associated mucin glycoproteins expressed by human mammary epithelium. *Proc Natl Acad Sci U S A.* 1987 Sep;84(17):6060-4.

Gendler SJ, Cohen EP, Craston A, Duhig T, Johnstone G, Barnes D. The locus of the polymorphic epithelial mucin (PEM) tumour antigen on chromosome 1q21 shows a high frequency of alteration in primary human breast tumours. *Int J Cancer*. 1990 Mar 15;45(3):431-5.

Gendler SJ, Spicer AP, Lalani EN, Duhig T, Peat N, Burchell J, Pemberton L, Boshell M, Taylor-Papadimitriou J. Structure and biology of a carcinoma-associated mucin, MUC1. *Am Rev Respir Dis*. 1991 Sep;144(3 Pt 2):S42-7.

Goldman SH, Walker SR, Merigan TC Jr, Gardner KD Jr, Bull JM. Hereditary occurrence of cystic disease of the renal medulla. *N Engl J Med*. 1966 May 5;274(18):984-92.

Gribouval O, Gonzales M, Neuhaus T, Aziza J, Bieth E, Laurent N, Bouton JM, Feuillet F, Makni S, Ben Amar H, Laube G, Delezoide AL, Bouvier R, Dijoud F, Ollagnon-Roman E, Roume J, Joubert M, Antignac C, Gubler MC. Mutations in genes in the renin-angiotensin system are associated with autosomal recessive renal tubular dysgenesis. *Nat Genet*. 2005 Sep;37(9):964-8.

Gribouval O, Morinière V, Pawtowski A, Arrondel C, Sallinen SL, Saloranta C, Clericuzio C, Viot G, Tantau J, Blesson S, Cloarec S, Machet MC, Chitayat D, Thauvin C, Laurent N, Sampson JR, Bernstein JA, Clemenson A, Prieur F, Daniel L, Levy-Mozziconacci A, Lachlan K, Alessandri JL, Cartault F, Rivière JP, Picard N, Baumann C, Delezoide AL, Belar Ortega M, Chassaing N, Labrune P, Yu S, Firth H, Wellesley D, Bitzan M, Alfares A, Braverman N, Krogh L, Tolmie J, Gaspar H, Doray B, Majore S, Bonneau D, Triau S, Loirat C, David A, Bartholdi D, Peleg A, Brackman D, Stone R, DeBerardinis R, Corvol P, Michaud A, Antignac C, Gubler MC. Spectrum of mutations in the renin-angiotensin system genes in autosomal recessive renal tubular dysgenesis. *Hum Mutat*. 2012 Feb;33(2):316-26.

Groopman EE, Marasa M, Cameron-Christie S, Petrovski S, Aggarwal VS, Milo-Rasouly H, Li Y, Zhang J, Nestor J, Krithivasan P, Lam WY, Mitrotti A, Piva S, Kil BH, Chatterjee D, Reingold R, Bradbury D, DiVecchia M, Snyder H, Mu X, Mehl K, Balderes O, Fasel DA, Weng C, Radhakrishnan J, Canetta P, Appel GB, Bomback AS, Ahn W, Uy NS, Alam S, Cohen DJ, Crew RJ, Dube GK, Rao MK, Kamalakaran S, Copeland B, Ren Z, Bridgers J, Malone CD, Mebane CM, Dagaonkar N, Fellström BC, Haefliger C, Mohan S, Sanna-Cherchi S, Kiryluk K, Fleckner J, March R, Platt A, Goldstein DB, Gharavi AG. Diagnostic Utility of Exome Sequencing for Kidney Disease. *N Engl J Med*. 2019 Jan 10;380(2):142-151.

Hanisch FG, Müller S. MUC1: the polymorphic appearance of a human mucin. *Glycobiology*. 2000 May;10(5):439-49.

Harris PA, Taylor R, Thielke R, Payne J, Gonzalez N, Conde JG. Research electronic data capture (REDCap)--a metadata-driven methodology and workflow process for providing translational research informatics support. *J Biomed Inform*. 2009 Apr;42(2):377-81.

Hart TC, Gorry MC, Hart PS, Woodard AS, Shihabi Z, Sandhu J, Shirts B, Xu L, Zhu H, Barmada MM, Bleyer AJ. Mutations of the UMOD gene are responsible for medullary cystic kidney disease 2 and familial juvenile hyperuricaemic nephropathy. *J Med Genet.* 2002 Dec;39(12):882-92.

Hartmannová H, Piherová L, Tauchmannová K, Kidd K, Acott PD, Crocker JF, Oussedik Y, Mallet M, Hodaňová K, Stránecký V, Přistoupilová A, Barešová V, Jedličková I, Živná M, Sovová J, Hůlková H, Robins V, Vrbacký M, Pecina P, Kaplanová V, Houštek J, Mráček T, Thibeault Y, Bleyer AJ, Kmoch S. Acadian variant of Fanconi syndrome is caused by mitochondrial respiratory chain complex I deficiency due to a non-coding mutation in complex I assembly factor NDUFAF6. *Hum Mol Genet.* 2016 Sep 15;25(18):4062-4079.

Hildebrandt F, Otto E. Molecular genetics of nephronophthisis and medullary cystic kidney disease. *J Am Soc Nephrol.* 2000 Sep;11(9):1753-1761.

Hill NR, Fatoba ST, Oke JL, Hirst JA, O'Callaghan CA, Lasserson DS, Hobbs FD. Global Prevalence of Chronic Kidney Disease - A Systematic Review and Meta-Analysis. *PLoS One.* 2016 Jul 6;11(7):e0158765.

Hodanová K, Majewski J, Kublová M, Vyletal P, Kalbáčová M, Stibůrková B, Hůlková H, Chagnon YC, Lanouette CM, Marinaki A, Fryns JP, Venkat-Raman G, Kmoch S. Mapping of a new candidate locus for uromodulin-associated kidney disease (UAKD) to chromosome 1q41. *Kidney Int.* 2005 Oct;68(4):1472-82.

Imbert Y, Foulks GN, Brennan MD, Jumblatt MM, John G, Shah HA, Newton C, Pouranfar F, Young WW Jr. MUC1 and estrogen receptor alpha gene polymorphisms in dry eye patients. *Exp Eye Res.* 2009 Mar;88(3):334-8.

Janssen R, Kruit A, Grutters JC, Ruven HJ, Gerritsen WB, van den Bosch JM. The mucin-1 568 adenosine to guanine polymorphism influences serum Krebs von den Lungen-6 levels. *Am J Respir Cell Mol Biol.* 2006 Apr;34(4):496-9.

Johannesen KM, Iqbal S, Guazzi M, Mohammadi NA, Pérez-Palma E, Schaefer E, De Saint Martin A, Abiwarde MT, McTague A, Pons R, Piton A, Kurian MA, Ambegaonkar G, Firth H, Sanchis-Juan A, Deprez M, Jansen K, De Waele L, Briltra EH, Verbeek NE, van Kempen M, Fazeli W, Striano P, Zara F, Visser G, Braakman HMH, Haeusler M, Elbracht M, Vaheer U, Smol T, Lemke JR, Platzer K, Kennedy J, Klein KM, Au PYB, Smyth K, Kaplan J, Thomas M, Dewenter MK, Dinopoulos A, Campbell AJ, Lal D, Lederer D, Liao VWY, Ahring PK, Møller RS, Gardella E. Structural mapping of GABRB3 variants reveals genotype-phenotype correlations. *Genet Med.* 2022 Mar;24(3):681-693.

Kirby A, Gnirke A, Jaffe DB, Barešová V, Pochet N, Blumenstiel B, Ye C, Aird D, Stevens C, Robinson JT, Cabili MN, Gat-Viks I, Kelliher E, Daza R, DeFelice M, Hůlková H, Sovová J, Vyletal P, Antignac C, Guttman M, Handsaker RE, Perrin D, Steelman S, Sigurdsson S, Scheinman SJ, Sougnez C, Cibulskis K, Parkin M, Green T, Rossin E, Zody

MC, Xavier RJ, Pollak MR, Alper SL, Lindblad-Toh K, Gabriel S, Hart PS, Regev A, Nusbaum C, Knoch S, Bleyer AJ, Lander ES, Daly MJ. Mutations causing medullary cystic kidney disease type 1 lie in a large VNTR in MUC1 missed by massively parallel sequencing. *Nat Genet.* 2013 Mar;45(3):299-303.

Kiser RL, Wolf MT, Martin JL, Zalewski I, Attanasio M, Hildebrandt F, Klemmer P. Medullary cystic kidney disease type 1 in large Native-American kindred. *Am J Kidney Dis.* 2004 Oct;44(4):611-7.

Klee GG, Schreiber WE. MUC1 gene-derived glycoprotein assays for monitoring breast cancer (CA 15-3, CA 27.29, BR): are they measuring the same antigen? *Arch Pathol Lab Med.* 2004 Oct;128(10):1131-5.

Köttgen A, Hwang SJ, Larson MG, Van Eyk JE, Fu Q, Benjamin EJ, Dehghan A, Glazer NL, Kao WH, Harris TB, Gudnason V, Shlipak MG, Yang Q, Coresh J, Levy D, Fox CS. Uromodulin levels associate with a common UMOD variant and risk for incident CKD. *J Am Soc Nephrol.* 2010 Feb;21(2):337-44.

Kovesdy CP. Epidemiology of chronic kidney disease: an update 2022. *Kidney Int Suppl* (2011). 2022 Apr;12(1):7-11.

Kroiss S, Huck K, Berthold S, Rüschemdorf F, Scolari F, Caridi G, Ghiggeri GM, Hildebrandt F, Fuchshuber A. Evidence of further genetic heterogeneity in autosomal dominant medullary cystic kidney disease. *Nephrol Dial Transplant.* 2000 Jun;15(6):818-21.

Lancaster CA, Peat N, Duhig T, Wilson D, Taylor-Papadimitriou J, Gendler SJ. Structure and expression of the human polymorphic epithelial mucin gene: an expressed VNTR unit. *Biochem Biophys Res Commun.* 1990 Dec 31;173(3):1019-29.

Levin A, Tonelli M, Bonventre J, Coresh J, Donner JA, Fogo AB, Fox CS, Gansevoort RT, Heerspink HJL, Jardine M, Kasiske B, Köttgen A, Kretzler M, Levey AS, Luyckx VA, Mehta R, Moe O, Obrador G, Pannu N, Parikh CR, Perkovic V, Pollock C, Stenvinkel P, Tuttle KR, Wheeler DC, Eckardt KU; ISN Global Kidney Health Summit participants. Global kidney health 2017 and beyond: a roadmap for closing gaps in care, research, and policy. *Lancet.* 2017 Oct 21;390(10105):1888-1917.

Lingenhel A, Lhotta K, Neyer U, Heid IM, Rantner B, Kronenberg MF, König P, von Eckardstein A, Schober M, Dieplinger H, Kronenberg F. Role of the kidney in the metabolism of apolipoprotein A-IV: influence of the type of proteinuria. *J Lipid Res.* 2006 Sep;47(9):2071-9.

Macao B, Johansson DG, Hansson GC, Härd T. Autoproteolysis coupled to protein folding in the SEA domain of the membrane-bound MUC1 mucin. *Nat Struct Mol Biol.* 2006 Jan;13(1):71-6.

- Mary S, Boder P, Padmanabhan S, McBride MW, Graham D, Delles C, Dominiczak AF. Role of Uromodulin in Salt-Sensitive Hypertension. *Hypertension*. 2022 Nov;79(11):2419-2429.
- Massari PU, Hsu CH, Barnes RV, Fox IH, Gikas PW, Weller JM. Familial hyperuricemia and renal disease. *Arch Intern Med*. 1980 May;140(5):680-4.
- Mochizuki T, Lemmink HH, Mariyama M, Antignac C, Gubler MC, Pirson Y, Verellen-Dumoulin C, Chan B, Schröder CH, Smeets HJ, et al. Identification of mutations in the alpha 3(IV) and alpha 4(IV) collagen genes in autosomal recessive Alport syndrome. *Nat Genet*. 1994 Sep;8(1):77-81.
- Mongeau JG, Worthen HG. Nephronophthisis and medullary cystic disease. *Am J Med*. 1967 Sep;43(3):345-55.
- Morris BJ, Cantanzaro DF, Hardman J, Mesterovic N, Tellam J, Hort Y, Shine J. Human renin gene sequence, gene regulation and prorenin processing. *J Hypertens Suppl*. 1984 Dec;2(3):S231-3.
- Morris BJ, Smith DL. Prorenin and gene activation. *Can J Physiol Pharmacol*. 1991 Sep;69(9):1367-74.
- Muchmore AV, Decker JM. Uromodulin. An immunosuppressive 85-kilodalton glycoprotein isolated from human pregnancy urine is a high affinity ligand for recombinant interleukin 1 alpha. *J Biol Chem*. 1986 Oct 15;261(29):13404-7.
- Neumann HP, Zäuner I, Strahm B, Bender BU, Schollmeyer P, Blum U, Rohrbach R, Hildebrandt F. Late occurrence of cysts in autosomal dominant medullary cystic kidney disease. *Nephrol Dial Transplant*. 1997 Jun;12(6):1242-6.
- Nobakht N, Hanna RM, Al-Baghdadi M, Ameen KM, Arman F, Nobakht E, Kamgar M, Rastogi A. Advances in Autosomal Dominant Polycystic Kidney Disease: A Clinical Review. *Kidney Med*. 2020 Feb 22;2(2):196-208.
- Pajic P, Shen S, Qu J, May AJ, Knox S, Ruhl S, Gokcumen O. A mechanism of gene evolution generating mucin function. *Sci Adv*. 2022 Aug 26;8(34):eabm8757.
- Patton S, Gendler SJ, Spicer AP. The epithelial mucin, MUC1, of milk, mammary gland and other tissues. *Biochim Biophys Acta*. 1995 Dec 20;1241(3):407-23.
- Pennica D, Kohr WJ, Kuang WJ, Glaister D, Aggarwal BB, Chen EY, Goeddel DV. Identification of human uromodulin as the Tamm-Horsfall urinary glycoprotein. *Science*. 1987 Apr 3;236(4797):83-8.
- Persson PB. Renin: origin, secretion and synthesis. *J Physiol*. 2003 Nov 1;552(Pt 3):667-71.

Pook MA, Jeremiah S, Scheinman SJ, Povey S, Thakker RV. Localization of the Tamm-Horsfall glycoprotein (uromodulin) gene to chromosome 16p12.3-16p13.11. *Ann Hum Genet.* 1993 Oct;57(4):285-90.

Popp B, Ekici AB, Knaup KX, Schneider K, Uebe S, Park J, Bafna V, Meiselbach H, Eckardt KU, Schiffer M, Reis A, Kraus C, Wiesener M. Prevalence of hereditary tubulointerstitial kidney diseases in the German Chronic Kidney Disease study. *Eur J Hum Genet.* 2022 Dec;30(12):1413-1422.

Pujol Gualdo N; Estonian Biobank Research Team; Mägi R, Laisk T. Genome-wide association study meta-analysis supports association between MUC1 and ectopic pregnancy. *Hum Reprod.* 2023 Dec 4;38(12):2516-2525.

Rahn JJ, Shen Q, Mah BK, Hugh JC. MUC1 initiates a calcium signal after ligation by intercellular adhesion molecule-1. *J Biol Chem.* 2004 Jul 9;279(28):29386-90.

Rampoldi L, Caridi G, Santon D, Boaretto F, Bernascone I, Lamorte G, Tardanico R, Dagnino M, Colussi G, Scolari F, Ghiggeri GM, Amoroso A, Casari G. Allelism of MCKD, FJHN and GCKD caused by impairment of uromodulin export dynamics. *Hum Mol Genet.* 2003 Dec 15;12(24):3369-84.

Rampoldi L, Scolari F, Amoroso A, Ghiggeri G, Devuyst O. The rediscovery of uromodulin (Tamm-Horsfall protein): from tubulointerstitial nephropathy to chronic kidney disease. *Kidney Int.* 2011 Aug;80(4):338-47.

Reeders ST, Breuning MH, Davies KE, Nicholls RD, Jarman AP, Higgs DR, Pearson PL, Weatherall DJ. A highly polymorphic DNA marker linked to adult polycystic kidney disease on chromosome 16. *Nature.* 1985 Oct 10-16;317(6037):542-4.

Richmond JM, Kincaid-Smith P, Whitworth JA, Becker GJ. Familial urate nephropathy. *Clin Nephrol.* 1981 Oct;16(4):163-8.

Saeki N, Saito A, Choi IJ, Matsuo K, Ohnami S, Totsuka H, Chiku S, Kuchiba A, Lee YS, Yoon KA, Kook MC, Park SR, Kim YW, Tanaka H, Tajima K, Hirose H, Tanioka F, Matsuno Y, Sugimura H, Kato S, Nakamura T, Nishina T, Yasui W, Aoyagi K, Sasaki H, Yanagihara K, Katai H, Shimoda T, Yoshida T, Nakamura Y, Hirohashi S, Sakamoto H. A functional single nucleotide polymorphism in mucin 1, at chromosome 1q22, determines susceptibility to diffuse-type gastric cancer. *Gastroenterology.* 2011 Mar;140(3):892-902.

Scolari F, Puzzer D, Amoroso A, Caridi G, Ghiggeri GM, Maiorca R, Aridon P, De Fusco M, Ballabio A, Casari G. Identification of a new locus for medullary cystic disease, on chromosome 16p12. *Am J Hum Genet.* 1999 Jun;64(6):1655-60.

Schaeffer C, Izzi C, Vettori A, Pasqualetto E, Cittaro D, Lazarevic D, Caridi G, Gnutti B, Mazza C, Jovine L, Scolari F, Rampoldi L. Autosomal Dominant Tubulointerstitial Kidney

Disease with Adult Onset due to a Novel Renin Mutation Mapping in the Mature Protein. *Sci Rep.* 2019 Aug 12;9(1):11601.

Schaeffer C, Merella S, Pasqualetto E, Lazarevic D, Rampoldi L. Mutant uromodulin expression leads to altered homeostasis of the endoplasmic reticulum and activates the unfolded protein response. *PLoS One.* 2017 Apr 24;12(4):e0175970.

Schlevogt B, Schlieper V, Krader J, Schröter R, Wagner T, Weiland M, Zibert A, Schmidt HH, Bergmann C, Nedvetsky PI, Krahn MP. A SEC61A1 variant is associated with autosomal dominant polycystic liver disease. *Liver Int.* 2023 Feb;43(2):401-412.

Schubert D, Klein MC, Hassdenteufel S, Caballero-Oteyza A, Yang L, Proietti M, Bulashevskaya A, Kemming J, Kühn J, Winzer S, Rusch S, Fliegau M, Schäffer AA, Pfeffer S, Geiger R, Cavalié A, Cao H, Yang F, Li Y, Rizzi M, Eibel H, Kobbe R, Marks AL, Peppers BP, Hostoffer RW, Puck JM, Zimmermann R, Grimbacher B. Plasma cell deficiency in human subjects with heterozygous mutations in Sec61 translocon alpha 1 subunit (SEC61A1). *J Allergy Clin Immunol.* 2018 Apr;141(4):1427-1438.

Schweda F, Friis U, Wagner C, Skott O, Kurtz A. Renin release. *Physiology (Bethesda).* 2007 Oct;22:310-9.

Sielecki AR, Hayakawa K, Fujinaga M, Murphy ME, Fraser M, Muir AK, Carilli CT, Lewicki JA, Baxter JD, James MN. Structure of recombinant human renin, a target for cardiovascular-active drugs, at 2.5 Å resolution. *Science.* 1989 Mar 10;243(4896):1346-51.

Sikora J, Kmochová T, Mušálková D, Pohludka M, Příkryl P, Hartmannová H, Hodaňová K, Trešlová H, Nosková L, Mrázová L, Stránecký V, Lunová M, Jirsa M, Honsová E, Dasari S, McPhail ED, Leung N, Živná M, Bleyer AJ, Rychlík I, Ryšavá R, Kmoch S. A mutation in the SAA1 promoter causes hereditary amyloid A amyloidosis. *Kidney Int.* 2022 Feb;101(2):349-359.

Smith CH, Graham JB. Congenital Medullary Cysts of the Kidneys with Severe Refractory Anemia. *Am J Dis Child.* 1945;69(6):369-377.

Stavrou C, Pierides A, Zouvani I, Kyriacou K, Antignac C, Neophytou P, Christodoulou K, Deltas CC. Medullary cystic kidney disease with hyperuricemia and gout in a large Cypriot family: no allelism with nephronophthisis type 1. *Am J Med Genet.* 1998 May 1;77(2):149-54.

Stibůrková B, Majewski J, Sebesta I, Zhang W, Ott J, Kmoch S. Familial juvenile hyperuricemic nephropathy: localization of the gene on chromosome 16p11.2 and evidence for genetic heterogeneity. *Am J Hum Genet.* 2000 Jun;66(6):1989-94.

Swallow DM, Gendler S, Griffiths B, Kearney A, Povey S, Sheer D, Palmer RW, Taylor-Papadimitriou J. The hypervariable gene locus PUM, which codes for the tumour associated

epithelial mucins, is located on chromosome 1, within the region 1q21-24. *Ann Hum Genet.* 1987 Oct;51(4):289-94.

Tamm I, Horsfall FL Jr. A mucoprotein derived from human urine which reacts with influenza, mumps, and Newcastle disease viruses. *J Exp Med.* 1952 Jan;95(1):71-97.

Tamm I, Horsfall FL Jr. Characterization and separation of an inhibitor of viral hemagglutination present in urine. *Proc Soc Exp Biol Med.* 1950 May;74(1):106-8.

Taylor-Papadimitriou J, Peterson JA, Arklie J, Burchell J, Ceriani RL, Bodmer WF. Monoclonal antibodies to epithelium-specific components of the human milk fat globule membrane: production and reaction with cells in culture. *Int J Cancer.* 1981 Jul 15;28(1):17-21.

Thielemans R, Speeckaert R, Delrue C, De Bruyne S, Oyaert M, Speeckaert MM. Unveiling the Hidden Power of Uromodulin: A Promising Potential Biomarker for Kidney Diseases. *Diagnostics (Basel).* 2023 Sep 28;13(19):3077.

Trudu M, Schaeffer C, Riba M, Ikehata M, Brambilla P, Messa P, Martinelli-Boneschi F, Rastaldi MP, Rampoldi L. Early involvement of cellular stress and inflammatory signals in the pathogenesis of tubulointerstitial kidney disease due to UMOD mutations. *Sci Rep.* 2017 Aug 7;7(1):7383.

Turner JJ, Stacey JM, Harding B, Kotanko P, Lhotta K, Puig JG, Roberts I, Torres RJ, Thakker RV. UROMODULIN mutations cause familial juvenile hyperuricemic nephropathy. *J Clin Endocrinol Metab.* 2003 Mar;88(3):1398-401.

Tzen CY, Tsai JD, Wu TY, Chen BF, Chen ML, Lin SP, Chen SC. Tubulointerstitial nephritis associated with a novel mitochondrial point mutation. *Kidney Int.* 2001 Mar;59(3):846-54.

Van Nieuwenhove E, Barber JS, Neumann J, Smeets E, Willemsen M, Pasciuto E, Prezzemolo T, Lagou V, Seldeslachts L, Malengier-Devlies B, Metzemaekers M, Haßdenteufel S, Kerstens A, van der Kant R, Rousseau F, Schymkowitz J, Di Marino D, Lang S, Zimmermann R, Schlenner S, Munck S, Proost P, Matthys P, Devalck C, Boeckx N, Claessens F, Wouters C, Humblet-Baron S, Meyts I, Liston A. Defective Sec61 α underlies a novel cause of autosomal dominant severe congenital neutropenia. *J Allergy Clin Immunol.* 2020 Nov;146(5):1180-1193.

Viering D, Schlingmann KP, Hureaux M, Nijenhuis T, Mallett A, Chan MMY, van Beek A, van Eerde AM, Coulibaly JM, Vallet M, Decramer S, Pelletier S, Klaus G, Kömhoff M, Beetz R, Patel C, Shenoy M, Steenbergen EJ, Anderson G, Bongers EMHF, Bergmann C, Panneman D, Rodenburg RJ, Kleta R, Houillier P, Konrad M, Vargas-Poussou R, Knoers NVAM, Bockenbauer D, de Baaij JHF; Genomics England Research Consortium. Gitelman-

Like Syndrome Caused by Pathogenic Variants in mtDNA. *J Am Soc Nephrol*. 2022 Feb;33(2):305-325.

Vivante A, Hildebrandt F. Exploring the genetic basis of early-onset chronic kidney disease. *Nat Rev Nephrol*. 2016 Mar;12(3):133-46..

Vylet'al P, Kidd K, Ainsworth HC, Springer D, Vrbacká A, Přistoupilová A, Hughey RP, Alper SL, Lennon N, Harrison S, Harden M, Robins V, Taylor A, Martin L, Howard K, Bitar I, Langefeld CD, Barešová V, Hartmannová H, Hodaňová K, Zima T, Živná M, Kmoch S, Bleyer AJ. Plasma Mucin-1 (CA15-3) Levels in Autosomal Dominant Tubulointerstitial Kidney Disease due to MUC1 Mutations. *Am J Nephrol*. 2021;52(5):378-387.

Vylet'al P, Kublová M, Kalbácová M, Hodanová K, Baresová V, Stibůrková B, Sikora J, Hůlková H, Zivný J, Majewski J, Simmonds A, Fryns JP, Venkat-Raman G, Elleder M, Kmoch S. Alterations of uromodulin biology: a common denominator of the genetically heterogeneous FJHN/MCKD syndrome. *Kidney Int*. 2006 Sep;70(6):1155-69.

Watson S, Padala SA, Hashmi MF, et al. Alport Syndrome. [Updated 2023 Aug 14]. In: *StatPearls* [Internet]. Treasure Island (FL): StatPearls Publishing; 2024 Jan-. Available from: <https://www.ncbi.nlm.nih.gov/books/NBK470419/>

Weinberg RB, Dantzker C, Patton CS. Sensitivity of serum apolipoprotein A-IV levels to changes in dietary fat content. *Gastroenterology*. 1990 Jan;98(1):17-24.

Witten VH, Sulzberger MB, Zimmerman EH, Shapiro AJ. A therapeutic assay of topically applied 9 alpha-fluorohydrocortisone acetate in selected dermatoses. *J Invest Dermatol*. 1955 Jan;24(1):1-4.

Wolf MT, Mucha BE, Attanasio M, Zalewski I, Karle SM, Neumann HP, Rahman N, Bader B, Baldamus CA, Otto E, Witzgall R, Fuchshuber A, Hildebrandt F. Mutations of the Uromodulin gene in MCKD type 2 patients cluster in exon 4, which encodes three EGF-like domains. *Kidney Int*. 2003 Nov;64(5):1580-7.

Xu X, Eales JM, Akbarov A, Guo H, Becker L, Talavera D, Ashraf F, Nawaz J, Pramanik S, Bowes J, Jiang X, Dormer J, Denniff M, Antczak A, Szulinska M, Wise I, Prestes PR, Glyda M, Bogdanski P, Zukowska-Szczehowska E, Berzuini C, Woolf AS, Samani NJ, Charchar FJ, Tomaszewski M. Molecular insights into genome-wide association studies of chronic kidney disease-defining traits. *Nat Commun*. 2018 Nov 22;9(1):4800.

Zikánová M, Wahezi D, Hay A, Stibůrková B, Pitts C 3rd, Mušálková D, Škopová V, Barešová V, Soucková O, Hodanová K, Živná M, Stránecký V, Hartmannová H, Hnízda A, Bleyer AJ, Kmoch S. Clinical manifestations and molecular aspects of phosphoribosylpyrophosphate synthetase superactivity in females. *Rheumatology (Oxford)*. 2018 Jul 1;57(7):1180-1185.

Živná M, Hůlková H, Matignon M, Hodanová K, Vyleťal P, Kalbáčová M, Baresová V, Sikora J, Blazková H, Živný J, Ivánek R, Stránecký V, Sovová J, Claes K, Lerut E, Fryns JP, Hart PS, Hart TC, Adams JN, Pawtowski A, Clemessy M, Gasc JM, Gübler MC, Antignac C, Elleder M, Kapp K, Grimbert P, Bleyer AJ, Kmoch S. Dominant renin gene mutations associated with early-onset hyperuricemia, anemia, and chronic kidney failure. *Am J Hum Genet.* 2009 Aug;85(2):204-13.

Živná M, Kidd KO, Barešová V, Hůlková H, Kmoch S, Bleyer AJ Sr. Autosomal dominant tubulointerstitial kidney disease: A review. *Am J Med Genet C Semin Med Genet.* 2022 Sep;190(3):309-324.

Živná M, Kidd K, Přistoupilová A, Barešová V, DeFelice M, Blumenstiel B, Harden M, Conlon P, Lavin P, Connaughton DM, Hartmannová H, Hodaňová K, Stránecký V, Vrbacká A, Vyleťal P, Živný J, Votruba M, Sovová J, Hůlková H, Robins V, Perry R, Wenzel A, Beck BB, Seeman T, Viklický O, Rajnochová-Bloudíčková S, Papagregoriou G, Deltas CC, Alper SL, Greka A, Bleyer AJ, Kmoch S. Noninvasive Immunohistochemical Diagnosis and Novel MUC1 Mutations Causing Autosomal Dominant Tubulointerstitial Kidney Disease. *J Am Soc Nephrol.* 2018 Sep;29(9):2418-2431.

3. Summary and Conclusions

Within this research framework [Figure 1], I have been able to carry out the specific aims of my doctoral programme:

1. To more accurately determine the prevalence of ADTKD by expanding outreach to families with this condition.

As part of my work, I developed and maintained websites to attract patients to our research. I developed a system for collecting laboratory samples from all over the world, isolating DNA, and preparing genotyping.

- I developed the REDCap database, which includes 1441 data elements.
- The current ADTKD registry has captured data on 1019 patients with ADTKD-*UMOD*, 930 patients with ADTKD-*MUC1* and 130 patients with ADTKD-*REN*.

- 25% of ADTKD families are direct family referrals.
- We have also established a large network of collaborators in the USA, European Union, United Kingdom, Canada, Australia, and South America.
- We work with 132 collaborators, who have provided over 1800 samples and/or clinical information for already diagnosed patients to increase our collective ADTKD registry by 457 ADTKD-*MUC1* patients, 363 ADTKD-*UMOD* patients and 102 ADTKD-*REN*.

2. To classify families with ADTKD genetically and identify new genetic causes of ADTKD.

- We analyzed the outcomes of 275 families referred with clinical features of ADTKD and have final genotyping results for *UMOD*, *MUC1*, *REN*, and *SEC61A1*. families (63%) were diagnosed with a type of ADTKD (*UMOD* n=98, *MUC1* n=65, *REN* n=7, and *SEC61A1* n=1).
- We have identified pathogenic variants in *APOA4* as a new cause of inherited kidney disease in five families.

3. To expand existing knowledge of ADTKD pathophysiology.

- Development of an *in-vitro* score based upon how retainment of aberrant mUMOD in the endoplasmic reticulum of cells transfected with the pathogenic variants compared to control/wild type UMOD. The score ranges from 1 (mild, little aberrant mUMOD retained) to 4 (severe, more aberrant mUMOD retained) and correlated significantly with age of ESKD in patients with each evaluated *UMOD* pathogenic variant.

- Identification of distinct cellular pathology in *ADTKD-REN* dependent upon location of the *REN* pathogenic variant. These distinct pathologies correlate to variability in clinical presentation, with pathogenic variants in the signal peptide being more severe as the aberrant peptide is unable to localize to the endoplasmic reticulum, pathogenic variants in the pro-peptide have an intermediate phenotype where the aberrant *REN* is retained in endoplasmic reticulum-Golgi intermediate compartment and reduced secretion of prorenin and mature *REN*, and pathogenic variants in the mature *REN* have a mild pathology with aberrant *REN* retained in ER, which prevents secretion of *REN* and prorenin.
- *ADTKD-MUC1* – we contributed to identification of retention of *MUC1*-fs in ERGIC due to interaction with quality control protein *TMED9* in patient kidney biopsies.
- *ADTKD-SEC61A1* – we found that mutations in *SEC61A1* in patients with *ADTKD* phenotype result in aberrant translocation capacity and mislocalization of mutated *SEC61A1* into the Golgi. It may affect processing and maturation process of all proteins with signal peptide targets to ER, such as *UMOD*, *REN* or *MUC1*.

4. To better characterize *ADTKD* clinically and identify factors associated with CKD progression.

- We described large cohorts of patients genotyped with *ADTKD-UMOD* (249 families and 722 individuals), *ADTKD-REN* (30 families and 111 individuals).
- We clinically evaluated a large cohort patients genotyped with *ADTKD-UMOD* (n=216) and *ADTKD-MUC1* (n=93).

- In ADTKD-*UMOD*, male gender, parent age of ESKD, family mean age of ESKD, and mother age of ESKD were predictive of disease progression.
 - The following genetic factors were not predictive of disease progression: rs4293393 genotype, mUMOD type, and mUMOD domain.
 - The following clinical factors were not predictive of disease progression: weight, BMI, smoking status, and presence of gout.
- Comparing clinical characteristics of patients with ADTKD-*UMOD* and ADTKD-*MUC1* identified gout is more prominent in ADTKD-*UMOD* patients and age of ESKD is younger in ADTKD-*MUC1* patients.
- In ADTKD-*REN*, clinical presentation of patients including age at presentation, anemia as a child, presence of gout, and age of ESKD is significantly impacted by location of the pathogenic variant within *REN*.
- Our current ADTKD registry contains 7,478 longitudinal serum creatinine values for 696 patients that is paired with additional clinical and genetic data ready for analysis and disease progression modeling.

5. To identify novel *MUC1* pathogenic variants in suspected ADTKD-*MUC1* families who tested negative for the cytosine duplication that commonly causes ADTKD-*MUC1*.

- We developed new diagnostic methods for detection of the MUC1-fs protein that leads to ADTKD-*MUC1* (smears, immunohistochemical detection of MUC1-fs in kidney biopsy, PacBio sequencing, MUC1 ELISA, and CA15-3)
- Using MUC1-fs screening and subsequent sequencing, we identified five novel *MUC1* VNTR pathogenic variants were identified: a +A insertion, +G insertion,

+16 base pair duplication, -C deletion +AT insertion, and another +C duplication found after a four-cytosine sequence.

- Two families with MUC1 pathogenic variants have been identified by whole-exome sequencing. One with a novel 25bp duplication and one with a +C duplication.
- Using a new PacBio workflow we have identified an additional 10 families with rare MUC1 pathogenic variants.

ADTKD is being increasingly recognized as a cause of inherited kidney disease and testing for pathogenic variants in genes that we initially identified as causative (*UMOD*, *REN*, and *MUC1*) is now available. There remain undiagnosed families in whom other genetic causes are likely to exist. We are working with newer techniques to identify these genes. We also continue to characterize these conditions clinically and pathophysiologically. Our next step is to identify new therapies for these conditions, based on the clinical and pathophysiologic findings we described.

4. Results

4.1 Outcomes of patient self-referral for the diagnosis of several rare inherited kidney diseases.

Bleyer AJ, **Kidd K**, Robins V, Martin L, Taylor A, Santi A, Tsoumas G, Hunt A, Swain E, Abbas M, Akinbola E, Vidya S, Moossavi S, Bleyer AJ Jr, Živná M, Hartmannová H, Hodaňová K, Vyleťal P, Votruba M, Harden M, Blumenstiel B, Greka A, Knoch S.

Genet Med. 2020 Jan;22(1):142-149.



Outcomes of patient self-referral for the diagnosis of several rare inherited kidney diseases

Anthony J. Bleyer, MD^{1,2,3}, Kendrah Kidd, MS^{1,2}, Victoria Robins, RN, BSN¹, Lauren Martin, MSW¹, Abbigail Taylor, BS¹, Annie Santi, MD⁴, Georgeanna Tsoumas, BS⁵, Alese Hunt, MD⁶, Elizabeth Swain, BS⁷, Marwan Abbas, MD⁸, Ebum Akinbola, MD⁹, Sri Vidya, MD¹⁰, Shahriar Moossavi, MD¹, Anthony J. Bleyer Jr., MD¹, Martina Živná, PhD², Hana Hartmannová, PhD², Kateřina Hodaňová, PhD², Petr Vyleťal, PhD², Miroslav Votruba, BS², Maegan Harden, PhD³, Brendan Blumenstiel, PhD³, Anna Greka, MD, PhD^{3,11,12} and Stanislav Kmoch, PhD^{1,2,3}

Purpose: To evaluate self-referral from the Internet for genetic diagnosis of several rare inherited kidney diseases.

Methods: Retrospective study from 1996 to 2017 analyzing data from an academic referral center specializing in autosomal dominant tubulointerstitial kidney disease (ADTKD). Individuals were referred by academic health-care providers (HCPs) nonacademic HCPs, or directly by patients/families.

Results: Over 21 years, there were 665 referrals, with 176 (27%) directly from families, 269 (40%) from academic HCPs, and 220 (33%) from nonacademic HCPs. Forty-two (24%) direct family referrals had positive genetic testing versus 73 (27%) families from academic HCPs and 55 (25%) from nonacademic HCPs ($P = 0.72$). Ninety-nine percent of direct family contacts were white and resided in zip code locations with a mean median income of $\$77,316 \pm 34,014$ versus US median income $\$49,445$.

Conclusion: Undiagnosed families with Internet access bypassed their physicians and established direct contact with an academic center specializing in inherited kidney disease to achieve a diagnosis. Twenty-five percent of all families diagnosed with ADTKD were the result of direct family referral and would otherwise have been undiagnosed. If patients suspect a rare disorder that is undiagnosed by their physicians, actively pursuing self-diagnosis using the Internet can be successful. Centers interested in rare disorders should consider improving direct access to families.

Genetics in Medicine (2020) 22:142–149; <https://doi.org/10.1038/s41436-019-0617-8>

Keywords: internet; rare disease; autosomal dominant tubulointerstitial kidney disease; uromodulin; mucin-1

INTRODUCTION

Poor access to health care often refers to individuals in need of care who cannot obtain it for socioeconomic reasons. Individuals with rare disorders also have difficulty accessing proper care, but their obstacles to care are unique. While it is estimated that 10% of individuals suffer from a rare disease,¹ each disease is unique, preventing a common pathway to diagnosis. Often, the patient's primary physician is unaware of the correct diagnosis and the presentation of a rare disorder. Other factors preventing a physician's search for a diagnosis include time constraints from a high patient caseload, a simple lack of interest, or a belief that securing the diagnosis will not alter the patient's treatment plan. Specialists likewise

may be unable to identify the disorder and do not explore further. If a researcher with expertise is identified, their practice may be very far from the patient, possibly on another continent. The plight of parents of children with undiagnosed, rare disorders has been described in the lay literature.^{2,3} Even physician-parents may be unsure how to pursue a diagnosis.⁴ While there are anecdotal reports of families finding a diagnosis when their physicians were unable,⁵ there have been no systematic investigations of individuals with rare disorders and their path to diagnosis.

The Internet has become increasingly important in the self-diagnosis of health conditions,^{6,7} and focused information on rare disorders may lead to increasing diagnoses of these

¹Section on Nephrology, Wake Forest School of Medicine, Winston-Salem, NC, USA; ²Research Unit for Rare Diseases, Department of Pediatrics and Adolescent Medicine, First Faculty of Medicine, Charles University, Prague, Czech Republic; ³Broad Institute of Harvard Medical School and Massachusetts Institute of Technology, Cambridge, MA, USA; ⁴Department of Anesthesiology, University of Pennsylvania School of Medicine, Philadelphia, PA, USA; ⁵Campbell University School of Osteopathic Medicine, Lillington, NC, USA; ⁶Children's Health of Carolina Pediatrics, Lumberton, NC, USA; ⁷West Virginia University School of Medicine, Morgantown, WV, USA; ⁸Giza Renal Center, Giza, Egypt; ⁹East Carolina University, Brody School of Medicine, Greenville, NC, USA; ¹⁰Peace Health Southwest Medical Center, Vancouver, WA, USA; ¹¹Division of Nephrology and Vascular Biology Research Center, Beth Israel Deaconess Medical Center, Boston, MA, USA; ¹²Brigham and Women's Hospital and Harvard Medical School, Boston, MA, USA.
Correspondence: Anthony J. Bleyer (ableyer@wakehealth.edu)

Submitted 29 March 2019; accepted: 11 July 2019
Published online: 24 July 2019

conditions. The Internet provides the patient with a rare disorder the opportunity to find the rare specialist interested in this disorder.

Background

Since 1999, our group has studied three rare genetic conditions that result in autosomal dominant tubulointerstitial kidney disease (ADTKD).⁸ The cardinal manifestations of these disorders include autosomal dominant inheritance of chronic kidney disease and a bland urinary sediment. Autosomal dominant inheritance results in many affected family members. Patients proceed to end-stage kidney disease requiring a kidney transplant or dialysis between the third and seventh decades. ADTKD-*MUC1* (OMIM 174000) is due to pathogenic variants in the *MUC1* gene and has no other associated symptoms.⁹ ADTKD-*UMOD* (OMIM 162000, 603860) is caused by pathogenic variants in the *UMOD* gene¹⁰ encoding uromodulin and is associated with a high prevalence of gout. ADTKD-*REN* (OMIM 613092) is caused by pathogenic variants in the gene encoding renin¹¹ and is associated with childhood anemia, gout, and hyperkalemia. These conditions present a diagnostic challenge because clinical findings are nonspecific, and the conditions are rare, recently identified, and not well known to nephrologists.

In 1999, there were fewer than ten US families with ADTKD described in the literature. After identification of the genetic cause of ADTKD-*UMOD*¹⁰ in 2002, a concerted attempt was made to identify as many ADTKD families as possible, communicating not only with health-care providers (HCPs), but also directly with families through Internet webpages.¹² In 2009, pathogenic variants in *REN*¹¹ and in 2014 pathogenic variants in *MUC1*⁹ were identified as causes of ADTKD. Due to complexities in sequencing *MUC1*, the Broad Institute is the only laboratory in the US that provides approved clinical testing for ADTKD-*MUC1*.¹³ All samples tested at the Broad Institute are first received and processed at Wake Forest School of Medicine. Thus, this investigation included all individuals in the US who underwent clinical genetic testing for ADTKD-*MUC1*.

The purpose of this analysis was to determine whether providing families with suspected rare disorders direct access to a research team through the Internet would result in genetic diagnoses of ADTKD and to compare direct access to families with indirect access to genetic testing through HCPs. As there was no diagnostic testing for these disorders prior to gene identification and we were the primary clinical academic center in the United States interested in and actively trying to identify families with these disorders, we were also able to characterize the natural history of how rare conditions are diagnosed after they are definitively characterized.

MATERIALS AND METHODS

Recruitment

The following multifaceted approach was used to educate and generate potential referrals: publication of articles,¹⁴ reviews,¹⁵

and a Kidney Disease: Improving Global Outcomes (KDIGO) consensus report,¹⁶ presentations at national meetings and invited lectures at academic centers; and publication in other venues, including GeneReviews[®], Renal and Urology News[®], and the medical information resource UpToDate[®]. In 2003, 1000 letters were mailed to US nephrologists requesting referral of any families with a suspected diagnosis of ADTKD. Several times over the last decade, Wake Forest School of Medicine sent brochures that included articles on ADTKD to US nephrologists. To encourage affected individuals or their families to contact us directly, a webpage was created.¹² Information was also provided through the National Organization of Rare Disorders.¹⁷

Family evaluation

UMOD and *REN* genetic analysis was performed by commercial laboratories or the laboratory of S.K.¹⁵ Genetic testing for ADTKD-*MUC1* has previously been described.¹³

Figures 1, S1, S2, and S3 provide flow diagrams of the evaluation process. All referrals were evaluated by the lead author. The study did not include data on bulk shipment of samples specifically for *MUC1* genetic analysis from international centers specializing in renal genetics. For HCP referrals, the HCP would provide patient contact information if the patient was agreeable. In some cases, a clinical diagnosis other than ADTKD was made (either before or after negative genetic testing), and the patients were referred for genetic testing elsewhere. If agreeable, patients were consented and arrangements were made for a local laboratory to obtain a blood sample for genetic analysis at no cost to the patient. If patients did not provide consent or provide blood samples after several reminders by email and phone over one year, they were considered to have declined participation. In all cases, genetic testing was provided free to patients. The characteristics of the person initially referred by HCPs or the first clinically affected family member who agreed to participate are described. Median income according to zip code was obtained from 2010 US Census data.¹⁸

Study data were collected and managed using REDCap electronic data capture tools hosted at Wake Forest School of Medicine.¹⁹ REDCap is a secure, web-based, National Institutes of Health (NIH)-sponsored application that supports confidential data capture for research studies.

This study was approved by the institutional review boards of Wake Forest School of Medicine; the First Faculty of Medicine, Charles University (Prague, Czech Republic); and the Broad Institute of MIT and Harvard (Cambridge, MA) and adhered to the Declaration of Helsinki.

Statistical analysis

Statistical analysis was performed with SAS statistical programming (Cary, NC). Chi-squared testing was used to compare the three referral groups. For continuous variables, a general linear model was created, with type III sums of squares reported and the direct family referral group selected as the reference group.

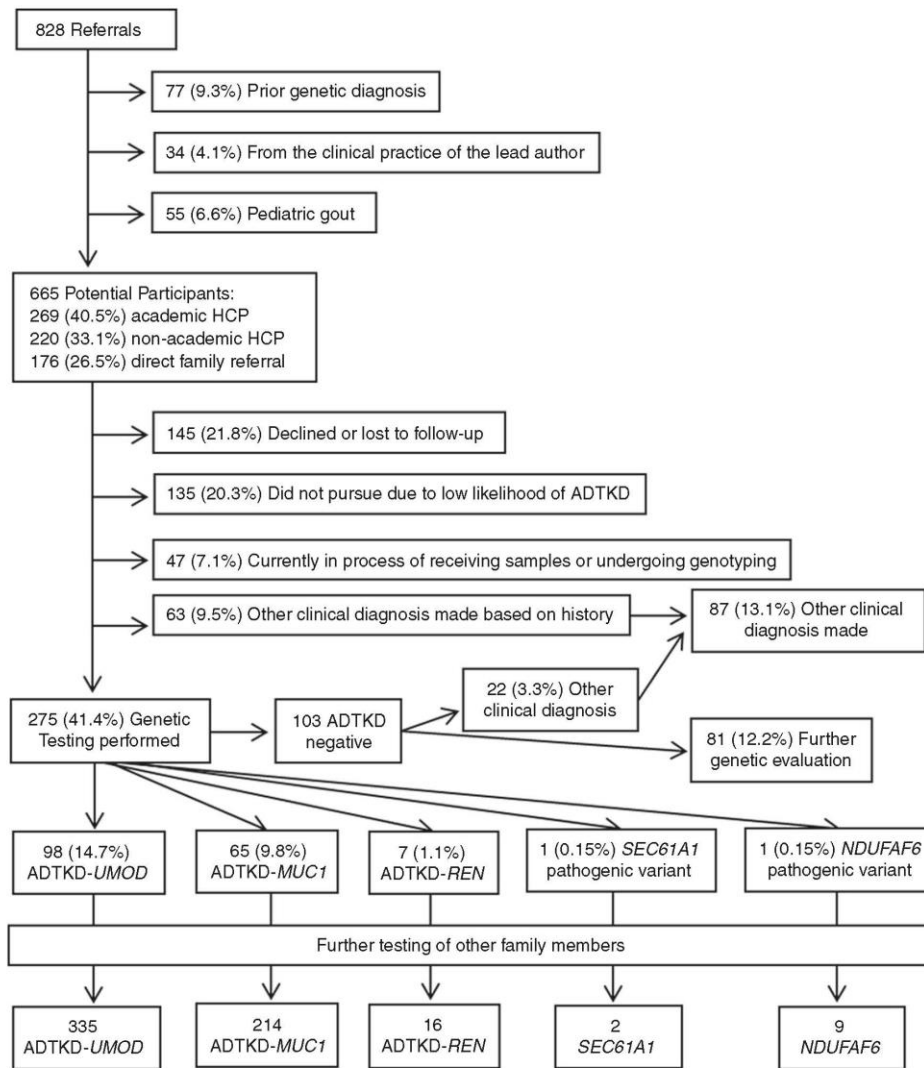


Fig. 1 Flow diagram of all referrals for evaluation for autosomal dominant tubulointerstitial kidney disease (ADTKD). Flow diagram of 828 family referrals for ADTKD evaluation. HCP health-care provider.

RESULTS

Over 21 years, there were 828 referrals. There were 77 individuals (9%) who already had a genetic diagnosis, 34 individuals (4%) referred directly from the first author's clinical practice, and 52 (6.3%) referrals specifically for pediatric gout. These three groups were excluded from further analysis. The remaining 665 referrals included 269 (41%) from HCPs at academic institutions, 220 (33%) from HCPs at nonacademic institutions, and 176 (27%) direct family referrals, defined as an affected or unaffected member of a family who does not have a known diagnosis of inherited disease contacting us through our website due to concerns

that they might have ADTKD, without the guidance or assistance from their health-care provider. Eight (1%) referrals from family members who were also physicians were included in the direct family referral group.

Of the 489 HCP referrals, 408 (83%) were from nephrologists, 46 (9%) non-nephrologist physicians, 30 (6%) geneticists or genetics counselors, and 5 (1%) HCPs not classified to other groups. There were 37 HCPs who referred 2 families, and 22 HCPs who referred 3 or more families. Referral sources are listed in Table S1. Multiple avenues led to referrals. Despite increasing availability of electronic media, 252 (52%) referrals were the result of some form of personal

contact, of which 97 (20%) were through personal acquaintance with the lead author, 96 (20%) were at the recommendation of a colleague, and 59 (12%) resulted from personal contact at meetings or lectures. There were 103 (21%) referrals via the Internet, including UpToDate® and GeneReviews®. There were 370 (76%) referrals from the United States, with 26 (5%) from Canada and 14 (3%) from Australia.

Of the 176 direct family referrals, 116 (66%) of the initial contacts were female, and 108 (61%) were affected personally. Of unaffected individuals referring their family, 27 (24%) were parents and 14 (13%) were spouses, with 46 (41%) unknown. There were 134 (76%) referrals from the United States, 7 (4%) from India, and 4 (2%) from Canada, with 2 or fewer referrals from 19 countries. All direct family referrals were through our website, except for one family that learned of our research through the Facebook page of an affected individual.

A higher number of affected family members could be a catalyst for trying to establish a diagnosis, especially in the case of direct family referrals. Therefore, the number of known, clinically affected individuals in each family was analyzed according to referral group. The number of affected family members was similar between groups (see Table S2), with 22% of direct family referrals having greater than five affected family members versus 25% for nonacademic HCPs and 28% for academic HCPs ($P = 0.17$).

Table 1 shows outcomes versus referral type. Thirty-one percent of direct family referrals were not pursued due to low likelihood of ADTKD versus 18% for academic HCP and 15% for nonacademic HCP referrals ($P = 0.0003$). Twenty-seven percent of nonacademic HCP and 22% of academic HCP referrals declined participation versus 17% of direct family referrals ($P = 0.04$). Twenty-four percent of direct family referrals underwent genetic testing that resulted in a diagnosis of ADTKD-*UMOD*/*MUC1*/*REN* versus 27% of academic HCP and 25% of nonacademic HCP referrals ($P = 0.72$). Two referrals from nonacademic providers led to the

identification of other new genetic causes of kidney disease.^{20,21} Heterozygous loss-of-function *SEC1A1* missense variants resulted in chronic tubulointerstitial kidney disease, congenital anemia, and pre- and postnatal growth retardation in one family and chronic kidney disease, anemia, and neutropenia in another family.²⁰ *NDUFA6* missense variants are responsible for autosomal recessive Fanconi syndrome associated with chronic kidney disease and progressive pulmonary fibrosis.²¹ Further testing of other family members (see Table S3) from direct family referrals resulted in the identification of 81 individuals with ADTKD-*UMOD*, 32 individuals with ADTKD-*MUC1*, and 3 with ADTKD-*REN*. Direct family referral resulted in the diagnosis of 116 of 565 (21%) individuals from all families identified with ADTKD. These families would have remained undiagnosed if family members had not independently sought a diagnosis on the Internet.

Characteristics of the initial contacts from direct family referrals who underwent sample collection (see Table 2) included a high proportion of white race, female gender, and higher median income by zip code. Of direct family referrals, 99% were white versus 93% from academic and 92% of nonacademic referrals ($P = 0.045$). Six (5%) academic HCP referrals were African American families versus 0 for both nonacademic HCPs and direct family referrals. The median income by zip code was substantially higher for direct family referrals ($\$77,316 \pm 34,014$ versus $\$65,301 \pm 29,741$ academic [$P = 0.04$] and $\$63,934 \pm 24,403$ nonacademic [$P = 0.03$]). Most individuals were referred with very advanced kidney disease, with 93% having an estimated glomerular filtration rate <45 ml/min/1.73 m² or on dialysis/transplanted.

Figures 2 and 3, Table S4, and Figs. S4, S5, S6, and S7 display the temporal and geographic distribution of referrals. While genetic testing was available for one form of ADTKD as early as 2002, referrals have continued to increase over time. Both patient and academic referrals from Internet sources increased in approximately 2009. Despite increasing Internet

Table 1 Outcomes according to referral type

	Direct family referrals ^a	Academic HCP ^a	Nonacademic HCP ^a	Total ^a	<i>P</i> value
Declined participation or lost to follow-up	29 (16.5)	57 (21.2)	59 (26.8)	145 (21.8)	0.04
Genetic diagnosis not pursued due to low likelihood of ADTKD	54 (30.7)	48 (17.8)	33 (15.0)	135 (20.3)	0.0003
In progress	7 (4.0)	21 (7.8)	19 (8.6)	47 (7.1)	0.16
ADTKD- <i>MUC1</i>	11 (6.3)	36 (13.4)	18 (8.2)	65 (9.8)	0.03
ADTKD- <i>UMOD</i>	30 (17.1)	33 (12.3)	35 (15.9)	98 (14.7)	0.32
ADTKD- <i>REN</i>	1 (0.6)	4 (1.5)	2 (0.9)	7 (1.1)	0.63
Genetic testing negative for ADTKD; pursuing other genes	19 (10.8)	32 (11.9)	28 (12.7)	79 (11.9)	0.84
Other clinical diagnosis	25 (14.2)	38 (14.1)	24 (10.9)	87 (13.1)	0.45
<i>SEC1A1</i> pathogenic variant	0	0	1 (0.45)	1 (0.15)	0.36
<i>NDUFA6</i> pathogenic variant	0	0	1 (0.45)	1 (0.15)	0.36
Total	176 (26.5)	269 (40.5)	220 (33.1)	665 (100)	

ADTKD autosomal dominant tubulointerstitial kidney disease.

^aData shown as number (%).

Table 2 Characteristics of first affected contact in families who underwent sample collection for the study

	Direct family referrals	Academic HCP	Nonacademic HCP	P value
N	68	120	101	
Gender (% male)	40 (58.8)	63 (52.5)	52 (51.5)	0.6
Race (% white)	67 (98.5)	111 (92.5)	93 (92.1)	0.045
Age (years)	47.9 ± 15.8 ^a	43.7 ± 17.2	44.7 ± 14.6	
End-stage kidney disease at referral (%)	32 (18.2)	47 (17.5)	38 (17.3)	0.97
Estimated glomerular filtration rate (mL/min/1.73 m ²) ^b	14.8 ± 20.1 ^c	22.4 ± 27.1	24.3 ± 26.7	
US referrals (%)	134 (76.1)	191 (71.0)	179 (81.4)	0.03
Mean median income by zip code (\$)	77,316 ± 34,014 ^d	65,301 ± 29,741	63,934 ± 24,403	

HCP health-care provider.

^aThere were no statistical differences between groups.

^bEstimated glomerular filtration rate defined as 0 mL/min/1.73 m² for individuals with end-stage kidney disease at the time of referral.

^cThe mean estimated glomerular filtration rate was significantly different for direct family referrals versus nonacademic referrals ($P = 0.03$), but not significantly different versus academic referrals ($P = 0.08$).

^dMedian income was significantly different for direct family referrals versus nonacademic referrals ($P = 0.03$) and versus academic referrals ($P = 0.04$).

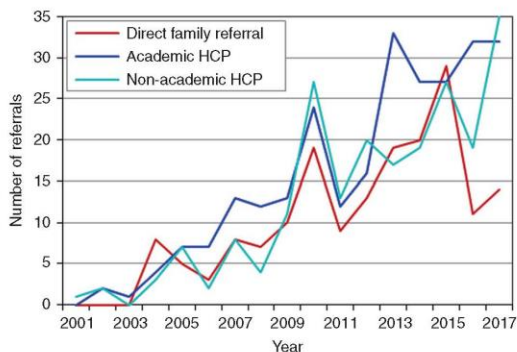


Fig. 2 Temporal distribution for referral type. Red represents direct family referrals, blue represents academic health-care providers (HCPs), and aqua represents nonacademic HCP.

resources, the primary source of HCP referrals continues to be some form of personal contact (personal knowledge of the author, referral at the suggestion of a colleague, or lectures), which has resulted in a rising number of referrals each year. Direct family referrals have decreased over the last two years, while HCP referrals have increased.

DISCUSSION

Comparison with prior work

While prior studies have questioned the effectiveness of Internet self-diagnosis,^{22,23} the current investigation showed that the Internet is an important tool for the self-diagnosis of rare disorders. Direct family referrals resulted in the diagnosis of 116 family members with ADTKD, none of whom would have received a diagnosis at that time if family members had not pursued self-diagnosis. Direct family referral via the Internet contributed 29% of the families and 21% of cases of these uncommon diseases, a major resource for clinical characterization and research. Importantly, patients originating from direct family referrals had similar frequencies of

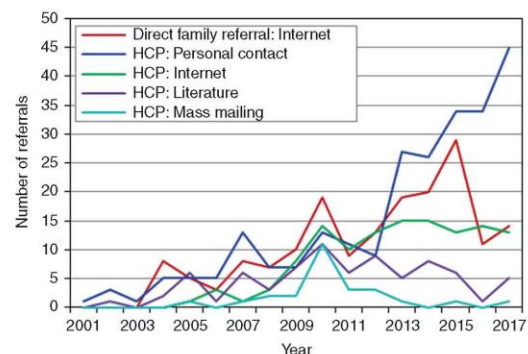


Fig. 3 Temporal distribution for method of referral. Red represents direct family referral via the Internet, with all family referrals being generated through Internet searches. Blue represents health-care provider (HCP) personal contact, including personal contact between the first author and the provider, colleague referral, and also lectures given by the first author. Green represents HCP referrals via Internet searches. Purple represents HCP referrals via reading of the literature. Aqua represents HCP referrals via mass mailing.

positive genetic diagnoses as referrals from HCPs. These observations provide insights about not only the self-diagnosis of rare inherited kidney diseases, but also the increasing empowerment of patients and families with rare disorders.²⁴

Principal results

This article highlights the strengths and weaknesses of direct Internet referral of individuals with rare disorders. Advantages include low cost, low manpower requirements for initial referral, and the ability to bypass nondiagnosis by physicians. We observed that patients made judicious decisions about initiating contact. Based on clinical characteristics, some conditions may lend themselves better to self-diagnosis. Family members were more likely to diagnose ADTKD-UMOD than ADTKD-MUC1 (see Table 1).

ADTKD-*UMOD* is more easily researched on the Internet due to the presence of both gout and inherited kidney disease, while ADTKD-*MUC1* is only associated with inherited kidney disease, making Internet searches nonspecific and more difficult. The presence of many affected family members in autosomal disorders provides more exposure to physicians and/or family members who might be interested to pursue diagnosis. Thus, 36% of our referrals were from families with four or more affected individuals. Autosomal recessive disorders, with only one or two affected individuals in each family, may be more difficult to diagnose.

This article also characterized the natural history of diagnosis once the genetic causes of ADTKD were identified. Though genetic testing was available for the first of these disorders in 2002, referrals from HCPs continue to increase over a decade later. Direct family referrals have begun to decrease, possibly due to better recognition by HCPs. Despite the increasing availability of Internet resources, physician education about these rare disorders appears to occur primarily through personal interaction, resulting in increasing referrals over time.

Limitations

A shortcoming of our study is that we only studied one center that specialized in ADTKD, provided current knowledge on the topic, and provided a path to diagnosis. Patients searching for other conditions may be unable to find accurate information or a path to diagnosis. One report found that only 20% of English searches for health information yielded relevant results.²⁵ Other studies have noted the poor quality of health information available on the Internet.^{22,23,26} Finding accurate information on the Internet is especially problematic for rare diseases, as approximately 50% of these disorders do not have a foundation providing specific patient information.¹ Despite studies showing frequent use of the Internet by parents of children with rare conditions,^{27–32} one study reviewing 693 websites about rare diseases found that in general the quality of information provided was poor.³³ Our results only describe outcomes that may occur when patients are provided with accurate information, personal contact, and a path to achieving diagnosis.

The potential use of the Internet for self-diagnosis also carries with it the inherent weaknesses of the digital divide. Almost all direct family referrals (99%) providing genetic samples were from white families. The median income of the zip codes from the site of referrals was \$77,316 ± 34,014, significantly higher than the 2010 US median household income of \$49,445.³⁴ There were no direct family referrals from African Americans, and few individuals from non-English speaking countries. There is no evidence that the pathogenic variants causing ADTKD would have a difference in prevalence between races. Factors that affect access to health care through the Internet include availability of devices connected to the Internet. Individuals who use the Internet on a daily basis (e.g., for work) are likely to have better Internet search skills. In addition, our webpage information was

provided only in English. An Italian study characterizing individuals who used the Internet to access a federation of associations of patients with rare diseases found that users were more likely to be female (68%), have higher education, and use the Internet at work (74%). Sixty-two percent of the respondents stated that the Internet helped them to achieve a diagnosis.

African Americans are more likely to have misgivings about research³⁵ and therefore may have been less likely to contact us, even though kidney disease is much more prevalent in African Americans. In a focus group study of African Americans' views on the trustworthiness of physicians, Jacobs *et al.* reported the importance of interpersonal competence of physicians.³⁶ Providing a more interpersonal experience on the Internet could include the use of more video material and providing faster methods of direct contact. Screening for genetic disorders in patients in dialysis centers would also provide a better interpersonal experience and enhance access to individuals across the digital divide.

African Americans were also less likely to be referred by their health-care providers. The high prevalence of chronic kidney disease in African Americans may have contributed to decreased consideration of a genetic diagnosis. Decreased access to health-care providers may have also contributed.

Despite many resources in the literature and on the Internet, 52% of HCP referrals were based on personal acquaintance with the lead author, lectures, or conversations with colleagues who had a personal knowledge of our research. Once nephrologists referred one family with ADTKD, they were likely to refer others. Unfortunately, most individuals from all three referral groups only undertook to establish a diagnosis when kidney disease was quite advanced and patients were near dialysis.

Strengths of this article include that this center was one of very few referral centers involved in the diagnosis of ADTKD-*UMOD* and the only center arranging clinical genetic testing for ADTKD-*MUC1*. Weaknesses of this study include the unknown prevalence of this disorder. An Austrian study by Lhotta and colleagues³⁷ estimated a prevalence of ADTKD-*UMOD* of 1.67 cases per million. Given a US population of 323 million, one would expect approximately 540 cases of ADTKD-*UMOD*, compared with the 283 cases that were identified. The relative contributions of our multifaceted interventions could not be determined. We could not account for how many families reviewed our website information and presented it to their physicians or how many individuals underwent commercial testing. We know that there were 2620 unique page views of our webpages in 2017. Similarly, for the National Organization of Rare Disorders (NORD) ADTKD website, there were 1518 unique page views in 2017 (Marsha Lanes, NORD, personal communication). Of note, 8.2 million users visited NORD webpages in 2017. We do not know how many families were tested at commercial laboratories for ADTKD-*UMOD*, though we know that all clinical diagnoses for ADTKD-*MUC1* were only made in our laboratory.

Conclusions

Despite these limitations, this investigation highlights the importance of providing direct knowledge and access to individuals with undiagnosed rare disorders through the Internet. Such direct access provided many families with a genetic diagnosis that had eluded them for generations. These families in turn provided a significant proportion of individuals willing to participate in clinical research. We believe that endeavors such as the Broad Institute Rare Genomes Project are likely to further empower patients to find the genetic causes of rare inherited diseases.³⁸ For aid in the diagnosis of rare inherited kidney diseases, please contact ableyer@wakehealth.edu.

SUPPLEMENTARY INFORMATION

The online version of this article (<https://doi.org/10.1038/s41436-019-0617-8>) contains supplementary material, which is available to authorized users.

ACKNOWLEDGEMENTS

This work was supported by NIH–National Institute of Diabetes and Digestive and Kidney Diseases (NIDDK_R21 DK106584), project NV17-29786A from the Ministry of Health of the Czech Republic, LQ1604 NPU II from the Ministry of Education of the Czech Republic, and by institutional programs of Charles University in Prague (UNCE 204064, PROGRES-Q26/LF1 and SVV 260367/2017), and the Carlos Slim Foundation.

DISCLOSURE

The authors declare no conflicts of interest.

Publisher's note: Springer Nature remains neutral with regard to jurisdictional claims in published maps and institutional affiliations.

REFERENCES

- Global Genes. Rare diseases: facts and statistics. <https://globalgenes.org/rare-diseases-facts-statistics/>. Accessed 22 July 2019.
- Bigelow B. Tess is not alone: a USP7 story. 2017. Accessed 22 July 2019.
- Mnookin S. One of a kind: what do you do if your child has a condition that is new to science? *New Yorker*. 14 July 2014. <https://www.newyorker.com/magazine/2014/07/14/one-of-a-kind-2>. Accessed 22 July 2019.
- Rule AR. I am that parent. *JAMA*. 2018;319:445.
- Bouwman MG, Teunissen QG, Wijburg FA, Linthorst GE. 'Doctor Google' ending the diagnostic odyssey in lysosomal storage disorders: parents using internet search engines as an efficient diagnostic strategy in rare diseases. *Arch Dis Child*. 2010;95:642–644.
- Patsos M. MSJAMA: the Internet and medicine: building a community for patients with rare diseases. *JAMA*. 2001;285:805.
- Kuehn BM. More than one-third of US individuals use the Internet to self-diagnose. *JAMA*. 2013;309:756–757.
- Bleyer AJ, Kidd K, Zivna M, Knoch S. Autosomal dominant tubulointerstitial kidney disease. *Adv Chronic Kidney Dis*. 2017;24:86–93.
- Kirby A, Gnirke A, Jaffe DB, et al. Mutations causing medullary cystic kidney disease type 1 lie in a large VNTR in MUC1 missed by massively parallel sequencing. *Nat Genet*. 2013;45:288–393.
- Hart TC, Gorry MC, Hart PS, et al. Mutations of the UMOD gene are responsible for medullary cystic kidney disease 2 and familial juvenile hyperuricaemic nephropathy. *J Med Genet*. 2002;39:882–892.
- Zivna M, Hulkova H, Marignon M, et al. Dominant renin gene mutations associated with early-onset hyperuricemia, anemia, and chronic kidney failure. *Am J Human Genet*. 2009;85:204–213.
- Bleyer AJ: Uromodulin Kidney Disease. <https://www.wakehealth.edu/Condition/u/Uromodulin-Kidney-Disease>. Accessed 22 July 2019.
- Blumentiel B, Defelice M, Bissoy O, et al. Development and validation of a mass spectrometry-based assay for the molecular diagnosis of mucin-1 kidney disease. *J Mol Diagn*. 2016;18:566–571.
- Bleyer AJ, Knoch S, Antignac C, et al. Variable clinical presentation of an MUC1 mutation causing medullary cystic kidney disease type 1. *Clin J Am Soc Nephrol*. 2014;9:527–535.
- Bleyer AJ, Hart PS, Knoch S. Hereditary interstitial kidney disease. *Semin Nephrol*. 2010;30:366–373.
- Eckardt KU, Alper SL, Antignac C, et al. Autosomal dominant tubulointerstitial kidney disease: diagnosis, classification, and management-A KDIGO consensus report. *Kidney Int*. 2015;88:676–683.
- National Organization of Rare Disorders. Autosomal dominant tubulointerstitial kidney disease. 2017. <https://rarediseases.org/rare-diseases/autosomal-dominant-interstitial-kidney-disease/>. Accessed 22 July 2019.
- United States Census Bureau. American Fact Finder. <https://factfinder.census.gov/faces/nav/jsf/pages/index.xhtml>. Accessed 22 July 2019.
- Harris PA, Taylor R, Thielke R, et al. Research electronic data capture (REDCap)—a metadata-driven methodology and workflow process for providing translational research informatics support. *J Biomed Inform*. 2009;42:377–381.
- Bolar NA, Golzio C, Zivna M, et al. Heterozygous loss-of-function SEC61A1 mutations cause autosomal-dominant tubulo-interstitial and glomerulocystic kidney disease with anemia. *Am J Hum Genet*. 2016;99:174–187.
- Hartmannova H, Piherovala L, Tauchmannova K, et al. Acadian variant of Fanconi syndrome is caused by mitochondrial respiratory chain complex I deficiency due to a non-coding mutation in complex I assembly factor NDUF6. *Hum Mol Genet*. 2016;25:4062–4079.
- Semigran HL, Linder JA, Gidengil C, Mehrotra A. Evaluation of symptom checkers for self diagnosis and triage: audit study. *BMJ*. 2015;351:h3480.
- Bisson LJ, Komm JT, Bernas GA, et al. How accurate are patients at diagnosing the cause of their knee pain with the help of a web-based symptom checker? *Orthop J Sports Med*. 2016;4:2325967116630286.
- Ayme S, Kole A, Groft S. Empowerment of patients: lessons from the rare diseases community. *Lancet*. 2008;371:2048–2051.
- Berland GK, Elliott MN, Morales LS, et al. Health information on the Internet: accessibility, quality, and readability in English and Spanish. *JAMA*. 2001;285:2612–2621.
- Eysenbach G, Powell J, Kuss O, Sa ER. Empirical studies assessing the quality of health information for consumers on the world wide web: a systematic review. *JAMA*. 2002;287:2691–2700.
- Nicholl H, Tracey C, Begley T, et al. Internet use by parents of children with rare conditions: findings from a study on parents' web information needs. *J Med Internet Res*. 2017;19:e51.
- Morgan T, Schmidt J, Haakonsen C, et al. Using the internet to seek information about genetic and rare diseases: a case study comparing data from 2006 and 2011. *JMIR Res Protoc*. 2014;3:e10.
- Hamilton JG, Hutson SP, Frohnmayer AE, et al. Genetic information-seeking behaviors and knowledge among family members and patients with inherited bone marrow failure syndromes. *J Genet Couns*. 2015;24:760–770.
- Schumacher KR, Stringer KA, Donohue JE, et al. Social media methods for studying rare diseases. *Pediatrics*. 2014;133:e1345–e1353.
- Davies W. Insights into rare diseases from social media surveys. *Orphanet J Rare Dis*. 2016;11:151.
- Babac A, Litzkendorf S, Schmidt K, et al. Shaping an effective health information website on rare diseases using a group decision-making tool: inclusion of the perspectives of patients, their family members, and physicians. *Interact J Med Res*. 2017;6:e23.
- Pauer F, Gobel J, Storf H, et al. Adopting quality criteria for websites providing medical information about rare diseases. *Interact J Med Res*. 2016;5:e24.
- United States Census Bureau. Income, poverty and health insurance coverage in the United States: 2010. September 2011. https://www.census.gov/newsroom/releases/pdf/2010_Report.pdf. Accessed 22 July 2019.

35. Scharff DP, Mathews KJ, Jackson P, et al. More than Tuskegee: understanding mistrust about research participation. *J Health Care Poor Underserved*. 2010;21:879–897.
36. Jacobs EA, Rolle I, Ferrans CE, et al. Understanding African Americans' views of the trustworthiness of physicians. *J Gen Intern Med*. 2006;21:642–647.
37. Lhotta K, Piret SE, Kramar R, et al. Epidemiology of uromodulin-associated kidney disease—results from a nation-wide survey. *Nephron Extra*. 2012;2:147–158.
38. Broad Institute. Rare Genomes Project. <https://raregenomes.org/home>. Accessed July 17 2019.

4.2 Genetic and Clinical Predictors of Age of ESKD in Individuals with Autosomal Dominant Tubulointerstitial Kidney Disease Due to *UMOD* Mutations.

Kidd K, Vylet'al P, Schaeffer C, Olinger E, Živná M, Hodaňová K, Robins V, Johnson E, Taylor A, Martin L, Izzi C, Jorge SC, Calado J, Torres RJ, Lhotta K, Steubl D, Gale DP, Gast C, Gombos E, Ainsworth HC, Chen YM, Almeida JR, de Souza CF, Silveira C, Raposeiro R, Weller N, Conlon PJ, Murray SL, Benson KA, Cavalleri GL, Votruba M, Vrbacká A, Amoroso A, Gianchino D, Caridi G, Ghiggeri GM, Divers J, Scolari F, Devuyst O, Rampoldi L, Kmoch S, Bleyer AJ.

Kidney Int Rep. 2020 Jul 3;5(9):1472-1485.

Genetic and Clinical Predictors of Age of ESKD in Individuals With Autosomal Dominant Tubulointerstitial Kidney Disease Due to *UMOD* Mutations



Kendrah Kidd^{1,2}, Petr Vyleťal², Céline Schaeffer³, Eric Olinger⁴, Martina Živná², Kateřina Hodaňová², Victoria Robins¹, Emily Johnson¹, Abigail Taylor¹, Lauren Martin¹, Claudia Izzi^{5,6}, Sofia C. Jorge⁷, Joaquim Calado⁸, Rosa J. Torres^{9,10}, Karl Lhotta¹¹, Dominik Steubl¹², Daniel P. Gale¹³, Christine Gast^{14,15}, Eva Gombos¹⁶, Hannah C. Ainsworth¹, Ying Maggie Chen¹⁷, Jorge Reis Almeida¹⁸, Cintia Fernandes de Souza¹⁸, Catarina Silveira¹⁹, Rita Raposeiro¹⁹, Nelson Weller¹, Peter J. Conlon^{20,21}, Susan L. Murray^{20,21}, Katherine A. Benson^{20,21}, Gianpiero L. Cavalleri^{20,21}, Miroslav Votruba², Alena Vrbacká², Antonio Amoroso²², Daniela Gianchino²³, Gianluca Caridi²⁴, Gian Marco Ghiggeri²⁴, Jasmin Divers¹, Francesco Scolari⁶, Olivier Devuyst^{4,25}, Luca Rampoldi³, Stanislav Kmoch^{1,2} and Anthony J. Bleyer^{1,2}

¹Section on Nephrology, Wake Forest School of Medicine, Winston-Salem, North Carolina, USA; ²Research Unit of Rare Diseases, Department of Pediatric and Adolescent Medicine, First Faculty of Medicine, Charles University, Prague, Czech Republic; ³Molecular Genetics of Renal Disorders, Division of Genetics and Cell Biology, Istituti di Ricovero e Cura a Carattere Scientifico (IRCCS) San Raffaele Scientific Institute, Milan, Italy; ⁴University of Zurich, Institute of Mechanisms of Inherited Kidney Disorders, Zurich, Switzerland; ⁵Division of Nephrology and Dialysis, University of Brescia and Montichiari Hospital, Brescia, Italy; ⁶Department of Medical and Surgical Specialties, Radiological Sciences, and Public Health, University of Brescia and Montichiari Hospital, Brescia, Italy; ⁷Department of Nephrology and Renal Transplant of Centro Hospitalar Universitário Lisboa Norte, EPE, Lisbon, Portugal; ⁸ToxOmics, Centre for Toxicogenomics and Human Health, NOVA Medical School, New University of Lisbon, Lisbon, Portugal; ⁹Foundation for Biomedical Research of La Paz University Hospital (FIBHULP), IdiPaz, Madrid, Spain; ¹⁰Center for Biomedical Network Research on Rare Diseases (CIBERER), Madrid, Spain; ¹¹Department of Internal Medicine, Academic Teaching Hospital Feldkirch, Feldkirch, Austria; ¹²Department of Nephrology, Klinikum rechts der Isar, Technical University of Munich, Munich, Germany; ¹³Department of Renal Medicine, University College London, London, UK; ¹⁴Wessex Kidney Centre, Queen Alexandra Hospital, Portsmouth Hospitals NHS Trust, Portsmouth, UK; ¹⁵Human Genetics and Genomic Medicine, Faculty of Medicine, University of Southampton, Southampton, UK; ¹⁶Department of Nephrology and Gastroenterology, Heim Pál Hospital for Children, Budapest, Hungary; ¹⁷Division of Nephrology, Washington University in St. Louis School of Medicine, St. Louis, Missouri, USA; ¹⁸Multi-User Laboratory to Support Research in Nephrology and Medical Sciences (LAMAP), Federal Fluminense University, Niterói, Rio de Janeiro, Brazil; ¹⁹GenoMed SA, Instituto de Medicina Molecular, Faculdade de Medicina, Universidade de Lisboa, Lisboa, Portugal; ²⁰Nephrology Department, Beaumont Hospital, Dublin, Ireland; ²¹Department of Medicine, Royal College of Surgeons in Ireland, Dublin, Ireland; ²²Medical Genetics, Department of Medical Sciences, University of Turin, Turin, Italy; ²³Department of Clinical and Biological Sciences, University of Turin, Turin, Italy; ²⁴Department of Nephrology and Transplantation, Istituto G. Gaslini Istituto di Ricovero e Cura a Carattere Scientifico (IRCCS), Genoa, Italy; and ²⁵Division of Nephrology, UCLouvain Medical School, Brussels, Belgium

Introduction: Autosomal dominant tubulo-interstitial kidney disease due to *UMOD* mutations (ADTKD-*UMOD*) is a rare condition associated with high variability in the age of end-stage kidney disease (ESKD). The minor allele of rs4293393, located in the promoter of the *UMOD* gene, is present in 19% of the population and downregulates uromodulin production by approximately 50% and might affect the age of ESKD. The goal of this study was to better understand the genetic and clinical characteristics of ADTKD-*UMOD* and to perform a Mendelian randomization study to determine if the minor allele of rs4293393 was associated with better kidney survival.

Methods: An international group of collaborators collected clinical and genetic data on 722 affected individuals from 249 families with 125 mutations, including 28 new mutations. The median age of ESKD was 47 years. Men were at a much higher risk of progression to ESKD (hazard ratio 1.78, $P < 0.001$).

Results: The allele frequency of the minor rs4293393 allele was only 11.6% versus the 19% expected ($P < 0.01$), resulting in Hardy-Weinberg disequilibrium and precluding a Mendelian randomization experiment.

Correspondence: Luca Rampoldi, IRCCS San Raffaele Scientific Institute, Via Olgettine 58, 20132 Milan, Italy. E-mail: rampoldi.luca@hsr.it; or Anthony J. Bleyer, Wake Forest School of

Medicine, Section on Nephrology, Winston-Salem, North Carolina 27157, USA. E-mail: ableyer@wakehealth.edu

Received 31 March 2020; revised 12 June 2020; accepted 24 June 2020; published online 3 July 2020

An *in vitro* score reflecting the severity of the trafficking defect of uromodulin mutants was found to be a promising predictor of the age of ESKD.

Conclusion: We report the clinical characteristics associated with 125 *UMOD* mutations. Male gender and a new *in vitro* score predict age of ESKD.

Kidney Int Rep (2020) 5, 1472–1485; <https://doi.org/10.1016/j.ekir.2020.06.029>

KEYWORDS: autosomal dominant uromodulin kidney disease; genotype; phenotype; rs4293393; uromodulin

© 2020 International Society of Nephrology. Published by Elsevier Inc. This is an open access article under the CC BY-NC-ND license (<http://creativecommons.org/licenses/by-nc-nd/4.0/>).

The cardinal manifestations of ADTKD-UMOD include autosomal dominant inheritance, precocious gout in some individuals, and slowly progressive chronic kidney disease.¹ Progression to ESKD is variable, occurring between ages 20 and 70 years.^{2–5} The reasons for this variation are unknown. Identification of the causes would lead to a better understanding of the pathogenesis of ADTKD-UMOD, identify individuals at risk of progression for clinical trials, and provide information about prognosis for patients.

In ADTKD-UMOD, retention of mutant uromodulin (mUMOD) protein in the endoplasmic reticulum (ER) of tubular epithelial cells in the thick ascending limb leads

to ER stress, tubular cell death, and chronic kidney disease.^{4,6–11} Uromodulin has a high cysteine content, resulting in a slow transit through the ER as disulfide bonds form.¹² Approximately two-thirds of the mutations causing ADTKD-UMOD (*mUMOD*) involve cysteine residues, and no mutations have been found resulting in truncation or loss of transcription.⁴ *Umod* knockout mice also do not develop the ADTKD phenotype.¹³ These findings implicate mUMOD as the principal pathophysiologic cause of ADTKD-UMOD. Based on these hypotheses, one could theorize the amount of mUMOD expressed and the type of mutation may contribute to the pathophysiology and age of ESKD onset.

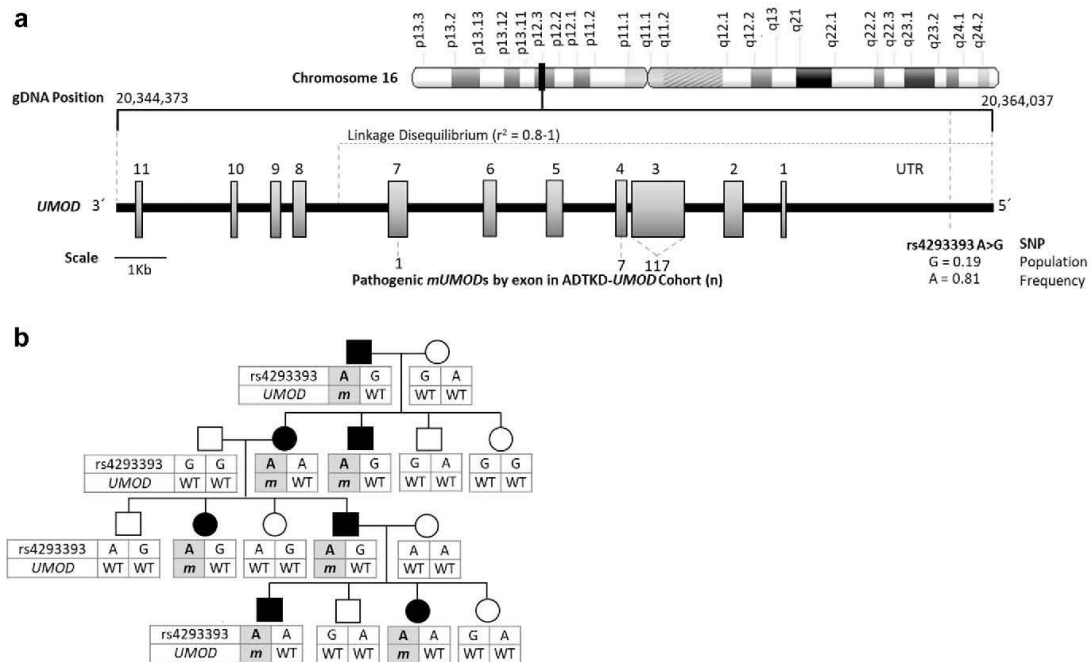


Figure 1. Genetic map of rs4293393 and *UMOD* with a representative autosomal dominant tubulo-interstitial kidney disease due to *UMOD* mutations (ADTKD-UMOD) pedigree demonstrating rs4293393-*UMOD* haplotype inheritance. (a) Genetic map of rs4293393 and *UMOD*, showing the linkage disequilibrium of rs4293393 with the *UMOD* mutations (*mUMOD*s) found in this cohort study; 124 of 125 *mUMOD*s occurred in exons 3 and 4 and were in a region of complete linkage disequilibrium with rs4293393. (b) Representative 4-generation ADTKD-UMOD pedigree. Genetically affected individuals are represented by black symbols, and the rs4293393-*mUMOD* haplotype is shaded gray. The rs4293393 allele (in this case “A”) is in phase with the *mUMOD* (designated *m*). In all genetically affected family members (due to linkage disequilibrium of rs4293393 and the *UMOD* gene [A]), the rs4293393-*mUMOD* haplotype is inherited together. In contrast, the rs4293393-wild-type *UMOD* (designated WT) haplotype inherited from the unaffected parent varies in subsequent generations based on the rs4293393-WT *UMOD* haplotypes of the unaffected parent. gDNA, genomic DNA; SNP, single nucleotide polymorphism; UTR, untranslated region.

There is a genetic variant (known as single nucleotide polymorphism [SNP] rs4293393) present in the *UMOD* promoter (Figure 1a). In 19% of Europeans, this SNP has a guanosine residue and results in an approximately 50% reduction in uromodulin expression as compared with the remaining 81% of the European population, which has an adenosine residue at this site.¹⁴ As rs4293393 resides in the promoter of the *UMOD* gene, it is virtually always inherited together with the *UMOD* gene on the same allele. Indeed, *UMOD* promoter variants are within a region of complete linkage disequilibrium that spans exons 1 to 5. Because more than 95% of *UMOD* mutations are within exons 3 and 4, this implies that for virtually all pedigrees the variants in the *UMOD* promoter and the causal *UMOD* mutation cosegregate. In a given family with ADTKD-*UMOD*, all affected individuals who inherit the *mUMOD* gene will inherit the same rs4293393 allele adjacent to *mUMOD* (Figure 1b). The rs4293393 variant that is present on the wild-type allele will be inherited from the unaffected parent and will not be the same for all affected family members (Figure 1b).

The primary aims of this investigation were to better characterize the genetic and clinical findings of ADTKD-*UMOD* in a large population of affected families and to perform a Mendelian randomization study of individuals affected with ADTKD-*UMOD*. In a Mendelian randomization study, one studies the effects of genetic variants randomly distributed in a population on an outcome (e.g., kidney failure). We hypothesized that the presence of the minor rs4293393 variant in the promoter of the *mUMOD* allele would lead to a decreased expression of *mUMOD*. Thus, families with the minor rs4293393 variant in the *mUMOD* promoter should have decreased expression of *mUMOD*, which might ameliorate mutant protein deposition, preserve the tubulo-interstitium, and slow progression of chronic kidney disease and development of ESKD. This decreased production of *mUMOD* would be similar to the administration of a medication from birth onward (with 100% compliance) that lowers *mUMOD* production by approximately 50%. Our goal was to determine if the presence of the rs4293393 minor SNP variant with the *mUMOD* allele results in a later age of onset of ESKD.

Another factor that could affect the age of ESKD onset is the nature of the *mUMOD* mutation and its effect on the transit of uromodulin and *mUMOD* through the ER and on apoptosis. Some mutations may have a more deleterious effect on uromodulin trafficking and consequently ER function.^{7,15} To this end, we quantified the *mUMOD* trafficking defect for 35 selected mutations (Supplementary Table S1) through an *in vitro* score and investigated whether this score correlated with the age of onset of ESKD.

The dataset included genetic information and age of ESKD from 12 international ADTKD research teams

(international cohort), as well as the Wake Forest ADTKD registry (WF cohort), which included additional clinical information (Figure 2). The data from the WF cohort and from the international cohort were combined to analyze genetic factors and gender, and the WF cohort data were then further analyzed to explore other factors that could affect the age of ESKD, including body mass index, smoking status, presence of gout, age of gout onset, and the mean age of ESKD for family members.

METHODS

The study was approved by the Wake Forest School of Medicine Institutional Review Board, all institutional review boards of participating centers, and was carried out in accordance with the Declaration of Helsinki.

Recruitment

(i) Most participants were from the WF cohort¹⁶ (Figure 2). Families were either referred by their physician or self-referred by a family member. A genetic diagnosis was made in the index case and then in as many family members as possible. A family tree was constructed that included the age of onset of ESKD in both living and deceased family members. A questionnaire containing demographic and clinical information was completed by as many affected family members as possible. (ii) Data obtained from affected individuals and families from the international cohort included the *UMOD* mutation, rs4293393 genotype when available, gender, and current kidney function or age of ESKD onset.

Genetic Evaluation

An index case in each family underwent mutational analysis and was found to have a *UMOD* mutation as described in the Supplementary Methods. As many family members as possible then underwent genetic testing for the at-risk *UMOD* mutation. Individuals found to be genetically affected underwent rs4293393 genotyping (Supplementary Methods).

In 209 of 240 families, genetic linkage was used to identify which of the rs4293393 alleles was present in the promoter of the *mUMOD* allele. In 18 families in whom DNA was available, the phase of the rs4293393 allele and *mUMOD* was established via cloning, genotyping, and sequencing of long-range polymerase chain reaction products encompassing the promoter and *UMOD* genomic sequence (Supplementary Methods). If the genotype and phase of the rs4293393 variant were established in at least 1 affected family member, it was assumed that all affected family members had the same rs4293393 variant, given the very high linkage disequilibrium. All available family members underwent rs4293393 variant testing to determine if results were consistent.

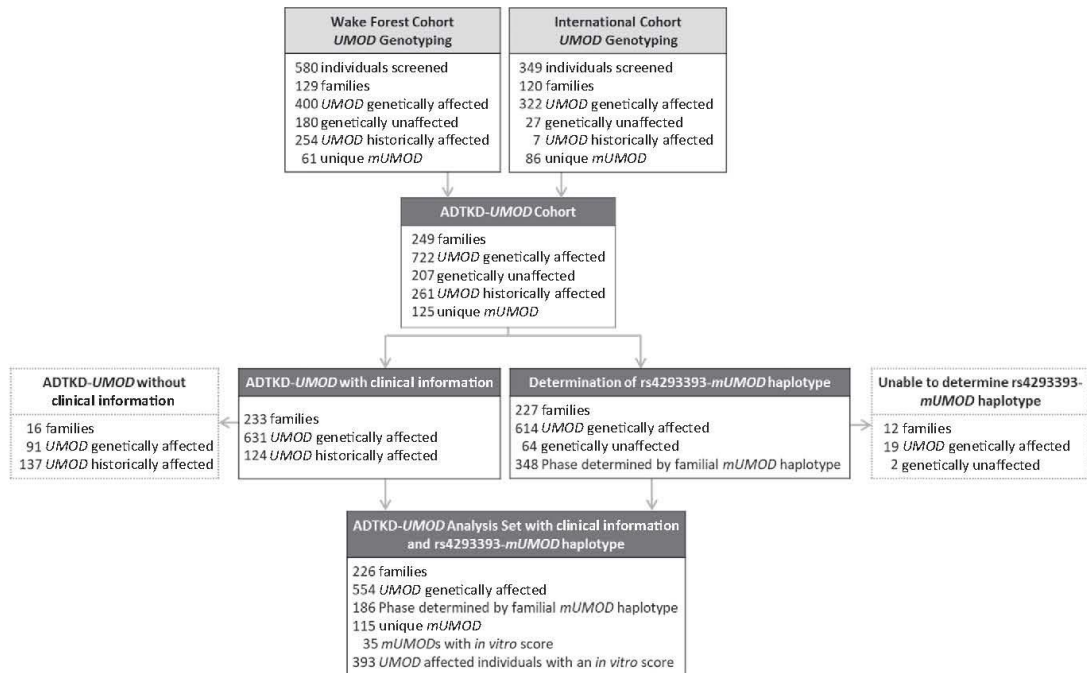


Figure 2. Flow diagram showing contribution of the Wake Forest and International cohorts to the development of the autosomal dominant tubulo-interstitial kidney disease due to *UMOD* mutations (ADTKD-*UMOD*) registry. A total of 929 individuals underwent genetic testing and 722 were documented to have a *UMOD* mutation (*UMOD* genetically affected), and 633 underwent further genetic testing for rs4293393. Historically affected individuals were from families genetically diagnosed with ADTKD-*UMOD* but in whom a DNA sample was unavailable. These individuals suffered from at least chronic kidney disease stage 3 and clinical findings were consistent with ADTKD-*UMOD*. Clinical information was available in most individuals from the Wake Forest cohort. *In vitro* scores were developed for 35 *UMOD* mutations to further understand disease progression.

DNA could not be obtained on some family members, most often because they were deceased. Individuals were considered historically affected if they met the following criteria: (i) a DNA sample for genetic diagnosis could not be obtained; (ii) there was a clinical history of at least chronic kidney disease stage 3 (estimated glomerular filtration rate <60 ml/min per 1.73 m²) that was consistent with ADTKD-*UMOD*; and (iii) the familial inheritance pattern was consistent with the individual being genetically affected.

In Vitro Score Determination

See [Supplementary Methods](#) for a full description. Thirty-five *UMOD* mutations were selected based on cohort prevalence and affected families having the youngest and oldest mean ages of ESKD onset. MDCK and/or HEK293 cell lines were transfected with expression vectors for each selected *mUMOD* and cell lysates analyzed by Western blots to evaluate uromodulin trafficking defects. *UMOD* mutation scoring was performed by quantifying the ratio between low- and high-molecular weight uromodulin glycoforms in 3 independent experiments.

Statistical Analysis

Descriptive statistics are shown as counts and proportions for categorical variables and mean \pm SD for continuous variables. For each variable, comparisons between WF and international cohorts were made using χ^2 and Fisher's exact tests for categorical variables and Wilcoxon rank-sum tests for continuous variables.

Testing for Hardy-Weinberg equilibrium was performed by adopting bootstrapping resampling methods with 1000 repeated sampling on the cohort subsets to estimate variance for the minor allele frequency.

A pedigree structure was built using Sequential Oligogenetic Linkage Analysis Routines (SOLAR) software (<http://solar-eclipse-genetics.org>) based on the reported family trees and used to create a kinship matrix with the R package "kinship2" (<https://cran.r-project.org/web/packages/kinship2/kinship2.pdf>). Survival analysis was then performed with the outcome being age of ESKD (defined as starting dialysis, receiving a kidney transplant, or dying from kidney failure without receiving dialysis). Individuals were censored if they had not yet received dialysis or if they died before

Table 1. Characteristics of individuals with ADTKD-UMOD who were genetically or historically affected, by cohort

Characteristic	WF cohort			International cohort	P value
	ADTKD-UMOD genotyped	ADTKD-UMOD historic	All		
ADTKD-UMOD genotyped	<i>n</i> = 400		400 (61%)	322 (98%)	
ADTKD-UMOD historic		<i>n</i> = 254	254 (39%)	7 (2%)	
Number of individuals who reached ESKD, <i>n</i> (%)	159 (40)	144 (57)	303 (53)	123 (37)	0.33 ^D
	4 (1) unknown	77 (30) unknown	81 (12) unknown	79 (24) unknown	
Age of ESKD	46.37	51.17	48.65	48.88	0.88
Male gender, <i>n</i> (%)	180 (48)	145 (57)	325 (50)	162 (49)	0.20 ^D
				2 (1) unknown	
Race, <i>n</i> (%)					<0.0001 ^B
White	380 (95)	247 (97)	627 (96)	271 (82)	
Black	3 (1)	0	3 (0.5)	0	
Hispanic	0	0	0	0	
Asian/Pacific Islander	11 (3)	5 (2)	16 (2)	0	
From India	1 (0.3)	1 (0.4)	2 (0.3)	0	
Other	0	0	0	0	
Unreported	5 (1)	1 (0.4)	6 (1)	58 (18)	
Ethnicity, <i>n</i> (%)					<0.0001 ^B
Hispanic or Latino	6 (2)	0	6 (1)	24 (7)	
Not Hispanic or Latino	374 (94)	239 (94)	613 (94)	251 (76)	
Other	8 (2)	5 (2)	13 (2)	0	
Unreported	12 (3)	10 (4)	22 (3)	54 (16)	
Smoking, <i>n</i> (%)					<0.0001 ^{A,C}
Never	228 (57)	8 (3)	236 (36)		
Current	23 (6)	1 (0.4)	24 (4)		
Former	69 (17)	5 (2)	74 (11)		
Uncertain	80 (20)	240 (94)	320 (49)		
Weight (kg)					0.24 ^C
Male and female	76.9 ± 19.9 (<i>n</i> = 287)	83.0 ± 22.2 (<i>n</i> = 20)	77.3 ± 20.2 (<i>n</i> = 307)		
Male	86.3 ± 19.2 (<i>n</i> = 127)	87.9 ± 18.4 (<i>n</i> = 11)	86.4 ± 19.1 (<i>n</i> = 138)		
Female	69.4 ± 17.1 (<i>n</i> = 160)	77.0 ± 25.9 (<i>n</i> = 9)	69.8 ± 17.6 (<i>n</i> = 169)		
Height (cm)					0.56 ^C
Male and Female	169.5 ± 12.0 (<i>n</i> = 287)	170.9 ± 10.0 (<i>n</i> = 20)	169.6 ± 11.8 (<i>n</i> = 307)		
Male	177.5 ± 11.8 (<i>n</i> = 127)	177.1 ± 6.3 (<i>n</i> = 11)	177.4 ± 11.5 (<i>n</i> = 138)		
Female	163.2 ± 7.5 (<i>n</i> = 160)	163.4 ± 8.4 (<i>n</i> = 9)	163.2 ± 7.5 (<i>n</i> = 169)		
BMI (kg/m ²)	26.5 ± 5.8 (<i>n</i> = 286)	28.15 ± 6.4 (<i>n</i> = 20)	26.6 ± 5.8 (<i>n</i> = 306)		0.27 ^C
Gout, <i>n</i> (%)					<0.0001 ^{A,C}
Yes					
Male and female	202 (50)	43 (17)	245 (37)		
Male	106 (59)	31 (21)	137 (42)		
Female	96 (44)	12(11)	108 (33)		
No					
Male and female	189 (47)	13 (5)	202 (31)		
Male	72 (40)	6(4)	78 (24)		
Female	117 (53)	7(6)	124 (38)		
Uncertain					
Male and female	9 (2)	198 (78)	207 (32)		
Male	2 (1)	108 (7)	110 (34)		
Female	7 (3)	90 (83)	97 (29)		
Age of gout onset (y)					0.15 ^C
Male and female	30.5 ± 11.5 (<i>n</i> = 197)	27.2 ± 9.5 (<i>n</i> = 20)	30.2 ± 11.4 (<i>n</i> = 217)		
Male	29.1 ± 9.9 (<i>n</i> = 105)	28.2 ± 10.4 (<i>n</i> = 13)	29.0 ± 9.9 (<i>n</i> = 118)		
Female	32.2 ± 12.9 (<i>n</i> = 92)	25.4 ± 8.0 (<i>n</i> = 7)	31.7 ± 12.7 (<i>n</i> = 99)		
Mutation type, <i>n</i> (%)					
p.H177-R185del (18%)	108 (27)	65 (26)	173 (26)	0	
p.V93-G97delinsAASC (8%)	42 (10)	30 (12)	72 (11)	2 (1)	
p.R178P (5%)	21 (5)	27 (11)	48 (7)	0	
p.C106F (5%)	26 (6)	21 (8)	47 (7)	0	
p.C148Y (3%)	12 (3)	11 (4)	23 (4)	2 (1)	
p.G88D (2%)	0	0	0	23 (7)	

(Continued on next page)

Table 1. (Continued) Characteristics of individuals with ADTKD-UMOD who were genetically or historically affected, by cohort

Characteristic	WF cohort			International cohort	P value
	ADTKD-UMOD genotyped	ADTKD-UMOD historic	All		
p.P236L (2%)	10 (2)	7 (3)	17 (3)	3 (1)	
p.C135Y (2%)	14 (4)	3 (1)	17 (3)	0	
p.S91del (2%)	0	1 (0.4)	1 (0.2)	16 (5)	
p.P236R (1%)	3 (1)	1 (0.4)	4 (1)	5 (2)	
Other mutation (54%)	164 (41)	88 (35)	252 (39)	278 (84)	

ADTKD-UMOD, autosomal dominant tubulo-interstitial kidney disease due to *UMOD* mutations; BMI, body mass index; ESKD, end-stage kidney disease; WF, Wake Forest.

^aChi-squared test.

^bFisher's exact test.

^cWF genotyped versus historic.

developing ESKD. Cox mixed effects models were built with the R package “coxme” (<https://cran.r-project.org/web/packages/coxme/coxme.pdf>) to incorporate the kinship matrix as the correlation structure and adjust for familial relationships. Univariate models were created for all parameters. Significant predictors from the univariate models were used to develop a best-fit multivariate model. Because of the absence of some data for individual variables (for example, parental age of ESKD), variables were included in modeling only if 100 events had occurred to protect the robustness of the data. This modeling adjusted for variable family sizes. The multivariate model was created in a forward stepwise manner with entry criteria of a *P* value <0.05. The model that resulted in the highest C-statistic was considered the most effective model.

RESULTS

In the WF cohort, 580 individuals from families with ADTKD-UMOD underwent genotyping, with 180 of 580 (31%) individuals being genetically unaffected and 400 of 580 (69%) individuals being genetically affected (Figure 2). There were 61 unique mutations in 129 families. An additional 254 individuals were considered historically affected, meaning that individuals were known to have ADTKD-UMOD as demonstrated by clinical findings and inheritance but did not undergo genotyping because they were deceased or otherwise unavailable to provide a DNA sample. The remaining data concern only individuals who were genetically affected or historically affected. Information regarding smoking history, body mass index, gout, and parental age of ESKD were available only in the WF cohort (Table 1).

For the international cohort, 349 individuals were screened from 120 affected families. There were 322 genetically affected, 27 genetically unaffected, and 7 historically affected. Table 1 compares characteristics of the 2 cohorts.

There was a total of 722 individuals from 249 families affected with ADTKD-UMOD, with 125 unique *mUMOD* mutations, including 28 mutations not previously described. Of the mutations, 117 (94%) were in exon 3, 7 (6%) in exon 4, and 1 in exon 7; 47% of mutations

resulted in the loss of a cysteine residue, 6% in the gain of a cysteine residue, and 6% resulted in a gain in hydrophobicity. Characteristics of individuals affected with the most common *UMOD* mutations are listed in Table 2 and Supplementary Table S1 for all mutations. This table is updated regularly at <http://j.mp/2q7Fi8f>. The median age of ESKD for the entire cohort was 47 years (range 18–87) and mean age 48.7 ± 12.7 years. Gender had a marked association with earlier age of ESKD (Figure 3), with an odds ratio of 1.78 (*P* = 0.00028). ESKD was uncommon before age 30, with approximately 50% of the male cohort reaching ESKD between 30 and 50, and 50% of the female cohort reaching ESKD between 30 and 60. In the WF cohort, 55% (245 of 447) of patients with ADTKD-UMOD developed gout. Figure 4 shows a survival curve with event defined as onset of gout for individuals with gout in whom an age of gout onset was known. The median age of gout onset was 28 years, with gout most commonly developing between ages 15 and 40. Of 180 men with information available, 106 (59%) developed gout at a mean age of 29.1 ± 9.9 years. Of 220 women with information available, 96 (44%) developed gout at a mean age of 32.2 ± 12.9 years.

Genetic Analysis

Genetic analysis was performed on both the WF and international cohorts, including 929 individuals from 249 families with 125 distinct *UMOD* mutations. Supplementary Table S1 shows a complete list of the number of individuals with each mutation, the median age and range of ESKD, and the *in vitro* score. A family was defined as a group of individuals from which 1 individual was referred, and in whom there were no family members known related to other referred families at the time of referral. The most common *mUMOD* was p.H177_R185del, with 173 individuals and 25 families from the WF cohort. The second most common *mUMOD* was p.V93_G97delinsAASC with 74 individuals and 11 families. This mutation originated in England.¹⁷ The statistical analysis performed (see Methods) adjusted for the large number of family members.

Table 2. Most common *UMOD* mutations (*mUMOD*) with *in vitro* score and age of ESKD

<i>mUMOD</i>	<i>In vitro</i> score	Families (n)	Individuals (n)	Median age ESKD	Range of ESKD	Families linked to major variant	Families linked to minor variant	Families with unknown linkage
p.H177_R185del	3	25	173	46	20–87	25	0	0
p.V93_G97delins AASC	2	11	74	48	27–75	10	0	1
p.R178P	4	9	48	53	39–79	8	0	1
p.C106F	1	11	47	55	35–72	11	0	0
p.C148Y	4	4	25	44	25–66	4	0	0
p.G88D	1	8	23	65.5	55–76	7	0	1
p.P236L	3	4	20	45	43–67	4	0	0
p.C135Y	4	2	17	41	37–47	2	0	0
p.S91del	2	5	17	50	37–66	5	0	0
p.P236R	4	5	9	40	24–50	4	0	1

ESKD, end-stage kidney disease.
Range of ESKD is earliest and latest ages of ESKD.

Genotyping of rs4293393 was performed in 633 of 722 genetically affected individuals and in 64 of 207 genetically unaffected individuals (Figure 2). With the aid of long-range sequencing in 18 families, it was possible to determine whether the minor or major allele was in phase with *mUMOD* in 614 individuals and 227 of 240 families. In 614 of 614 cases, rs4293393 testing results were consistent with inheritance of the same rs4293393-*mUMOD* haplotype throughout each family.

In 348 individuals (92 genetically affected and 256 historically affected) who were not rs4293393 genotyped, the allele in phase with *mUMOD* was assigned based on familial results.

Distribution of the rs4293393 SNP Variant in Families With ADTKD-UMOD

When performing a Mendelian randomization study, one must first determine that the genetic

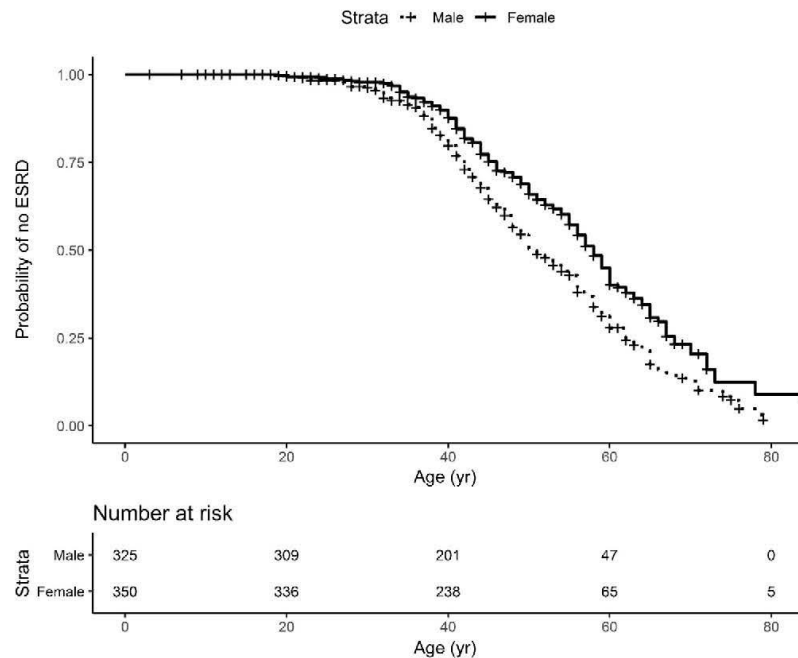


Figure 3. End-stage kidney disease (ESKD) survival according to gender in autosomal dominant tubulo-interstitial kidney disease due to *UMOD* mutations (ADTKD-*UMOD*). This analysis included 675 individuals with ADTKD-*UMOD* with known gender and clinical information. An event was defined as starting dialysis, receiving a transplant, or dying of kidney failure. Censoring occurred for death before ESKD or if the individual had not reached ESKD by the end of the study period. ESKD rarely occurred before age 30, with most patients requiring dialysis by age 70. Male gender was associated with an increased risk of reaching ESKD at an earlier age (hazard ratio 0.562, 0.00028). ESRD, end-stage renal disease.

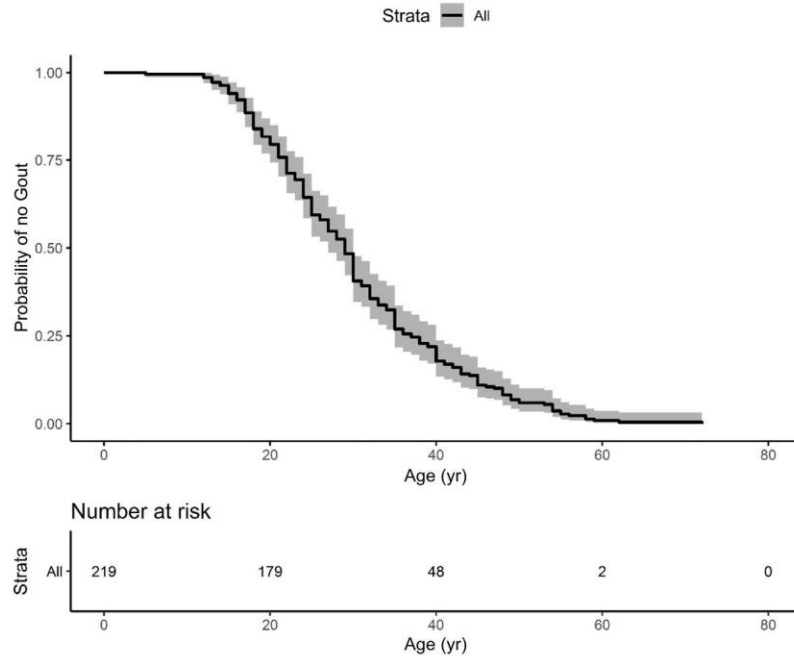


Figure 4. Survival curve of gout onset in individuals with autosomal dominant tubulo-interstitial kidney disease due to *UMOD* mutations (ADTKD-*UMOD*). This analysis included only 219 individuals who developed gout. An event was defined as age to onset of gout. Gout rarely occurred before age 15, with the vast majority of affected individuals developing gout between the ages of 20 and 40.

variant under study is randomly distributed in the population being investigated. Approximately 19% of the European population has the minor rs4293393 allele (G) (defined as the minor allele frequency [MAF]).¹⁴ In patients with ADTKD-*UMOD*, for the rs4293393 allele inherited from the unaffected parent, the MAF was 0.17, which is similar to reference populations (Table 3). We then sought to determine if the rs4293393 minor variant linked to the *mUMOD* allele was distributed in the same proportion as the general population. As some of the families under study might be distantly related, we assumed that all individuals with the

same rs4293393-*mUMOD* haplotype were one family. Using this approach, there were 123 families with the major rs4293393 allele linked to *mUMOD* and 24 families with the minor rs4293393 allele linked to *mUMOD*. For 9 *mUMOD*s, there were families with the minor allele-*mUMOD* haplotype and also families with the major allele-*mUMOD* haplotype. For the rs4293393 variant linked to -*mUMOD*, the MAF was only 0.12 versus the MAF of 0.19 to 0.20 in the TOPMED, gnomAD, and 1000 genome populations, which statistically deviated from expected proportions ($P = 0.0037$, Table 3). In other words, the SNP minor allele, associated with

Table 3. Comparison of minor allele frequencies of the rs4293393 SNP in phase and out of phase with the mutated *UMOD* (*mUMOD*)

Testing	Population	<i>n</i>	Observed MAF (minor, major)	Comparison database	MAF in comparison group	<i>P</i> value
rs4293393 in phase with <i>mUMOD</i>	1 per haplotype present in cohort	129 ^a	0.1163 (G, A)	TOPMED	0.18639	0.0147
				gnomAD	0.1924	0.0082
				1000 genomes	0.20	0.0037
rs4293393 out of phase with <i>mUMOD</i>	<i>UMOD</i> genotyped, rs4293393 genotyped	554	0.1645 (G, A)	TOPMED	0.18639	0.2693
				gnomAD	0.1924	0.1629
				1000 Genomes	0.20	0.07958

MAF, minor allele frequency.

^aThere were 129 unique rs4293393/*mUMOD* haplotypes.

Conservative testing was used, in which it was assumed that all individuals with the same rs4293393-*mUMOD* haplotype were related. The MAF of the test population was compared with the MAF found in TOPMED, gnomAD, and 1000 genomes registries.¹⁶ All comparisons showed that the MAF deviates from expected population frequencies. The MAF was then determined in available samples for the *UMOD* allele that was inherited from the unaffected parents. This allele was found to have similar allele frequencies as the control populations.

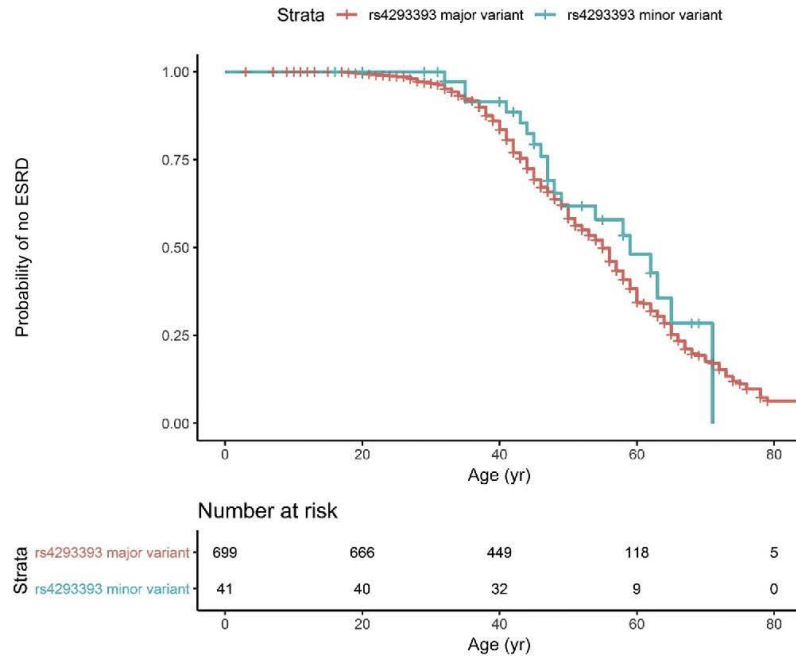


Figure 5. Survival curves according to the rs4293393 allele in phase with mutant *UMOD* (*mUMOD*). This analysis included 668 individuals with autosomal dominant tubulo-interstitial kidney disease due to *UMOD* mutations (ADTKD-*UMOD*) with clinical information available in addition to determined rs4293393-*mUMOD* haplotype. An event was defined as end-stage kidney disease (ESKD) by starting dialysis, receiving a transplant, or dying of kidney failure. Censoring occurred for death before ESKD or if the individual had not reached ESKD by the end of the study period. There were only 41 individuals with the minor allele (G) in phase with *mUMOD*, resulting in insufficient power to detect a difference in survival. ESRD, end-stage renal disease.

lower uromodulin production, is underrepresented when associated with *mUMOD* mutation, whereas this is not the case when it is associated with a wild-type *UMOD* allele. Given that the rs4293393 variant was not randomly distributed in this population, a Mendelian randomization experiment could not be performed.

ESKD Survival by rs4293393 Allele

Figure 5 shows the ESKD survival curves for individuals according to the rs4293393-*mUMOD* haplotype. There were 699 (94.5%) genotyped and historic individuals with the major allele (A) in phase with *mUMOD* and 41 (5.5%) genotyped and historic individuals with the minor rs4293393 allele (G) in

Table 4. Univariate models for individuals with ADTKD-*UMOD*

Parameter	Observations (n)	Events	Reference category	Hazard ratio	C-statistic	P value
Gender	675	342	Male	1.78	0.556	0.0028
rs4293393 minor variant in phase with <i>mUMOD</i>	668	337	A (major)	0.6885	0.507	0.36
rs4293393 minor variant in phase with <i>wtUMOD</i>	494	221	A (major)	0.6152	0.529	0.064
rs4293393 variant (at least 1 G allele present)	499	224	2 A alleles present	0.6943	0.528	0.13
<i>mUMOD</i> type	675	342	p.(H177_R185del)		0.561	
Cysteine gain				0.9234		0.88
Cysteine loss				0.9995		1.0
Deletion/insertion				0.6369		0.3
Hydrophobic amino acid gain				0.3197		0.066
Proline gain				0.5321		0.13
Other				0.6155		0.15
<i>In vitro</i> score	393	198		1.5457	0.591	0.0022
Cysteine-rich domains	675	342	All other domains	0.8247	0.521	0.38

ADTKD-*UMOD*, autosomal dominant tubulo-interstitial kidney disease due to *UMOD* mutations; *mUMOD*, mutant uromodulin; *wtUMOD*, wild-type uromodulin. Data combine Wake Forest and International cohorts.

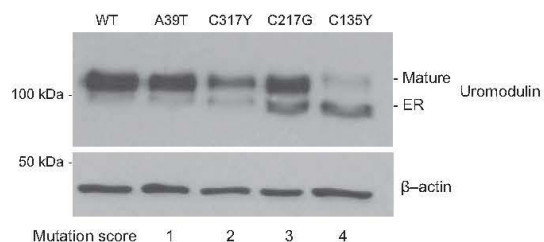


Figure 6. Representative Western blot results from mutant *UMOD* (*mUMOD*) *in vitro* experiments (Supplementary Methods). Western blot analysis of HEK cells stably expressing wild-type (WT) or mutant uromodulin isoforms. An *in vitro* score reflecting the severity of trafficking defect was assigned to each mutation. The scoring was performed by quantifying the ratio between endoplasmic reticulum (ER)-retained and mature uromodulin glycoforms in cell lysates.

phase with *mUMOD*. A univariate model (Table 4) was underpowered because of the presence of only 41 individuals with the minor allele phased with *mUMOD*.

Scoring of *UMOD* Mutations

The trafficking of 35 *mUMOD* isoforms was characterized *in vitro* (Figure 6, Table 2, Supplementary Table S1, and Supplementary Figures S1 and S2). MDCK and/or HEK293 cell lines were transfected with expression vectors coding for different *mUMODs*. As previously described,⁸ Western blot revealed 2 bands: a lower molecular weight glycoform corresponding to the uromodulin precursor in the ER that carries Endo H-sensitive N-glycans, and a higher molecular weight glycoform that carries post-Golgi, Endo H-resistant type of glycans. The higher molecular weight form corresponds to fully glycosylated, mature protein that proceeded along the secretory pathway into post-Golgi compartments (trans-Golgi network, secretory vesicles, plasma membrane). *UMOD* mutation scoring was performed by quantifying the ratio between low- and high-molecular weight uromodulin glycoforms in cell lysates, as a measure of trafficking defect. We normalized these values to the ratio obtained for the well-characterized, paradigm mutation C150S that consistently shows strong ER retention. Mutations were then subdivided into 4 distinct subgroups based on the generated ratio before statistical correlation with age of ESKD (Figure 6).

The different cellular phenotypes of *mUMOD* forms and their severity were reproducible between independent experiments (Supplementary Figure S1) and conserved when expressed in different cell lines (e.g., HEK293 vs. MDCK) (Figure 6 and Supplementary Figure S3), regardless of the expression system (transient or stable transfection) (Supplementary Figure S4).

UMOD Mutation Type and ESKD Survival

In univariate models, we found no difference in survival for the different mutation types but did show an association with the *in vitro* score (Table 5 and ESKD survival curve in Figure 7). For individuals with *mUMOD* mutations that less hindered uromodulin export to the cell surface (Group 1), renal survival was significantly improved.

Multivariate Model

A multivariate model was then created based on the genetic factors present in both cohorts. In the multivariate model, the presence of gender and *in vitro* score provided the highest correlation (Table 6). We did not find that the type of mutation was predictive of age of ESKD (data not shown). There were no significant interaction terms.

Analysis of Genetic and Clinical Factors for the WF Cohort

Analysis of clinical and genetic factors was performed on the WF cohort (Table 7). The presence of gout was not associated with age of ESKD; however, a younger age of gout for individuals who developed gout was highly correlated with a younger age of ESKD ($P < 0.0001$). In univariate analysis (Table 7), maternal age was highly associated with survival ($P = 0.0017$), whereas the paternal age was not ($P = 0.23$). When looking at subgroups, daughter and maternal age of ESKD were most highly correlated, followed by son and maternal age of ESKD (Supplementary Figures S1 and S2).

Multivariate clinical and genetic/clinical models were then created using the WF cohort (Table 8). The combination of gender and the family mean age of ESKD were found to be the best predictors of survival. There were no significant interaction terms.

DISCUSSION

This is the largest study that has been performed in individuals with ADTKD-*UMOD* and is the result of a large multinational collaboration that included 13

Table 5. Mean age of end-stage kidney disease in individuals with ADTKD-*UMOD* according to *in vitro* score

<i>In vitro</i> score	Observations (n)	Age (mean \pm SD)
1	42	59.4 \pm 11.0
2	56	50.4 \pm 11.0
3	90	48.5 \pm 12.1
4	59	47.2 \pm 11.7
Not available	179	46.3 \pm 13.1

ADTKD-*UMOD*, autosomal dominant tubulo-interstitial kidney disease due to *UMOD* mutations.
Data include only individuals who reached end-stage kidney disease.

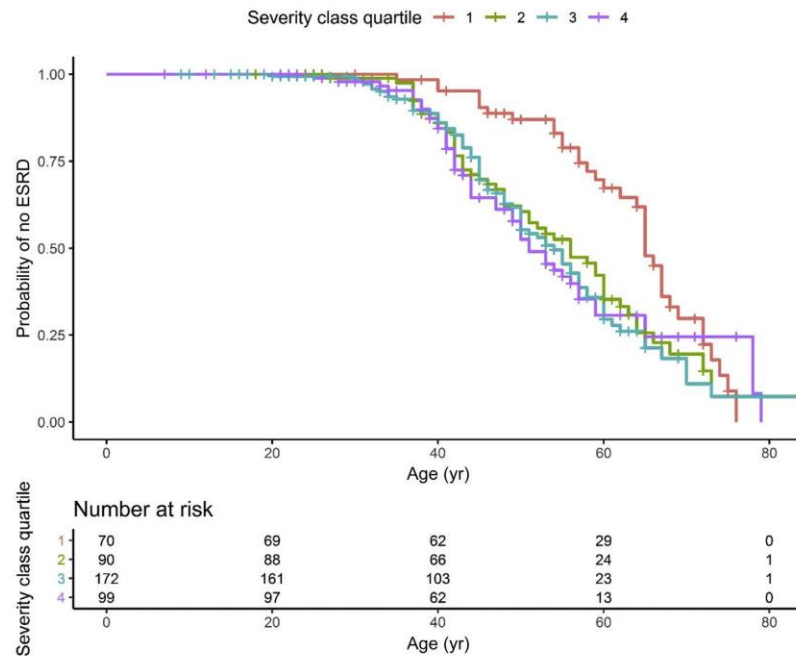


Figure 7. End-stage kidney disease (ESKD) survival in individuals with autosomal dominant tubulo-interstitial kidney disease due to *UMOD* mutations (ADTKD-*UMOD*) according *in vitro* score. This analysis included 393 individuals with 1 of the 35 *UMOD* mutations receiving an *in vitro* score. An event was defined as ESKD by starting dialysis, receiving a transplant, or dying of kidney failure. Censoring occurred for death before ESKD or if the individual had not reached ESKD by the end of the study period. ESRD, end-stage renal disease.

different research groups. The age of ESKD onset in individuals with ADTKD-*UMOD* ranges from 20 to >70, and the goal of this study was to identify factors associated with the highly variable age of ESKD onset. The principal findings of the study included the following: (i) the rs4293393 SNP in the mutant *UMOD* promoter was not randomly distributed in families with ADTKD-*UMOD*, with the minor allele (G) postulated to produce decreased mUMOD significantly underrepresented. (ii) An *in vitro* score that measured the effect of the specific *mUMOD* mutation on uromodulin trafficking was significantly correlated with kidney survival. (iii) Women had significantly better renal survival than men (hazard ratio 1.78, $P < 0.001$). (iv) The maternal age of ESKD was significantly associated with the child’s age of ESKD, particularly for women; however, there remained significant variation. (v) A younger age of gout was associated with a younger age

of ESKD. (vi) Twenty-eight new mutations were described.

A major finding of the study was that the MAF of the rs4293393 minor variant linked to *mUMOD* was only 11% in affected families as opposed to the 18% to 20% found in the general population ($P < 0.001$) and as opposed to the observed MAF of the rs4293393 allele in phase with wild-type *UMOD* allele (17%). We postulate that the decreased allele frequency is due to decreased *mUMOD* expression and hence a milder form of ADTKD-*UMOD* associated with later age of ESKD onset. Families with a later age of ESKD onset would be less likely to be identified with ADTKD-*UMOD* and less likely to be referred for evaluation and potential entry into a disease registry. Because of the rs4293393 MAF of 19% in the general population, we anticipated the need to collect a large number of affected individuals for the study. The further decrease in allele

Table 6. Best-fit multivariate model for individuals with ADTKD-*UMOD* using gender and *in vitro* score

Parameter	Observations (n)	Events	Reference category	Hazard ratio	C-statistic	P value
Gender	393	198	Male	0.53	0.61	0.002
<i>In vitro</i> score				1.5		0.00085

ADTKD-*UMOD*, autosomal dominant tubulo-interstitial kidney disease due to *UMOD* mutations.

Table 7. Univariate models for clinical characteristics for the WF cohort

Parameter	Observations (n)	Events	Reference category	Hazard ratio	C-statistic	P value
Weight	301	130		0.9967	0.545	0.23
BMI	300	130		0.9617	0.564	0.069
Smoking (active or former)	337	197	Nonsmoker	0.7185	0.533	0.17
Gout (y/h)	417	178	No	1.2549	0.52	0.29
Age of gout onset	209	110		0.9452	0.666	0.000053
Parental age ESKD	229	101		0.9701	0.629	0.0045
Family mean age ESKD	429	217		0.9706	0.619	0.009
Mother's age ESKD	111	53		0.9593	0.667	0.0017
Father's age ESKD	114	47		0.9816	0.559	0.23

BMI, body mass index; ESKD, end-stage kidney disease; WF, Wake Forest.

frequency resulted in a marked decrease in the number of individuals with the minor allele and hence a loss of statistical power for the study. As the rs4293393 minor SNP variant was not randomly distributed in the ADTKD-UMOD population, we were not able to perform a Mendelian randomization study. We did not find a difference in survival between families with major versus minor rs4293393-*mUMOD* haplotypes, which may have been the result of lack of statistical power, the fact that there was no difference, or the fact that families with milder disease due to minor allele rs4293393-*mUMOD* haplotypes were undetected.

We found that mutation class (e.g., loss or gain of polarity or a cysteine residue) was not correlated with the age of ESKD. This absence of correlation may have been because of the conservative statistical analysis, which adjusted for the large number of individuals in different families. An *in vitro* score reflecting the severity of the trafficking defect caused by specific *mUMOD* mutations was found to be a promising predictor of the age of ESKD. In addition, this finding points to enhanced transit of *mUMOD* through the ER as a potential therapeutic approach. [Supplementary Table S1](#) provides information on all *in vitro* scores, as well as the median age of ESKD for each mutation. Based on the *in vitro* score, we would predict that the type of mutation, but not the class of amino acid substitution (e.g., cysteine vs. noncysteine substitution) does have an effect on ESKD survival. Other investigators have also studied the interaction between genotype and phenotype in ADTKD-UMOD. Bollee and colleagues³ reported on 109 patients from 45 families with 37 distinct *UMOD* mutations and a median age of ESKD of 54. These authors found a high intrafamilial variability in the age of ESKD, with only a modest,

nonsignificant effect of the type of mutation on survival. In a review of the literature, Moskowitz and colleagues⁴ identified 202 patients from 74 families with 59 different *UMOD* mutations and a median age of ESKD of 56. Onset of ESKD was significantly earlier with mutations in the epidermal growth factor domains 2 and 3 (range 45–52 years) compared with the cysteine-rich domains (range 60–65 years) using a shared frailty model. The *in vitro* score is novel and should be considered a research test at this time. Further development and validation are required to assess its relevance as a clinical test that could be useful in predicting the age of ESKD for individuals with *de novo* mutations or from smaller families in which the age of ESKD is not well characterized.

Male gender was a significant predictor of worse renal outcomes, with a hazard ratio of 1.78, $P < 0.001$. This was similar to the finding of Moskowitz *et al.*⁴ of an increased risk of ESKD in men (hazard ratio 2.09, $P = 0.04$) in their cohort.

As part of this study, we were able to produce a catalog of *UMOD* mutations, including the median age of ESKD onset and *in vitro* score, which is included in [Supplementary Table S1](#) and available in an updated form online at <http://j.mp/2q7Fi8f>. We believe that this information will be helpful to clinicians working with families with ADTKD-UMOD.

A primary weakness of this article was the lack of power to better detect statistical differences among groups, a major obstacle in the study of rare diseases. Another weakness was the retrospective nature of the study and limited clinical data from the international cohort. For instance, information on gout was missing from many of the historically affected individuals, and this may have affected our ability to identify

Table 8. Multivariate model for the Wake Forest cohort

Parameter	Observations (n)	Events	Reference category	Hazard ratio	C-statistic	P value
Gender	429	217	Male	0.6380	0.634	0.0054
Family mean age ESKD				0.9591		<0.0001

ESKD, end-stage kidney disease.

significant findings. Formation of a registry of individuals with ADTKD who contribute genetic samples, as well as clinical information, will be helpful to overcome this obstacle in the future. In addition, we were not able to explain fully the interfamilial and intrafamilial variation in the age of ESKD onset.

In summary, we studied genetic and clinical factors associated with the age of ESKD onset. An *in vitro* score of mUMOD transit was a predictor of the age of onset of ESKD, as was the presence of gout, age of gout onset, and parental age of ESKD. The rs4293393 *UMOD* minor allele, associated with decreased uromodulin production, was underrepresented in families with ADTKD-UMOD.

DISCLOSURE

All the authors declared no competing interests.

ACKNOWLEDGMENTS

We thank all participating patients and families, and the referring physicians. We acknowledge Sebastiano Regina (San Luigi Gonzaga University Hospital) and Alessandra Cuccurullo (University of Turin) for genotyping, Alessandra Pelle (University of Turin) for genetic counseling, and Elena Pasqualetto (San Raffaele Scientific Institute) for *in vitro* studies.

This study was funded by National Institutes of Health (NIH)-National Institute of Diabetes and Digestive and Kidney Diseases R21 DK106584. Wake Forest also thanks the Black-Brogan Foundation for support. YMC was supported by NIH grants R01 DK105056A1, R03DK106451, and K08DK089015; The Assistant Secretary of Defense for Health Affairs endorsed by the Department of Defense, Award Number W81XWH-19-1-0320. PV, MŽ, and SK were supported by grant NV17-29786A from the Ministry of Health of the Czech Republic and by institutional programs of Charles University in Prague (UNCE/MED/007 and PROGRES-Q26/LF1); they thank The National Center for Medical Genomics (LM2015091) for help in genotyping. EO is supported by the Fonds National de la Recherche Luxembourg (6903109). OD is supported by the European Reference Network for Rare Kidney Diseases (ERKNet), project ID No. 739532; the National Centre for Competence in Research Kidney CH program; and the Swiss National Science Foundation 310030-189044. LR was supported by the Italian Society of Nephrology (SIN) under the "Adotta un progetto di ricerca" program, Telethon-Italy (GGP14263); the Ministry of Health of Italy (grant RF-2010-2319394 and RF-2016-02362623), Soli Deo Gloria.

SUPPLEMENTARY MATERIALS

Supplementary File (PDF)

Table S1. Clinical characteristics according to *UMOD* mutation.

Figure S1. Subgroup comparison of parental age of ESKD versus child's age of ESKD.

Figure S2. Histogram of difference in years between daughter's age of ESKD versus mother's age of ESKD.

Figure S3. Western blot analysis of the indicated uromodulin mutant isoforms stably expressed in MDCK cells.

Figure S4. Western blot analysis of the indicated uromodulin mutant isoforms transiently expressed in MDCK cells.

Supplementary Methods. Genetic evaluation and *UMOD* mutational sequencing, rs4293393 genotyping, rs4293393 and *UMOD* mutation phase determination, and *in vitro* score determination

Supplementary References.

REFERENCES

1. Bleyer AJ, Hart PS, Knoch S. Autosomal dominant tubulointerstitial kidney disease, UMOD-related. 2016. *GeneReviews [Internet]*. Seattle, WA: University of Washington, Seattle, 1993-2020.
2. Bleyer AJ, Woodard AS, Shihabi Z, et al. Clinical characterization of a family with a mutation in the uromodulin (Tamm-Horsfall glycoprotein) gene. *Kidney Int.* 2003;64:36-42.
3. Bollee G, Dahan K, Flamant M, et al. Phenotype and outcome in hereditary tubulointerstitial nephritis secondary to UMOD mutations. *Clin J Am Soc Nephrol.* 2011;6:2429-2438.
4. Moskowitz JL, Piret SE, Lhotta K, et al. Association between genotype and phenotype in uromodulin-associated kidney disease. *Clin J Am Soc Nephrol.* 2013;8:1349-1357.
5. Devuyst O, Olinger E, Weber S, Eckardt KU, et al. Autosomal dominant tubulointerstitial kidney disease. *Nat Rev Dis Primers.* 2019;5:60.
6. Vylet'al P, Kublova M, Kalbacova M, et al. Alterations of uromodulin biology: a common denominator of the genetically heterogeneous FJHN/MCKD syndrome. *Kidney Int.* 2006;70:1155-1169.
7. Scolari F, Caridi G, Rampoldi L, et al. Uromodulin storage diseases: Clinical aspects and mechanisms. *Am J Kidney Dis.* 2004;44:987-999.
8. Bernascone I, Vavassori S, Di PA, et al. Defective intracellular trafficking of uromodulin mutant isoforms. *Traffic.* 2006;7:1567-1579.
9. Rampoldi L, Caridi G, Santon D, et al. Allelism of MCKD, FJHN and GCKD caused by impairment of uromodulin export dynamics. *Hum Mol Genet.* 2003;12:3369-3384.
10. Williams SE, Reed AA, Galvanovskis J, et al. Uromodulin mutations causing familial juvenile hyperuricaemic nephropathy lead to protein maturation defects and retention in the endoplasmic reticulum. *Hum Mol Genet.* 2009;18:2963-2974.

11. Dahan K, Devuyt O, Smaers M, et al. A cluster of mutations in the UMOD gene causes familial juvenile hyperuricemic nephropathy with abnormal expression of uromodulin. *J Am Soc Nephrol*. 2003;14:2883–2893.
12. Serafini-Cessi F, Malagolini N, Hoops TC, Rindler MJ. Biosynthesis and oligosaccharide processing of human Tamm-Horsfall glycoprotein permanently expressed in HeLa cells. *Biochem Biophys Res Commun*. 1993;194:784–790.
13. Raffi H, Bates JM, Laszik Z, Kumar S. Tamm-Horsfall protein knockout mice do not develop medullary cystic kidney disease. *Kidney Int*. 2006;69:1914–1915.
14. Trudu M, Janas S, Lanzani C, et al. Common noncoding UMOD gene variants induce salt-sensitive hypertension and kidney damage by increasing uromodulin expression. *Nat Med*. 2013;19:1655–1660.
15. Vyletal P, Bleyer AJ, Knoch S. Uromodulin biology and pathophysiology - an update. *Kidney Blood Press Res*. 2010;33:456–475.
16. Bleyer AJ, Kidd K, Robins V, et al. Outcomes of patient self-referral for the diagnosis of several rare inherited kidney diseases. *Genet Med*. 2019;22:142–149.
17. Smith GD, Robinson C, Stewart AP, et al. Characterization of a recurrent in-frame UMOD indel mutation causing late-onset autosomal dominant end-stage renal failure. *Clin J Am Soc Nephrol*. 2011;6:2766–2774.
18. Karczewski KJF, Francioli LC, Tiao G, et al. Variation across 141,456 human exomes and genomes reveals the spectrum of loss-of-function intolerance across human protein-coding regions. *Nature*. 2020;581:434–443.

4.3 **An International Cohort Study of Autosomal Dominant Tubulointerstitial Kidney Disease due to *REN* Mutations Identifies Distinct Clinical Subtypes.**

Živná M, **Kidd K**, Zaidan M, Vyleťal P, Barešová V, Hodaňová K, Sovová J, Hartmannová H, Votruba M, Trešlová H, Jedličková I, Sikora J, Hůlková H, Robins V, Hnízda A, Živný J, Papagregoriou G, Mesnard L, Beck BB, Wenzel A, Tory K, Häeffner K, Wolf MTF, Bleyer ME, Sayer JA, Ong ACM, Balogh L, Jakubowska A, Łaszkiewicz A, Clissold R, Shaw-Smith C, Munshi R, Haws RM, Izzi C, Capelli I, Santostefano M, Graziano C, Scolari F, Sussman A, Trachtman H, Decramer S, Matignon M, Grimbert P, Shoemaker LR, Stavrou C, Abdelwahed M, Belghith N, Sinclair M, Claes K, Kopel T, Moe S, Deltas C, Knebelmann B, Rampoldi L, Knoch S, Bleyer AJ.

Kidney Int. 2020 Aug 1:S0085-2538(20)30838-3.

An international cohort study of autosomal dominant tubulointerstitial kidney disease due to *REN* mutations identifies distinct clinical subtypes

see commentary on page 1397



Martina Živná¹, Kendrah Kidd^{1,2}, Mohamad Zaidan³, Petr Vyletal¹, Veronika Barešová¹, Kateřina Hodaňová¹, Jana Sovová¹, Hana Hartmannová¹, Miroslav Votruba¹, Helena Trešlová¹, Ivana Jedličková¹, Jakub Sikora¹, Helena Hůlková¹, Victoria Robins², Aleš Hnízda⁴, Jan Živný⁵, Gregory Papagregoriou⁶, Laurent Mesnard⁷, Bodo B. Beck^{8,9}, Andrea Wenzel^{8,9}, Kálmán Tory^{10,11}, Karsten Häeffner¹², Matthias T.F. Wolf¹³, Michael E. Bleyer², John A. Sayer^{14,15,16}, Albert C.M. Ong¹⁷, Lídia Balogh¹¹, Anna Jakubowska¹⁸, Agnieszka Łaszkiwicz¹⁹, Rhian Clissold²⁰, Charles Shaw-Smith²⁰, Raj Munshi²¹, Robert M. Haws²², Claudia Izzì²³, Irene Capelli²⁴, Marisa Santostefano²⁵, Claudio Graziano²⁶, Francesco Scolari²³, Amy Sussman²⁷, Howard Trachtman²⁸, Stephane Decramer^{29,30,31}, Marie Maignon^{32,33}, Philippe Grimbert^{32,33,34}, Lawrence R. Shoemaker³⁵, Christoforos Stavrou³⁶, Mayssa Abdelwahed³⁷, Neila Belghith^{37,38}, Matthew Sinclair^{39,40}, Kathleen Claes^{41,42}, Tal Kopel⁴³, Sharon Moe⁴⁴, Constantinos Deltas⁵, Bertrand Knebelmann^{45,46,47}, Luca Rampoldi⁴⁸, Stanislav Kmoč^{1,2} and Anthony J. Bleyer^{1,2}

¹Research Unit of Rare Diseases, Department of Pediatric and Inherited Metabolic Disorders, First Faculty of Medicine, Charles University, Prague, Czech Republic; ²Section on Nephrology, Wake Forest School of Medicine, Winston-Salem, North Carolina, USA; ³Service de Néphrologie–Transplantation, Hôpital de Bicêtre, Le Kremlin Bicêtre, France; ⁴Department of Biochemistry, University of Cambridge, Cambridge, UK; ⁵Institute of Pathophysiology, First Faculty of Medicine, Charles University, Prague, Czech Republic; ⁶Center of Excellence in Biobanking and Biomedical Research, Molecular Medicine Research Center, University of Cyprus, Nicosia, Cyprus; ⁷Sorbonne Université, Urgences Néphrologiques et Transplantation Rénale, Assistance Publique–Hôpitaux de Paris (APHP), Hôpital Tenon, Paris, France; ⁸University of Cologne, Faculty of Medicine and University Hospital Cologne, Institute of Human Genetics, Cologne, Germany; ⁹University of Cologne, Faculty of Medicine and University Hospital Cologne, Center for Molecular Medicine Cologne (CMMC) and Center for Rare Diseases Cologne(ZSEK), Cologne, Germany; ¹⁰MTA-SE Lendület Nephrogenetic Laboratory, Semmelweis University, Budapest, Hungary; ¹¹First Department of Pediatrics, Semmelweis University, Budapest, Hungary; ¹²Department of General Pediatrics, Adolescent Medicine and Neonatology, Medical Center, Faculty of Medicine, Universitätsklinikum Freiburg, Freiburg, Germany; ¹³Pediatric Nephrology, University of Texas Southwestern Medical Center, Dallas, Texas, USA; ¹⁴Renal Services, The Newcastle Hospitals NHS Foundation Trust, Newcastle upon Tyne, UK; ¹⁵Translational and Clinical Research Institute, Faculty of Medical Sciences, Newcastle University, Newcastle upon Tyne, UK; ¹⁶NIHR Newcastle Biomedical Research Centre, Newcastle University, Newcastle upon Tyne, UK; ¹⁷Kidney Genetics Group, Academic Nephrology Unit, Department of Infection, Immunity and Cardiovascular Disease, University of Sheffield Medical School, Sheffield, UK; ¹⁸Department of Pediatric Nephrology Medical University Wrocław, Poland; ¹⁹Laboratory of Molecular and Cellular Immunology, Hirsfeld Institute of Immunology and Experimental Therapy, Polish Academy of Sciences, Wrocław, Poland; ²⁰Exeter Kidney Unit, Royal Devon and Exeter NHS Foundation Trust, Exeter, Devon, UK; ²¹Division of Nephrology, Department of Pediatrics, Seattle Children's Hospital, University of Washington, Seattle, Washington, USA; ²²Pediatrics–Nephrology, Marshfield Medical Center, Marshfield, Wisconsin, USA; ²³Division of Nephrology and Dialysis, Department of Medical and Surgical Specialties, Radiological Sciences, and Public Health, University of Brescia and Montichiari Hospital, Brescia, Italy; ²⁴Department of Experimental Diagnostic and Specialty Medicine, Nephrology, Dialysis and Renal Transplant Unit, S. Orsola Hospital, University of Bologna, Bologna, Italy; ²⁵Division of Nephrology, Ospedale Sant'Orsola–Malpighi, Bologna, Italy; ²⁶Medical Genetics Unit, Policlinico S. Orsola–Malpighi, Bologna, Italy; ²⁷Department of Medicine, Division of Nephrology, University of Arizona Health Sciences Center, Tucson, Arizona, USA; ²⁸Division of Nephrology, Department of Pediatrics, New York University School of Medicine, New York, New York, USA; ²⁹Pediatric Nephrology, Centre Hospitalier Universitaire de Toulouse (CHU de Toulouse), Toulouse, France; ³⁰France Rare Renal Disease Reference Centre (SORARE), Toulouse, France; ³¹Centre Hospitalier Universitaire de Toulouse (CHU de Toulouse), Toulouse, France; ³²AP-HP (Assistance Publique–Hôpitaux de Paris), Nephrology and Renal Transplantation Department, Institut Francilien de Recherche en Néphrologie et Transplantation (IFRNT), Groupe Hospitalier Henri-Mondor/Albert-Chenevier, Créteil, France; ³³Université Paris-Est-Créteil, (UPEC), DHU (Département Hospitalo-Universitaire) VIC (Virus-Immunité-Cancer), IMRB (Institut Mondor de Recherche Biomédicale), Equipe 21, INSERM U 955, Créteil, France; ³⁴AP-HP (Assistance Publique–Hôpitaux de Paris), CIC-BT 504, Créteil, France; ³⁵Division of Nephrology, Department of Pediatrics, University of Florida, Gainesville, Florida, USA; ³⁶Department of Nephrology, Evangelismos Private Hospital, Pafos, Cyprus; ³⁷Laboratory of Human Molecular Genetics, Faculty of Medicine, University of Sfax, Sfax, Tunisia; ³⁸Medical Genetics Department of Hedi Chaker Hospital, Sfax, Tunisia; ³⁹Division of Nephrology, Department of Medicine, Duke University School of Medicine, Durham, North Carolina, USA; ⁴⁰Department of Pediatrics, University of Washington, Seattle, Washington, USA; ⁴¹Department of Pediatrics, Marshfield Medical Center, Marshfield, Wisconsin, USA; ⁴²Department of Pediatrics, Marshfield Medical Center, Marshfield, Wisconsin, USA; ⁴³Department of Pediatrics, Marshfield Medical Center, Marshfield, Wisconsin, USA; ⁴⁴Department of Pediatrics, Marshfield Medical Center, Marshfield, Wisconsin, USA; ⁴⁵Department of Pediatrics, Marshfield Medical Center, Marshfield, Wisconsin, USA; ⁴⁶Department of Pediatrics, Marshfield Medical Center, Marshfield, Wisconsin, USA; ⁴⁷Department of Pediatrics, Marshfield Medical Center, Marshfield, Wisconsin, USA; ⁴⁸Department of Pediatrics, Marshfield Medical Center, Marshfield, Wisconsin, USA

Correspondence: Anthony J. Bleyer, Section on Nephrology, Wake Forest School of Medicine, Winston-Salem, North Carolina 27157, USA. E-mail: ableyer@wakehealth.edu

Received 23 April 2020; revised 9 June 2020; accepted 11 June 2020; published online 1 August 2020

Carolina, USA;⁴⁰Duke Clinical Research Institute, Durham, North Carolina, USA;⁴¹Department of Nephrology and Renal Transplantation, University Hospitals Leuven, Leuven, Belgium;⁴²Laboratory of Nephrology, Department of Microbiology and Immunology, Katholieke Universiteit (KU) Leuven, Leuven, Belgium;⁴³Nephrology Division, University of Montreal Hospital Centre, Hopital Saint-Luc, Montréal, Québec, Canada;⁴⁴Division of Nephrology, Indiana University School of Medicine, Indianapolis, Indiana, USA;⁴⁵Department of Nephrology–Transplantation, Necker Hospital, APHP, Paris, France;⁴⁶Paris Descartes University, Sorbonne Paris Cité, Paris, France;⁴⁷Département Biologie cellulaire, INSERM U1151, Institut Necker Enfants Malades, Paris, France; and⁴⁸Molecular Genetics of Renal Disorders, Division of Genetics and Cell Biology, IRCCS San Raffaele Scientific Institute, Milan, Italy

There have been few clinical or scientific reports of autosomal dominant tubulointerstitial kidney disease due to *REN* mutations (ADTKD-REN), limiting characterization. To further study this, we formed an international cohort characterizing 111 individuals from 30 families with both clinical and laboratory findings. Sixty-nine individuals had a *REN* mutation in the signal peptide region (signal group), 27 in the prosegment (prosegment group), and 15 in the mature renin peptide (mature group). Signal group patients were most severely affected, presenting at a mean age of 19.7 years, with the prosegment group presenting at 22.4 years, and the mature group at 37 years. Anemia was present in childhood in 91% in the signal group, 69% prosegment, and none of the mature group. *REN* signal peptide mutations reduced hydrophobicity of the signal peptide, which is necessary for recognition and translocation across the endoplasmic reticulum, leading to aberrant delivery of preprorenin into the cytoplasm. *REN* mutations in the prosegment led to deposition of prorenin and renin in the endoplasmic reticulum-Golgi intermediate compartment and decreased prorenin secretion. Mutations in mature renin led to deposition of the mutant prorenin in the endoplasmic reticulum, similar to patients with ADTKD-*UMOD*, with a rate of progression to end stage kidney disease (63.6 years) that was significantly slower vs. the signal (53.1 years) and prosegment groups (50.8 years) (significant hazard ratio 0.367). Thus, clinical and laboratory studies revealed subtypes of ADTKD-REN that are pathophysiologically, diagnostically, and clinically distinct.

Kidney International (2020) 98, 1589–1604; <https://doi.org/10.1016/j.kint.2020.06.041>

KEYWORDS: autosomal dominant tubulointerstitial kidney disease; characterization; mutation; prosegment; renin; signal peptide

Copyright © 2020, International Society of Nephrology. Published by Elsevier Inc. All rights reserved.

Autosomal dominant tubulointerstitial kidney disease (ADTKD) is characterized by autosomal dominant inheritance, bland urinary sediment, and slowly progressive chronic kidney disease (CKD), leading to end-stage kidney disease (ESKD) at between 30 and 80 years of age.¹ Although ADTKD was described in <10 families before 1990, genetic testing has led to increased detection, with over 300 families reported.^{2–5} ADTKD due to mutations in the *REN* gene encoding renin (ADTKD-REN) is one of the least common forms of ADTKD,⁵ with only 8 families and 28 individuals reported before 2020.^{5–11}

Renin is a hormone primarily produced in the kidney that is requisite for tubulogenesis¹² and embryonic kidney formation.¹³ The renin–angiotensin system is a key modulator of blood pressure¹⁴ and CKD progression.¹⁵ Renin biosynthesis constitutes the first enzymatic steps in the renin–angiotensin system. The human renin precursor is synthesized in the juxtaglomerular cells of the macula densa as a 406-amino-acid preprorenin, composed of a 23-amino-acid N-terminal signal peptide, a 43-amino-acid prosegment, and a 340-amino-acid mature renin peptide.¹⁶ During biosynthesis, the signal peptide mediates insertion of the nascent preprorenin into the translocation channel in the endoplasmic reticulum (ER) and initiates cotranslational translocation of preprorenin into the ER lumen, where glycosylation and proteolytic processing of the nascent preprorenin occur, conditioning further transit of prorenin and renin through the constitutive and regulated secretory pathways.¹⁷

In ADTKD-REN, heterozygous *REN* mutations lead to decreased synthesis of prorenin and renin, resulting in mild hyperkalemia, anemia, hyperuricemia, and a predisposition to the development of acute kidney injury.⁵ *REN* mutations have been reported in the segment of the *REN* gene encoding the signal peptide^{5–8} and the mature renin protein.^{9,10} Mutations in the prosegment—a segment of the gene after the signal peptide that assists in protein folding—have not been reported. The lack of case reports of ADTKD-REN has prevented clinical correlation with mutation type and identification of risk factors for progression to ESKD.

To better characterize this condition, we performed an international retrospective cohort study and collected clinical and genetic data on 111 individuals from 30 families with heterozygous *REN* mutations. We performed laboratory investigations on 10 representative mutations (5 in the signal peptide, 3 in the prosegment, and 2 in mature renin) and characterized 2 missense *REN* variants of unknown significance found in African Americans, p.P8A and p.R33W.

RESULTS

Of the 111 individuals from 30 families (Table 1, and Supplementary Figures S1 and S2), 69 (62%) individuals had a mutation in the signal peptide, 27 (24%) in the prosegment, and 15 (14%) in the mature renin peptide. A mutation in p.S45N was identified in 1 individual with ADTKD of unknown cause. This mutation did not segregate with disease and was determined to be nonpathogenic; it was included as a control for laboratory investigations. While searching variant databases, we noticed 2 additional rare missense variants (AA-*REN* variants) found specifically in African Americans, a

Table 1 | Distribution of heterozygous mutations causing ADTKD-REN mutations by mutation group and family

Mutation group	Nucleotide change	Mutation	Families (n)	Individuals (n)
Signal	c.28T>C	p.Trp10Arg	1	5
	c.35T>C	p.Leu12Pro	1	1
	c.38T>A	p.Leu13Gln	1	1
	c.45_47del	p.delLeu16	6	28
	c.47T>C	p.Leu16Pro	3	11
	c.47T>G	p.Leu16Arg	2	9
	c.49T>C	p.Trp17Arg	4	9
	c.58T>C	p.Cys20Arg	3	5
Signal total			21	69
Prosegment	c.77C>T	p.Thr26Ile	2	19
	c.116T>A	p.Met39Lys	1	5
	c.142G>A	p.Glu48Lys	1	3
Prosegment total			4	27
Mature	c.973T>C	p.Cys325Arg	1	3
	c.1097T>A	p.Ile366Asn	1	2
	c.1142T>C	p.Leu381Pro	1	5
	c.1172C>G	p.Thr391Arg	1	4
	c.255G>C	p.Gln85His	1	1
Mature total			5	15
Total			30	111

group with an increased prevalence of low-renin hypertension and CKD.¹⁸ These variants encode p.P8A in the signal peptide and p.R33W in the prosegment of preprorenin. Their allelic frequencies in African Americans are 0.007 and 0.001, respectively.

Effect of mutation class on clinical characteristics

Presentation. After excluding patients with missing data ($n = 14$) and those identified by genetic screening ($n = 16$), 81 patients were available for analysis (Table 2, and Supplementary Table S1, which shows clinical characteristics according to each mutation). Patients in the signal group were the most severely affected and presented at the youngest age. The mean age of clinical presentation was 19.7 ± 15.7 years for the signal group, 22.4 ± 20.2 years for the prosegment group, and 37.0 ± 12.4 years for the mature group ($P < 0.001$ for comparison of the mature group vs. signal and prosegment groups). Only patients in the signal group presented with acute kidney injury (10%) or acidosis, anemia, and kidney failure (13%). Thirty-one percent of patients in the signal group and 50% of patients in the prosegment group presented with anemia. Patients in the mature group presented only with gout (75%) or CKD (25%). The mean age of presentation was similar for men and women (19.3 ± 13.7 vs. 19.9 ± 19.4 years, $P = 0.6$).

Kidney function. Kidney function was less severely affected in the mature group vs. the signal and prosegment groups. Figure 1a displays all estimated glomerular filtration (eGFR) values obtained for the entire cohort of patients. An eGFR of 10 ml/min per 1.73 m^2 was assigned at the age of ESKD.

Patients in the signal and prosegment groups presented much earlier in life. At earliest clinical presentation, the majority of eGFR readings in these groups were $<60 \text{ ml/min per } 1.73 \text{ m}^2$, suggesting that decreased kidney function is present at birth in most patients. Despite early decreased function, eGFR values tended to remain relatively stable during childhood and through adolescence. Figure 1b shows data for 13 children in the signal group with multiple eGFR measurements. In almost all cases, eGFR remained steady with minimal decline, including 1 patient whose eGFR remained stable at approximately 30 ml/min per 1.73 m^2 from ages 2 through 16 (p.C20R with red marking in Figure 1b). Another patient (p.M39K) presented during infancy with an eGFR of 19 ml/min per 1.73 m^2 and had a relatively stable eGFR through childhood before proceeding to renal replacement therapy at 15 years of age, being the only individual reaching ESKD before age 30. After adolescence, there was, in general, a slow decline in eGFR in the signal and prosegment groups (Figure 1a). The median age of ESKD was 57 years in the signal group, 62 years in the prosegment group, and 68 years in the mature group (Figure 2). Patients in the mature group had no laboratory values until age 20, due to milder

Table 2 | Characteristics according to mutation group

	Signal	Prosegment	Mature	P value
Individuals	69 (62)	27 (24)	15 (14)	
Families	21 (70)	4 (13)	5 (17)	
Age at presentation ^a	23 (39)	11 (61)	0	0.003
<10 yr				
Age at presentation ^a	19 (32)	2 (11)	0	0.02
10 to <20 yr				
Age at presentation ^a	17 (29)	5 (28)	12 (100)	<0.001
>20 yr				
Age at presentation, yr ^{a,b}	19.7 ± 15.7	22.4 ± 20.2	37.0 ± 12.4^b	
Reason for presentation ^{a,b}				0.014
Acute kidney injury	5/55 (10)	0	0	
Anemia, acidosis, kidney failure	7/55 (13)	0	0	
Anemia	17/55 (31)	7/14 (50)	0	
Chronic kidney disease	12/55 (22)	2/14 (14)	3/12 (25)	
Gout	14/55 (25)	5/14 (36)	9/12 (75)	
Total, n	55	14	12	
Anemia as child	39/43 (91)	11/16 (69)	0/7 (0)	<0.001
Gout developed during course of disease	31/55 (56)	13/20 (65)	9/14 (64)	0.74
Age at first gout attack, yr	29.7 ± 9.9	25.7 ± 8.2	32.9 ± 11.2	0.4
Age at ESKD onset, yr	53.1 ± 10.6	50.8 ± 17.6	63.6 ± 7.6^b	

ESKD, end-stage kidney disease.

^aExcluding individuals who presented for asymptomatic genetic screening. Six of 61 (10%) patients in the signal group, 7 of 21 (33%) in the prosegment group, and 3 of 15 (20%) in the mature group were identified by asymptomatic genetic screening.

^b $P < 0.001$ vs. the other 2 groups.

Data are n (%) or mean \pm SD, unless otherwise noted.

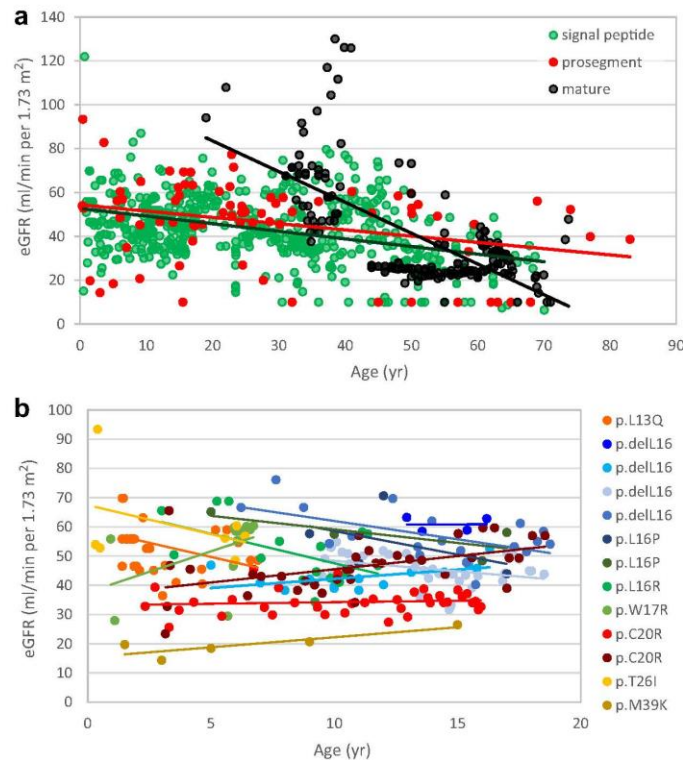


Figure 1 | Age versus estimated glomerular filtration (eGFR) rate in ADTKD-REN patients. (a) All eGFR measurements for each group are included (green, signal group; red, prosegment group; black, mature group). A best-fit line is included for each group. Patients in the mature group presented later in life and had normal kidney function at the earliest measurement. Patients in the signal and prosegment groups often presented early in life, and eGFR was significantly decreased from the time of first measurement in most patients. (b) eGFR values in 13 children with longitudinal follow-up from the signal group. Each child is represented by a different color with a best-fit line, and the *REN* mutation is given in the legend. Despite having low eGFR values at the earliest measurement, kidney function remained stable until 20 years of age in most patients.

manifestations (Figure 1a). Patients in the mature group presenting at this age appeared to have normal kidney function.

To evaluate risk factors for ESKD progression, univariate Cox proportional hazards models were created, with the event being age of ESKD. Patients in the mature group had a significantly decreased risk of developing ESKD over time as compared with the signal and prosegment groups combined, with a hazard ratio of 0.37 ($P = 0.023$) (Table 3 and Figure 2). In other univariate models, anemia in childhood (hazard ratio 2.82, $P = 0.03$) (Table 3 and Figure 3) was significantly associated with an earlier age of ESKD, whereas gender was not associated with progression to ESKD. The best-fit Cox proportional hazards model included only anemia in childhood (Table 3 and Figure 3).

Anemia. Figure 4a shows hemoglobin levels in patients not on erythropoietin. The lowest hemoglobin value was 7.5 g/dl. The mean hemoglobin levels were 9.6 ± 1.04 g/dl for those <10 years, 10.1 ± 1.1 g/dl for those 10 to <15 years,

and 10.5 ± 1.2 g/dl for those 15 to <20 years of age. Females were more likely to have anemia as children (97% vs. 46%, $P = 0.005$) and have lower hemoglobin levels (Table 4 and Figure 4a). Hemoglobin levels in women tended to remain low over time, whereas, in men, hemoglobin levels appeared to rise after age 20. For 14 children who never received erythropoietin, the mean hemoglobin level was 9.8 ± 1.2 g/dl (range 7.4–13.8 g/dl) for children who received erythropoietin, whereas for those not receiving erythropoietin the mean hemoglobin level was 10.1 ± 1.3 g/dl (range 7.6–12.6 g/dl).

Hyperkalemia and acidemia. Hyperkalemia was present but rarely reached life-threatening levels. Figure 4 shows serum potassium values according to age (Figure 4b) and eGFR (Figure 4c). Serum bicarbonate levels vs. age are depicted in Figure 4d. Serum bicarbonate values were frequently <24 mEq/l.

Gout. In individuals not taking allopurinol or febuxostat, males had a higher mean serum urate level than women (9.4

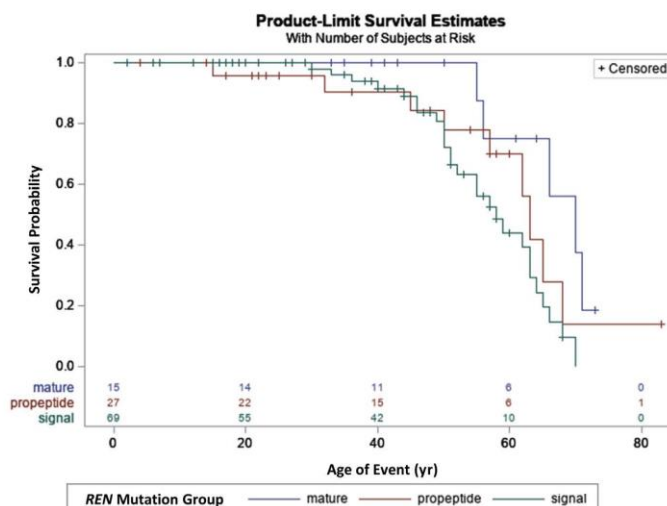


Figure 2 | End-stage kidney disease (ESKD) survival in ADTKD-REN individuals according to REN mutation group. The analysis included 111 individuals. An event was defined as starting dialysis or receiving a transplant. Censoring occurred if the individual had not reached ESKD by the end of the study period. Patients in the mature group had a later age of onset of ESKD compared with the signal and prosegment groups (hazard ratio = 0.237, $P = 0.023$).

± 2.7 vs. 7.7 ± 1.6 mg/dl, $P = 0.02$) and were more likely to have gout (49.3% vs. 39.5%, $P < 0.01$).

Renin levels. Plasma renin levels were low, with the mean random plasma renin activity (normal range 2.9 to 24 ng/ml per hour) 0.5 ± 0.8 ng/ml per hour in the signal group ($n = 18$), 0.5 ± 0.6 ng/ml per hour in the prosegment group ($n = 4$), and 0.8 ± 0.7 ng/ml per hour in the mature group ($n = 5$).

Fludrocortisone. Fludrocortisone was administered to 2 patients consistently and in 7 patients for a short period of time. There were no adverse effects from fludrocortisone. In 1 patient, the drug was taken consistently from age 11 onward, and in another patient from age 13 (Figure 5). The serum potassium values were lower in 9 individuals while taking versus not taking fludrocortisone (4.37 ± 0.54 vs. 4.77 ± 0.55 mEq/l, $P < 0.01$). The serum bicarbonate values were also higher (25.9 ± 2.3 vs. 23.7 ± 3.5 mEq/l, $P = 0.003$).

In silico analysis. Figure 6a displays the REN mutations identified in ADTKD families. Except for the p.T26I and the nonpathogenic p.S45N, all amino acid residues at mutation sites were absolutely conserved across species (Figure 6b). SignalP 4.1 prediction software¹⁹ indicated that all signal peptide mutations except p.C20R decreased the cleavage site prediction scores (C-score) (Figure 6c), suggesting a decrease in the efficacy of the signal peptidase-mediated release of the signal peptide from preprorenin. Scores for the AA_REN p.P8A variant were similar to those of wild-type (Figure 6c). The mutations in the prosegment, including the AA_REN variant p.R33W, are categorized by the Mendelian Clinically Applicable Pathogenicity classifier²⁰ as either likely benign (p.T26I, p.M39K, and p.S45N [nonpathogenic]) or possibly

pathogenic (p.R33W). Mutations in mature renin (p.C325R and p.I366N) are classified as possibly pathogenic (Figure 6d).

All mutations have significant effects on prorenin structure (Figure 7) and may modulate renin activity by affecting the folding, constitutive secretion, and proteolytic processing of prorenin.^{21–23}

Functional studies of identified REN variants

Wild-type and mutant proteins were transiently expressed in human embryonic kidney 293 cells (Figure 8). Western blot and immunodetection of corresponding proteins showed that the wild-type protein was present in the cell lysate in 3 major forms (Figure 8a) corresponding to preprorenin (45 kDa), prorenin (47 kDa), and renin (43 kDa), with preprorenin being less abundant. Only prorenin was detected in the culture media (Figure 8b). Except for the p.L16del mutation that allows partial translocation, processing, and secretion, proteins with other mutations in the signal peptide were present

Table 3 | Proportional hazards models including all individuals, with event being age of ESKD

Model	Risk	Reference	Hazard ratio	P value
Univariate Mutation affecting mature renin		Mutations affecting signal peptide and prosegment	0.367	0.023
Univariate Anemia in childhood		No anemia in childhood or unknown	2.82	0.003
Univariate Male		Female	0.92	0.80

ESKD, end-stage kidney disease. The univariate model showing anemia in childhood was also the best-fit multivariate model.

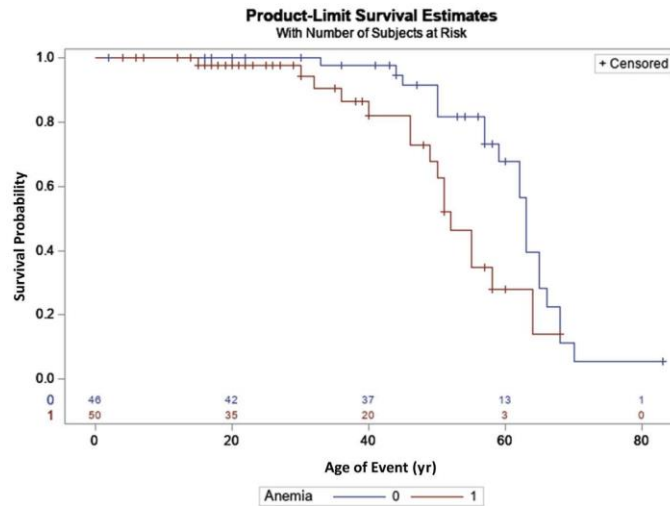


Figure 3 | End-stage kidney disease (ESKD) survival according to presence of anemia in childhood. The analysis included 111 ADTKD-REN individuals. An event was defined as starting dialysis or receiving a transplant. Censoring occurred if the individual had not reached ESKD by the end of the study period. A diagnosis of anemia in childhood was associated with a worse prognosis (hazard ratio = 2.82, $P = 0.03$).

in cell lysates, mostly in the form of prorenin, with no prorenin or renin detected in the culture media. Proteins with mutations p.T26I and p.M39K in the prosegment were

present in cell lysates in all 3 forms similar to the wild-type protein, whereas the nonpathogenic p.S45N was present mostly in the form of prorenin. Prosegment mutations

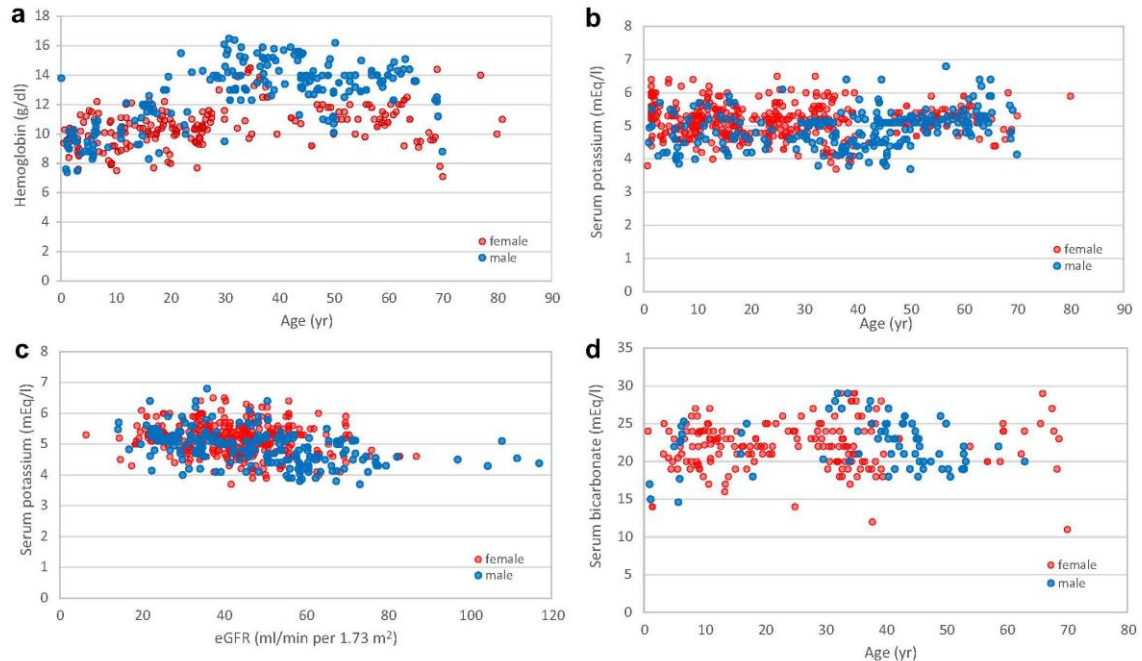


Figure 4 | Hemoglobin, hyperkalemia, and acidemia in ADTKD-REN patients. (a) Hemoglobin values according to age. For females, hemoglobin values were low throughout the period of measurement. For males, hemoglobin values began to rise at 20 years of age. (b) Serum potassium values according to age. Values remained consistent over time. (c) Serum potassium according to estimated glomerular filtration rate (eGFR). (d) Serum bicarbonate values according to age. Many of the serum bicarbonate values were <24 mEq/l.

Table 4 | Characteristics of presentation according to gender for patients with signal peptide or prosegment mutations

	Female	Male	P value
Individuals, n	44	52	0.41
Age at presentation ^a <10 yr	18/35 (48.6)	17/43 (39.5)	0.42
Age at presentation ^a 10 to <20 yr	9/35 (25.7)	12/43 (27.9)	0.85
Age at presentation ^a >20 yr	9/35 (25.7)	13/43 (30.2)	0.66
Age at presentation, yr	19.9 ± 19.4	19.3 ± 13.7	0.6
Anemia as child	31/32 (96.7)	19/27 (45.8)	0.005
Gout	15/38 (39.5)	29/37 (49.3)	0.0006
Age at first gout attack, yr	30.3 ± 9.6	27.8 ± 9.7	0.45
Age at ESKD onset, yr	50.1 ± 11.4	55.8 ± 10.5	0.25
Serum potassium, mEq/l	5.1 ± 0.5	5.1 ± 0.6	0.75
Serum bicarbonate, mEq/l	21.3 ± 0.4	22.2 ± 2.5	0.38
Serum urate without urate-lowering therapy, mg/dl	7.7 ± 1.6	9.4 ± 2.7	0.02

ESKD, end-stage kidney disease.

^aExcluding individuals who presented for asymptomatic genetic screening.

Data are n (%) or mean ± SD, unless otherwise noted.

affected secretion of p.M39K prorenin into culture media, but secretion of p.T26I and p.S45N was unaffected. Proteins with mutations in the mature renin were present in cell lysate predominantly as prorenin and were not secreted into culture media. Proteins with AA_REN variants in the signal peptide (p.P8A) or prosegment (p.R33W) showed similar profiles to wild-type protein in cell lysates. The mutation p.R33W affected secretion of prorenin into culture media (Figure 8a and b). Quantitative immunoradiometric assay (Figure 8c and d) showed that mutations in the signal peptide either significantly reduced (p.L16del) or entirely prevented renin and prorenin synthesis in cells and their secretion into culture media. Mutations in the prosegment had either no effect or a marginal effect (p.M39K) on renin and prorenin synthesis but affected secretion of p.T26I and p.M39K into culture media. Secretion of nonpathogenic p.S45N was unaffected. Mutations in the mature renin led to the synthesis of prorenin and renin that were either inactive or undetectable by the antibody used in the assay. The AA_REN variant p.P8A had no effect on renin and prorenin synthesis in cells and secretion of prorenin and renin into the culture media. For the AA_REN

variant p.R33W, there was reduced secretion of prorenin into the culture media (Figure 8c and d). Proteolytic activity assay showed that mutations in the signal peptide either reduced (p.L16del) or entirely abolished renin activity in culture media. Mutations in the prosegment led either to a production of proteolytically “hyperactive” prorenin (p.M39K) or reduced the activity of renin in the culture media (p.T26I, p.S45N). Mutations in the mature renin abolished production of active renin. The AA_REN variant p.P8A had no effect on the proteolytic activity of secreted renin and prorenin. The AA_REN variant p.R33W reduced renin activity via low prorenin secretion (Figure 8e and f). Mutated proteins had altered intracellular localization (Figure 9, and Supplementary Figures S3 and 4A). Wild-type protein was present in coarsely granular structures that were localized in the cytoplasm and in the lysosome-associated membrane protein-2 (LAMP-2)-positive lysosomal-like structures. Proteins with signal peptide mutations demonstrated mostly diffuse cytoplasmic staining. Proteins with prosegment mutations were localized mainly to the ER intermediate compartment. Proteins with mutations in the mature renin formed intracellular clumps

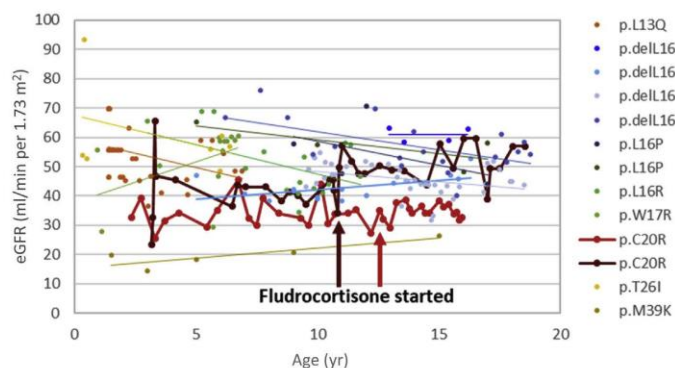


Figure 5 | ADTKD-REN treatment with fludrocortisone. Thirteen young patients in the signal (n = 11) and prosegment (n = 2) groups with mutations are listed in the column at right. The patient denoted with burgundy-colored marking (p.C20R) began fludrocortisone at 11 years of age, with an increase in estimated glomerular filtration rate (eGFR) that was sustained. The patient denoted with red-colored marking (p.C20R) started fludrocortisone at age 13.

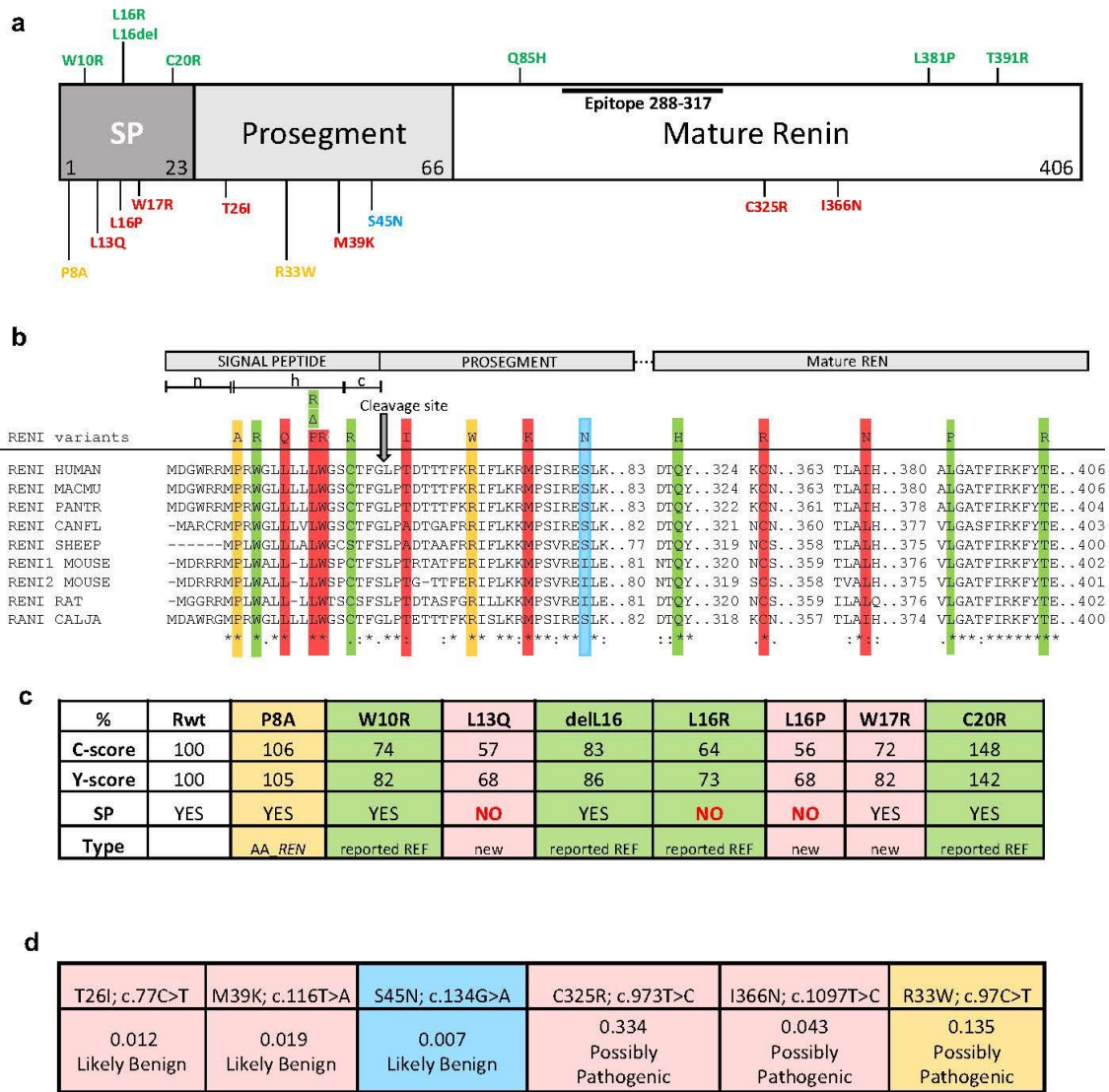


Figure 6 | In silico analysis of REN variants. (a) Preprorenin, a precursor of prorenin and renin, consists of (i) the signal peptide (SP) essential for targeting and insertion of the synthesized protein into the endoplasmic reticulum (ER) membrane; (ii) the prosegment that determines the biosynthesis, cellular trafficking, and enzymatic activity; and (iii) the mature enzymatically active renin that is formed upon the proteolytic cleavage of prorenin. Novel pathogenic mutations identified and characterized in this study are shown in red. Previously reported dominant mutations associated with ADTKD are shown in green. The p.S45N is considered nonpathogenic and is shown in blue. Variants of unknown significance identified in African American variants are shown in yellow. Epitope 288–317 denotes the protein segment recognized by the anti-preprorenin antibody used in this study. The n-, h-, and c-regions, respectively, denote stretches of positively charged amino acids (n-region), hydrophobic amino acids (h-region) essential for targeting and insertion of the signal peptide into ER membrane, and polar amino acids (c-region), forming a recognition site for the signal peptidase that releases translocated preproprotein from its ER membrane–anchored signal peptide. (b) Amino acids conservation across mutated segments of REN in higher mammals. Asterisks (*) indicate amino acid residues that are absolutely conserved, a colon (:) indicates residues with strong conservation, and a dot (.) indicates residues with weak conservation between species. (c) Computational prediction by the SignalP 4.1 server of the impact of missense REN mutations located in the signal peptide on the conformation of the signal peptide cleavage site location (C-score) and on the sequence characteristics of the signal peptide (Y-score). SP denotes presence (yes/no) of the signal peptidase cleavage site within the given sequence. The first 60 N-terminal amino acids of REN were used for this calculation. (d) Computational prediction by Mendelian Clinically Applicable Pathogenicity score of the pathogenicity of missense REN mutations located in the propeptide and mature renin.

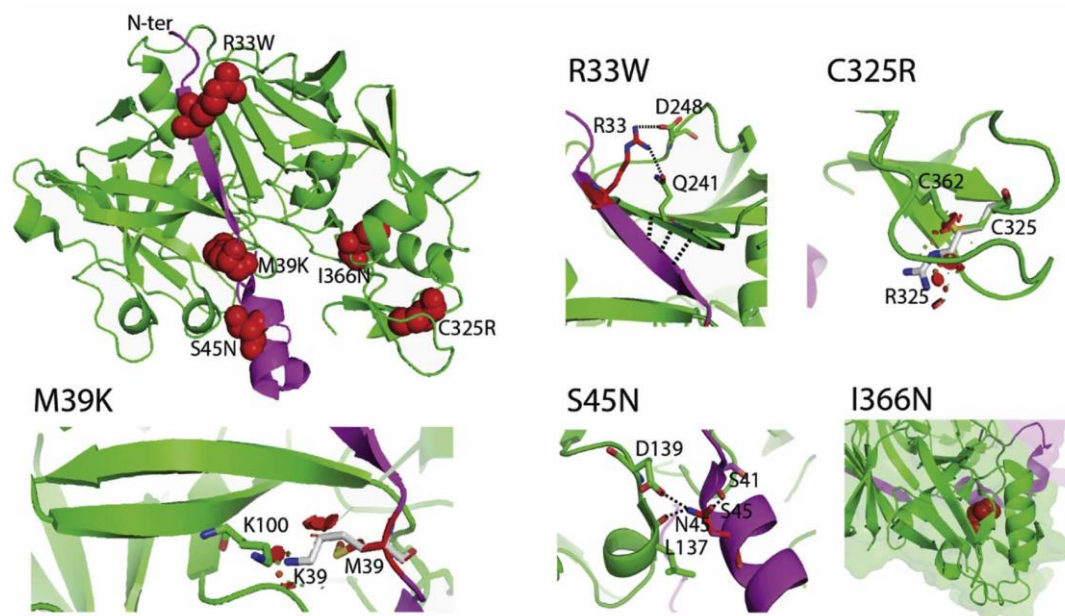


Figure 7 | Structural topology and impact of prosegment and *REN* mutations. The crystal structure of prorenin (PDB ID 3VCM) was used for modeling. The prorenin segment (amino acid residues 24–66) and the renin core (amino acid residues 67–406) are colored in magenta and green, respectively. The location of mutated residues is shown in the full structural model using red spheres. The effects of each mutation are illustrated in detail in individual images. Mutated residues and their interactions are highlighted as sticks and dashed lines. The mutation p.R33W loses polar contacts with p.Q241 and p.D248. Possible compensatory interactions between the proximal 2 β sheets are highlighted as 3 dashed lines. These changes decrease affinity between prorenin and renin. The mutation p.M39K causes steric clashes and charge repulsion with K100, resulting in decreased affinity between prorenin and renin. The nonpathogenic mutation p.S45N changes the interaction network, with p.S45 interacting with p.S41, and with p.N45 interacting with p.L137 and p.D139. These changes increase affinity due to a changed interaction network. The mutation p.C325R disrupts a disulfide bridge (highlighted as sticks), and incorporation of the arginine residue causes steric clashes (shown as red areas). The mutation p.I366N results in the loss of hydrophobic contacts (shown by red spheres) in the renin core.

localized in the ER (Figure 9, and Supplementary Figures S4 and S5). There was little renin staining in the Golgi apparatus for wild-type and *REN* mutations (Supplementary Figure S6). Wild-type protein and proteins with prosegment mutations were localized in lysosomes, whereas proteins with signal peptide mutations (except for p.L16del) and proteins with mutations in the mature renin were not (Supplementary Figure S7). All functional data are summarized in Table 5.

DISCUSSION

In this work we describe distinct clinical and pathophysiologic differences (Figure 10) in signal, prosegment, and mature peptide mutations of the *REN* gene in a cohort of 111 patients from 30 families with ADTKD-REN.

Patients with mutations in the signal peptide region were the most severely affected. One third of the patients presented before 10 years of age, with 10% having acute kidney injury and 13% presenting with anemia, acidosis, and kidney failure. The mean age of presentation was lower than in the other 2 groups (19.7 ± 15.7 vs. 22.4 ± 20.2 years and 37.0 ± 12.4 years, respectively). We demonstrated that transiently expressed proteins with mutations in the signal peptide lead

to proteosynthesis of prorenin that, according to immunofluorescence studies, is probably located in the cytoplasm or faces the cytoplasmic side of the ER or the ER intermediate compartment membranes. This phenomenon has been described previously in a case of signal peptide mutations of preproinsulin leading to β -cell failure and autosomal dominant diabetes,^{24,25} and in a mutation in the preproparathyroid hormone (*PTH*) gene, resulting in familial isolated hypoparathyroidism.²⁶ The effects of aberrant renin production not only resulted in manifestations of clinical renin deficiency but likely also affected normal renal embryogenesis, resulting in decreased kidney function at birth. The presence of significantly decreased renin activity in the setting of a heterozygous mutation was likely due to the mutated protein blocking the translocon and affecting synthesis of functional renin from the wild-type allele, a phenomenon that has been observed in ADTKD caused by mutations of translocon subunit alpha 1 (*SEC61A1*)⁴ or in preproinsulin signal peptide mutations, resulting in permanent neonatal diabetes despite the presence of a wild-type insulin allele.²⁷

Sixty-one percent of individuals in the prosegment group presented at <10 years of age (61%), often presenting with

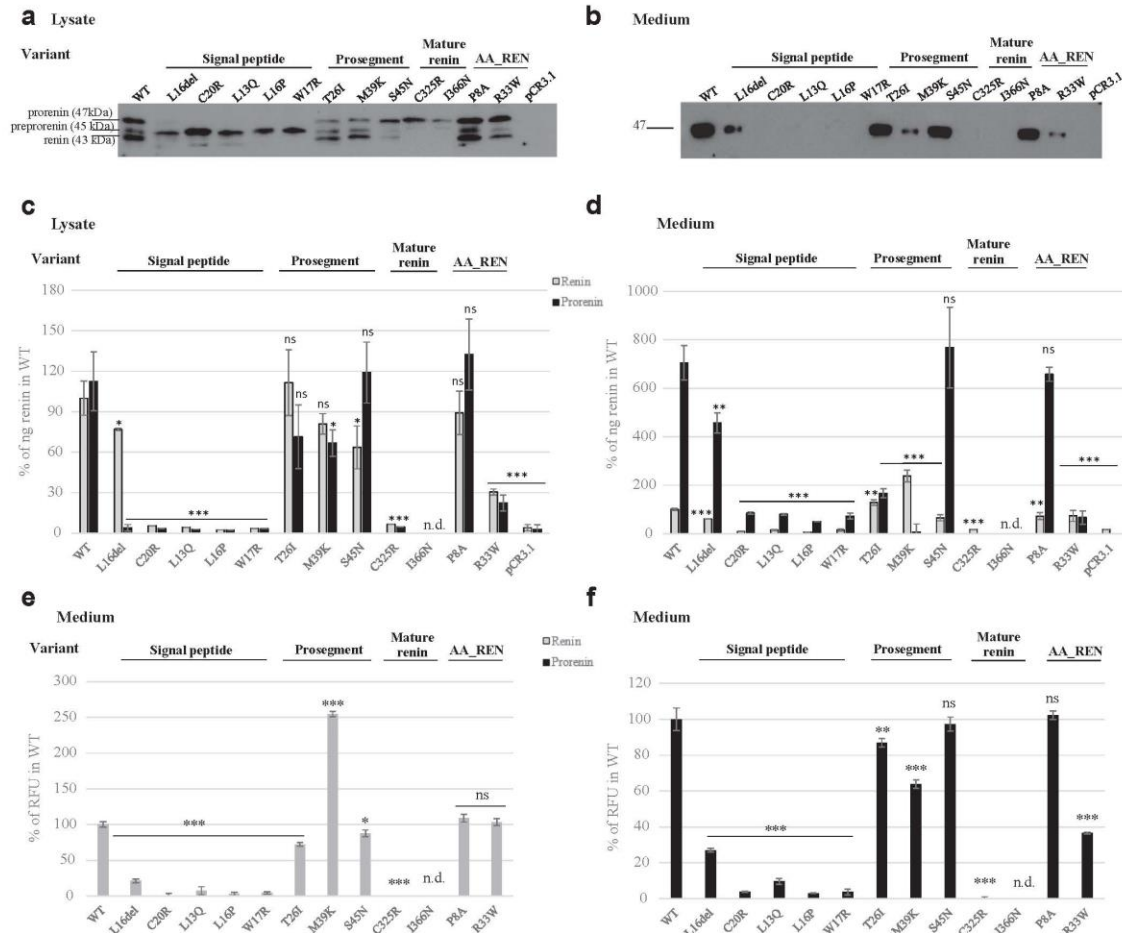


Figure 8 | Transient expression and functional characterization of REN variants in human embryonic kidney 293 cells. The wild-type (WT) renin; signal peptide, prosegment, and mature renin mutations; African American (AA_REN) variants; and empty vector were analyzed. (a,b) Western blot analysis of (a) cell lysates and (b) culture media. Molecular weights of immunoreactive proteins present in the WT lysates correspond with expected molecular weights of prorenin (47 kDa), preprorenin (45 kDa), and renin (43 kDa). (c,d) Immunoradiometric assay (IRMA) of prorenin and renin amounts in (c) cell lysates and (d) culture media employing a radiolabeled antibody that specifically recognizes the active site of renin. The concentration of prorenin was calculated as the difference between the renin concentration measured before and after trypsin treatment, which activates renin by proteolytic cleavage of the prosegment from prorenin. Amounts of mutated renin (gray bars) and prorenin (black bars) were normalized to the amount of WT renin. The values represent mean \pm SD. Measurements were performed in 3 independent clones for each of the constructs. The individual measurements were carried out in triplicate. The statistical significance of the differences between the WT and renin variant protein amounts was assessed by *t* test. **P* < 0.05; ***P* > 0.01; ****P* > 0.001; n.d., not done. (e,f) Enzymatic activity of (e) mature renin secreted into culture media and (f) prorenin secreted into culture media. Values were normalized to the WT (100%) and represent the mean \pm SD of relative fluorescent units (RFU) generated by renin-mediated cleavage of the 5-FAM- and QXL520-conjugated renin substrate. Measurements were performed in 3 independent clones for each of the constructs. The individual measurements were carried out in triplicate. The statistical significance of the differences between activity of the WT renin and renin variants was assessed by *t* test. **P* < 0.05; ***P* > 0.01; ****P* > 0.001; n.d., not done.

gout (36%) and anemia (50%). The prosegment (propeptide) is a structural element that determines the biosynthesis, cellular trafficking, and function of most proteases,²⁸ including prorenin.^{21–23} Mutations in the prosegment leading to dominant phenotypes have been reported in several other preproteins, including proinsulin (leading to diabetes)²⁹

and factor IX deficiency (hemophilia).³⁰ The prosegment mutations in prorenin described herein are classified as likely benign by various pathogenicity prediction programs. However, based on structural studies, they are predicted to change interactions of the prosegment region with renin that are critical for the maintenance of the protease in its inactive

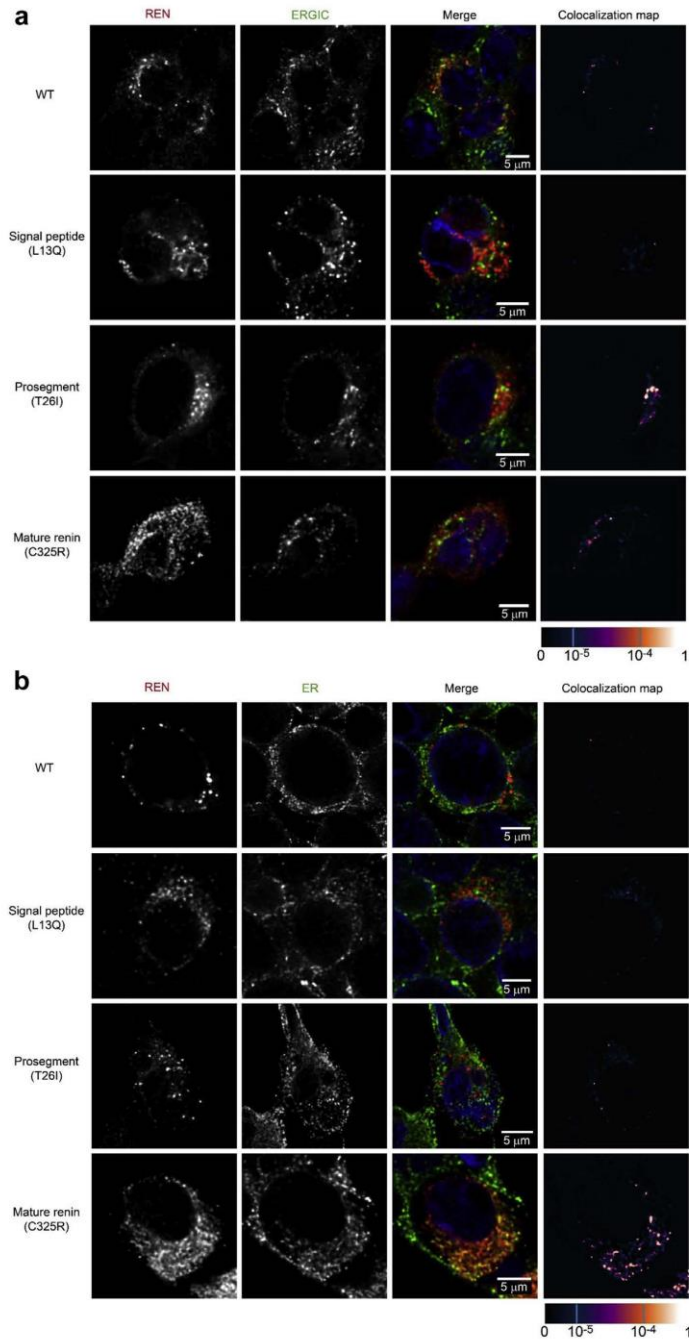


Figure 9 | Transient expression and intracellular localization of transiently expressed mutated preprorenin, prorenin, and renin in human embryonic kidney 293 cells. (a) Preprorenin, prorenin, and renin were detected using an antibody recognizing the epitope 288–317 of preprorenin and colocalized with a marker of endoplasmic reticulum–Golgi intermediate compartment (ERGIC53); wild-type (WT) protein was present in coarsely granular structures that were localized exclusively in the cytoplasm. Proteins with signal peptide mutations (represented here by the p.L13Q mutation) demonstrate intense diffuse cytoplasmic staining (see [Supplementary Figure S3](#) for detailed renin staining). Proteins with prosegment mutations (represented here by the p.T26I mutation) demonstrated a less distinct and diffuse (continued)

state.²⁴ Accordingly, found that mutations in the prosegment do not significantly affect the amounts of synthesized prorenin and renin, but instead they alter secretion and enzyme activity—regulating properties of the prosegment, as demonstrated by altered proportions of synthesized, enzymatically active renin and prorenin (Table 5). This altered proportion may also reflect the effect of prosegment mutations on trafficking through the intracellular vesicular network, within which processing of prorenin to renin occurs. Such an effect is suggested by specific accumulation of proteins with prosegment mutations (vs. other *REN* mutations) in the ER–Golgi intermediate compartment, where the quality control system of the early secretory pathway and the concentration process of nascent secretory proteins into secretory granules take place.³¹ The age of presentation and severity of prosegment mutations may vary significantly due to the type of mutation and its specific effects on biosynthesis, cellular trafficking, and proteolytic processing of prorenin and renin activity regulation. In addition to causing cellular toxicity, these dominant negative effects may be due to abnormal interactions between the mutant and wild-type proteins that are being processed in parallel, as seen in early-onset insulin-deficient diabetes.³² The nonpathogenic p.S45N variant showed normal *in vitro* scores and normal (actually increased) enzyme activity. However, accumulation in the ER intermediate compartment suggests that the p.S45N mutation affects protein trafficking and could potentially lead to late-onset CKD.

Mutations in the genetic region encoding the mature renin peptide had a much milder course compared with patients with mutations in the region encoding the signal peptide or prorenin, as first noted by Schaeffer *et al.* in their case report of a family with the p.L381P *REN* mutation.¹¹ In contrast to patients in the signal and prosegment groups, who often present in childhood, patients in the mature group first present in their 20s with gout or present later in life with unexplained CKD. These patients appear to have normal kidney function early in life. It is unclear whether individuals in the mature group had anemia in childhood, but, if so, it was asymptomatic in the patients in our cohort. Although patients in this group presented later and had a higher mean age of ESKD, they appeared to have a faster rate of eGFR decline in adulthood (Figure 1b) than the other 2 groups. This finding may have been related to the small sample size, fewer measurements of eGFR earlier in life, and/or case ascertainment bias. Two mutations in mature renin were studied *in vitro*. These mutations destabilize renin structure and produce an enzymatically inactive prorenin that is trapped within the ER, similar to the mature *REN* mutation

p.L381P.¹¹ The localization of the mutated mature renin protein and pathophysiologic changes are very similar to changes found in ADTKD due to *UMOD* mutations, and the 2 conditions are quite similar clinically. Better clinical outcomes in the mature group may be due to decreased cellular toxicity of the mature renin mutations and decreased effects on cellular processing of the wild-type renin produced by the normal allele, similar to mutations in the mature insulin peptide found in diabetes mellitus, with onset of symptoms in adulthood.^{33–35}

REN mutations identified in African Americans

We also evaluated 2 missense *REN* variants of unknown significance, p.P8A and p.R33W, both located in the signal peptide and prosegment of prorenin and are present in relatively high frequencies in African Americans. Individuals of African descent show a higher prevalence of low-renin hypertension and ESKD,¹⁸ and we sought to evaluate their functional impact. Our analyses demonstrate that, although the p.P8A variant had no effect, the p.R33W variant showed altered properties very similar to those of other ADTKD-*REN* prosegment mutations. With population frequencies of 0.001, the p.R33W may thus represent a genetic factor contributing to heritability of low circulating plasma renin and CKD in a small group of African Americans. We were unable to recruit and study any individuals with the p.R33W mutation, who could have mild hyperkalemia, gout, and CKD with aging.

Although this is the largest study of patients with ADTKD-*REN*, the small number of participants still limited our ability to assess the effects of fludrocortisone. Moreover, data were limited in teenage males and patients in the mature group. As the study was retrospective and these individuals were asymptomatic, there was no need for clinicians to perform laboratory studies earlier in life. We are interested in adding more families to our registry to improve clinical characterization, and we would appreciate information on other families with this disorder (contact ableyer@wakehealth.edu).

In summary, families with ADTKD-*REN* can be divided into 3 groups. Patients with mutations in the region encoding the mature peptide present with gout in early adulthood or CKD later in life. Their course is milder than in patients with mutations in the regions encoding the signal peptide and prosegment. In these latter 2 groups, kidney function appears to be decreased starting from birth in many patients but remains stable through early adulthood. Anemia, hyperkalemia, and acidosis are frequently present, with acidosis being inadequately treated in a number of patients. Fludrocortisone raises eGFR, lowers serum potassium, and improves serum

Figure 9 (continued) pattern localized mainly to ERGIC. Mutations in mature renin portion (represented here by the p.C325R mutation) demonstrated a less distinct and more diffuse pattern. See Supplementary Figures S4A and S5 for renin and ERGIC staining of other mutations. **(b)** Co-staining of renin with protein disulfide isomerase (PDI), a marker of ER demonstrating localization of mature renin mutations (represented here by the p.C325R mutation) in the ER. See Supplementary Figure S4B for renin and ER staining of other mature renin mutations. The degree of renin colocalization with selected markers is demonstrated by the fluorescent signal–overlap coefficient values ranging from 0 to 1. The resulting overlap coefficient values are presented as the pseudo color (scale shown in corresponding lookup table). To optimize viewing of this image, please see the online version of this article at www.kidney-international.org/.

Table 5 | REN mutations—a summary of *in vitro* characteristics

Localization of the mutation	Cell lysate				Culturing medium				Cellular localization				
	Preprorenin (WB)	Prorenin (WB) IRMA % WT renin	Renin (WB) IRMA % WT	Prorenin / renin ratio	Prorenin (WB)	Renin (WB) % WT renin	Prorenin / renin ratio	Prorenin activity % WT renin		Renin activity % WT renin	Prorenin / renin ratio		
WT protein	+	112 ± 19	+	100 ± 13	1.1	+	705 ± 71	100 ± 4	7.5	100 ± 6	100 ± 4	1	Immunofluorescence using anti-human preprorenin 288-317 antibody detecting prorenin + prorenin + renin
Signal peptide del16L	+	4 ± 3	+	77 ± 1	0.1	+	457 ± 41	61 ± 1	7.5	27 ± 1	21 ± 3	1.3	Coarsely granular structures exclusively in cytoplasm
Signal peptide missense	+	2-3	-	2-6	0	-	51-85	7-15	0	3-10	0-7	0	Less-distinct granular structures
Prosegment T26L, M39K	+	67-72	+	81-112	0.6-0.8	+	7-167	130-238	0.03-1.3	64-87	72-255	0.3-1.2	Diffuse cytoplasmic staining
Prosegment VUS_S45N	+	119 ± 23	+	64 ± 16	1.9	+	768 ± 170	66 ± 12	11.6	97 ± 4	88 ± 5	1.1	Less-distinct cytoplasmic granular structures with diffuse staining localized partly to ERGIC.
Mature renin C325R	-	5	+	7	0	-	0	0	0	10 ± 0.1	0	0	Intracellular clumps localized to ER
AA variants													
Signal peptide P8A	+	132 ± 26	+	89 ± 16	1.5	+	658 ± 29	73 ± 14	9	102 ± 2	109 ± 5	0.9	Similar to WT
Prosegment R33W	+	22 ± 6	+	30 ± 3	0.7	+	67 ± 7	74 ± 22	0.9	37 ± 1	103 ± 5	0.4	More-diffuse pattern localized to ERGIC.

AA, amino acid; ER, endoplasmic reticulum; ERGIC, endoplasmic reticulum-Golgi intermediate compartment; IRMA, immunoradiometric assay; WB, Western blot; WT, wild-type. Bold values are significantly different from WT.

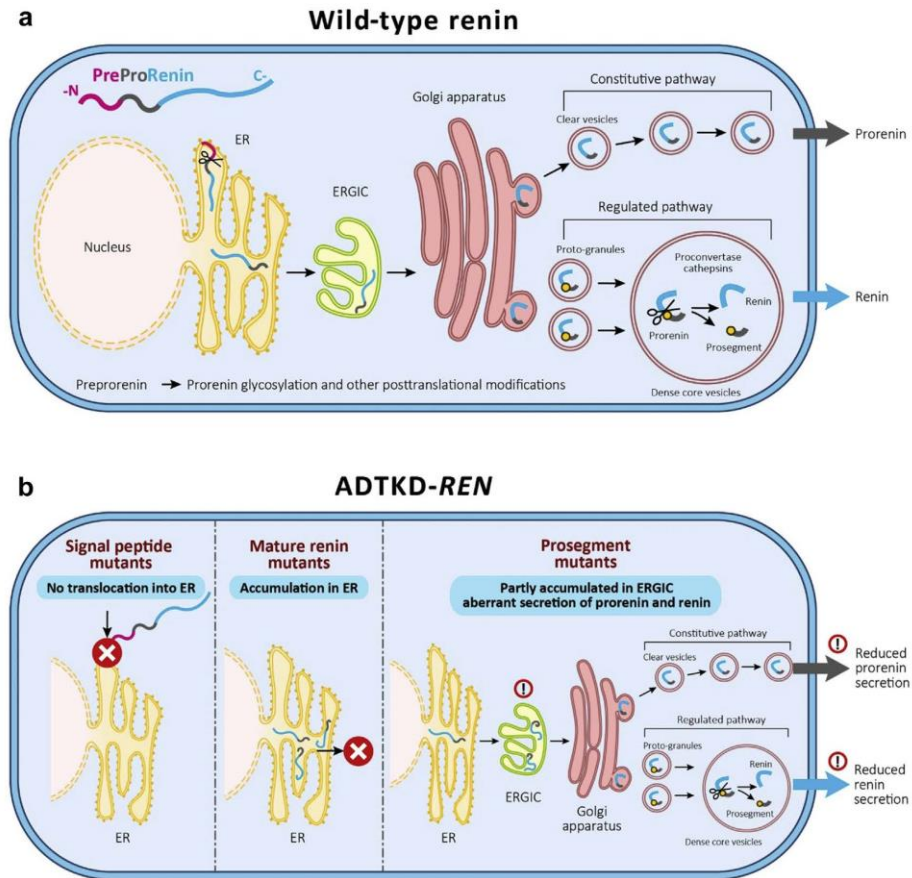


Figure 10 | Pathophysiology of ADTKD-REN. (a) Wild-type preprorenin is cotranslationally translocated into the endoplasmic reticulum (ER). The signal sequence is cleaved during translocation, and nascent prorenin is glycosylated. Prorenin then transits through the ER–Golgi intermediate compartment (ERGIC), which monitors proper protein folding and detects aberrant protein forms. In the Golgi apparatus, prorenin is both sorted to clear vesicles and constitutively secreted to protogranules, where it is proteolytically processed to renin, which is later subjected to regulated secretion. (b) Mutations in the signal peptide prevent translocation across the ER membrane and the preprorenin is aberrantly located in the cytoplasm. This results in clinical renin deficiency and ER stress in renin-producing cells. Mutations in the mature renin lead to retention of mutated protein in ER. This initiates ER stress similar to that seen in *UMOD* mutations and uromodulin retention in ADTKD-*UMOD*. Mutations in the prosegment introduce structural changes affecting protein biosynthesis, folding, and travel along the secretory pathway, causing clinical renin deficiency and potentially also cellular toxicity, leading to chronic kidney disease.

bicarbonate; however, only a few patients received treatment with this medication, limiting our ability to understand the advantages and disadvantages of treatment.

METHODS

This investigation was approved by the institutional review boards of the participating centers and was carried out in accordance with the Declaration of Helsinki.

Identification of cases

Between January 1, 2019 and February 29, 2020, the literature was reviewed for families reported with heterozygous *REN* mutations, and the authors were contacted for additional

information regarding affected patients. Academic centers with an interest in ADTKD were contacted and asked to provide clinical and genetic data from families with ADTKD-*REN* that had not been reported (Supplementary Figure S1). Investigators were asked to provide the following information for each individual from birth through February 29, 2020: mutation; age and reason for presentation; all hemoglobin values and use of erythropoietin; all serum electrolyte, uric acid, blood urea nitrogen, and creatinine values; age of onset of ESKD; and use of fludrocortisone, allopurinol, or alkali supplementation. These mutations were not present in the Genome Aggregation Database³⁶ and segregated with disease in affected families, with the exception of p.S45N, which was found not to segregate with disease in the 1 family found to have this mutation.

Genetic evaluation

REN mutations were identified using either Sanger sequencing of individual REN exons, panel sequencing, or whole-exome sequencing, essentially as described elsewhere.^{4,5}

Calculation of eGFR

The eGFR was determined using the Pottel equation.³⁷ This equation takes into account age, gender, and serum creatinine values. It was specifically chosen because it has been shown to be accurate in all age groups and allows for a continued comparison of data from childhood into adulthood,³⁷ a critical period of analysis in this cohort.

Statistical analysis

Statistical analysis was carried out using SAS statistical software (SAS, Inc, Cary, NC), using standard analytical tests such as the *t* test, chi-square test, multivariate regression, and Cox proportional hazards regression. For comparison of laboratory values (including serum potassium, uric acid, hemoglobin, and bicarbonate), the mean values for each patient were determined and compared with the mean values of other patients. This analysis was chosen to maximize the use of data while also controlling for an increased number of measurements for some individuals.

In silico analysis

Properties of the signal sequences were assessed as described elsewhere.^{5,6} Mutations were mapped into the prorenin structure (PDB ID 3VCM). Structural models were visualized using PyMOL viewer (DeLano Scientific, Palo Alto, CA).

Transient expression of preprorenin in human embryonic kidney 293 cells

Wild-type REN cloned into pCR3.1 a eukaryotic expression vector was used and the corresponding mutated constructs were prepared by site-directed mutagenesis, as in our previous study.^{5,6} Transfection and qualitative and quantitative assays and immunofluorescence analysis of renin were performed as described elsewhere^{5,6} and in the Supplementary Methods.

DISCLOSURE

All the authors declared no competing interests.

ACKNOWLEDGMENTS

The authors thank all participating patients and families, and the referring physicians. We also thank Dr. Heike Göbel (Institute of Pathology, University Hospital of Cologne, Cologne, Germany) and Dr. Helmut Hopfer (Institute of Pathology, University Hospital Basel, Basel, Switzerland) for providing renal sections. This study was supported by a grant from the Ministry of Health of the Czech Republic (NV17-29786A) and by institutional programs of Charles University in Prague, Czech Republic (UNCE/MED/007 and PROGRES-Q26/LF1). Sequencing and genotyping were kindly provided by the National Center for Medical Genomics (LM2018132). AJB was funded by the Slim Health Foundation, the Black-Brogan Foundation, and the National Institutes of Health (NIH) (National Institute of Diabetes and Digestive and Kidney Diseases [NIDDK] R21 DK106584). KT was supported by an MTA-SE Lendulet research grant (LP2015-11/2015). JAS was supported by Kidney Research UK and the Northern Counties Kidney Research Fund. BBB and AW were supported by intramural grants from the Koeln Fortune Program/Faculty of Medicine (KF Nr 245/2011, KF Nr 172/2013, and KF 472/18), University of Cologne, Germany. LR was supported by the Italian Society of Nephrology under the "Adotta un progetto di ricerca" program, Telethon-Italy (GGP14263), and a grant from the Italian Ministry of Health (RF-2010-2319394), Soli Deo Gloria. MTFW

received grants from the NIH/NIDDK, Children's Health Dallas, and the Department of Defense, during this study.

SUPPLEMENTARY MATERIAL

Supplementary File (PDF)

Figure S1. Flow diagram of the ADTKD-REN international cohort.

Figure S2. Representative family trees from 3 families with dominant REN mutations.

Figure S3. Intracellular localization of transiently expressed mutated preprorenin, prorenin, and renin in HEK293 cells.

Figure S4. Transient expression and intracellular localization of transiently expressed mutated preprorenin, prorenin, and renin in HEK293 cells.

Figure S5. Colocalization of transiently expressed mutated preprorenin, prorenin, and renin in ERGIC of HEK293 cells.

Figure S6. Localization of transiently expressed mutated preprorenin, prorenin, and renin in Golgi apparatus of HEK293 cells.

Figure S7. Localization of transiently expressed mutated preprorenin, prorenin, and renin in lysosomes of HEK293 cells.

Table S1. Clinical characteristics of each ADTKD-REN mutation by preprorenin domain.

Supplementary Methods. Transient expression of preprorenin in HEK293 cells, Western blot analysis, quantitative analysis of renin and prorenin by immunoradiometric assay (IRMA), measurement of the enzymatic activity of renin secreted into the culture media, confocal microscopy, and image acquisition and analysis.

Supplementary References.

REFERENCES

- Devuyst O, Olinger E, Weber S, et al. Autosomal dominant tubulointerstitial kidney disease. *Nat Rev Dis Primers*. 2019;5:60.
- Hart TC, Gorry MC, Hart PS, et al. Mutations of the UMOD gene are responsible for medullary cystic kidney disease 2 and familial juvenile hyperuricaemic nephropathy. *J Med Genet*. 2002;39:882–892.
- Kirby A, Gnirke A, Jaffe DB, et al. Mutations causing medullary cystic kidney disease type 1 lie in a large VNTR in MUC1 missed by massively parallel sequencing. *Nat Genet*. 2013;45:288–393.
- Bolar NA, Golzio C, Zivna M, et al. Heterozygous loss-of-function SEC61A1 mutations cause autosomal-dominant tubulo-interstitial and glomerulocystic kidney disease with anemia. *Am J Hum Genet*. 2016;99:174–187.
- Zivna M, Hulkova H, Marignon M, et al. Dominant renin gene mutations associated with early-onset hyperuricemia, anemia, and CKD. *Am J Human Genet*. 2009;85:204–213.
- Bleyer AJ, Zivna M, Hulkova H, et al. Clinical and molecular characterization of a family with a dominant renin gene mutation and response to treatment with fludrocortisone. *Clin Nephrol*. 2010;74:411–422.
- Beck BB, Trachtman H, Gitman M, et al. Autosomal dominant mutation in the signal peptide of renin in a kindred with anemia, hyperuricemia, and CKD. *Am J Kidney Dis*. 2011;58:821–825.
- Clissold RL, Clarke HC, Spasic-Boskovic O, et al. Discovery of a novel dominant mutation in the REN gene after forty years of renal disease: a case report. *BMC Nephrol*. 2017;18:234.
- Petrijan T, Menih M. Discovery of a novel mutation in the REN gene in patient with chronic progressive kidney disease of unknown etiology presenting with acute spontaneous carotid artery dissection. *J Stroke Cerebrovasc Dis*. 2019;28:104302.
- Abdelwahed M, Chaabouni Y, Michel-Calemard L, et al. A novel disease-causing mutation in the Renin gene in a Tunisian family with autosomal dominant tubulointerstitial kidney disease. *Int J Biochem Cell Biol*. 2019;117:105625.
- Schaeffer C, Izzi C, Vettori A, et al. Autosomal dominant tubulointerstitial kidney disease with adult onset due to a novel renin mutation mapping in the mature protein. *Sci Rep*. 2019;9:11601.
- Gribouval O, Gonzales M, Neuhaus T, et al. Mutations in genes in the renin-angiotensin system are associated with autosomal recessive renal tubular dysgenesis. *Nat Genet*. 2005;37:964–968.
- Gomez RA, Sequiera-Lopez MLS. Renin cells in homeostasis, regeneration and immune defence mechanisms. *Nat Rev Nephrol*. 2018;14:231–245.

14. Pugliese NR, Masi S, Taddei S. The renin-angiotensin-aldosterone system: a crossroad from arterial hypertension to heart failure. *Heart Fail Rev.* 2020;25:31–42.
15. Sparks MA, Crowley SD, Gurley SB, Mirosou M, Coffman TM. Classical renin-angiotensin system in kidney physiology. *Compr Physiol.* 2014;4:1201–1228.
16. Imai T, Miyazaki H, Hirose S, et al. Cloning and sequence analysis of cDNA for human renin precursor. *Proc Natl Acad Sci USA.* 1983;80:7405–7409.
17. Schweda F, Friis U, Wagner C, et al. Renin release. *Physiology (Bethesda).* 2007;22:310–319.
18. Sagnella GA. Why is plasma renin activity lower in populations of African origin? *J Hum Hypertens.* 2001;15:17–25.
19. Petersen TN, Brunak S, von Heijne G, Nielsen H. SignalP 4.0: discriminating signal peptides from transmembrane regions. *Nat Methods.* 2011;8:785–786.
20. Jagadeesh KA, Wenger AM, Berger MJ, et al. M-CAP eliminates a majority of variants of uncertain significance in clinical exomes at high sensitivity. *Nat Genet.* 2016;48:1581–1586.
21. Nagahama M, Nakayama K, Hori H, Murakami K. Expression of a deletion mutant of the prosegment of human prorenin in Chinese hamster ovary cells. *FEBS Lett.* 1989;259:202–204.
22. Nakayama K, Nagahama M, Kim WS, et al. Prorenin is sorted into the regulated secretory pathway independent of its processing to renin in mouse pituitary AT-20 cells. *FEBS Lett.* 1989;257:89–92.
23. Mercure C, Thibault G, Lussier-Cacan S, et al. Molecular analysis of human prorenin prosegment variants in vitro and in vivo. *J Biol Chem.* 1995;270:16355–16359.
24. Guo H, Xiong Y, Witkowski P, et al. Inefficient translocation of preproinsulin contributes to pancreatic beta cell failure and late-onset diabetes. *J Biol Chem.* 2014;289:16290–16302.
25. Liu M, Lara-Lemus R, Shan SO, et al. Impaired cleavage of preproinsulin signal peptide linked to autosomal-dominant diabetes. *Diabetes.* 2012;61:828–837.
26. Arnold A, Horst SA, Gardella TJ, et al. Mutation of the signal peptide-encoding region of the preproparathyroid hormone gene in familial isolated hypoparathyroidism. *J Clin Invest.* 1990;86:1084–1087.
27. Hussain S, Mohd Ali J, Jalaludin MY, Harun F. Permanent neonatal diabetes due to a novel insulin signal peptide mutation. *Pediatr Diabetes.* 2013;14:299–303.
28. Demiduk IV, Shubin AV, Gasanov EV, Kostrov SV. Propeptides as modulators of functional activity of proteases. *Biomol Concepts.* 2010;1:305–322.
29. Weiss MA. Diabetes mellitus due to the toxic misfolding of proinsulin variants. *FEBS Lett.* 2013;587:1942–1950.
30. Bentley AK, Rees DJ, Rizza C, Brownlee GG. Defective propeptide processing of blood clotting factor IX caused by mutation of arginine to glutamine at position -4. *Cell.* 1986;45:343–348.
31. Saraste J, Marie M. Intermediate compartment (IC): from pre-Golgi vacuoles to a semi-autonomous membrane system. *Histochem Cell Biol.* 2018;150:407–430.
32. Liu M, Sun J, Cui J, et al. INS-gene mutations: from genetics and beta cell biology to clinical disease. *Mol Aspects Med.* 2015;42:3–18.
33. Given BD, Mako ME, Tager HS, et al. Diabetes due to secretion of an abnormal insulin. *N Engl J Med.* 1980;302:129–135.
34. Sakura H, Iwamoto Y, Sakamoto Y, et al. Structurally abnormal insulin in a diabetic patient. Characterization of the mutant insulin A3 (Val—Leu) isolated from the pancreas. *J Clin Invest.* 1986;78:1666–1667.
35. Shoelson S, Fickova M, Haneda M, et al. Identification of a mutant human insulin predicted to contain a serine-for-phenylalanine substitution. *Proc Natl Acad Sci USA.* 1983;80:7390–7394.
36. Genome Aggregation Database. Available at: https://gnomad.broadinstitute.org/gene/ENSG00000143839?dataset=gnomad_r3. Accessed April 9, 2020.
37. Pottel H, Hoste L, Dubourg L, et al. An estimated glomerular filtration rate equation for the full age spectrum. *Nephrol Dial Transplant.* 2016;31:798–806.

4.4 Clinical and genetic spectra of autosomal dominant tubulointerstitial kidney disease due to mutations in *UMOD* and *MUC1*.

Olinger E, Hofmann P, **Kidd K**, Dufour I, Belge H, Schaeffer C, Kipp A, Bonny O, Deltas C, Demoulin N, Fehr T, Fuster DG, Gale DP, Goffin E, Hodaňová K, Huynh-Do U, Kistler A, Morelle J, Papagregoriou G, Pirson Y, Sandford R, Sayer JA, Torra R, Venzin C, Venzin R, Vogt B, Živná M, Greka A, Dahan K, Rampoldi L, Kmoch S, Bleyer AJ Sr, Devuyst O.

Kidney Int. 2020 Sep;98(3):717-731.

***EO, PH, and KO are co-first authors**

Clinical and genetic spectra of autosomal dominant tubulointerstitial kidney disease due to mutations in *UMOD* and *MUC1*



see commentary on page 549
OPEN

Eric Olinger^{1,2,16,23}, Patrick Hofmann^{1,3,23}, Kendrah Kidd^{4,20,23}, Inès Dufour^{1,9}, Hendrica Belge⁵, Céline Schaeffer⁶, Anne Kipp¹, Olivier Bonny⁷, Constantinos Deltas⁸, Nathalie Demoulin^{9,10}, Thomas Fehr^{1,11}, Daniel G. Fuster², Daniel P. Gale¹², Eric Goffin^{9,10}, Kateřina Hodaňová²⁰, Uyen Huynh-Do², Andreas Kistler¹³, Johann Morelle^{9,10}, Gregory Papagregoriou⁸, Yves Pirson⁹, Richard Sandford¹⁴, John A. Sayer^{15,16}, Roser Torra¹⁷, Christina Venzin¹⁸, Reto Venzin¹⁹, Bruno Vogt², Martina Živná²⁰, Anna Greka^{21,22}, Karin Dahan⁵, Luca Rampoldi⁶, Stanislav Kmoč²⁰, Anthony J. Bleyer Sr^{4,20,24} and Olivier Devuyst^{1,9,24}

¹Institute of Physiology, University of Zurich, Zurich, Switzerland; ²Department of Nephrology and Hypertension, Inselspital Bern University Hospital, Bern, Switzerland; ³Department of Internal Medicine, Hospital Uster, Uster, Switzerland; ⁴Section on Nephrology, Wake Forest School of Medicine, Winston-Salem, North Carolina, USA; ⁵Center for Human Genetics, Institute of Pathology and Genetics, Gosselies, Belgium; ⁶Division of Genetics and Cell Biology, San Raffaele Scientific Institute, Milan, Italy; ⁷Service of Nephrology, Lausanne University Hospital, Lausanne, Switzerland; ⁸Molecular Medicine Research Center, Department of Biological Sciences, University of Cyprus, Nicosia, Cyprus; ⁹Division of Nephrology, Cliniques Universitaires Saint-Luc, Brussels, Belgium; ¹⁰Institut de Recherche Expérimentale et Clinique, Université catholique de Louvain, Brussels, Belgium; ¹¹Department of Internal Medicine, Cantonal Hospital Graubünden, Chur, Switzerland; ¹²Department of Nephrology, University College of London, London, UK; ¹³Department of Internal Medicine, Cantonal Hospital Frauenfeld, Frauenfeld, Switzerland; ¹⁴Department of Medical Genetics, Cambridge Biomedical Campus, Cambridge, UK; ¹⁵Renal Services, Newcastle upon Tyne Hospitals National Health Service Trust, Newcastle upon Tyne, UK; ¹⁶Translational and Clinical Research Institute, Faculty of Medical Sciences, Newcastle University, Newcastle upon Tyne, UK; ¹⁷Inherited Renal Disorders, Nephrology Department, Fundació Puigvert, Spanish Renal Research Network (REDinREN), Instituto de Investigaciones Biomédicas Sant Pau, Universitat Autònoma de Barcelona, Barcelona, Spain; ¹⁸Division of Nephrology, Department of Internal Medicine, Hospital Davos, Davos, Switzerland; ¹⁹Division of Nephrology, Department of Internal Medicine, Cantonal Hospital Graubünden, Chur, Switzerland; ²⁰Research Unit for Rare Diseases, Department of Pediatrics and Adolescent Medicine, First Faculty of Medicine, Charles University, Prague, Czech Republic; ²¹Department of Medicine, Brigham and Women's Hospital, Harvard Medical School, Boston, Massachusetts, USA; and ²²Broad Institute of MIT and Harvard, Massachusetts Institute of Technology, Cambridge, Massachusetts, USA

Autosomal dominant tubulointerstitial kidney disease (ADTKD) is an increasingly recognized cause of end-stage kidney disease, primarily due to mutations in *UMOD* and *MUC1*. The lack of clinical recognition and the small size of cohorts have slowed the understanding of disease ontology and development of diagnostic algorithms. We analyzed two registries from Europe and the United States to define genetic and clinical characteristics of ADTKD-*UMOD* and ADTKD-*MUC1* and develop a practical score to guide genetic testing. Our study encompassed 726 patients from 585 families with a presumptive diagnosis of ADTKD along with clinical, biochemical, genetic and radiologic data. Collectively, 106 different *UMOD* mutations were detected in 216/562 (38.4%) of families with ADTKD (303 patients), and 4 different *MUC1* mutations in 72/205 (35.1%) of the families that are *UMOD*-negative (83 patients). The median kidney survival was significantly shorter in patients with ADTKD-*MUC1* compared to ADTKD-*UMOD* (46 vs. 54 years, respectively), whereas the median gout-free survival was dramatically reduced in patients

with ADTKD-*UMOD* compared to ADTKD-*MUC1* (30 vs. 67 years, respectively). In contrast to patients with ADTKD-*UMOD*, patients with ADTKD-*MUC1* had normal urinary excretion of uromodulin and distribution of uromodulin in tubular cells. A diagnostic algorithm based on a simple score coupled with urinary uromodulin measurements separated patients with ADTKD-*UMOD* from those with ADTKD-*MUC1* with a sensitivity of 94.1%, a specificity of 74.3% and a positive predictive value of 84.2% for a *UMOD* mutation. Thus, ADTKD-*UMOD* is more frequently diagnosed than ADTKD-*MUC1*, ADTKD subtypes present with distinct clinical features, and a simple score coupled with urine uromodulin measurements may help prioritizing genetic testing.

Kidney International (2020) 98, 717–731; <https://doi.org/10.1016/j.kint.2020.04.038>

KEYWORDS: diagnostic score; dominant kidney disease; gout; mucin-1; uromodulin

Copyright © 2020, International Society of Nephrology. Published by Elsevier Inc. This is an open access article under the CC BY-NC-ND license (<http://creativecommons.org/licenses/by-nc-nd/4.0/>).

Correspondence: Eric Olinger or Olivier Devuyst, University of Zurich, Winterthurerstrasse 190, 8057 Zurich, Switzerland. E-mail: eric.olinger@nclac.uk or olivier.devuyst@uzh.ch or Anthony J. Bleyer, Sr., Section on Nephrology, Wake Forest School of Medicine, Medical Center Boulevard, Winston-Salem, North Carolina 27157, USA; ableyer@wakehealth.edu

²³EO, PH, and KK are co-first authors.

²⁴AJB and OD are co-last authors.

Received 5 January 2020; revised 23 March 2020; accepted 2 April 2020; published online 22 May 2020

Autosomal dominant tubulointerstitial kidney disease (ADTKD) is characterized by tubular damage and interstitial fibrosis of the kidney in the absence of glomerular lesions. Affected individuals present with progressive chronic kidney disease (CKD), normal-to-mild proteinuria, and normal-sized kidneys, often with a positive family history.^{1,2} The disease invariably progresses to end-stage kidney disease (ESKD). Dominant mutations in *UMOD* were first associated with ADTKD.^{3,4} *UMOD* encodes uromodulin, a kidney-specific protein that is abundant in normal urine and plays multiple roles in the kidney.⁴ Mutations in *MUC1* were subsequently identified as a cause for ADTKD.⁵ *MUC1* encodes the glycoprotein mucin-1, which is important in epithelial barrier function and intracellular signaling.^{6–8} Rare forms of ADTKD have also been associated with mutations in *HNF1B*, which encodes the transcription factor hepatocyte nuclear factor 1β^{9,10}; *REN*, which encodes preprorenin, the precursor of renin¹¹; and *SEC61A1*, which encodes the α1 subunit of the SEC61 complex that forms the core of the endoplasmic reticulum (ER) translocon.¹²

Due to the nonspecific nature of the clinical, biological, and pathological findings, ADTKD is underdiagnosed. In a recent study of whole exome sequencing in ~3000 patients with CKD, *UMOD* mutations were detected in 3% of patients with a monogenic cause of CKD, making it the sixth most common genetic diagnosis in CKD.¹³ A single tertiary center survey in England estimated that up to 2% of patients with ESKD had ADTKD-*UMOD*, that is, the most common monogenic kidney disease after autosomal dominant polycystic kidney disease.¹⁴ The prevalence of ADTKD-*MUC1* remains unclear, as mutations in *MUC1* are not detected by next-generation sequencing and require specialized genetic testing.^{5,13} However, previous studies have identified ADTKD-*MUC1* and ADTKD-*UMOD* as the most common subtypes of ADTKD.^{8,15} The pathophysiology of ADTKD-*UMOD* involves retention of mutant *UMOD* in the ER with ensuing ER stress (“gain of toxic function”) and a cascade leading to inflammatory cell infiltrate, tubular dysfunction, and interstitial fibrosis.^{16–18} ADTKD-*MUC1* is caused by mutations in the variable number of tandem repeat (VNTR) region of *MUC1*, leading to the formation of a frameshift, truncated protein (*MUC1fs*) that accumulates in intracellular vesicles and causes tubulointerstitial damage.¹⁹

To date, the largest clinical analysis of ADTKD-*UMOD* was performed in a cohort of French and Belgian patients with ADTKD-*UMOD* ($n = 70$ from 38 families), showing a median renal survival of 54 years and a 66% prevalence of gout.²⁰ The phenotype of ADTKD-*MUC1* was reported in a cohort of 95 patients from 24 families, with an age of onset of ESKD ranging from 16 to 80 years and a 24% prevalence of gout.⁸ A Spanish cohort of 90 patients with ADTKD-*MUC1* (16 families) showed a trend toward earlier age at ESKD and a lower prevalence of gout compared with that of patients with ADTKD-*UMOD* ($n = 41$ from 9 families). The small size of these cohorts prevented the detection of significant differences between ADTKD subtypes.¹⁵

Because of the nonspecific presentation and relative rarity, a clinical characterization of ADTKD subtypes and practical tools to guide genetic testing for suspected ADTKD are missing. Here, we compared the phenotype of the ADTKD-*UMOD* and ADTKD-*MUC1* subgroups in 2 large cohorts from Europe (Belgo-Swiss ADTKD registry) and the United States (US ADTKD registry), representing the largest multicenter ADTKD cohort (726 patients from 585 families) to date. We observed distinct features among these ADTKD subtypes and established a simple score to orient diagnosis and prioritize genetic testing in ADTKD.

RESULTS

Clinical and genetic characteristics of patients with ADTKD

The International ADTKD Cohort included 726 patients from 585 families: 451 patients from 429 families from the US ADTKD registry and 275 patients from 156 families from the Belgo-Swiss ADTKD registry (Figure 1).² In the international cohort, 84% of patients presented with CKD and 43% had reached ESKD. Gout had an overall prevalence of 66% and a family history of either CKD and/or gout was reported in 92% of all cases (Table 1). The main differences between the Belgo-Swiss and US registries included age at presentation, which was older, and prevalence of ESKD, which was higher in the US registry, possibly due to a higher rate of patient self-referral when the disease became symptomatic.

Most patients (703 of 726), from 562 of 585 families, underwent mutational screening in the *UMOD* gene as a first diagnostic test. *UMOD* mutations were detected in 216 of 562 tested families (38.4%), corresponding to 303 of 703 tested patients (43.1%) (Figure 1). The *UMOD* mutation detection rate was 40.0% in the US registry and 34.6% in the Belgo-Swiss registry (Table 1). Next, mutations in *MUC1* were screened in 218 patients who were *UMOD*-negative, from 205 families that were *UMOD*-negative, mostly from the US registry. Of these, 83 patients from 72 families screened positive for *MUC1* mutations, yielding a proportion of 35.1% (72 of 205) of families with ADTKD-*MUC1* among families with *UMOD*-negative ADTKD. Of note, a subset of 23 patients from 23 families with ADTKD (most of them previously linked to chromosome 1q22) were first screened for *MUC1*, with a mutation in *MUC1* detected in 21 patients in this group (Figure 1). At the end of the screening process, 135 patients from 133 families were negative for mutations in both *UMOD* and *MUC1* (Figure 1). Based on these genetic results, the prevalence for ADTKD-*UMOD* is 37.1% [(216 positive) / (585 – 2) tested families] and for ADTKD-*MUC1* is 21.0% [(93 positive) / (585 – 141) tested families] among ADTKD families in this real-life cohort.

Spectrum of *UMOD* and *MUC1* mutations

A total of 106 different *UMOD* mutations were detected in the 216 families with ADTKD-*UMOD* (Figure 2a; Supplementary Table S1). Variant calling was based on *in silico* prediction tools, previous reports, and/or family segregation analysis for undescribed variants. Missense mutations were by far the most

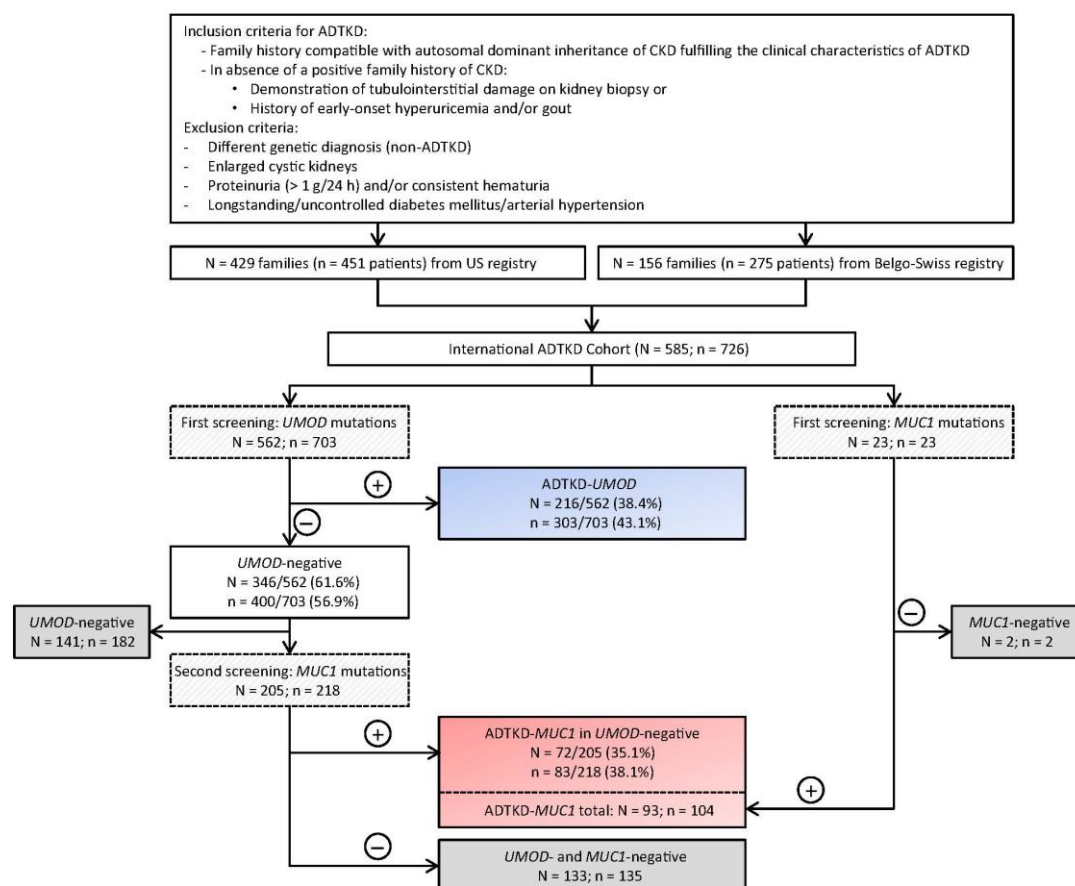


Figure 1 | Design and flowchart of mutation detection in the International ADTKD Cohort. Clinical characteristics of autosomal dominant tubulointerstitial kidney disease (ADTKD) are based on the Kidney Disease: Improving Global Outcomes consensus report²; see the Methods for more details. CKD, chronic kidney disease; n, number of patients; N, number of families.

common type of *UMOD* mutations (101 of 106, 95.3%). Four different deletions (H177-R185del, E188-L221del, K246-S252del, Y272del) and 1 indel (V93-G97del4ins) mutations were found. Of 106 mutations, 95 (89.6%) were clustered in exon 3 of the *UMOD* gene. Of the 101 missense mutations, 57 (56.4%) involved cysteine bonds, either by substituting a cysteine residue by another amino acid or by inserting a new cysteine (Figure 2b). Among the 17 mutations not described before (Supplementary Table S1), 6 involve a previously reported amino acid (N85S, C92G, C120R, C135W, V273L, C300S); 2 (Y272del, G201D) were validated in segregation analyses; and 1 (L284P) was clearly associated with ER retention in functional studies, similar to paradigm mutation C150S (Supplementary Figure S1), along with family history (3 generations with CKD and gout, bland urine sediment) and the absence of this substitution in the Genome Aggregation Database. Using *in silico* prediction tools, the remaining 8 mutations were predicted to be disease-causing (Supplementary Table S2).

We detected 2 families with genetically proven *de novo* *UMOD* mutations c.855C>A (p.A285E) and c.707C>T (p.P236L) and 1 family with clinically suspected neomutation c.707C>T (p.P236L). We did not detect *UMOD* mutations in the homozygous state.

Four different types of *MUC1* mutations (27dupC, 28dupA, 26_27insG, 23delinsAT) in the VNTR domain of *MUC1* were detected in this cohort (nomenclature based on the mutation position inside the canonical 60 nucleotide-long wild-type VNTR repeat as identified by *MUC1* VNTR sequencing⁷). Their localization inside the *MUC1* VNTR as well as their effect on the *MUC1* structure are shown in Figure 2c. All these mutations are predicted to lead to the same frameshift and premature stop codon.⁷ Among the 93 families with ADTKD-*MUC1*, 87 presented with a cytosine duplication (27dupC, 93.5%), 3 with an adenine duplication (28dupA, 3.2%), 2 with a guanine insertion (26_27insG, 2.2%), and 1 with a small indel (23delinsAT, 1.1%) (Figure 2d).

Table 1 | Clinical and genetic characteristics of patients with ADTKD

Characteristic	International ADTKD Cohort (N = 726)	Belgo-Swiss ADTKD registry (n = 275)	US ADTKD registry (n = 451)	n (BE-CH/US)
Number of families	585	156	429	
Sex, female	332/726 (46)	115/275 (42)	217/451 (48)	
Age at presentation (yr)	45 (31, 58)	34 (22, 49)	49 (37, 62)	174/377
Positive family history, gout and/or CKD	625/679 (92)	191/227 (84)	434/451 (96)	
eGFR at diagnosis (ml/min)	44.3 ± 30.0	45.1 ± 20.9	43.8 ± 34.3	137/229
CKD	492/586 (84)	205/258 (80)	287/328 (88)	
ESKD	216/503 (43)	70/258 (27)	146/245 (60)	
Age at ESKD (yr)	44 (32, 55)	44 (33, 56)	44 (32, 55)	245/146
Serum uric acid (μmol/l)	472 ± 141	479 ± 145	455 ± 128	173/74
Female	452 ± 149	457 ± 158	443 ± 129	67/33
Male	485 ± 134	494 ± 135	464 ± 129	106/41
Gout	305/461 (66)	130/218 (60)	175/243 (72)	
Female	98/256 (38)	40/91 (44)	58/165 (35)	
Male	207/305 (68)	90/127 (71)	117/178 (66)	
Age at gout onset (yr)	30 (20, 45)	31 (20, 47)	30 (21, 40)	235/160
Female	35 (22, 50)	40 (23, 56)	35 (22, 50)	98/55
Male	28 (20, 40)	30 (20, 41)	28 (20, 40)	135/105
<i>UMOD</i> mutations	216/562 (38.4)	54/156 (34.6)	162/406 (40.0)	

ADTKD, autosomal dominant tubulointerstitial kidney disease; BE-CH, Belgo-Swiss; CKD, chronic kidney disease; eGFR, estimated glomerular filtration rate; ESKD, end-stage kidney disease.

Quantitative parameters are presented as medians (interquartile ranges) or means ± SD. Qualitative parameters are presented as fractions with percentages. n (BE-CH/US) denotes the number of patients from the Belgo-Swiss and US registries analyzed for the respective parameter.

Clinical characteristics of ADTKD-*UMOD* and ADTKD-*MUC1*

The size of the International ADTKD Cohort allowed us to analyze the clinical characteristics of ADTKD-*UMOD* and ADTKD-*MUC1* subtypes (Figure 3). Age at presentation (first patient contact) was earlier (median: 42 years [interquartile range (IQR): 27, 53] vs. 47 years [IQR: 37, 57], $P = 0.005$) and a positive family history of CKD and/or gout was more frequent (95% vs. 86%, $P = 0.007$) in patients with ADTKD-*UMOD* than in patients with ADTKD-*MUC1*. While the overall prevalence of CKD was significantly higher in patients with ADTKD-*UMOD*, ESKD was significantly more prevalent (44% vs. 58%, $P = 0.04$) and of earlier onset (median: 46 years [IQR: 39, 57] vs. 36 years [IQR: 30, 46], $P < 0.001$) in patients with ADTKD-*MUC1* (Figure 3b, upper panel). Conversely, the prevalence of gout was significantly higher (79% vs. 26%, $P < 0.001$) and gout onset was significantly earlier (median: 27 years [IQR: 19, 37] vs. 45 years [IQR: 29, 51], $P = 0.001$) in patients with ADTKD-*UMOD* (Figure 3b, lower panel). These findings were generally consistent in both sexes. In patients with ADTKD-*UMOD*, gout onset was significantly earlier in men than in women (median: 26 years [IQR: 18, 34] vs. 30 years [IQR: 21, 43], $P = 0.013$) (Figure 3a).

The key differences in terms of renal function and uric acid handling were substantiated by survival curves depicting freedom from ESKD and gout (Figure 4). Renal survival was significantly shorter in ADTKD-*MUC1* than in ADTKD-*UMOD* (median: 54 years, 95% confidence interval [CI]: 51.5–56.5 in ADTKD-*UMOD* vs. 46 years, 95% CI: 39.3–52.7 in ADTKD-*MUC1*, log rank test: $P = 0.013$) (Figure 4a). Conversely, gout-free survival was dramatically shorter in ADTKD-*UMOD* than in ADTKD-*MUC1* (median: 30 years,

95% CI: 27.3–32.7 in ADTKD-*UMOD* vs. 67 years, 95% CI: 57.9–76.1 in ADTKD-*MUC1*, log rank test: $P < 0.001$) (Figure 4b).

Among patients with ADTKD-*UMOD*, carriers of missense mutations involving cysteines (either by substituting a cysteine residue by another amino acid or by inserting a new cysteine) did not experience a worse prognosis in terms of onset of ESKD or age of gout onset when compared with patients with non-cysteine-involving ADTKD-*UMOD* (Supplementary Figure S2).

Comparing ADTKD-*UMOD* with ADTKD-NOS (not otherwise specified, i.e., no mutation detected) in the US ADTKD registry, we found that CKD (94.0% vs. 82.7%, $P < 0.001$) and ESKD (46.5% vs. 26.2%, $P < 0.001$) were more prevalent and the estimated glomerular filtration rate (eGFR) at diagnosis lower (34.7 ml/min vs. 48.1 ml/min, $P < 0.001$) in ADTKD-*UMOD* versus ADTKD-NOS, respectively. Similarly, CKD and ESKD were more prevalent in ADTKD-*MUC1* than in ADTKD-NOS (86.4% vs. 82.7%, $P < 0.001$ and 54.8% vs. 26.2%, $P < 0.001$, respectively) (Supplementary Table S3). These findings suggest a more severe kidney phenotype in ADTKD-*UMOD* and ADTKD-*MUC1* than in ADTKD cases without genetic diagnosis—a finding confirmed in the Belgo-Swiss registry.

UMOD biology in ADTKD-*UMOD* and ADTKD-*MUC1*

Given the colocalization of *MUC1* with *UMOD* in the kidney tubule⁶ and the fact that *MUC1* accumulates in several tissues without causing extrarenal manifestations,⁷ we tested the hypothesis that *MUC1*s might interact with *UMOD* processing in the thick ascending limb (TAL) in ADTKD-*MUC1*. We used a validated enzyme-linked immunosorbent assay²¹ to assess the

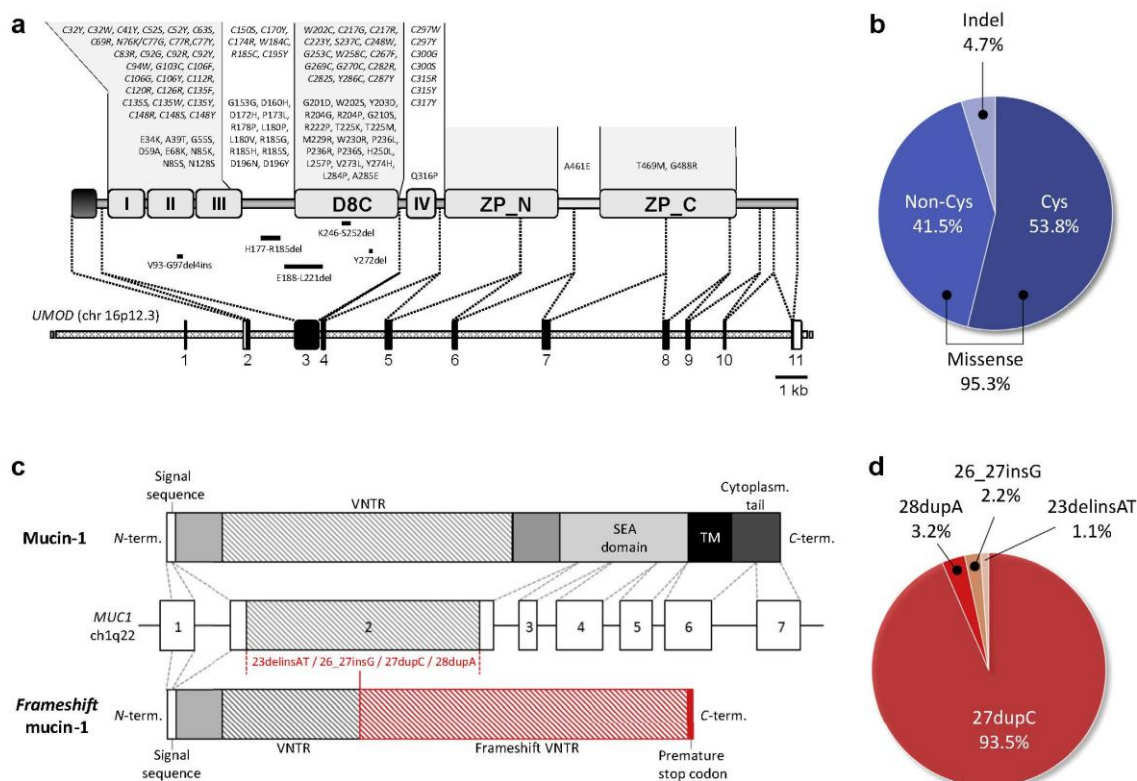


Figure 2 | Spectrum of mutations in *UMOD* and *MUC1*. (a) *UMOD* gene and protein domain structure with the 106 *UMOD* mutations reported in the international cohort depicted relative to domain localization. Mutations involving cysteine residues are indicated in italics, on top of each box. (b) The prevalence of different *UMOD* mutations: missense mutations (101 of 106; 95.3%), affecting cysteine ([Cys]; 57 of 106; 53.8%) or noncysteine (44 of 106; 41.5%) amino acids and indels (5 of 106; 4.7%). (c) *MUC1* gene exon-intron structure (middle panel) and normal protein structure (above) with the 4 detected mutations (in red) in the variable number tandem repeat (VNTR) domain and the consequence on protein structure (below). (d) Prevalence of identified *MUC1* mutations in reported families with autosomal dominant tubulointerstitial kidney disease (ADTKD)-*MUC1*. SEA, self-cleavage module; term, terminal; TM, transmembrane domain.

levels of urinary *UMOD* in a population-based cohort (Cohorte Lausannoise), confirming the positive correlation between urinary *UMOD* (mg/g creatinine) and eGFR between 15 and 90 ml/min per 1.73 m² (test for linear trend: $P = 0.001$) (Supplementary Figure S3A), as previously described.²² Normalizing urinary *UMOD* for eGFR (by dividing *UMOD* concentrations by urinary creatinine and by eGFR) mitigated the linear dependency (test for linear trend: $P = 0.54$) (Supplementary Figure S3B), allowing a more robust comparison of urinary *UMOD* levels between patients and controls. We next measured urinary *UMOD* levels in patients with ADTKD-*MUC1* and ADTKD-*UMOD* compared with levels in controls ($n = 180$) from the population-based cohort strictly matched for eGFR (45–60 ml/min per 1.73 m²). In contrast to patients with ADTKD-*UMOD*, who showed strongly reduced urinary *UMOD* levels (median: 2.8 vs. 14.7 mg/g creatinine, $P < 0.0001$), patients with ADTKD-*MUC1* showed urinary levels of *UMOD* similar to those of controls (median: 15.7 vs.

14.7 mg/g creatinine, $P = 0.99$) (Figure 5a, left panel). Normalizing urinary *UMOD* levels to eGFR [(mg/g creatinine)/eGFR] confirmed strongly reduced levels in patients with ADTKD-*UMOD* versus in controls ($n = 2717$) with eGFR spanning 15 to 90 ml/min per 1.73 m² {(0.05 vs. 0.23 mg/g creatinine)/eGFR}, $P < 0.0001$, respectively, in contrast with unchanged levels in patients with ADTKD-*MUC1* versus in controls {(0.29 vs. 0.23 mg/g creatinine)/eGFR}, $P = 0.29$, respectively) (Figure 5a, right panel).

Next, we performed immunofluorescence staining for *UMOD* on kidney biopsies from healthy individuals (normal human kidney), from 2 patients with ADTKD-*UMOD*, and from 2 patients with ADTKD-*MUC1*. While we were able to see the characteristic intracellular *UMOD* deposits in the patients with ADTKD-*UMOD*, *UMOD* staining was largely confined to the apical membrane in patients with ADTKD-*MUC1*, similar to the pattern observed in normal kidney (Figure 5b). The accumulation of mutant *UMOD* in the TAL

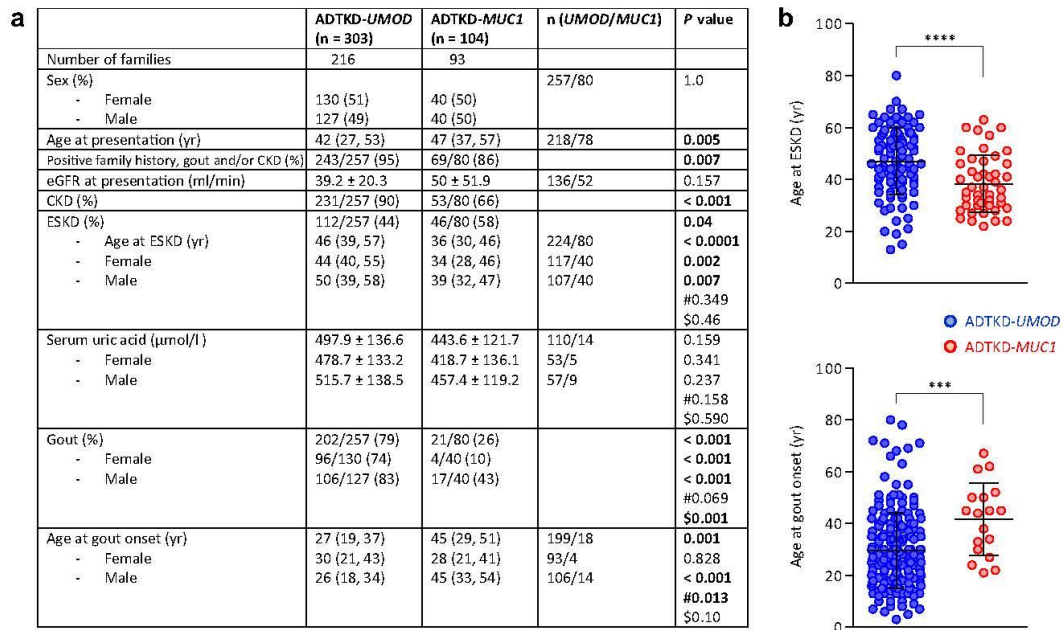


Figure 3 | Clinical characteristics of autosomal dominant tubulointerstitial kidney disease (ADTKD)-*UMOD* and ADTKD-*MUC1*. (a) Quantitative parameters are presented as medians and interquartile ranges or means ± SD. Qualitative parameters are presented as fractions with percentages. χ^2 test for categorical variables and Mann-Whitney *U* test and unpaired *t* test for quantitative parameters were used. #, \$Sex comparison within ADTKD-*UMOD* and ADTKD-*MUC1*, respectively. The n (*UMOD/MUC1*) column denotes the number of patients with ADTKD-*UMOD* and ADTKD-*MUC1* analyzed for the respective parameter. (b) Scatter plots for age at end-stage kidney disease (ESKD) and onset of gout for patients with ADTKD-*UMOD* and ADTKD-*MUC1*. Bars indicate means ± SD. ****P* < 0.001, *****P* < 0.0001. CKD, chronic kidney disease; eGFR, estimated glomerular filtration rate.

cells from patients with ADTKD-*UMOD* induced ER stress, as shown by colocalization with the unfolded protein response regulator glucose-regulated protein 78 ([GRP78], also known as binding Ig protein). Conversely, GRP78 could not be detected in the TALs of patients with ADTKD-*MUC1* (Figure 5b; Supplementary Figure S4).

Establishment of a clinical *UMOD*-score in the Belgo-Swiss ADTKD registry

Based on the Belgo-Swiss ADTKD registry with detailed phenotyping, including 54 families that are *UMOD*-positive (*n* = 132 patients) and 102 families that are *UMOD*-negative (*n* = 143 patients) (Figure 1; Supplementary Figure S5), we designed a clinical score to estimate the probability of ADTKD-*UMOD*. Clinical characteristics in patients with ADTKD with or without *UMOD* mutations guided the scoring system (Supplementary Figure S6). Compared with patients who are *UMOD*-negative, patients with a *UMOD* mutation had a more frequent family history of CKD and/or gout (90% vs. 76%, *P* < 0.001); a higher prevalence of CKD (83% vs. 75%, *P* = 0.03) and ESKD (33% vs. 20%, *P* = 0.02), with earlier onset of CKD (median: 32 years vs. 42 years, *P* = 0.002) and ESKD (median: 42 years vs. 48 years, *P* = 0.007); a higher level of serum uric acid (mean: 507.0 ± 131 vs. 454.5

± 153.4 μmol/l, *P* = 0.017); and an earlier onset of gout (median: 24 years vs. 33 years, *P* = 0.001). Of note, the prevalence of renal cysts, as detected by sonography and/or computed tomography or magnetic resonance imaging, was lower in patients with ADTKD-*UMOD* compared with in patients who were *UMOD*-negative (36% vs. 57%, *P* = 0.001) (Supplementary Figure S6).

The weighted *UMOD*-score was developed on 8 items using these discriminative clinical, biochemical, histological, and imaging characteristics of ADTKD-*UMOD* (Figure 6a). The maximal item value of +3 points was attributed to gout before 30 years and uricemia >500 μmol/l, which are the most specific discriminants (Supplementary Figure S6). Because the prevalence of CKD and autosomal dominant inheritance was higher in ADTKD-*UMOD*, these criteria were weighted with +2 points. Clinical findings suggesting an alternative diagnosis (e.g., proteinuria, uncontrolled hypertension) were attributed negative points. Values for each available item are added to obtain a final additive score for each patient. The clinical *UMOD*-score was applied on patients with ADTKD from the Belgo-Swiss registry, for which information for at least 5 of the 8 items were present (*n* = 211 patients: 106 *UMOD*-positive and 105 *UMOD*-negative). The receiver-operating characteristics curve, with *UMOD*

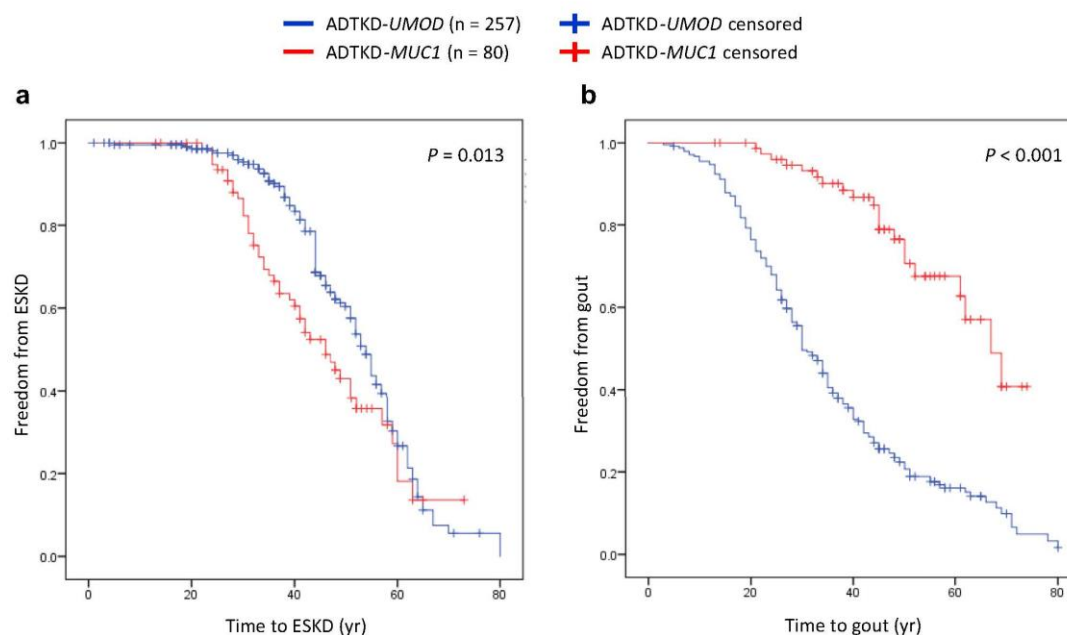


Figure 4 | Freedom from end-stage kidney disease (ESKD) and gout in autosomal dominant tubulointerstitial kidney disease (ADTKD)-*UMOD* and ADTKD-*MUC1*. (a) Kaplan-Meier curve of renal survival in patients with ADTKD-*UMOD* and ADTKD-*MUC1*. Median renal survival was 54 years (95% confidence interval [CI]: 51.5–56.5) in ADTKD-*UMOD* and 46 years (95% CI: 39.3–52.7) in ADTKD-*MUC1*. (b) Kaplan-Meier gout-free survival curve in patients with ADTKD-*UMOD* and ADTKD-*MUC1*. Median gout-free survival was 30 years (95% CI: 27.3–32.7) in ADTKD-*UMOD* and 67 years (95% CI: 57.9–76.1) in ADTKD-*MUC1*. Log rank test was used. Censored: event of interest has not occurred during the follow-up time.

mutation status as the dependent variable yielded an area under the curve (AUC) of 0.72 (95% CI: 0.66–0.79, $P < 0.001$) (Figure 6b). The *UMOD*-score cut-off of ≥ 5 was selected, yielding a sensitivity of 98.1% and specificity of 41.4% for positive *UMOD* mutation testing, corresponding to a negative predictive value (NPV) of 94.3% and a positive predictive value (PPV) of 59.1% (Figure 6c; Supplementary Table S4). This cut-off also proved to be optimal for group discrimination corresponding to a Youden index (sensitivity + specificity – 1) of 0.395 (Supplementary Table S4).

***UMOD*-score and urine *UMOD* levels to guide genetic testing in ADTKD**

The score was validated in patients that were *UMOD*-positive ($n = 124$) and *UMOD*-negative ($n = 183$) from the US ADTKD registry, yielding similarly high sensitivity and low specificity for *UMOD* mutations using a cut-off of ≥ 5 (sensitivity: 97.6%, specificity: 16.4%, NPV: 91.0%, PPV: 44.2%, data not shown), altogether making ADTKD-*UMOD* very unlikely for score results < 5 . We tested how the clinical score separated the 2 most common etiologies of ADTKD in a subset of patients with ADTKD-*UMOD* ($n = 125$) and ADTKD-*MUC1* ($n = 80$) from the US registry for which at least 5 of the 8 clinical items and/or urinary *UMOD* levels

were available. The clinical *UMOD*-score alone separated the 2 entities with an AUC of 0.69 (95% CI: 0.62–0.77, $P = 0.037$) (Figure 7a, left panel). However, the specificity for *UMOD* increased considerably with higher *UMOD*-score values (for instance, a score ≥ 8 had a sensitivity of 48.8%, a specificity of 83.7%, an NPV of 50.8% and a PPV of 81.3% for *UMOD* mutation) (Supplementary Table S5). Only a few patients, mostly those with ADTKD-*MUC1*, had score results of < 5 (Figure 7a, right panel).

We next investigated whether addition of urinary *UMOD* levels to the clinical score improved its ability to discriminate ADTKD-*UMOD* from ADTKD-*MUC1*. Based on the normalized urinary *UMOD* values in the reference population [(mg/g creatinine)/eGFR] (Figure 5a, right panel), we assigned, respectively, +1 and +3 points for urinary *UMOD* values between the median and 25th percentile [(0.14–0.23 mg/g creatinine)/eGFR] and below the 25th percentile. Similarly, we assigned, respectively, –1 and –3 points for urinary *UMOD* values between the median and 75th percentile [(0.23–0.35 mg/g creatinine)/eGFR] and above the 75th percentile. Applied to a cohort of 51 patients with ADTKD-*UMOD* and 35 patients with ADTKD-*MUC1* for which urinary *UMOD* data were available, this combined clinical and biochemical score separated ADTKD-*UMOD* from ADTKD-*MUC1* with an improved AUC of 0.89 (95%

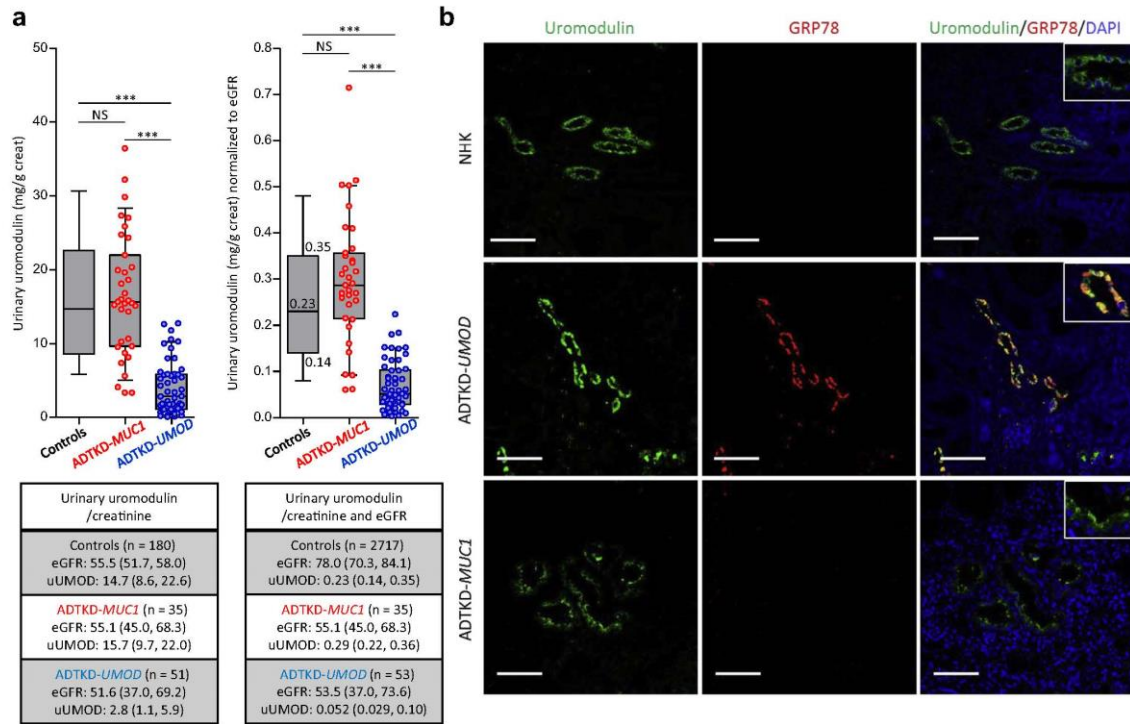


Figure 5 | UMOD processing in autosomal dominant tubulointerstitial kidney disease (ADTKD)-*UMOD* and ADTKD-*MUC1*. (a) Urinary UMOD excretion normalized to urinary creatinine (creat) (left panel) and normalized to urinary creatinine and estimated glomerular filtration rate (eGFR) (right panel) in patients with ADTKD-*MUC1* and ADTKD-*UMOD* and a reference population (controls). Median, 25th percentile, and 75th percentile values in the reference population are indicated (right panel). Numerical values (medians and interquartile ranges) for urinary UMOD (uUMOD), eGFR, and sample size are below the graph. Outlier removed with GraphPad (*ROUT* $Q = 1\%$), 1-way analysis of variance $P < 0.0001$ for both graphs, and Tukey's multiple comparison test was applied with not significant (NS) and $***P < 0.0001$. (b) Immunofluorescence staining for UMOD (green) and glucose-regulated protein 78 (GRP78; red) in ADTKD-*MUC1*, ADTKD-*UMOD*, and normal human kidney (NHK) biopsy. Bars = 50 μm. DAPI, 4',6-diamidino-2-phenylindole. To optimize viewing of this image, please see the online version of this article at www.kidney-international.org.

CI: 0.82–0.96, $P < 0.001$). The cut-off value of ≥ 5 still appears as the optimal cut-off value to discriminate ADTKD-*UMOD* from ADTKD-*MUC1* (Youden index: 0.684) with a sensitivity of 94.1%, a specificity of 74.3%, an NPV of 89.7%, and a PPV of 84.2% for a *UMOD* mutation (Figure 7b; Supplementary Table S5). Based on the clinical and biochemical *UMOD*-score, we suggest a diagnostic algorithm to guide genetic testing in ADTKD (Figure 8).^{1,23,24}

DISCUSSION

This international cohort study represents the largest dataset of patients with ADTKD-*UMOD* and ADTKD-*MUC1* reported to date, providing new insights into the phenotype and disease progression of the main subtypes of ADTKD. Because of the autosomal dominant inheritance and regional familial clustering, considerable differences in the prevalence of ADTKD subgroups are mentioned in national cohorts.^{2,15,20} In the International ADTKD Cohort, ADTKD-*UMOD* represents the most

frequent subtype of ADTKD with an estimated prevalence of 37.1%, followed by ADTKD-*MUC1* in 35.1% of families that are *UMOD*-negative, and an estimated overall prevalence of 21.0%. Of note, a systematic effort to screen for mutations in *HNF1B*, *REN*, *DNAJB11*, and *SEC61A1* is ongoing in the 133 families that are *UMOD*-negative and *MUC1*-negative and for mutations in *MUC1* in the 141 families that are *UMOD*-negative in the registry.

Based on the large sample size, we observed distinct features in the clinical presentation of ADTKD-*UMOD* and ADTKD-*MUC1*, with relevance for clinical practice and patient counselling. Kidney disease appears more severe in patients with ADTKD-*MUC1*, with a higher prevalence of ESKD (58% vs. 44% in ADTKD-*UMOD*, $P = 0.04$), an earlier onset of ESKD (36 years vs. 46 years in ADTKD-*UMOD*, $P < 0.001$), and a shorter median renal survival (46 years vs. 54 years in ADTKD-*UMOD*, $P = 0.013$). Previous studies reported an older age at ESKD (mean: 44.9 years) in patients with ADTKD-*MUC1*,⁸ which could be explained by inclusion

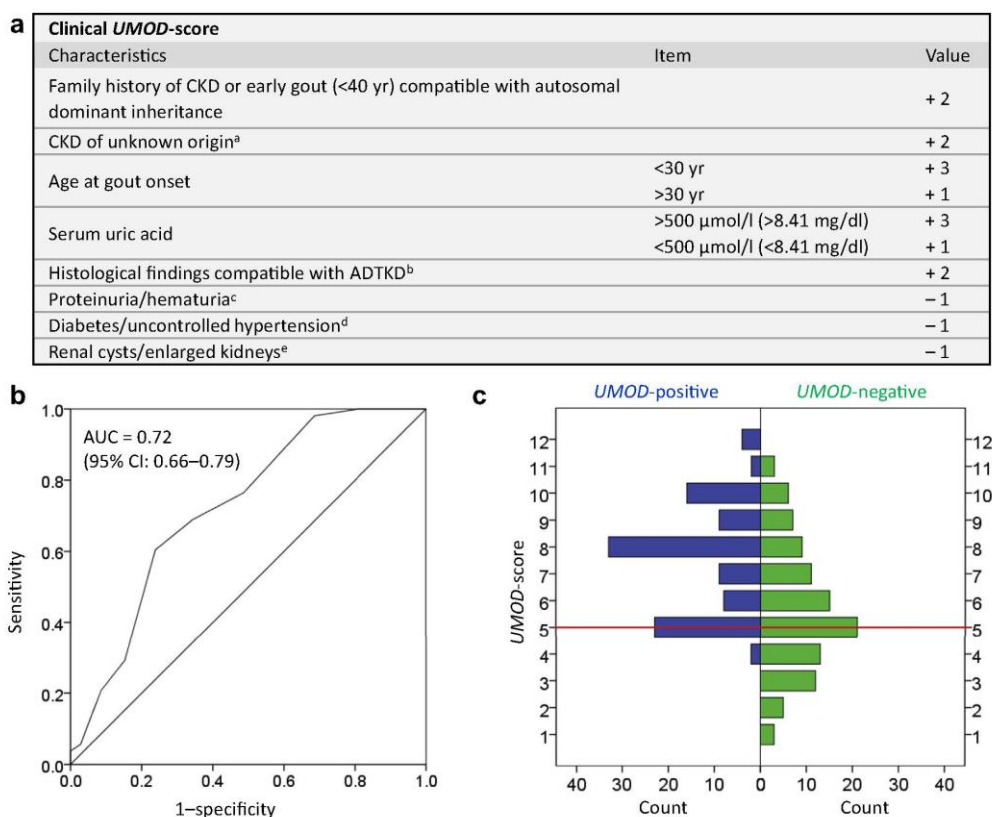


Figure 6 | Clinical *UMOD*-score and performance in the Belgo-Swiss ADTKD registry. (a) Clinical *UMOD*-score based on clinical, biochemical, histological, and imaging data. Attributed points for specific characteristics are shown on the right. ^aAfter routine work-up including urinary sediment and urinalysis and kidney imaging. ^bInterstitial fibrosis, tubular atrophy, thickening and lamellation of tubular basement membranes, tubular dilatation (microcysts), negative immunofluorescence for complement, and Igs. ^cProteinuria >300 mg/dl, persistent hematuria (both eumorphic and dysmorphic) in repeated urinalysis. ^dHemoglobin A1c >10% or repeated blood pressure measurements > 160/100 mm Hg and/or corresponding clinical findings of hypertensive cardiopathy and/or nephropathy. ^eAt least 1 cyst at any location diagnosed by ultrasonography, computed tomography scan, or magnetic resonance imaging. Example: 35-year-old patient, gout onset at 32 years (+1); serum uric acid 550 $\mu\text{mol/l}$ (+3); estimated glomerular filtration rate 55 ml/min per 1.73 m², bland urine analysis and sediment, kidneys without cysts and normal size on magnetic resonance imaging, no diabetes or hypertension (+2 for chronic kidney disease [CKD] of unknown origin); and family history of CKD documented on 3 generations (+2) yields a total clinical *UMOD*-score of 8 points. **(b)** Receiver-operating characteristics curve of the clinical *UMOD*-score in the Belgo-Swiss registry ($n = 211$ patients with autosomal dominant tubulointerstitial kidney disease [ADTKD] with available data) are as follows: area under the curve (AUC): 0.72; 95% confidence interval (CI): 0.66–0.79; $P < 0.001$; the cut-off value of ≥ 5 has a sensitivity of 98.1% and specificity of 41.4% for *UMOD* mutation; negative predictive value: 94.3%; positive predictive value: 59.1%. **(c)** Histogram of clinical *UMOD*-score results in patient who are *UMOD*-positive ($n = 106$) and *UMOD*-negative ($n = 105$). The red horizontal line indicates the cut-off value of 5.

of historically affected patients (clinically affected relatives of genetically diagnosed patients), whereas we only included individuals with an established genetic diagnosis. The heterogeneity of ADTKD-*MUC1* in terms of CKD and/or renal disease progression is intriguing and suggests considerable modifier effects.

Gout has been classically described in patients with *UMOD* mutations. Indeed, our data suggest that gout is strikingly more prevalent and of significantly earlier onset in ADTKD-*UMOD* than in ADTKD-*MUC1*. Defective urinary concentration resulting in polydipsia and polyuria has been

described in patients with ADTKD-*UMOD*, most likely because of impaired activity of TAL-based $\text{Na}^+\text{-K}^+\text{-2Cl}^-$ -cotransporter.^{15,17} Plasma volume contraction and compensatory higher reabsorption activity of the proximal tubule including upregulation of Na^+ -coupled urate transporters most likely explain the hyperuricemia phenotype in ADTKD-*UMOD*.^{25,26} A similar mechanism was shown in aged *Umod* knockout mice that displayed reduced activity of the $\text{Na}^+\text{-K}^+\text{-2Cl}^-$ -cotransporter.²⁶ Even though ADTKD-*MUC1* presumably originates from the distal tubule, gout was considerably less prevalent in this disorder.

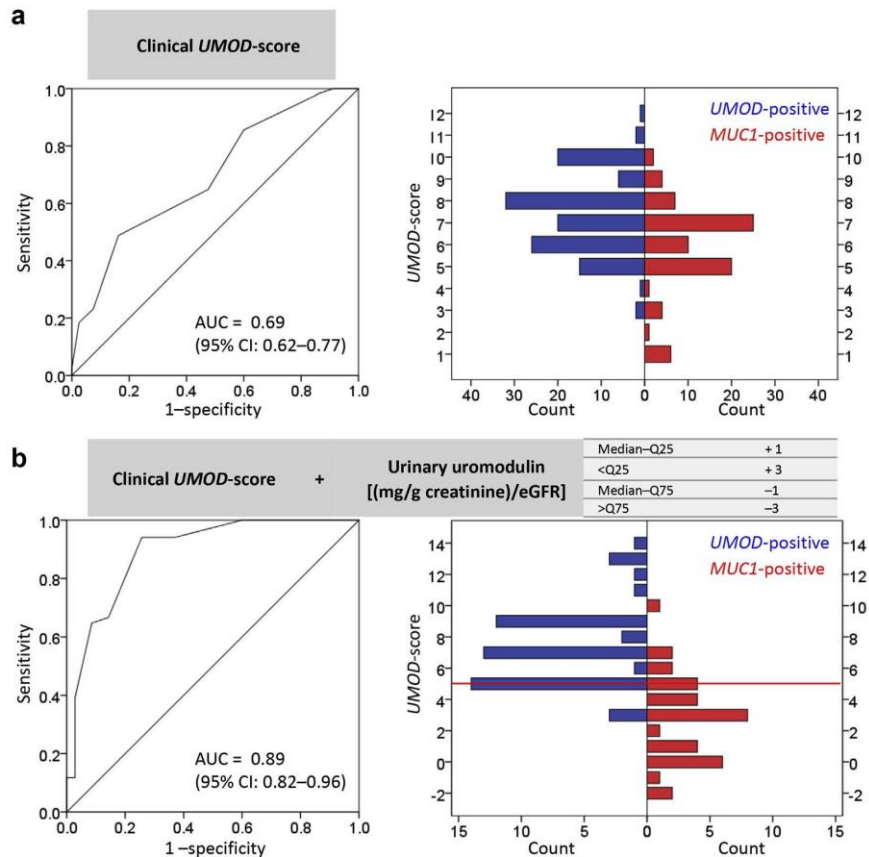


Figure 7 | *UMOD*-score comparing autosomal dominant tubulointerstitial kidney disease (ADTKD)-*UMOD* versus ADTKD-*MUC1* in the US ADTKD registry. (a, left panel) Receiver-operating characteristics curve of the clinical *UMOD*-score in the US registry ($n = 205$ patients with ADTKD-*UMOD* and ADTKD-*MUC1* with available data) are as follows: area under the curve (AUC): 0.69; 95% confidence interval (CI): 0.62–0.77; $P < 0.037$. A cut-off value of ≥ 8 has a sensitivity of 48.8% and specificity of 83.7% for *UMOD* mutations, while a cut-off value of ≥ 5 has a sensitivity of 97.6% and specificity of 15.0% for *UMOD* mutations. (a, right panel) Histogram of clinical *UMOD*-score results in patients with ADTKD-*UMOD* ($n = 125$) and ADTKD-*MUC1* ($n = 80$). (b, left panel) Receiver-operating characteristics curve of the clinical *UMOD*-score including urine *UMOD* levels in the US registry ($n = 86$ patients with ADTKD-*UMOD* and ADTKD-*MUC1* with available urinary *UMOD* data) are as follows: AUC: 0.89; 95% CI: 0.82–0.96; $P < 0.001$. The cut-off value of ≥ 5 has the highest Youden index for discrimination (0.684) and has a sensitivity of 94.1% and specificity of 74.3% for *UMOD* mutation; negative predictive value: 89.7%; positive predictive value: 84.2%. (b, right panel) Histogram of clinical + urinary *UMOD*-score results in patients with ADTKD-*UMOD* ($n = 51$) and ADTKD-*MUC1* ($n = 35$). The red horizontal line indicates the cut-off value of 5. Q, quartile.

We investigated 2 cardinal biological features described in ADTKD-*UMOD* with likely pathophysiological relevance: aberration in *UMOD* export mechanisms and induction of ER stress. Based on the observation that *MUC1* is expressed in the distal kidney tubule including the TAL where it colocalizes with *UMOD*⁵ and on the observation that *MUC1*fs is accumulating in other *MUC1*-expressing tissues (skin, breast, lung, colon) without causing extrarenal manifestations,⁷ one could hypothesize that *MUC1*fs might interact with *UMOD* in TAL. Yet, in contrast to ADTKD-*UMOD*, we found no difference in the urinary level of *UMOD* between patients with ADTKD-*MUC1* and the normal population. Furthermore, analysis of *MUC1*-mutant

kidney biopsies revealed a normal distribution of *UMOD* in TAL cells, without evidence for ER stress (GRP78 expression), which is a hallmark of ADTKD-*UMOD*. These novel findings suggest that the processing of *UMOD* is not altered in ADTKD-*MUC1* and that ER stress is not a main finding in ADTKD-*MUC1*. Along the same line, a recent study found entrapment of *MUC1*fs in vesicles of the early secretory pathway in models of ADTKD-*MUC1*.¹⁹

Previous reports described intracellular accumulation of *UMOD* in kidney biopsies from patients with ADTKD-*UMOD*.^{1,2} However, such staining is not available in a large number of patients, preventing us from speculating on its value in clinical decision making. In our experience, the

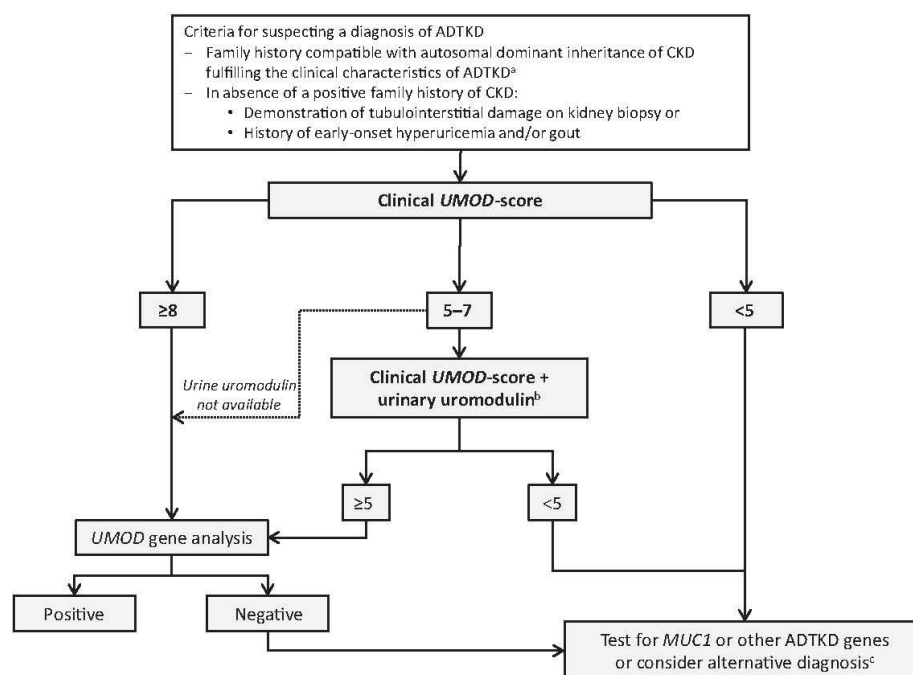


Figure 8 | Diagnostic algorithm for suspected autosomal dominant tubulointerstitial kidney disease (ADTKD) based on clinical UMOD-score and urinary UMOD levels. ^aProgressive loss of renal function, bland urinary sediment, normal-to-mild albuminuria and/or proteinuria, normal-sized kidneys on ultrasound, and no consumption of drugs linked to tubulointerstitial nephritis. ^bAssessed by validated enzyme-linked immunosorbent assay and normalized to urinary creatinine and estimated glomerular filtration rate. Obtained values should be interpreted against family members who are *UMOD*-negative or reference populations.^{23,24} See Results and Discussion sections for more details. ^cFor diagnostic algorithm including other ADTKD genes, refer to Devuyst *et al.*¹ Alternative diagnoses include nephronophthisis (autosomal recessive), autosomal dominant polycystic kidney disease (large cystic kidneys), autosomal dominant glomerulopathies (proteinuria and/or hematuria), other causes of tubulointerstitial kidney disease (autoimmune, tubulointerstitial nephritis, and uveitis syndrome) including drugs and toxins (nonsteroidal anti-inflammatory drugs, aristolochic acid, calcineurin inhibitors, lithium), CKD, chronic kidney disease.

UMOD staining is operator-dependent, requiring rigorous positive and negative controls, and it might depend on the underlying *UMOD* mutation. Furthermore, the availability of kidney biopsies is restricted. The assessment of urinary *UMOD* levels in patients at time of diagnosis and during disease progression might offer a noninvasive diagnostic tool and biomarker in ADTKD-*UMOD*. Because urinary *UMOD* levels show a positive correlation with eGFR (for eGFR < 90 ml/min per 1.73 m²) and tubular mass,^{23,24} they need to be normalized for residual eGFR and interpreted against matched controls. Based on data from a large control cohort, we show here that urinary *UMOD* (in mg/g creatinine to account for urine concentration) normalized for eGFR can be applied in the clinical setting of ADTKD.

A recent study based on exome sequencing reported mutations in *UMOD* accounting for $\sim 3\%$ of all patients with a genetic finding in this cohort.¹³ However, considerable hurdles in the diagnostic approach of ADTKD subtypes persist. These include but are not limited to (i) limited availability of *MUC1* testing due to technical challenges, (ii) lack of

validated diagnostic or genetic algorithm due to unappreciated clinical differences between ADTKD subtypes, and (iii) missing disease biomarkers due to small and scattered disease cohorts. For everyday practice and cost-effectiveness, practical tools such as scoring systems are very useful to guide genetic testing.¹ The Belgo-Swiss registry was instrumental in delineating a clinical *UMOD*-score because it revealed key discriminatory clinical features, including positive family history of CKD and/or gout, age at presentation, prevalence of kidney disease and progression to ESKD, and history of gout. Of interest, renal cysts are less common in patients with ADTKD-*UMOD*, which is in line with previous studies.^{8,15,20} The delineated clinical *UMOD*-score showed an excellent NPV for *UMOD* mutations (cut-off ≥ 5) in the Belgo-Swiss (NPV: 94.3%) and US (NPV: 91.0%) registries. As ADTKD-*UMOD* and ADTKD-*MUC1* present considerable clinical overlap, we were not surprised that the clinical *UMOD*-score separated modestly between these 2 entities (AUC: 0.69). Yet, higher *UMOD*-score values showed a solid specificity for *UMOD* mutations (e.g., cut-off ≥ 8 : specificity of 83.7% and

PPV of 81.3% for an *UMOD* mutation). Adding urinary *UMOD* measurements, a pathophysiological biomarker for ADTKD-*UMOD*, considerably increased the discriminating power of the score (AUC: 0.89) with a PPV of 84.2% for an *UMOD* mutation (cut-off ≥ 5 points). Because the progression of kidney disease and the prevalence and onset of gout seem dependent on the underlying genetic diagnosis, a genetic diagnosis is recommended as it might impact on the management of patients with ADTKD (e.g., follow-up, scheduling of renal transplantation, and gout-preventive strategies). Furthermore, targeted therapies might be in reach at least for ADTKD-*MUC1*.

The limits of this study include the retrospective “real-life” cohort design of consecutively recruited patients, with inherent difficulties such as limited access to full clinical information, missing DNA samples for further genetic testing, and lack of strict inclusion and exclusion criteria. We included all genetically resolved cases of a given family, potentially introducing the risk for selection bias. However, we estimate that this represents a negligible risk as in general only 1 to 2 patients were included per family and considerable intrafamilial clinical variability exists in ADTKD.^{8,20} Because kidney biopsies are rarely performed in these diseases and yield nonspecific findings (e.g., interstitial fibrosis, tubular atrophy), we did not include histopathology information in the analysis. A survey of histopathology results from the Belgo-Swiss registry showed that interstitial fibrosis with tubular atrophy (in $\sim 60\%$ of available pathology reports) and interstitial nephritis (in $\sim 40\%$ of available pathology reports) were the preponderant histological findings in patients with ADTKD-*UMOD* and those who were *UMOD*-negative. A more detailed histological description of biopsies performed in ADTKD-*UMOD* and ADTKD-*MUC1* warrants a dedicated analysis.

It should be pointed out that systematic screening for *UMOD* mutations in all 10 coding exons has only been performed in a subset of patients with ADTKD. Based on previous screens and whole exome sequencing, we estimate that very few *UMOD* mutations outside exons 3 and 4 might have been missed in ADTKD-*UMOD*.^{13,15} Furthermore, large deletions or insertions in *UMOD* are not detected by direct sequencing methods. With the availability of gene panel testing and next-generation sequencing approaches, the utility of a clinical score in directing targeted gene testing will probably decrease. However, at the current stage, *MUC1* mutations are missed by next-generation sequencing and availability of specialized testing is limited. To the best of our knowledge, clinical-grade genetic testing for *MUC1* is only performed by the Broad Institute. For these reasons, we estimate that simple clinical and biochemical tools to estimate pretest probability impacts on diagnostic work-up and potentially reduces the costs associated with unjustified genotyping.

In conclusion, this large international retrospective cohort study provides a detailed phenotype analysis of patients with ADTKD-*UMOD* and ADTKD-*MUC1*. The clinical hallmarks

of the 2 most common ADTKD subtypes are hyperuricemia and early gout in ADTKD-*UMOD* and a heterogeneous, but generally more severe kidney disease in ADTKD-*MUC1*. The clinical *UMOD*-score is a sensitive and, coupled to urinary *UMOD* levels, potentially specific tool to select patients for genetic *UMOD* testing. These results should help clinicians to improve diagnostic rates, clinical management, and patient counselling in ADTKD.

METHODS

International ADTKD Cohort

The International ADTKD Cohort consists of patients from the Belgo-Swiss ADTKD registry and the US ADTKD registry. The inclusion criteria were those defined by the Kidney Disease: Improving Global Outcomes consensus² and included the following in any combination: a family history compatible with autosomal dominant inheritance of CKD with features of ADTKD, including progressive loss of kidney function, bland urinary sediment, absent-to-mild albuminuria and/or proteinuria, normal-sized or small-sized kidneys on ultrasound; and/or (in absence of a positive family history of CKD) a history of early-onset hyperuricemia and/or gout and/or the presence of interstitial fibrosis and/or tubular atrophy on kidney biopsy. Exclusion criteria included the following: a different genetic diagnosis (non-ADTKD), the presence of enlarged cystic kidneys, proteinuria (>1 g/24 h) and/or consistent hematuria, long-standing or uncontrolled diabetes mellitus or arterial hypertension, and the consumption of drugs linked to tubulointerstitial nephritis. Only patients screened for mutations of *UMOD* and/or *MUC1* were included in the cohort. Anonymized demographics and clinical and genetic information were recorded in a database. This study was approved by the institutional review board of Wake Forest School of Medicine, the Université catholique de Louvain (UCL) Medical School, and the European Community's Seventh Framework Programme “European Consortium for High-Throughput Research in Rare Kidney Diseases (EURenOmics).

Belgo-Swiss ADTKD registry. The Belgo-Swiss ADTKD registry includes patients referred to UCLouvain and University of Zurich (UZH) by clinical partners mostly from Europe (Supplementary Appendix S1). In 2019, the registry included 275 patients who had been enrolled since 2003. The clinical data included a family pedigree, onset and evolution of kidney function decline, onset of hyperuricemia and/or gout (age of gout onset was defined as the patient's age at the first episode of gouty arthritis) and fractional excretion of uric acid, imaging and histopathology data (where available), and information on potential extrarenal manifestations (e.g., pancreatic enzymes, liver function tests). ESKD was defined as eGFR < 10 ml/min or initiation of renal replacement therapy (dialysis or kidney transplantation).

US ADTKD registry. The US ADTKD registry includes families with tubulointerstitial kidney disease referred to Wake Forest School of Medicine since 1999 (Supplementary Appendix S1). Information collected included demographics, pedigree, age of ESKD, laboratory values, and ultrasound results.

Genetic testing

Informed written consent was obtained from all patients. Genomic DNA was isolated from peripheral blood leukocytes using standard procedures and DNA was stored at 4 °C.

Direct sequencing of *UMOD* exons was initially performed by Sanger sequencing, as previously described.²⁷ More recently, the

UMOD gene is analyzed by massive parallel sequencing using a tubulopathy gene panel designed by the work package tubulopathies of the European Consortium EUREnOmics.^{28,29} Mutational analysis was carried out in exons 3 and 4 for all enrolled patients and in all 10 coding exons for a subset of patients.

MUC1 genotyping was performed using a *MUC1* VNTR sequencing approach coupled with a spectrometry-based probe extension assay as previously described.^{7,30} *MUC1* testing was provided by the Broad Institute of MIT and Harvard³⁰ and the First Faculty of Medicine, Charles University.⁷ Nucleotide numbering reflects cDNA numbering with +1 corresponding to the A of the ATG translation initiation codon in the reference sequence (NM_003361.3). Alamut Visual software (Interactive Biosoftware, Rouen, France; www.interactivebiosoftware.com) was used to assist in determining variant pathogenicity. Identified variants were successively checked against relevant databases, such as Clinvar (National Center for Biotechnology Information, Bethesda, MD; <https://www.ncbi.nlm.nih.gov/clinvar/>), Human Gene Mutation Database (Institute of Medical Genetics in Cardiff, Cardiff, UK; <http://www.hgmd.cf.ac.uk/ac/index.php>), VarSome (Saphetor, Lausanne, Switzerland; <https://varsome.com/>), and local databases to assess for previous publication.

Variants were considered disease-causing based on previous reports, family segregation analysis, or prediction algorithms (Sorting Intolerant from Tolerant [SIFT], Align GVD, mutation taster, and Polymorphism Phenotyping v2 [PolyPhen-2]) for pathogenicity.

The variants were classified according to the guidelines published by the American College of Medical Genetics in 2015.³¹ Variants of interest were verified by Sanger sequencing.

Measurements of urinary levels of *UMOD*

A validated enzyme-linked immunosorbent assay method was used to measure urinary *UMOD* levels (second morning urine sample) from 86 patients with ADTKD.²¹ Urinary creatinine was measured using a Synchro DXC800 analyzer (Beckman Coulter, Fullerton, CA). The reference samples ($n = 2717$) were obtained from the Cohorte Lausannoise, a population-based study including 6000 people 35 to 75 years of age from the city of Lausanne, Switzerland.²² eGFR was calculated using the Chronic Kidney Disease Epidemiology Collaboration equation. Informed consent was obtained from all participating individuals.

UMOD expression constructs

cDNA of human wild-type *UMOD* was cloned in pcDNA 3.1(+) (Thermo Fisher Scientific, Waltham, MA) and a hemagglutinin tag was inserted after the leader peptide in between T26 and S27 in the protein sequence.³² The C150S and L284P mutant isoforms were obtained by mutagenesis using the QuikChange Lightning mutagenesis kit (Agilent, Santa Clara, CA) following the manufacturer's instructions. Primers were designed using the software QuikChange Primer Design Program (Agilent). Primers used for mutation C150S: forward (5'→3') gatggcactgtgagctctccccggctctg, reverse (5'→3') caggagccggggaggactcacagtggccac and for mutation L284P: forward (5'→3') cccgagtgctaccggcgctactgcaca, reverse (5'→3') tgtgcagtacgcccggctgactcggg.

Cell culture conditions

HEK293 cells were grown in Dulbecco's modified Eagle's medium supplemented with 10% fetal bovine serum, 200 U/ml penicillin, 200 µg/ml streptomycin, and 2 mmol/l glutamine at 37 °C, 5% CO₂. HEK293 cells were transfected using Lipofectamine 2000 (Thermo

Fisher Scientific) following the manufacturer's protocol and analyzed 24 hours after transfection.

Western blot

Cells were lysed in octylglucoside lysis buffer (50 mmol/l Tris-HCl, pH 7.4, 150 mmol/l NaCl, 60 mmol/l octyl β-D-glucopyranoside, 10 mmol/l NaF, 0.5 mmol/l sodium orthovanadate, 1 mmol/l glycerophosphate and protease inhibitor cocktail [Sigma-Aldrich, St. Louis, MO]) for 1 hour at 4 °C followed by 10 minutes of centrifugation at 17,000g. Soluble fractions were quantified by the Bio-Rad Protein Assay (Bio-Rad Laboratories, Hercules, CA). Western blot experiments were performed as described in Schaeffer *et al.*³² Antibodies used were mouse purified anti-HA.11 Epitope Tag antibody (dilution 1:1000; 901502; BioLegend, San Diego, CA) and mouse monoclonal anti-β-actin (dilution 1:20,000; A2228; Sigma-Aldrich).

Immunofluorescence

Kidney biopsies. Immunodetection of *UMOD* and GRP78 was performed on 5-µm-thick kidney sections obtained from nephrectomy samples of patients with ADTKD-*UMOD* (female, 41 years old, ESKD; male, 42 years old, ESKD) and ADTKD-*MUC1* (female, 60 years old, ESKD; male, 47 years old, ESKD). Slides were deparaffinized in xylene and rehydrated in a graded ethanol series. Antigen retrieval was carried out for 10 minutes with citrate buffer (pH 6.0) at 98 °C. After 20 minutes in blocking solution, slides were incubated overnight with GRP78 primary antibody (1:300; ab21685; Abcam, Cambridge, UK), followed by incubation with AlexaFluor555-conjugated goat anti-rabbit antibody for 45 minutes (1:200; Invitrogen, Thermo Fisher Scientific). The slides were probed with sheep anti-*UMOD* primary antibody (1:800; K90071C; Meridian Life Science Inc., Memphis, TN), followed by AlexaFluor488-conjugated donkey anti-sheep (1:200; Invitrogen). Coverslips were mounted with Prolong gold antifade reagent with 4',6-diamidino-2-phenylindole (Invitrogen) and analyzed under a Zeiss LSM 510 Meta confocal microscope (Carl Zeiss, Jena, Germany) with high numerical aperture lenses (Plan-Neofluar 20×/0.5). The use of these samples has been approved by the Université catholique de Louvain Ethical Review Board.²³

HEK293 cells. Cells grown on coverslip were fixed in 4% paraformaldehyde for 15 minutes, permeabilized 10 minutes with 0.5% Triton, and blocked 30 minutes with 10% donkey serum. Cells were labelled for 1 hour, 30 minutes at room temperature with a mouse purified anti-HA.11 Epitope Tag antibody (dilution 1:500; 901502; BioLegend) and a rabbit polyclonal anti-calreticulin (dilution 1:500; C4606; Sigma-Aldrich) followed by incubation for 1 hour with the appropriate AlexaFluor conjugated secondary antibodies (dilution 1:500; Thermo Fisher Scientific). Cells were stained with 4',6-diamidino-2-phenylindole and mounted using fluorescence mounting medium (Dako; Agilent). All pictures were taken with an UltraVIEW ERS spinning disk confocal microscope (UltraVIEW ERS-Imaging Suite Software; Zeiss 63X/1.4; PerkinElmer Life and Analytical Sciences, Boston, MA). All images were imported in Photoshop CS (Adobe Systems, Mountain View, CA) and adjusted for brightness and contrast.

Generation and validation of the ADTKD *UMOD*-score

The weighted *UMOD*-score was based on ADTKD criteria, specific clinical characteristics of ADTKD-*UMOD* (i.e., early gout onset and hyperuricemia), and parameters that are negatively associated with ADTKD (i.e., providing alternative explanation for CKD: proteinuria and/or hematuria, diabetes and/or uncontrolled hypertension, renal

cysts and/or enlarged kidneys).^{2,15,20} For weighting the items of the score, we used integer values between -1 and $+3$. A score of $+2$ was given for the general ADTKD criteria,² $+1$ or $+3$ for the *UMOD*-specific clinical and laboratory findings, and -1 for each negatively associated item. The score was first tested in the Belgo-Swiss ADTKD registry and validated in the US ADTKD registry. To discriminate ADTKD-*UMOD* from ADTKD-*MUC1*, we defined a normal range of urinary *UMOD* [(mg/g creatinine)/eGFR] using 2717 urine samples from the general population. Based on the pathophysiology of ADTKD-*UMOD*, on previous reports,³⁴ as well as on our findings (Figure 5a), we assigned, respectively, $+1$ and $+3$ points for urinary *UMOD* values between the median and 25th percentile and below the 25th percentile of normal urinary *UMOD* levels. Similarly, we assigned, respectively, -1 and -3 points for urinary *UMOD* values between the median and 75th percentile and above the 75th percentile of normal urinary *UMOD* levels. Conceptualization of the score was based on the previously published hepatocyte nuclear factor 1 β score.³⁵

Statistical analysis

Quantitative parameters are presented as median and IQR (25th, 75th percentiles) (for scale variables) or means \pm SD (for continuous variables), and qualitative parameters are presented as fractions with percentages. Categorical variables were compared using the χ^2 test. Continuous variables were compared using the Mann-Whitney U test or unpaired *t* test. Analysis of variance testing with Tukey's multiple comparison test was used to compare urinary *UMOD* levels. Kaplan-Meier curves were generated to display ESKD-free and gout-free survival. Patients who had not reached ESKD or developed gout at the end of the study (outcome of interest not occurred during follow-up time) were considered censored individuals. Censoring time was defined as age at last follow-up. A log-rank test was used for comparison of survival curves. The performance of the *UMOD*-score was assessed by calculating the AUC of the receiver-operating characteristic curve. The Youden index was used to define the optimal discriminatory cut-off point for the *UMOD*-score. Statistical analysis was performed using SPSS Statistics (IBM Corp., Armonk, NY). $P < 0.05$ was considered statistically significant, 2-sided tests were used.

DISCLOSURE

All the authors declared no competing interests.

ACKNOWLEDGMENTS

EO is supported by the Fonds National de la Recherche Luxembourg (grant 6903109), the University Research Priority Program "Integrative Human Physiology, ZIHP" of the University of Zurich, and an Early Postdoc Mobility-Stipendium of the Swiss National Science Foundation (P2ZHP3_195181). LR is supported by the Italian Society of Nephrology (SIN) under the "Adotta un progetto di ricerca" program, Telethon-Italy (grant GGP14263) and the Italian Ministry of Health (grant RF-2010-2319394). KK and AJB are supported by National Institutes of Health-National Institute of Diabetes and Digestive and Kidney Diseases (grant R21 DK106584). MZ, KH, and SK were supported by the Ministry of Health of the Czech Republic (grant NV17-29786A), the Ministry of Education of the Czech Republic (grant LTAUSA19068), and by Charles University in Prague (institutional programs UNCE/MED/007 and PROGRES-Q26/LF1). They thank the National Center for Medical Genomics (grant LM2015091) for help with *UMOD* and *MUC1* sequencing. OD is supported by the European Community's Seventh Framework Programme (grant 305608), the European Reference Network for Rare Kidney Diseases (project ° 739532), the Swiss National Science Foundation's National Center of Competence in Research Kidney Control of Homeostasis program, and the Swiss National Science Foundation (grant 310030-

189044). OD and OB were supported by the Gebert-Rüf Foundation for research on ADTKD-*UMOD*. JAS is supported by Kidney Research UK and the Northern Counties Kidney Research Fund. RT is funded by Instituto de Salud Carlos III: Redes Temáticas de Investigación Cooperativa Red de Investigación Renal (grant RD16/0009) and Fondo de Investigación Sanitarias Fondo Europeo de Desarrollo Regional (grant PI15/01824, PI18/00362). JM is supported by the Fonds de la Recherche Scientifique-Communauté Française de Belgique. DGF was supported by the Swiss National Centre of Competence in Research TransCure, the Swiss National Centre of Competence in Research Kidney Control of Homeostasis program, and the Swiss National Science Foundation (grants 31003A_152829 and 331C30_166785/1). Genetic testing for *MUC1* is supported by the Slim Initiative for Genomic Medicine in the Americas, a collaboration of the Broad Institute with the Carlos Slim Foundation.

We thank all participating patients and families. The Cohorte Lausannoise is acknowledged for providing reference urine samples and eGFR information. We are grateful to Maegan Harden and her team on the Broad Genomics Platform for expert assistance with genetic testing for *MUC1*.

Parts of these data were presented as a poster during the 2017 American Society of Nephrology Kidney Week (October 31–November 5, 2017, New Orleans, Louisiana).

SUPPLEMENTARY MATERIAL

Supplementary File (PDF)

Appendix S1. Referring Physicians.

Figure S1. The L284P uromodulin shows trafficking defect.

Figure S2. Freedom from ESKD and gout in ADTKD-*UMOD* according to noncysteine versus cysteine mutations.

Figure S3. Association between urinary uromodulin and glomerular filtration in the general population.

Figure S4. Uromodulin processing in ADTKD-*UMOD* and ADTKD-*MUC1*.

Figure S5. Design and flowchart of the Belgo-Swiss ADTKD registry.

Figure S6. Clinical characteristics of *UMOD*-positive and *UMOD*-negative patients in the Belgo-Swiss ADTKD registry.

Table S1. List of the 106 *UMOD* mutations in the Belgo-Swiss and US ADTKD registries.

Table S2. Allele frequency and pathogenicity scores for novel *UMOD* variants.

Table S3. Clinical characteristics of ADTKD patients in the US ADTKD registry according to genetic diagnosis.

Table S4. Coordinates of the receiver-operating characteristics (ROC) curve of the clinical *UMOD*-score in the Belgo-Swiss ADTKD registry (*UMOD*-positive and *UMOD*-negative patients) ($n = 211$ patients with available data).

Table S5. Coordinates of the receiver-operating characteristics (ROC) curve of the *UMOD*-score in the US ADTKD registry (patients with ADTKD-*UMOD* and ADTKD-*MUC1*) without and with urinary uromodulin ($n = 205$ and $n = 86$ with urinary uromodulin).

REFERENCES

- Devuyst O, Olinger E, Weber S, et al. Autosomal dominant tubulointerstitial kidney disease. *Nat Rev Dis Primers*. 2019;5:60.
- Eckardt KU, Alper SL, Antignac C, et al. Autosomal dominant tubulointerstitial kidney disease: diagnosis, classification, and management—a KDIGO consensus report. *Kidney Int*. 2015;88:676–683.
- Hart TC, Gorry MC, Hart PS, et al. Mutations of the *UMOD* gene are responsible for medullary cystic kidney disease 2 and familial juvenile hyperuricaemic nephropathy. *J Med Genet*. 2002;39:882–892.
- Devuyst O, Olinger E, Rampoldi L. Uromodulin: from physiology to rare and complex kidney disorders. *Nat Rev Nephrol*. 2017;13:525–544.
- Kirby A, Gnirke A, Jaffe DB, et al. Mutations causing medullary cystic kidney disease type 1 lie in a large VNTR in *MUC1* missed by massively parallel sequencing. *Nat Genet*. 2013;45:299–303.

6. Knaup KX, Hackenbeck T, Popp B, et al. Biallelic expression of mucin-1 in autosomal dominant tubulointerstitial kidney disease: implications for nongenetic disease recognition. *J Am Soc Nephrol.* 2018;29:2298–2309.
7. Zivna M, Kidd K, Pristoupilova A, et al. Noninvasive immunohistochemical diagnosis and novel MUC1 mutations causing autosomal dominant tubulointerstitial kidney disease. *J Am Soc Nephrol.* 2018;29:2418–2431.
8. Bleyer AJ, Kmoch S, Antignac C, et al. Variable clinical presentation of an MUC1 mutation causing medullary cystic kidney disease type 1. *Clin J Am Soc Nephrol.* 2014;9:527–535.
9. Bingham C, Ellard S, van't Hoff WG, et al. Atypical familial juvenile hyperuricemic nephropathy associated with a hepatocyte nuclear factor-1beta gene mutation. *Kidney Int.* 2003;63:1645–1651.
10. Faguer S, Decramer S, Chassaing N, et al. Diagnosis, management, and prognosis of HNF1B nephropathy in adulthood. *Kidney Int.* 2011;80:768–776.
11. Zivna M, Hulkova H, Matignon M, et al. Dominant renin gene mutations associated with early-onset hyperuricemia, anemia, and chronic kidney failure. *Am J Hum Genet.* 2009;85:204–213.
12. Bolar NA, Golzio C, Zivna M, et al. Heterozygous loss-of-function SEC61A1 mutations cause autosomal-dominant tubulo-interstitial and glomerulocystic kidney disease with anemia. *Am J Hum Genet.* 2016;99:174–187.
13. Groopman EE, Marasa M, Cameron-Christie S, et al. Diagnostic utility of exome sequencing for kidney disease. *N Engl J Med.* 2019;380:142–151.
14. Gast C, Marinaki A, Arenas-Hernandez M, et al. Autosomal dominant tubulointerstitial kidney disease-UMOD is the most frequent non polycystic genetic kidney disease. *BMC Nephrol.* 2018;19:301.
15. Ayasreh N, Bullich G, Miquel R, et al. Autosomal dominant tubulointerstitial kidney disease: clinical presentation of patients with ADTKD-UMOD and ADTKD-MUC1. *Am J Kidney Dis.* 2018;72:411–418.
16. Trudu M, Schaeffer C, Riba M, et al. Early involvement of cellular stress and inflammatory signals in the pathogenesis of tubulointerstitial kidney disease due to UMOD mutations. *Sci Rep.* 2017;7:7383.
17. Bemascone I, Janas S, Ikehata M, et al. A transgenic mouse model for uromodulin-associated kidney diseases shows specific tubulo-interstitial damage, urinary concentrating defect and renal failure. *Hum Mol Genet.* 2010;19:2998–3010.
18. Johnson BG, Dang LT, Marsh G, et al. Uromodulin p.Cys147Trp mutation drives kidney disease by activating ER stress and apoptosis. *J Clin Invest.* 2017;127:3954–3969.
19. Dvela-Levitt M, Kost-Altimova M, Emani M, et al. Small molecule targets TMED9 and promotes lysosomal degradation to reverse proteinopathy. *Cell.* 2019;178:521–535.e523.
20. Bollée G, Dahan K, Flamant M, et al. Phenotype and outcome in hereditary tubulointerstitial nephritis secondary to UMOD mutations. *Clin J Am Soc Nephrol.* 2011;6:2429–2438.
21. Youhanna S, Weber J, Beaujean V, et al. Determination of uromodulin in human urine: influence of storage and processing. *Nephrol Dial Transplant.* 2014;29:136–145.
22. Pruijm M, Ponte B, Ackermann D, et al. Associations of urinary uromodulin with clinical characteristics and markers of tubular function in the general population. *Clin J Am Soc Nephrol.* 2016;11:70–80.
23. Troyanov S, Delmas-Frenette C, Bollée G, et al. Clinical, genetic, and urinary factors associated with uromodulin excretion. *Clin J Am Soc Nephrol.* 2016;11:62–69.
24. Olden M, Corre T, Hayward C, et al. Common variants in UMOD associate with urinary uromodulin levels: a meta-analysis. *J Am Soc Nephrol.* 2014;25:1869–1882.
25. Scolari F, Caridi G, Rampoldi L, et al. Uromodulin storage diseases: clinical aspects and mechanisms. *Am J Kidney Dis.* 2004;44:987–999.
26. Liu Y, Goldfarb DS, El-Achkar TM, et al. Tamm-Horsfall protein/ uromodulin deficiency elicits tubular compensatory responses leading to hypertension and hyperuricemia. *Am J Physiol Renal Physiol.* 2018;314:F1062–F1076.
27. Dahan K. A cluster of mutations in the UMOD gene causes familial juvenile hyperuricemic nephropathy with abnormal expression of uromodulin. *J Am Soc Nephrol.* 2003;14:2883–2893.
28. Ashton EJ, Legrand A, Benoit V, et al. Simultaneous sequencing of 37 genes identified causative mutations in the majority of children with renal tubulopathies. *Kidney Int.* 2018;93:961–967.
29. Hureauux M, Ashton E, Dahan K, et al. High-throughput sequencing contributes to the diagnosis of tubulopathies and familial hypercalcemia hypocalciuria in adults. *Kidney Int.* 2019;96:1408–1416.
30. Blumenstiel B, DeFelice M, Birsoy O, et al. Development and validation of a mass spectrometry-based assay for the molecular diagnosis of mucin-1 kidney disease. *J Mol Diagn.* 2016;18:566–571.
31. Richards S, Aziz N, Bale S, et al. Standards and guidelines for the interpretation of sequence variants: a joint consensus recommendation of the American College of Medical Genetics and Genomics and the Association for Molecular Pathology. *Genet Med.* 2015;17:405–424.
32. Schaeffer C, Santambrogio S, Perucca S, et al. Analysis of uromodulin polymerization provides new insights into the mechanisms regulating ZP domain-mediated protein assembly. *Mol Biol Cell.* 2009;20:589–599.
33. Dahan K, Devuyt O, Smaers M, et al. A cluster of mutations in the UMOD gene causes familial juvenile hyperuricemic nephropathy with abnormal expression of uromodulin. *J Am Soc Nephrol.* 2003;14:2883–2893.
34. Bleyer AJ, Hart TC, Shihabi Z, et al. Mutations in the uromodulin gene decrease urinary excretion of Tamm-Horsfall protein. *Kidney Int.* 2004;66:974–977.
35. Faguer S, Chassaing N, Bandin F, et al. The HNF1B score is a simple tool to select patients for HNF1B gene analysis. *Kidney Int.* 2014;86:1007–1015.

4.5 **Autosomal dominant ApoA4 mutations present as tubulointerstitial kidney disease with medullary amyloidosis.**

Kmochová T, **Kidd KO**, Orr A, Hnízda A, Hartmannová H, Hodaňová K, Vyleťal P, Naušová K, Brinsa V, Trešlová H, Sovová J, Barešová V, Svojšová K, Vrbacká A, Stránecký V, Robins VC, Taylor A, Martin L, Rivas-Chavez A, Payne R, Bleyer HA, Williams A, Rennke HG, Weins A, Short PJ, Agrawal V, Storsley LJ, Waikar SS, McPhail ED, Dasari S, Leung N, Hewlett T, Yorke J, Gaston D, Geldenhuys L, Samuels M, Levine AP, West M, Hůlková H, Pompach P, Novák P, Weinberg RB, Bedard K, Živná M, Sikora J, Bleyer AJ Sr, Kmoch S.

Kidney Int. 2023 Dec 12;. doi: 10.1016/j.kint.2023.11.021

Autosomal dominant ApoA4 mutations present as tubulointerstitial kidney disease with medullary amyloidosis

Tereza Kmochová^{1,2,3}, Kendrah O. Kidd^{1,2,23}, Andrew Orr^{3,4,23}, Aleš Hnízda¹, Hana Hartmannová¹, Kateřina Hodaňová¹, Petr Vyleťal¹, Karolína Naušová¹, Vítězslav Brinsa¹, Helena Trešlová¹, Jana Sovová¹, Veronika Barešová¹, Klára Svojšová¹, Alena Vrbacká¹, Viktor Stránecký¹, Victoria C. Robins², Abbigail Taylor², Lauren Martin², Ana Rivas-Chavez², Riley Payne², Heidi A. Bleyer², Adrienne Williams², Helmut G. Rennke⁵, Astrid Weins⁵, Patrick J. Short⁶, Varun Agrawal⁷, Leroy J. Storsley⁸, Sushrut S. Waikar⁹, Ellen D. McPhail¹⁰, Surendra Dasari¹¹, Nelson Leung¹², Tom Hewlett¹³, Jake Yorke⁴, Daniel Gaston⁴, Laurette Geldenhuys⁴, Mark Samuels^{14,15,16}, Adam P. Levine¹⁷, Michael West¹³, Helena Hůlková^{1,18}, Petr Pompach¹⁹, Petr Novák¹⁹, Richard B. Weinberg^{20,21}, Karen Bedard²², Martina Živná^{1,2}, Jakub Sikora^{1,18}, Anthony J. Bleyer Sr.^{1,2} and Stanislav Kmoch^{1,2}

¹Research Unit for Rare Diseases, Department of Pediatrics and Inherited Metabolic Disorders, First Faculty of Medicine, Charles University, Prague, Czech Republic; ²Section on Nephrology, Wake Forest University School of Medicine, Winston-Salem, North Carolina, USA; ³Department of Ophthalmology and Visual Sciences, Dalhousie University, Halifax, Nova Scotia, Canada; ⁴Department of Pathology, Faculty of Medicine, Dalhousie University, Halifax, Nova Scotia, Canada; ⁵Pathology Department, Brigham and Women's Hospital, Harvard Medical School, Boston, Massachusetts, USA; ⁶Sano Genetics Limited, London, UK; ⁷Division of Nephrology and Hypertension, Larner College of Medicine, University of Vermont, Burlington, Vermont, USA; ⁸Department of Medicine, University of Manitoba, Winnipeg, Manitoba, Canada; ⁹Section of Nephrology, Boston University Chobanian and Avedisian School of Medicine, Boston, Massachusetts, USA; ¹⁰Department of Laboratory Medicine and Pathology, Mayo Clinic, Rochester, Minnesota, USA; ¹¹Department of Quantitative Health Sciences, Mayo Clinic, Rochester, Minnesota, USA; ¹²Division of Nephrology and Hypertension, Division of Hematology, Mayo Clinic, Rochester, Minnesota, USA; ¹³Division of Nephrology, Department of Medicine, Faculty of Medicine, Dalhousie University, Halifax, Nova Scotia, Canada; ¹⁴Department of Medicine Université de Montréal, Montreal, Quebec, Canada; ¹⁵Department of Biochemistry, Université de Montréal, Montreal, Quebec, Canada; ¹⁶Centre de Recherche du CHU Ste-Justine, Montreal, Quebec, Canada; ¹⁷Research Department of Pathology, University College London, London, UK; ¹⁸Institute of Pathology, First Faculty of Medicine, Charles University, Prague, Czech Republic; ¹⁹Institute of Microbiology of the Czech Academy of Sciences, Vestec, Czech Republic; ²⁰Section on Gastroenterology, Department of Internal Medicine, Wake Forest University School of Medicine, Winston-Salem, North Carolina, USA; ²¹Department of Physiology and Pharmacology, Wake Forest University School of Medicine, Winston-Salem, North Carolina, USA; and ²²Department of Pathology and Laboratory Medicine, Izaak Walton Killam Hospital, Halifax Nova Scotia, Canada

Sporadic cases of apolipoprotein A-IV medullary amyloidosis have been reported. Here we describe five families found to have autosomal dominant medullary amyloidosis due to two different pathogenic APOA4 variants. A large family with autosomal dominant chronic kidney disease (CKD) and bland urinary sediment underwent whole genome sequencing with identification of a chr11:116692578 G>C (hg19) variant encoding the missense mutation p.L66V of the ApoA4 protein. We identified two other distantly related families from our registry with the same variant and two other distantly related families with a chr11:116693454 C>T (hg19) variant encoding the missense mutation p.D33N. Both

mutations are unique to affected families, evolutionarily conserved and predicted to expand the amyloidogenic hotspot in the ApoA4 structure. Clinically affected individuals suffered from CKD with a bland urinary sediment and a mean age for kidney failure of 64.5 years. Genotyping identified 48 genetically affected individuals; 44 individuals had an estimated glomerular filtration rate (eGFR) under 60 ml/min/1.73 m², including all 25 individuals with kidney failure. Significantly, 11 of 14 genetically unaffected individuals had an eGFR over 60 ml/min/1.73 m². Fifteen genetically affected individuals presented with higher plasma ApoA4 concentrations. Kidney pathologic specimens from four individuals revealed amyloid deposits limited to the medulla, with the mutated ApoA4 identified by mass-spectrometry as the predominant amyloid constituent in all three available biopsies. Thus, ApoA4 mutations can cause autosomal dominant medullary amyloidosis, with marked amyloid deposition limited to the kidney medulla and presenting with autosomal dominant CKD

Correspondence: Anthony J. Bleyer, Sr., Section on Nephrology, Wake Forest School of Medicine, One Medical Center Boulevard, Winston-Salem, North Carolina 27157, USA. E-mail: ableyer@wakehealth.edu

²³These authors contributed equally to the work.

Received 13 April 2023; revised 3 November 2023; accepted 10 November 2023

with a bland urinary sediment. Diagnosis relies on a careful family history, *APOA4* sequencing and pathologic studies.

Kidney International (2024) ■, ■-■; <https://doi.org/10.1016/j.kint.2023.11.021>

KEYWORDS: AApoA-IV; ApoA4; autosomal dominant tubulointerstitial kidney disease; medullary amyloidosis

Copyright © 2023, International Society of Nephrology. Published by Elsevier Inc. All rights reserved.

Lay Summary

In this article, we identify changes (“mutations”) in the gene *APOA4* as a cause of inherited kidney disease. Apolipoprotein A-IV (ApoA4) is a protein that transports fat molecules from the intestines via the bloodstream to cells throughout the body. After the fat molecules are removed from ApoA4, it is filtered by the kidney and reabsorbed back into the bloodstream. In this study of 5 families, we identified 1 mutation in 3 families, and another mutation in 2 families. In both cases, the mutations affect the ApoA4 structure and result in deposition of abnormal ApoA4 in the middle (medulla) of the kidney. This abnormal protein deposition leads to slowly progressive kidney failure, often leading to the need for dialysis later in life. The article is important because it identifies a new form of inherited kidney disease. Now patients can be tested for the disease, and scientists can start to develop treatments.

Genetic causes increasingly are being identified in families presenting with chronic kidney disease (CKD) with a bland urinary sediment and autosomal dominant inheritance.¹ The most common causes are autosomal dominant tubulointerstitial kidney disease (ADTKD) due to *UMOD*² or *MUC1*³ mutations, each accounting for approximately 0.3% of cases of kidney failure resulting in the need for dialysis or kidney transplantation in the US.^{4–6} Other families also have an ADTKD-like presentation (autosomal dominant CKD with a bland urinary sediment) in which the genetic cause of kidney disease has not been identified.

In this investigation, we identify 2 different variants in the *APOA4* gene encoding human apolipoprotein A-IV (ApoA4) in 48 individuals from 5 families with an ADTKD-like presentation. ApoA4 is a 46-kDa apolipoprotein that is synthesized in intestinal enterocytes in response to dietary fat absorption⁷ and incorporated onto the surface of nascent chylomicrons. Once chylomicrons enter the circulation, ApoA4 dissociates from the chylomicron and circulates in a manner loosely associated with high-density lipoproteins⁸ as a lipid-free glycoprotein with a molecular weight of 46 kD⁹ and as a stable homodimer with a molecular weight of 92 kD.¹⁰ The kidney plays a major role in ApoA4 metabolism. Monomeric ApoA4 is small enough to undergo glomerular filtration,¹¹ with subsequent reabsorption and degradation in proximal and distal tubules.¹¹

ApoA4 has been found in rare cases to be the primary constituent of amyloid deposits occurring exclusively in the kidney medulla, with 13 cases of sporadic AApoAIV (amyloid-ApoAIV) medullary amyloidosis having been described in the literature^{12–14} or presented as an abstract (Sheikh SN, Li T, Kunjal RA. Apolipoprotein A-IV amyloidosis: an unusual cause of renal amyloidosis and CKD. Presented at: American Society of Nephrology Kidney Week. October 23–25, 2018; San Diego, CA. TH-PO523). In all cases, AApoAIV deposition was limited to the kidney medulla. Of the 13 cases, 12 presented with CKD and a bland urinary sediment with minimal proteinuria; 1 presented with advanced CKD and 5.8 g/d of urinary protein.¹³

As in reports of sporadic AApoAIV medullary amyloidosis, pathologic examination of kidney tissue from 4 genetically affected individuals from our investigation revealed isolated medullary amyloid deposition, with mass-spectrometric analysis of tissue available from 3 patients revealing mutated ApoA4 protein as the predominant constituent. Thus, in this investigation, we report for the first time cases of *APOA4* variants causing autosomal dominant medullary amyloidosis and a presentation of CKD with a bland urinary sediment.

METHODS

This investigation was approved by the institutional review boards of Wake Forest School of Medicine (Winston-Salem, NC, United States), Charles University (Prague, Czech Republic), and Nova Scotia Health (Halifax, Nova Scotia, Canada).

The Wake Forest Rare Inherited Kidney Disease Registry includes DNA from 429 families with autosomal dominant CKD with a bland urinary sediment.¹⁵ Participants with autosomal dominant CKD with a bland urinary sediment who are not found to have a known causative mutation then undergo whole-exome or whole-genome analysis with systematic reanalysis for unsolved cases.

Genetic evaluation

Genomic DNA of all available individuals was extracted from whole blood or saliva. Sanger sequencing, whole-exome and whole-genome sequencing, data analysis, variant prioritization, and targeted genotyping were performed as described.¹⁶ Obligate heterozygotes were included in the analysis only if age of initiation of dialysis or transplantation was available.

In silico analysis

Mutations were mapped into the ApoA4 crystal structure¹⁷ or a theoretical model of the dimeric full-length protein generated by AlphaFold2-multimer available via ColabFold.¹⁸ Structural models were visualized with PyMOL viewer (Schrodinger Inc.) and UCSF ChimeraX (DeLano Scientific). Amyloidogenic regions in ApoA4 were identified using MetAmyl¹⁹ and AmyloPred2.²⁰

Amyloid proteomic analysis

The proteomic content of microdissected amyloid deposits from pathologic specimens was analyzed as previously described.¹³

Histopathologic, immunohistochemical, immunofluorescent, and ultrastructural electron microscopic analyses of kidney biopsies

Standard staining was performed as previously described.⁶ See the [Supplementary Methods](#) for information on the specific antibodies that were used.

Immunoblot analysis of ApoA4 in plasma

Plasma samples were separated by non-denaturing polyacrylamide gel electrophoresis, and ApoA4 was immunodetected as previously described.²¹ For immunodetection, mouse anti-human ApoA4 antibody (G-8) (sc-374543, Santa Cruz) was used. Immunoaffinity enrichment of plasma ApoA4 with mass spectrometry analysis typing was performed as previously described,²² with details provided in the [Supplementary Methods](#).

Statistical analysis

Standard statistical analyses were performed with SAS (SAS Institute). Estimated glomerular filtration rate (eGFR) was calculated with the Chronic Kidney Disease Epidemiology Collaboration (CKD-EPI) equation.²³ To assess the differences in plasma ApoA4 levels between those with *APOA4* risk genotypes and those unaffected, a mixed-effects model with compound-symmetry covariance structure was applied to account for the correlation between related individuals.

RESULTS

The index case III.12 from Family 1 ([Figure 1](#)) is a male patient who presented at age 54 years with CKD of unknown cause. In his early 40s, the patient was diagnosed with hypertension, gout, and hypercholesterolemia. The patient was placed on atorvastatin, 60 mg daily, for

hyperlipidemia. The patient never experienced a cardiovascular event. The patient's father died in his 80s without CKD, and his mother's eGFR was 55 ml/min per 1.73 m² at age 90 years. A sister of the proband (III.9) underwent kidney transplantation at age 68 years, and a brother's (III.11) eGFR was 19 ml/min per 1.73 m² at age 57 years. Cardiovascular disease occurred only after age 50 years in family members with and without CKD. Physical examination was unremarkable. The patient's urinalysis was bland, with pH 5.5 and no urinary protein. The eGFR was 44 ml/min per 1.73 m². A fasting lipid panel of the patient at age 52 years while on atorvastatin revealed a total cholesterol of 193 mg/dl (normal range [nr] 25–200 mg/dl), triglycerides 176 mg/dl (nr <150 mg/dl), high-density lipoprotein cholesterol 49.6 mg/dl (nr 35–135 mg/dl), and low-density lipoprotein cholesterol 108 mg/dl (nr <130 mg/dl). On kidney imaging at age 55 years, the right kidney was 11.3 cm with 2 cortical cysts, and the left kidney was 12.7 cm with a simple cyst. A kidney biopsy at age 54 years ([Table 1](#)) revealed advanced chronic changes in all compartments of the kidney parenchyma, with about 60% globally sclerotic glomeruli, tubular atrophy, interstitial fibrosis, and severe vascular sclerotic changes. No amyloid deposition was noted. CKD progressed to initiation of

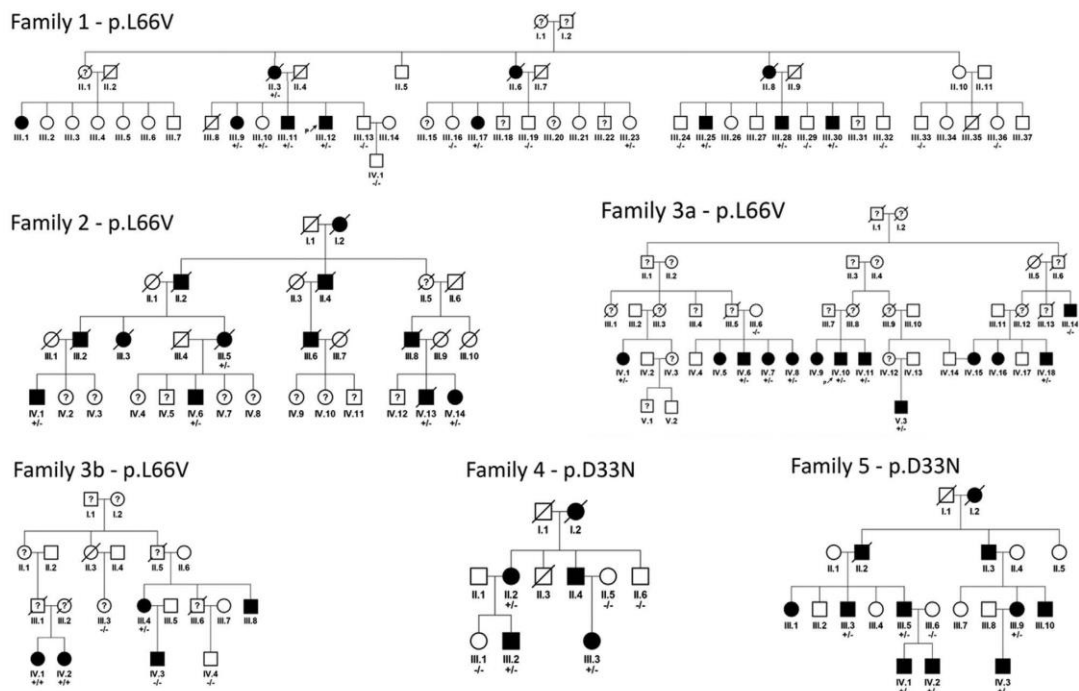


Figure 1 | Family pedigrees. Filled-in shapes denote chronic kidney disease, and unshaded shapes denote normal kidney function. A question mark (?) denotes lack of information on clinical status. A plus sign (+) indicates the presence of the p.L66V or p.D33N *APOA4* variant, and a minus sign (-) indicates the presence of the wild-type *APOA4* variant in a genotyped individual. Two plus signs (++) indicates the presence of 2 p.L66V *APOA4* variants. Unfortunately, no clinical and/or laboratory data were available for the parents of the 2 homozygotes in Family 3b, IV.1 and IV.2. Additional pedigree branches of Family 3 are presented in [Supplementary Figure S1](#).

Table 1 | Pathologic findings

Individual and mutation	eGFR at time of biopsy, ml/min per 1.73 m ²	Bx type	Glomeruli	Tubule changes	Tubulointerstitium	Microvascular changes	EM	Medulla	CR/ApoA4 staining
Family 1, III.12 p.L66V	54	Core	Glomerulo-sclerosis. Double contours of GBMs	TA	IF	Severe vascular sclerotic changes	The displaced glomerular endothelium has developed a newly formed thin layer of basement membrane material	Not present	CR staining and ApoA4 staining revealed no interstitial amyloid, amyloid casts, or abnormal cytoplasmic ApoA4 signal.
Family 1, III.12 p.L66V	10	Nx	Global glomerulo-sclerosis. No double contours seen.	TA	Marked IF	Moderate sclerosis	Fibrils approximately 8.5 nm in diameter in criss-crossing bundles (Figure 5b)	Extensive deposition of amorphous eosinophilic material	Strongly congophilic with apple-green birefringence limited to inner medulla
Family 2, IV.1 p.L66V	46	Core	Glomerulosclerosis	Basement membrane thickening and atrophy	Mild chronic inflammatory cell infiltrate with fibrosis	Vessels are mildly thickened and demonstrate hyaline changes in the vessel walls	Fine non-branching fibrils arranged in criss-crossing bundles, confirming the presence of amyloid	Advanced involvement of the tubules and interstitium by a hyaline, "brittle" material, which is PAS-negative.	CR stains demonstrate positive staining in the hyaline areas, which appear under polarization as apple-green birefringence
Family 2, V.3 p.L66V	53	Core	Glomerulo-sclerosis. Bowman's capsule is thickened and lamellated.	Atrophic tubules. TBM shows areas of lamellation.	Scattered chronic inflammation. Increased collagen.	Focal hyalinosis	No EDD	No medulla present	CR staining and ApoA4 staining revealed no interstitial amyloid, amyloid casts, or abnormal cytoplasmic ApoA4 signal.
Family 4, III.2 p.D33N	73	Core	Glomerulo-sclerosis. Wrinkling of the GBM	Mild patchy TA. No tubulitis	Patchy interstitial mononuclear inflammatory cell infiltrate.	Unremarkable	Unavailable	No medulla present	CR staining and ApoA4 staining revealed no interstitial amyloid, amyloid casts, or abnormal cytoplasmic ApoA4 signal.
Family 4, III.3 p.D33N	39	Core	Glomerular hypertrophy. Focal global glomerulosclerosis, moderate	Focal TBM multi-lamellation. Diffuse TA	Mild chronic inflammatory infiltrate of mononuclear leukocytes	Mild to moderate ARS	No comment	No medulla present	CR staining and ApoA4 staining revealed no interstitial amyloid, amyloid casts, or abnormal cytoplasmic ApoA4 signal.
Family 3a, III.14 p.L66V	On dialysis	Nx	Extensive glomerulosclerosis. Basement membrane wrinkling	Marked TA and IF	Moderate patchy interstitial lymphoid infiltrate	Marked arterial and ARS	Unavailable	Amyloid deposition. Focal calcification and ossification	Positive CR staining—salmon pink with apple-green birefringence
Family 3a, IV.10 p.L66V	61	Core	Medulla only	Unremarkable medullary tubules	Unremarkable medullary tubules	No arteries identified	Unavailable, no glomeruli	Amyloid deposition	Positive CR staining—salmon pink with apple-green birefringence

ARS, arteriosclerosis; Bx, biopsy; CR, Congo Red; EDD, electron-dense deposit; eGFR, estimated glomerular filtration rate; EM, electron microscopy; GBM, glomerular basement membrane; IF, interstitial fibrosis; Nx, nephrectomy; PAS, periodic acid-Schiff; TA, tubular atrophy; TBM, tubular basement membrane.

dialysis at age 66 years. Family history revealed numerous family members who were affected similarly clinically, with an autosomal dominant inheritance pattern (Figure 1).

Genetic analysis

Upon negative results of *UMOD* and *MUC1* genotyping, whole-genome sequencing was performed in 5 clinically affected individuals from family 1 (III.9, III.11, III.12, III.25, and III.30). A search for shared genetic material identified only one ~15-megabase pair (Mbp)-sized genomic region on chromosome 11 (chr11: 110012896-124998347), with only one relevant candidate variant—chr11:116692578 G>C (hg19)—encoding for a missense mutation in *APOA4* (NM_000482.4): c.196C>G (p.L66V). No other rare protein coding or conserved regulatory variants were shared by affected individuals elsewhere in their genomes. Using Sanger sequencing and segregation analysis, we genotyped 19 individuals from Family 1. Of 11 genetically affected individuals (10 genotyped and one obligate heterozygote), 9 had CKD, with 2 female members (III.10 and III.23) being as yet clinically unaffected (eGFR 100 ml/min per 1.73 m² at age 55 years, and eGFR 86 ml/min per 1.73 m² at age 54 years, respectively). Of 9 genetically unaffected individuals, the lowest eGFR was 59 ml/min per 1.73 m² at age 69 years (Figure 2a).

A search for rare *APOA4* variants from our internal whole-genome sequencing/whole-exome sequencing database revealed the following results:

- (i) The same chr11:116692578 G>C (p.L66V) variant was present in 7 clinically affected individuals (5 genotyped and 2 obligate heterozygotes) from Family 2 (Figure 1) and in the proband IV.10 from Family 3a, who was later
- (ii) The chr11:116693454 C>T (hg19) variant encoding for another missense mutation in *APOA4* (NM_000482.4): c.97G>A (p.D33N) was identified in 5 clinically affected individuals (3 genotyped and 2 obligate heterozygotes)

found to be part of a large kindred from a rural area in Nova Scotia, Canada, where an unusually high incidence of CKD had been noted by researchers from Dalhousie University. The different branches of this kindred are displayed as Families 3a and 3b in Figure 1, and Families 3c–f in Supplementary Figure S1. High-density single-nucleotide polymorphism genotyping was carried out on 13 affected members of the Nova Scotia pedigrees and an analysis was performed using the combinatorial conflicting homozygosity (CCH) method, an efficient nonparametric technique that is well suited to identifying haplotypes shared identical-by-descent in founder populations.²⁴ This revealed a 2.8-Mbp region at chr11: 116369171-119235404 shared by all 13 individuals. Taken together with the mapping described above, this narrowed the critical interval to an ~1 Mbp-sized region at chr11: 116369171-117651600, still containing *APOA4*. The p.L66V variant segregated with affected status. In further analysis, the p.L66V variant was identified in 17 individuals, all of whom were clinically affected. Two clinically affected individuals were genetically unaffected: III.14 from Family 3a, with an eGFR of 12 ml/min per 1.73 m² at age 94 years, and IV.3 from Family 3b, with an eGFR of 30 ml/min per 1.73 m² at age 77 years (Figure 2a). Two individuals homozygous for the p.L66V variant (IV.1 and IV.2 from Family 3b) had clinical findings similar to those for heterozygous individuals (Figure 2a).

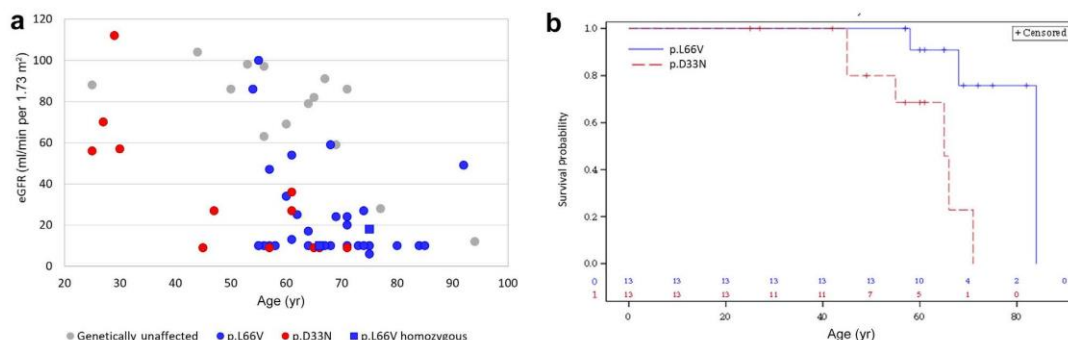


Figure 2 | Kidney function in affected individuals. (a) The most recent estimated glomerular filtration rate (eGFR, ml/min per 1.73 m²) versus age in individuals affected with the ApoA4 p.D33N mutation, the ApoA4 p.L66V mutation, and genetically unaffected individuals from the 5 families. Individuals on dialysis/transplanted were assigned an eGFR of 10 ml/min per 1.73 m² at the time of first initiation of dialysis or transplantation. All genetically unaffected individuals had an eGFR \geq 59 ml/min per 1.73 m². Individuals affected with the p.L66V mutation started dialysis or underwent kidney transplantation at a later age and had milder eGFR decline than individuals with the p.D33N mutation. Two individuals affected with the p.L66V variant had an eGFR > 80 ml/min per 1.73 m² at age >50 years, and one genetically affected individual with the p.L66V variant had an eGFR of 58 ml/min per 1.73 m² at age 91 years. The genetically unaffected individuals had normal kidney function, except for 3 individuals—one patient had an eGFR of 59 ml/min per 1.73 m² at age 69 years, another had an eGFR of 30 ml/min per 1.73 m² at age 77 years, and another had an eGFR of 12 ml/min per 1.73 m² at age 94 years. (b) Survival curve to first initiation of dialysis or kidney transplantation according to mutation and sex. Events included start of dialysis, date of preemptive kidney transplantation, and date of death from uremia. Censoring occurred at end of follow-up or at death from non-kidney causes.

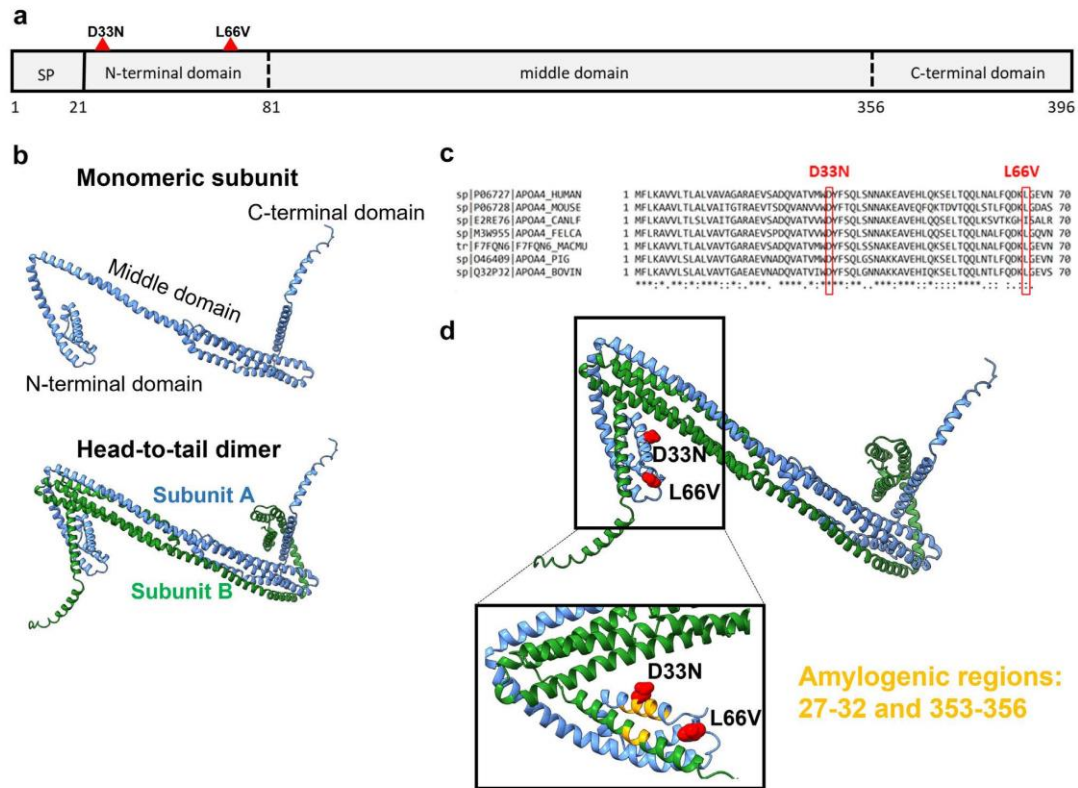


Figure 3 | Structural impact of ApoA4 mutations. (a) Domain architecture of ApoA4, with the signal peptide (SP) spanning amino acid (aa) residues 1–20 and the mature protein (aa 21–396) composed of the N-terminal, middle, and C-terminal domains. Red triangles show the locations of the identified mutations. (b) Theoretical model of dimeric ApoA4 molecule generated by AlphaFold2-Multimer. Upper and lower panels illustrate the domain architectures of the ApoA4 monomer and the tail-to-head oriented dimer. Each ApoA4 subunit is depicted in a different color. (c) Homology of the mutant and wild-type ApoA4 N-terminal domain with those of higher mammals shows a high degree of sequence conservation at the mutated residues. (d) Localization of mutations in the structural model of mature ApoA4 is highlighted by red spheres in a single subunit of dimeric assembly. Amyloidogenic regions predicted by MetAmyl¹⁹ and AmyloPred2²⁰ software are detailed in orange.

from Family 4, and 8 clinically affected individuals (6 genotyped and 2 obligate heterozygotes) from Family 5. Thus, the identified *APOA4* variants segregated in an autosomal dominant pattern. In summary, 44 of 48 genetically affected individuals had an eGFR <60 ml/min per 1.73 m², and 11 of 14 genetically unaffected individuals had an eGFR >60 ml/min per 1.73 m² (Figure 2a; $P < 0.0001$). All 25 of the 25 individuals who developed the need for dialysis or kidney transplantation were genetically affected.

Examination of haplotypes across the *APOA4* genomic region showed that probands carrying the same variant shared identical mutation-carrying chromosomal segments from a common ancestor, indicating that affected families are highly likely to be related. Both genetic variants reside on the “wild-type” ApoA4-1 isoform in all families.²⁵ Neither of these variants have been reported in The Genome Aggregation Database (gnomAD), and both affect an evolutionarily conserved amino acid located in the ApoA4 N-terminal amyloidogenic domain (Figure 3; Supplementary Figure S2).²⁶

Clinical findings in the 5 families

Urinary protein/creatinine measurements (Supplementary Figure S3) were <300 mg/g in 10 of 11 genetically affected individuals, with one individual with an eGFR of 52 ml/min per 1.73 m² having a measurement of 867 mg/g, consistent with proteinuria in CKD due to reduced nephron mass.²⁷ In 8 patients with urinary albumin/creatinine measurements, 6 were <250 mg/g, with one patient with an eGFR of 25 ml/min per 1.73 m² having a measurement of 949 mg/g, and another with an eGFR of 30 ml/min per 1.73 m² having a measurement of 720 mg/g. Kidney function in genetically unaffected versus genetically affected individuals is shown in Figure 2a. Two individuals are affected with the p.L66V variant, with an eGFR > 80 ml/min per 1.73 m² at age >50 years, and one individual is genetically affected with the p.L66V variant, with an eGFR of 58 ml/min per 1.73 m² at age 91 years. Two patients homozygous for the p.L66V mutation had rates of eGFR decline similar to those of heterozygous individuals (Figure 2a). Kidney imaging was consistent with

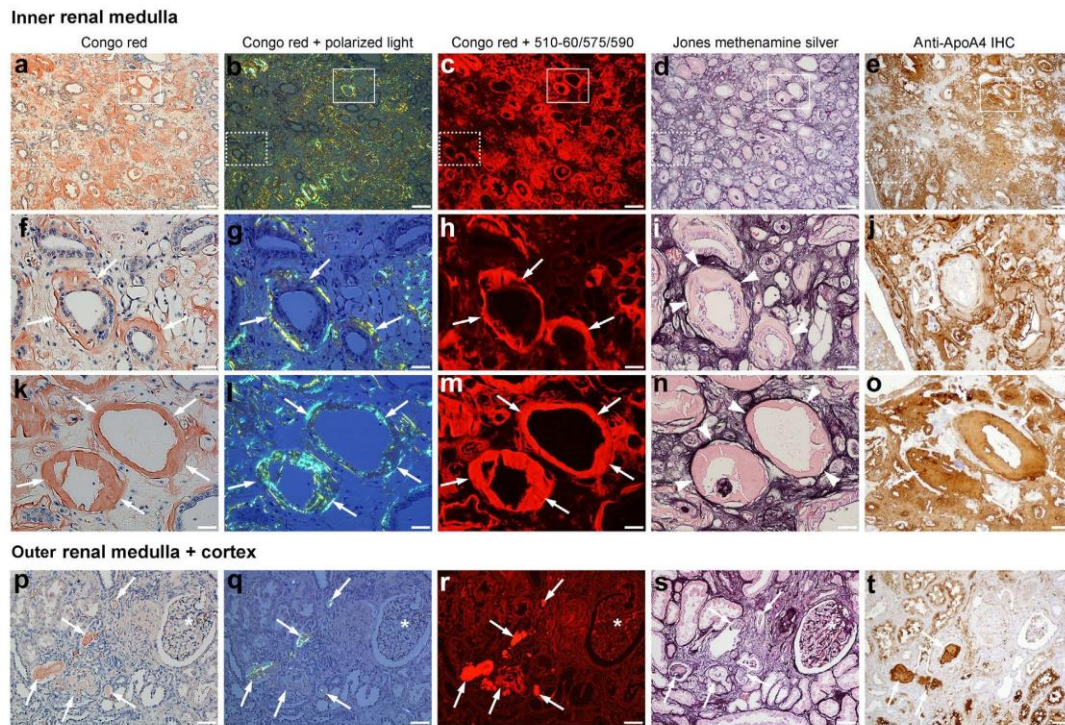


Figure 4 | Light microscopy, including Congo-red staining, of the cortex and medulla in the nephrectomy specimen from an affected individual. Three serial sections were stained with (a–c, f–h, k–m, p–r), Congo red (d, i, n, s) Jones methenamine silver, and (e, j, o, t) anti-ApoA4 Ab. Dashed white rectangles in (c–e) correspond to areas shown in (f–j), respectively. White solid rectangles in (a–e) correspond to areas shown in (k–o), respectively. Identical fields of view in Congo-red staining are shown under (a, f, k, p) normal transmitted light, (b, g, l, q) polarized light, and (c, h, m, r) epifluorescence (for example, BP 510-560/DM575/LP 590). Amyloid accumulation can be seen in the inner medulla (kidney papilla). Amyloid localizes interstitially but also under the epithelia of collecting ducts. (f–h, i) Subepithelial amyloid accumulation is highlighted by white arrows (white arrowheads mark the epithelial basal membranes). (k–n) Some of the collecting ducts are completely lined by amyloid deposits and lack surface epithelium. (n) Residual epithelial basal membranes are highlighted by white arrowheads. (e, j, o) Amyloid deposits (variably) stain with anti-ApoA4 Ab, compared to corresponding serial sections stained by (c, h, m) Congo red and (d, i, n) Jones methenamine silver. (p–t) Numerous amyloid tubular casts can be found in outer kidney medulla and cortex (highlighted by white arrows). Similar intratubular casts can be also found in inner medulla collecting ducts (not shown). Asterisks highlight one glomerulus. Bar = (a–e) 200 μ m; (f–o) 50 μ m; and (p–t) 100 μ m. IHC, immunohistochemical. To optimize viewing of this image, please see the online version of this article at www.kidney-international.org.

CKD. **Supplementary Figure S4A** shows a similar figure by sex and pathogenic variant, including genetically unaffected individuals, obligate carriers, and clinically affected individuals (CKD stage $\geq 3b$) in whom DNA could not be obtained. The mean age of initiation of dialysis or kidney transplantation was 58.2 ± 11.1 years (range: 45–71 years) for individuals with the p.D33N variant, and 66.7 ± 10.2 years (range: 55–85 years) for individuals with the p.L66V variant ($P = 0.1$). To compare disease severity between the p.D33N and the p.L66V variants, survival curves (**Figure 2b**; **Supplementary Figure S4B**) and a Cox proportional hazards model were created with the outcome variable being age of first initiation of dialysis or kidney transplantation, and with independent variables including sex and mutation. In univariate models, the hazard ratio for the p.D33N genotype was 7.8 (95% confidence interval [CI] 1.30–46.97, $P = 0.01$), and for male

sex, it was 4.51 (95% CI 0.75–27.27), $P = 0.07$. The best-fit model included only genotype.

In 22 genetically affected individuals with available data, 4 suffered cardiac events at age 55, 58, 65, and 70 years. Eight of 24 affected individuals were receiving lipid-lowering agents. Lipid profiles were available in 5 genetically affected individuals who were not receiving statins. The mean cholesterol level was 199 ± 49 mg/dl; high-density lipoprotein cholesterol was 62.4 ± 20.1 mg/dl; very-low-density lipoprotein cholesterol was 13 ± 1.4 mg/dl (nr 2–30 mg/dl); and low-density lipoprotein cholesterol was 118 ± 50 mg/dl.

To identify other potential clinical manifestations of amyloidosis, a chart review and/or interview revealed normal serum alkaline phosphatase and normal serum albumin levels in 9 of 9 available patients. In surveying 14 genetically affected

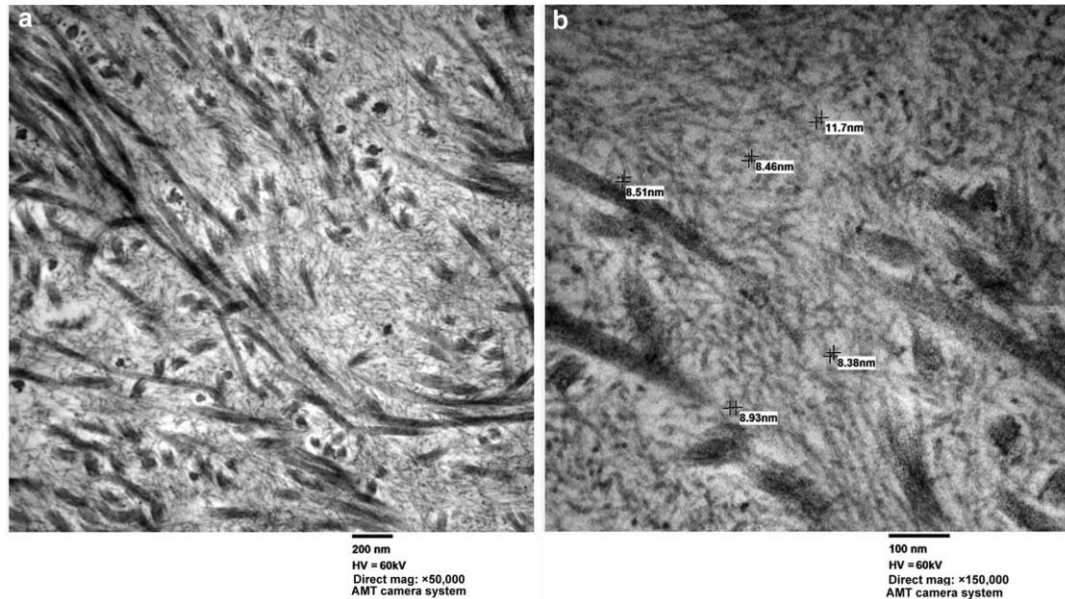


Figure 5 | Electron microscopy of amyloid fibrils at (a) x50,000 and (b) x150,000 demonstrates a crisscrossing pattern with a fibril diameter of approximately 8.5 nm.

individuals, 1 of 14 (Family 5, III.3) had heart failure (diagnosed with cardiac transthyretin amyloidosis), and 0 of 14 had hepatomegaly or chronic problems with diarrhea or constipation. Three of 14 patients, all aged >60 years and with advanced CKD, reported increased susceptibility to bruising that had not required physician referral. Besides the cardiac biopsy showing transthyretin amyloidosis, 0 of 14 patients underwent biopsies of the intestine, heart, liver, or other organs, except for the kidney.

Histopathologic, immunohistochemical, and proteomic analyses

Pathologic findings from 8 kidney specimens are presented in Table 1. Pathology consistently showed secondary global glomerulosclerosis and tubulointerstitial fibrosis. Four of 8 pathologic specimens contained inner medulla, with all showing hyaline material restricted to the medulla (Figure 4). Of the 4 cases with inner medulla, 2 were nephrectomy samples (III.12 from Family 1 and III.14 from Family 3a), 1 was a core biopsy with limited material (IV.10 from Family 3a), and in 1 case (IV.1 from Family 2), only a biopsy report was available. In 3 of the 4 cases, hyaline deposits consistent with amyloid deposition were noted only in secondary analysis after the mutation had been identified. Congo-red staining revealed apple-green birefringence under polarized light (Table 1; Figure 4; Supplementary Figure S5) in all 4 cases. For III.12, electron microscopy of the medulla showed fine nonbranching fibrils approximately 8.5 nm in diameter arranged in crisscrossed bundles (Figure 5a). Similar findings appeared in the electron microscopy report from IV.1. Four

biopsies containing only kidney cortex showed no pathologic staining with Congo red or ApoA4 (Table 1).

Patient III.12 underwent nephrectomy at age 67 years after a genetic diagnosis had been made, allowing detailed immunohistologic examination of both the cortex and medulla. Examination of the kidney cortex revealed tubular atrophy, and interstitial fibrosis with advanced global glomerulosclerosis (Figure 4). In the inner medulla (kidney papilla), extensive amyloid accumulation was present in the interstitium and under the epithelia of collecting ducts. Some of the collecting ducts were completely lined by amyloid and lacked surface epithelium. Numerous amyloid intratubular casts were found in the medulla and cortex. We categorized the tubules containing amyloid casts as collecting ducts based on their light microscopic morphology, localization, and distribution in the tissue. No cytoplasmic amyloid deposits in the tubular epithelia were detected anywhere in the tissue.

Aside from the normal granular ApoA4 signal in epithelia of proximal tubules, we identified an abnormal and intense diffuse ApoA4 signal in the cytoplasm of epithelia of a fraction of cortical and medullary tubules that were uromodulin-negative. Lack of the granular cytoplasmic ApoA4 signal, together with absence of uromodulin in these abnormally ApoA4-stained epithelia, suggested that they were likely collecting ducts. The majority of the interstitial amyloid deposits stained positive with ApoA4 antibody (Figure 4; Supplementary Figures S5, S6, and S7).

Congo red-positive amyloid deposits were laser-microdissected and subjected to proteomics analysis

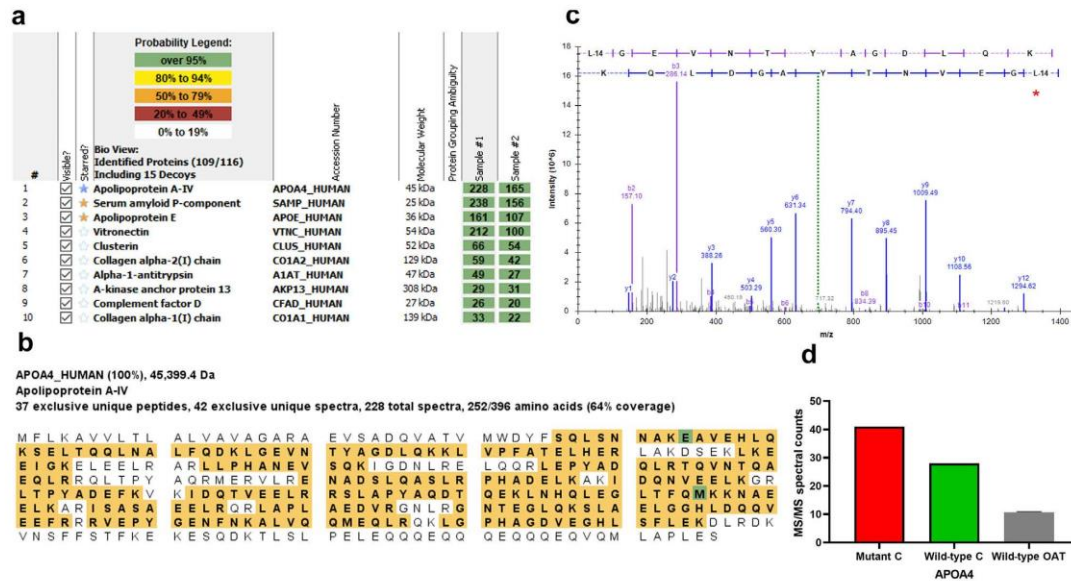


Figure 6 | Proteomic identification of mutant ApoA4 in amyloid deposits. Congo red–positive amyloid deposits were laser microdissected and subjected to proteomics analysis. Two independent microdissections were performed, and each was analyzed separately. **(a)** Protein identification profile showing top 10 proteins detected in the patient amyloid deposits. The yellow star highlights universal amyloid signature proteins. The blue star represents amyloidogenic protein in the patient’s amyloid deposits. Values in green boxes are the total number of tandem mass spectrometry (MS/MS) spectra matching to the corresponding protein in each sample. **(b)** Sequence coverage of ApoA4 protein detected in the patient. Bold letters on yellow highlighted background represent the portions of protein detected in the patient. **(c)** The MS/MS spectrum corresponding to the p.L66V is shown. The red asterisk shows the mutated amino acid. **(d)** Mutant-C and wild type-C represent the total number of MS/MS spectra matching to the p.L66V peptide and the corresponding wild-type ApoA4 peptide present in the patient’s amyloid deposit. Wild type-OAT (other amyloid type) represents the average total number of MS/MS spectra matching to the same wild-type ApoA4 peptide in non-AApoAIV kidney amyloidosis cases (N = 905). The p.L66V mutant peptide was not detected in these N = 905 non-AApoAIV kidney amyloidosis cases.

(Figure 6). Approximately 100 proteins were in the deposit, with the mutant ApoA4 being the most abundant amyloidogenic protein. Approximately 350 spectral counts of ApoA4 were present, similar to cases of sporadic AApoAIV amyloidosis. The ratio of the ApoA4 peptide containing the mutated p.L66V residue to wild-type ApoA4 was 1.46 to 1.

The nephrectomy sample from III.14 showed extensive amyloid deposition (see Supplementary Figure S5) and positive ApoA4 immunohistochemical staining. The tissue was from a patient with advanced kidney failure on dialysis, precluding detailed analysis of ApoA4 deposition similar to that of the specimen from III.12. Laser microdissection and proteomic analysis revealed approximately 121 proteins in the deposit, with the mutant ApoA4 being the most abundant amyloidogenic protein. Approximately 137 spectral counts of ApoA4 were present, similar to cases of sporadic AApoAIV amyloidosis. The ratio of the ApoA4 peptide containing the mutated p.L66V residue to wild-type ApoA4 was approximately 2 to 1. The needle biopsy from IV.10 revealed amyloid deposition in the medulla, but no tissue remained for ApoA4 immunostaining. Laser microdissection and proteomic analysis revealed approximately 335 spectral counts of ApoA4. The ratio of the ApoA4 peptide containing the mutated p.L66V residue to wild-type ApoA4 was approximately 2 to 1.

Skin biopsy samples were available from two family 1 members, III.12 and III.28. Amyloid deposits were not detected in these samples using Congo-red staining (not shown).

Plasma ApoA4 analysis

Plasma ApoA4 was immunodetected in 15 individuals with the ApoA4 variants (7 with the p.D33N variant, and 8 with the p.L66V variant), and 49 controls (6 genetically unaffected family members, 6 with MUC1 mutations, 12 with UMOD mutations, and 24 population controls; Figure 7a and b). Plasma total ApoA4 levels were increased for patients with ApoA4 mutations versus controls (840 ± 226 vs. 515 ± 188 ng, P = 0.0001), as well as plasma monomeric ApoA4 (578 ± 151 vs. 406 ± 110 ng, P = 0.0001) and plasma dimeric ApoA4 (262 ± 83 vs. 109 ± 132 ng, P = 0.06). Immunoaffinity enrichment with mass spectrometry analysis revealed that the ratio of mutated ApoA4 and wild-type ApoA4 was approximately 1 to 1 (Supplementary Figure S8).

In silico analysis

ApoA4 consists of a middle domain comprised of 13 proline-punctuated amphipathic helices (residues 84–355) and globular and/or coiled domains at the N- and C-terminus

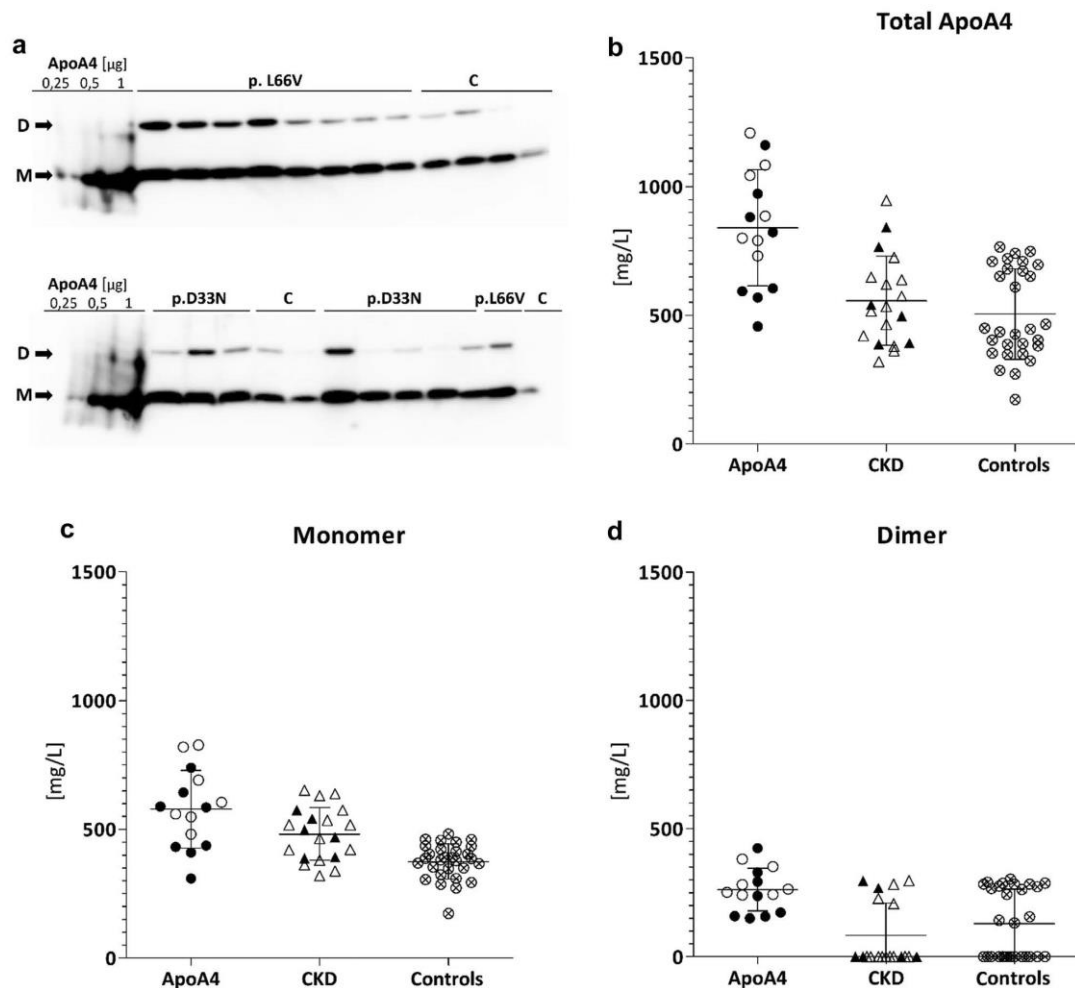


Figure 7 | Plasma ApoA4 concentrations. (a) 1 μ l of plasma was separated on 3%–25% gradient native polyacrylamide gel electrophoresis polyacrylamide gel; monomeric (M) and dimeric (D) fractions were immunodetected and quantified by densitometry with recombinant ApoA4 as a calibrator. (b) The graph represents concentrations of monomer, dimer, and total ApoA4 in genetically affected individuals, individuals with chronic kidney disease (CKD), individuals with *UMOD*, *MUC1*, and *APOA4* mutations, and controls. Black circles indicate individuals with the ApoA4 p.L66V mutation. Unshaded circles indicate individuals with the ApoA4 p.D33N mutation. Black triangles indicate individuals with *MUC1* mutations, and unshaded triangles indicate individuals with *UMOD* mutations. (b–d) Plasma levels of total ApoA4 and monomeric ApoA4 were significantly different between individuals with ApoA4 and unaffected individuals (including individuals with *UMOD* and *MUC1* mutations and controls), whereas dimeric levels were not ($P = 0.06$). Plasma levels were not significantly different in comparisons between genetically affected and individuals with *UMOD* or *MUC1* mutations or between genetically affected individuals and controls, likely due to lack of statistical power.

(residues 21–83 and 356–394, respectively; Figure 3a). These terminal domains are involved in transient interactions among themselves and with the central helical domains²⁸ (Figure 3b), which play a major role in stabilizing ApoA4 tertiary and quaternary structure.

The p.D33N and p.L66V mutations are located at the structurally flexible N-terminal domain (Figure 3c). The altered charge and size of the substituted amino acid

residues may disturb the association with other protein domains, such as the C-terminus²⁹ and may thereby alter protein stability, self-association, and/or lipid binding. Destabilization of the ApoA4 helical structure by amino acid substitutions could also induce formation of alternate secondary structures—including beta-sheets, a basic structural unit of amyloid fibrils (Figure 3d; Supplementary Figure S2).

Two *in silico* prediction programs consistently revealed 2 amyloidogenic regions at the N- and C-terminal domains overlapping at positions of 27–32 and 353–356 (Supplementary Figure S2). Notably, these regions form several contacts in the structural model generated by AlphaFold-Oligomer and may thus form a single amyloidogenic hotspot in the ApoA4 structure. In addition, both pathogenic mutations are near this hotspot. The p.D33N mutation is located in the proximate vicinity, whereas the p.L66V mutation is found in the adjacent interhelical loop. In the analysis of specific mutations, p.D33N caused an expansion of the amyloidogenic region, with both predictive software tools. Similar expansion was found for the p.L66V mutant, using the MetAmyl, but not the AmyloPred2, program.

DISCUSSION

In this investigation, we identified 2 pathogenic variants in *APOA4* as causes of autosomal dominant CKD with a bland urinary sediment in 48 individuals from 5 families. In all, 44 of 47 family members with an eGFR < 60 ml/min per 1.73 m² carried an *APOA4* pathogenic variant, and neither variant has been found in the general population. Both variants are evolutionarily conserved and encode for missense mutations in the N-terminal domain relevant to oligomerization of ApoA4.³⁰ All clinically affected individuals presented with a bland urinary sediment, CKD, and, no clinical evidence of systemic amyloidosis. Routine kidney biopsies limited to the kidney cortex showed tubulointerstitial fibrosis and secondary glomerulosclerosis and no amyloid deposition. Four genetically affected individuals were identified with isolated medullary deposition of amyloid, with mass spectrometry showing the mutated ApoA4 as the primary constituent in 3 available cases.

The majority of filtered ApoA4 likely undergoes intact proximal tubular reabsorption¹¹ through vesicular transport,³¹ similar to albumin.³² Immunohistochemical studies in normal kidney have demonstrated the presence of ApoA4 in proximal tubular cells, capillaries, blood vessels, and the lymphatic system, but not in glomeruli or distal tubular cells. In proximal tubules, ApoA4 was present in the brush border and in intracellular granules and plasma membranes. ApoA4 was not found in the tubulointerstitium, with no *APOA4* mRNA expression detected in the kidney.³³ These findings are all consistent with reabsorption and degradation of the majority of filtered ApoA4 in proximal tubule cells.

We hypothesize that the amino acid substitutions alter the tertiary or quaternary structure of the mutated ApoA4, leading to increased plasma and primary urine concentrations and isolated medullary amyloid deposition, a finding that is specific to AApoIV amyloidosis—in both sporadic cases^{12–14} and patients who have ApoA4 mutations. Pathologic studies performed on the kidney of the proband demonstrated ApoA4-positive amyloid casts in the outer kidney medulla, cortex, and the inner medulla collecting ducts, indicating the ability of ApoA4 to transit the glomerular basement membrane. Abundant ApoA4 staining in the proximal tubule cells indicated

increased proximal tubular reabsorption consistent with increased plasma apo4 levels. The mutant ApoA4 is then preferentially deposited in amyloid form in the medulla, possibly because of the increased concentration and due to the medullary gradient and the lower pH environment of the kidney medulla. In fact, the pH of the kidney medulla, approximately 5.5,³⁴ is very close to the ApoA4 isoelectric point of 5.13,⁹ where it denatures and aggregates. Alternatively, N-terminal pathogenic variants may impair intramolecular electron transfer,³⁵ thus impairing its antioxidant properties³⁶ and rendering it more vulnerable to free radical attack in the relatively hypoxic environment of the kidney medulla. The deposition of amyloid leads to slowly progressive CKD. As the condition does not primarily affect the glomerulus, the urinary sediment contains no blood or protein.

Identification of pathogenic *APOA4* variants will be clinically challenging for several reasons. Patients present with the mundane clinical findings of slowly progressive CKD with a bland urinary sediment. Given the relatively late onset of kidney disease and the incomplete penetrance in some individuals, the genetic nature of the condition may be missed. In addition, nephrologists may not perform a kidney biopsy due to the slowly progressive nature of the disease and the bland urinary sediment. If a biopsy is performed, it often will include only cortical tissue and result in a nonspecific diagnosis, as occurred in 4 of 6 needle biopsies in this study. Similar to the findings for our proband, Rosenstiel and Alves reported on a patient with sporadic medullary amyloidosis that was found after nephrectomy but not on a prior biopsy.¹⁴ In addition, amyloid deposition was initially missed on 3 of 4 pathologic specimens containing medulla. Thus, diagnosis will rely on a careful family history, *APOA4* sequencing, and ApoA4 immunostaining.

The identification of several genetically affected family members with well-preserved kidney function suggests that environmental or genetic factors may ameliorate the course of disease in this condition. ApoA4 is produced in the intestinal epithelium in response to dietary fat consumption.⁷ Reduction in dietary fat content lowers plasma ApoA4 levels,⁷ and in the absence of enteral intake, as in patients on total parenteral nutrition, plasma ApoA4 levels fall to nearly undetectable levels.³⁷ Less ApoA4 production may result in decreased kidney deposition of the mutant protein and could potentially ameliorate kidney disease. We are pursuing investigations in this area. A shortcoming of our study was the small patient population. Given the late onset of disease and its autosomal dominant inheritance, a number of large families have likely suffered from this condition for generations, similar to families with *UMOD*^{38–40} and *MUC1* mutations.^{41,42} A limitation of this study is the lack of other organ or tissue biopsies to definitively rule out AApoAIV deposition occurring outside of the kidney. Systematic investigations with echocardiography, computed tomography scanning, and ¹²⁵I-labeled serum amyloid P component (SAP) scintigraphy should be performed in the future to rule out systemic amyloid deposition in these patients.

In summary, we describe 5 families presenting with autosomal dominant medullary amyloidosis due to *APOA4* mutations. ApoA4 is a small protein produced by the small intestine to facilitate fat uptake. Once fat is transported, ApoA4 is filtered by the glomerulus and undergoes tubular reabsorption. Pathogenic *APOA4* variants produce small changes in ApoA4 that do not show clinical signs of affecting lipid transport. However, when mutant ApoA4 is filtered by the glomerulus, the mutation results in fibril formation and amyloid deposition isolated to the kidney medulla, with no clinical evidence of non-kidney deposition. Routine kidney biopsies (which often do not sample the kidney medulla) often show only secondary nephrosclerosis and tubulointerstitial sclerosis but no amyloid deposition. Thus, diagnosis relies on genetic testing. In addition, if medullary amyloidosis is identified in the kidney, formal diagnosis of AApoAIV medullary amyloidosis relies on the identification of the mutated protein either by mass spectrometry, or if the mutation is not known, by the number of spectral counts in the deposits.¹² If the condition is found, patients should undergo genetic analysis of the *APOA4* gene via commercial testing or consultation with an academic center interested in this disorder.

DISCLOSURE

All the authors declared no competing interests.

DATA STATEMENT

Many of the study participants provided consent more than 10 years ago and belonged to very small family units from geographically defined areas with pathogenic variants that are easily identifiable. Given this, the Wake Forest Institutional Review Board did not give permission to share DNA in a repository, due to possible breaches of privacy. However, we can share genetic data from this cohort based on specific data requests, following Wake Forest Institutional Review Board approval of the proposal and a signed data access agreement.

ACKNOWLEDGMENTS

The authors thank all participating patients and families, and the referring physicians. This study was supported by the National Institute for Treatment of Metabolic and Cardiovascular Diseases (CarDia; LX22NPO5104) from the Ministry of Education, Youth and Sports of the Czech Republic, by grants NU21-07-00033 and NV19-08-00137 from the Ministry of Health of the Czech Republic, by the project TN02000132/National Centre for New Methods of Diagnosis, Monitoring, Treatment and Prevention of Genetic Diseases and by institutional programs of Charles University in Prague (UNCE/MED/007 and Cooperation). The National Center for Medical Genomics (LM2023067) kindly provided sequencing and genotyping. CF Structural mass spectrometry of CIISB, Instruct-CZ Centre was supported by MEYS CR (LM2023042), and the European Regional Development Fund-Project "UP CIISB" (No. CZ.02.1.01/0.0/0.0/18_046/0015974) provided proteomic analyses. AJB was funded by the Slim Health Foundation, the Black-Brogan Foundation, and Soli Deo Gloria.

SUPPLEMENTARY MATERIAL

Supplementary File (Word)

Supplementary Figure S1. Additional pedigree branches of Family 3.

Supplementary Figure S2. Amyloidogenic prediction.

Supplementary Figure S3. Urine protein:creatinine ratios for the Wake Forest cohort, and urine albumin:creatinine ratios for the Nova Scotia cohort, according to kidney function and mutation type.

Supplementary Figure S4. Kidney function according to sex. (A) Kidney function in affected individuals according to mutation and sex. (B) Survival analysis.

Supplementary Figure S5. Light microscopy, including Congo-red staining, of the cortex and medulla in the nephrectomy specimen from an affected individual.

Supplementary Figure S6. Immunodetection patterns of uromodulin (Tamm-Horsfall protein) and ApoA4 in the kidney cortex and outer kidney medulla of the proband (III.12, Family 1).

Supplementary Figure S7. Control autopsic kidney tissue from an unrelated individual. Immunodetection patterns of uromodulin (Tamm-Horsfall protein) and ApoA4 in the kidney cortex and outer kidney medulla.

Supplementary Figure S8. Plasma ApoA4 immunoaffinity enrichment with mass spectrometry analysis.

Supplementary Methods.

Supplementary Reference.

REFERENCES

- Zivna M, Kidd KO, Baresova V, et al. Autosomal dominant tubulointerstitial kidney disease: a review. *Am J Med Genet C Semin Med Genet.* 2022;190:309–324.
- Hart TC, Gorry MC, Hart PS, et al. Mutations of the *UMOD* gene are responsible for medullary cystic kidney disease 2 and familial juvenile hyperuricaemic nephropathy. *J Med Genet.* 2002;39:882–892.
- Kirby A, Gnirke A, Jaffe DB, et al. Mutations causing medullary cystic kidney disease type 1 lie in a large VNTR in *MUC1* missed by massively parallel sequencing. *Nat Genet.* 2013;45:288–393.
- Groopman EE, Marasa M, Cameron-Christie S, et al. Diagnostic utility of exome sequencing for kidney disease. *N Engl J Med.* 2019;380:142–151.
- Devuyst O, Olinger E, Weber S, et al. Autosomal dominant tubulointerstitial kidney disease. *Nat Rev Dis Primers.* 2019;5:60.
- Zivna M, Kidd K, Pristoupilova A, et al. Noninvasive immunohistochemical diagnosis and novel *MUC1* mutations causing autosomal dominant tubulointerstitial kidney disease. *J Am Soc Nephrol.* 2018;29:2418–2431.
- Weinberg RB, Dantzker C, Patton CS. Sensitivity of serum apolipoprotein A-IV levels to changes in dietary fat content. *Gastroenterology.* 1990;98:17–24.
- Duverger N, Ghalim N, Ailhaud G, et al. Characterization of apoA-IV-containing lipoprotein particles isolated from human plasma and interstitial fluid. *Arterioscler Thromb.* 1993;13:126–132.
- Weinberg RB, Scanu AM. Isolation and characterization of human apolipoprotein A-IV from lipoprotein-depleted serum. *J Lipid Res.* 1983;24:52–59.
- Ledford AS, Weinberg RB, Cook VR, et al. Self-association and lipid binding properties of the lipoprotein initiating domain of apolipoprotein B. *J Biol Chem.* 2006;281:8871–8876.
- Lingenhel A, Lhotta K, Neyer U, et al. Role of the kidney in the metabolism of apolipoprotein A-IV: influence of the type of proteinuria. *J Lipid Res.* 2006;47:2071–2079.
- Sethi S, Theis JD, Shiller SM, et al. Medullary amyloidosis associated with apolipoprotein A-IV deposition. *Kidney Int.* 2012;81:201–206.
- Dasari S, Amin MS, Kurtin PJ, et al. Clinical, biopsy, and mass spectrometry characteristics of renal apolipoprotein A-IV amyloidosis. *Kidney Int.* 2016;90:658–664.
- Rosenstiel PE, Alves T. Diagnosis of AApoAIV medullary amyloidosis at radical nephrectomy. *Kidney Int.* 2022;101:423.
- Bleyer AJ, Kidd K, Robins V, et al. Outcomes of patient self-referral for the diagnosis of several rare inherited kidney diseases. *Genet Med.* 2020;22:142–149.
- Hartmannova H, Piherova L, Tauchmannova K, et al. Acadian variant of Fanconi syndrome is caused by mitochondrial respiratory chain complex I deficiency due to a non-coding mutation in complex I assembly factor NDJFAF6. *Hum Mol Genet.* 2016;25:4062–4079.

17. RCSB. Protein data bank. Accessed April 13, 2023. www.rcsb.org/structure/3584
18. Mirdita M, Schütze K, Moriwaiki Y, et al. ColabFold: making protein folding accessible to all. *Nat Methods*. 2022;19:679–682.
19. Emily M, Talvas A, Delamarche C. MetAmyl: a META-predictor for AMYloid proteins. *PLoS One*. 2013;8:e79722.
20. Tsolis AC, Papandreou NC, Iconomidou VA, Hamodrakas SJ. A consensus method for the prediction of 'aggregation-prone' peptides in globular proteins. *PLoS One*. 2013;8:e54175.
21. Weinberg RB, Spector MS. Lipoprotein affinity of human apolipoprotein A-IV during cholesterol esterification. *Biochem Biophys Res Commun*. 1986;135:756–763.
22. Dvorak J, Novakova J, Kraftova L, et al. The rapid detection of procalcitonin in septic serum using immunoaffinity MALDI chips. *Clin Proteomics*. 2023;20:20.
23. Levey AS, Stevens LA, Schmid CH, et al. A new equation to estimate glomerular filtration rate. *Ann Intern Med*. 2009;150:604–612.
24. Levine AP, Connor TM, Oyar DD, et al. Combinatorial conflicting homozygosity (CCH) analysis enables the rapid identification of shared genomic regions in the presence of multiple phenocopies. *BMC Genomics*. 2015;16:163.
25. Weinberg RB, Hopkins RA, Jones JB. Purification, isoform characterization, and quantitation of human apolipoprotein A-IV. *Methods Enzymol*. 1996;263:282–296.
26. Weinberg RB. Identification of functional domains in the plasma apolipoproteins by analysis of inter-species sequence variability. *J Lipid Res*. 1994;35:2212–2222.
27. Wen Y, Shah S, Campbell KN. Molecular mechanisms of proteinuria in focal segmental glomerulosclerosis. *Front Med (Lausanne)*. 2018; 5:98.
28. Walker RG, Deng X, Melchior JT, et al. The structure of human apolipoprotein A-IV as revealed by stable isotope-assisted cross-linking, molecular dynamics, and small angle x-ray scattering. *J Biol Chem*. 2014;289:5596–5608.
29. Tubb MR, Silva R, Pearson KJ, et al. Modulation of apolipoprotein A-IV lipid binding by an interaction between the N and C termini. *J Biol Chem*. 2007;282:28385–28394.
30. Weinberg RB, Spector MS. The self-association of human apolipoprotein A-IV. Evidence for an in vivo circulating dimeric form. *J Biol Chem*. 1985;260:14279–14286.
31. Russo LM, Sandoval RM, McKee M, et al. The normal kidney filters nephrotic levels of albumin retrieved by proximal tubule cells: retrieval is disrupted in nephrotic states. *Kidney Int*. 2007;71:504–513.
32. Comper WD, Vuchkova J, McCarthy KJ. New insights into proteinuria/albuminuria. *Front Physiol*. 2022;13:991756.
33. Haiman M, Salvenmoser W, Scheiber K, et al. Immunohistochemical localization of apolipoprotein A-IV in human kidney tissue. *Kidney Int*. 2005;68:1130–1136.
34. Zalyapin EA, Bouley R, Hasler U, et al. Effects of the renal medullary pH and ionic environment on vasopressin binding and signaling. *Kidney Int*. 2008;74:1557–1567.
35. Weinberg RB. Exposure and electronic interaction of tyrosine and tryptophan residues in human apolipoprotein A-IV. *Biochemistry*. 1988;27:1515–1521.
36. Wong WM, Gerry AB, Putt W, et al. Common variants of apolipoprotein A-IV differ in their ability to inhibit low density lipoprotein oxidation. *Atherosclerosis*. 2007;192:266–274.
37. Weinberg RB, Sherman JR. Serum apolipoprotein A-IV and lipoprotein cholesterol in patients undergoing total parenteral nutrition. *Gastroenterology*. 1988;95:394–401.
38. Valluru MK, Chung NK, Gilchrist M, et al. A founder UMOD variant is a common cause of hereditary nephropathy in the British population. *J Med Genet*. 2023;60:397–405.
39. Smith GD, Robinson C, Stewart AP, et al. Characterization of a recurrent in-frame UMOD indel mutation causing late-onset autosomal dominant end-stage renal failure. *Clin J Am Soc Nephrol*. 2011;6:2766–2774.
40. Bleyer AJ, Woodard AS, Shihabi Z, et al. Clinical characterization of a family with a mutation in the uromodulin (Tamm-Horsfall glycoprotein) gene. *Kidney Int*. 2003;64:36–42.
41. Stavrou C, Pierides A, Zouvani I, et al. Medullary cystic kidney disease with hyperuricemia and gout in a large cyprriot family: no allelism with nephronophthisis type 1. *Am J Med Genet*. 1998;77:149–154.
42. Kiser RL, Wolf MTF, Martin JL, et al. Medullary cystic kidney disease type 1 in a large Native-American kindred. *Am J Kidney Dis*. 2004;44:611–617.

5. List of Publications, Awards, Grants, and Presentations

5.1 Publications

Cochran B, Kovačiková T, Hodaňová K, Živná M, Hnízda A, Niehaus AG, Bonnacaze A, Balasubraminiam G, Ceballos-Picot I, Hawfield A, **Kidd K**, Kmoch S, Bleyer AJ. Chronic tubulointerstitial kidney disease in untreated adenosine phosphoribosyl transferase (APRT) deficiency: A case report. *Clin Nephrol*. 2018 Oct;90(4):296-301. **Impact Factor = 1.2**

Bleyer AJ, Scavo VA, Wilson SE, Browne BJ, Ferris BL, Ozaki CK, Lee T, Peden EK, Dixon BS, Mishler R, O'Connor TP, **Kidd K**, Burke SK; PATENCY-1 Investigators. A randomized trial of vonapanitase (PATENCY-1) to promote radiocephalic fistula patency and use for hemodialysis. *J Vasc Surg*. 2019 Feb;69(2):507-515. **Impact Factor = 4.3**

Cormican S, Connaughton DM, Kennedy C, Murray S, Živná M, Kmoch S, Fennelly NK, O'Kelly P, Benson KA, Conlon ET, Cavalleri G, Foley C, Doyle B, Dorman A, Little MA, Lavin P, **Kidd K**, Bleyer AJ, Conlon PJ. Autosomal dominant tubulointerstitial kidney disease (ADTKD) in Ireland. *Ren Fail*. 2019 Nov;41(1):832-841. **Impact Factor = 3.2**

Bleyer AJ, **Kidd K**, Johnson E, Robins V, Martin L, Taylor A, Pinder AJ, Bowline I, Frankova V, Živná M, Taylor KB, Kim N, Baek JJ, Hartmannová H, Hodaňová K, Vyleťal P, Votruba M, Kmoch S. Quality of life in patients with autosomal dominant tubulointerstitial kidney disease. *Clin Nephrol*. 2019 Dec;92(6):302-311. **Impact Factor = 1.2**

Murray SL, Dorman A, Benson KA, Connaughton DM, Stapleton CP, Fennelly NK, Kennedy C, McDonnell CA, **Kidd K**, Cormican SM, Ryan LA, Lavin P, Little MA, Bleyer AJ, Doyle B, Cavalleri GL, Hildebrandt F, Conlon PJ. Utility of Genomic Testing after Renal Biopsy. *Am J Nephrol*. 2020;51(1):43-53. **Impact Factor = 4.2**

Bleyer AJ, **Kidd K**, Robins V, Martin L, Taylor A, Santi A, Tsoumas G, Hunt A, Swain E, Abbas M, Akinbola E, Vidya S, Moossavi S, Bleyer AJ Jr, Živná M, Hartmannová H, Hodaňová K, Vyleťal P, Votruba M, Harden M, Blumenstiel B, Greka A, Kmoch S. Outcomes of patient self-referral for the diagnosis of several rare IKDs. *Genet Med*. 2020 Jan;22(1):142-149. **Impact Factor = 8.8**

Cormican S, Kennedy C, Connaughton DM, O'Kelly P, Murray S, Živná M, Kmoch S, Fennelly NK, Benson KA, Conlon ET, Cavalleri GL, Foley C, Doyle B, Dorman A,

Little MA, Lavin P, **Kidd K**, Bleyer AJ, Conlon PJ. Renal transplant outcomes in patients with autosomal dominant tubulointerstitial kidney disease. *Clin Transplant*. 2020 Feb;34(2):e13783. **Impact Factor = 3.5**

Kidd K, Vyleťal P, Schaeffer C, Olinger E, Živná M, Hodaňová K, Robins V, Johnson E, Taylor A, Martin L, Izzi C, Jorge SC, Calado J, Torres RJ, Lhotta K, Steubl D, Gale DP, Gast C, Gombos E, Ainsworth HC, Chen YM, Almeida JR, de Souza CF, Silveira C, Raposeiro R, Weller N, Conlon PJ, Murray SL, Benson KA, Cavalleri GL, Votruba M, Vrbacká A, Amoroso A, Gianchino D, Caridi G, Ghiggeri GM, Divers J, Scolari F, Devuyst O, Rampoldi L, Knoch S, Bleyer AJ. Genetic and Clinical Predictors of Age of ESKD in Individuals With Autosomal Dominant Tubulointerstitial Kidney Disease Due to *UMOD* Mutations. *Kidney Int Rep*. 2020 Jul 3;5(9):1472-1485. **Impact Factor = 6.0**

Živná M, **Kidd K**, Zaidan M, Vyleťal P, Barešová V, Hodaňová K, Sovová J, Hartmannová H, Votruba M, Trešlová H, Jedličková I, Sikora J, Hůlková H, Robins V, Hnízda A, Živný J, Papagregoriou G, Mesnard L, Beck BB, Wenzel A, Tory K, Häeffner K, Wolf MTF, Bleyer ME, Sayer JA, Ong ACM, Balogh L, Jakubowska A, Łaszkiwicz A, Clissold R, Shaw-Smith C, Munshi R, Haws RM, Izzi C, Capelli I, Santostefano M, Graziano C, Scolari F, Sussman A, Trachtman H, Decramer S, Matignon M, Grimbert P, Shoemaker LR, Stavrou C, Abdelwahed M, Belghith N, Sinclair M, Claes K, Kopel T, Moe S, Deltas C, Knebelmann B, Rampoldi L, Knoch S, Bleyer AJ. An International Cohort Study of Autosomal Dominant Tubulointerstitial Kidney Disease due to *REN* Mutations Identifies Distinct Clinical Subtypes. *Kidney Int*. 2020 Aug 1:S0085-2538(20)30838-3. **Impact Factor = 18.9**

Olinger E, Hofmann P, **Kidd K**, Dufour I, Belge H, Schaeffer C, Kipp A, Bonny O, Deltas C, Demoulin N, Fehr T, Fuster DG, Gale DP, Goffin E, Hodaňová K, Huynh-Do U, Kistler A, Morelle J, Papagregoriou G, Pirson Y, Sandford R, Sayer JA, Torra R, Venzin C, Venzin R, Vogt B, Živná M, Greka A, Dahan K, Rampoldi L, Knoch S, Bleyer AJ Sr, Devuyst O. Clinical and genetic spectra of autosomal dominant tubulointerstitial kidney disease due to mutations in *UMOD* and *MUC1*. *Kidney Int*. 2020 Sep;98(3):717-731. **Impact Factor = 18.9**

Živná M, **Kidd K**, Knoch S, Bleyer AJ. Autosomal Dominant Tubulointerstitial Kidney Disease – *REN*. 2011 Apr 5 [updated 2020 Dec 10]. In: Adam MP, Everman DB, Mirzaa GM, Pagon RA, Wallace SE, Bean LJH, Gripp KW, Amemiya A, editors. GeneReviews® [Internet]. Seattle (WA): University of Washington, Seattle; 1993–2022.

Bleyer AJ, Wolf MT, **Kidd KO**, Živná M, Kmoch S. Autosomal dominant tubulointerstitial kidney disease: more than just HNF1β. *Pediatr Nephrol*. 2022 May;37(5):933-946. **Impact Factor = 3.6**

Vyleťal P, **Kidd K**, Ainsworth HC, Springer D, Vrbacká A, Přistoupilová A, Hughey RP, Alper SL, Lennon N, Harrison S, Harden M, Robins V, Taylor A, Martin L, Howard K, Bitar I, Langefeld CD, Barešová V, Hartmannová H, Hodaňová K, Zima T, Živná M, Kmoch S, Bleyer AJ. Plasma Mucin-1 (CA15-3) Levels in Autosomal Dominant Tubulointerstitial Kidney Disease due to *MUC1* Mutations. *Am J Nephrol*. 2021;52(5):378-387. **Impact Factor = 4.2**

Buglioni A, Hasadsri L, Nasr SH, Hogan MC, Moyer AM, Siddique K, **Kidd K**, Kmoch S, Hodaňová K, Bleyer AJ, Alexander MP. Mitochondriopathy Manifesting as Inherited Tubulointerstitial Nephropathy Without Symptomatic Other Organ Involvement. *Kidney Int Rep*. 2021 Jun 12;6(9):2514-2518. **Impact Factor = 6.0**

Kim Y, Wang Z, Li C, **Kidd K**, Wang Y, Johnson BG, Kmoch S, Morrissey JJ, Bleyer AJ, Duffield JS, Singamaneni S, Chen YM. Ultrabright plasmonic fluor nanolabel-enabled detection of a urinary ER stress biomarker in autosomal dominant tubulointerstitial kidney disease. *Am J Physiol Renal Physiol*. 2021 Aug 1;321(2):F236-F244. **Impact Factor = 4.2**

Bleyer AJ, Živná M, **Kidd K**, Kmoch S. Autosomal Dominant Tubulointerstitial Kidney Disease – *MUC1*. 2013 Aug 15 [updated 2021 Oct 21]. In: Adam MP, Everman DB, Mirzaa GM, Pagon RA, Wallace SE, Bean LJH, Gripp KW, Amemiya A, editors. GeneReviews® [Internet]. Seattle (WA): University of Washington, Seattle; 1993–2022.

Bleyer AJ, **Kidd K**, Živná M, Kmoch S. Autosomal Dominant Tubulointerstitial Kidney Disease – *UMOD*. 2007 Jan 12 [updated 2021 Dec 23]. In: Adam MP, Everman DB, Mirzaa GM, Pagon RA, Wallace SE, Bean LJH, Gripp KW, Amemiya A, editors. GeneReviews® [Internet]. Seattle (WA): University of Washington, Seattle; 1993–2022.

Elhassan EAE, Murray SL, Connaughton DM, Kennedy C, Cormican S, Cowhig C, Stapleton C, Little MA, **Kidd K**, Bleyer AJ, Živná M, Kmoch S, Fennelly NK, Doyle B, Dorman A, Griffin MD, Casserly L, Harris PC, Hildebrandt F, Cavalleri GL, Benson KA, Conlon PJ. The utility of a genetic kidney disease clinic employing a broad range of genomic testing platforms: experience of the Irish Kidney Gene Project. *J Nephrol*. 2022 Jul;35(6):1655-1665. **Impact Factor = 3.4**

Olinger E, Schaeffer C, **Kidd K**, Elhassan EAE, Cheng Y, Dufour I, Schiano G, Mabillard H, Pasqualetto E, Hofmann P, Fuster DG, Kistler AD, Wilson IJ, Kmoch S, Raymond L, Robert T; Genomics England Research Consortium, Eckardt KU, Bleyer AJ Sr, Köttgen A, Conlon PJ, Wiesener M, Sayer JA, Rampoldi L, Devuyst O. An intermediate-effect size variant in *UMOD* confers risk for CKD. *Proc Natl Acad Sci USA*. 2022 Aug 16;119(33):e2114734119. **Impact Factor = 11.0**

Živná M, **Kidd KO**, Barešová V, Hůlková H, Kmoch S, Bleyer AJ Sr. Autosomal dominant tubulointerstitial kidney disease: A review. *Am J Med Genet C Semin Med Genet*. 2022 Sep;190(3):309-324. doi: 10.1002/ajmg.c.32008. Epub 2022 Oct 17. **Impact Factor = 3.1**

Bleyer AJ, **Kidd KO**, Williams AH, Johnson E, Robins V, Martin L, Taylor A, Kim A, Bowline I, Connaughton DM, Langefeld C, Živná M, Kmoch S. Maternal health and pregnancy outcomes in autosomal dominant tubulointerstitial kidney disease. *Obstetric Medicine*. 2022;0(0). **Impact Factor = 0.7**

Al-Bataineh MM, Kinlough CL, Marciszyn A, Lam T, Ye L, **Kidd K**, Maggiore JC, Poland PA, Kmoch S, Bleyer A, Bain DJ, Montalbetti N, Kleyman TR, Hughey RP, Ray EC. Influence of glycoprotein MUC1 on trafficking of the Ca(2+)-selective ion channels, TRPV5 and TRPV6, and on in vivo calcium homeostasis. *J Biol Chem*. 2023 Mar;299(3):102925. **Impact Factor = 4.8**

Airik M, Arbore H, Childs E, Huynh AB, Phua YL, Chen CW, Aird K, Bharathi S, Zhang B, Conlon P, Kmoch S, **Kidd K**, Bleyer AJ, Vockley J, Goetzman E, Wipf P, Airik R. Mitochondrial ROS Triggers KIN Pathogenesis in FAN1-Deficient Kidneys. *Antioxidants (Basel)*. 2023 Apr 8;12(4). **Impact Factor = 7.0**

de Haan A, van Eerde AM, Eijgelsheim M, Rump P, van der Zwaag B, Hennekam E, Živná M, Kmoch S, Bleyer AJ, **Kidd K**, Vogt L, Knoers NVAM, de Borst MH. Novel *MUC1* variant identified by massively parallel sequencing explains interstitial kidney disease in a large Dutch family. *Kidney Int*. 2023 May;103(5):986-989. **Impact Factor = 18.9**

Jorge S, **Kidd K**, Vylet'al P, Nogueira E, Martin L, Howard K, Barešová V, Hodaňová K, Hnízda A, Moldovan O, Silveira C, Coutinho AM, Lopes JA, Bleyer AJ, Kmoch S, Živná M. Bi-allelic REN Mutations and Undetectable Plasma Renin Activity in a Patient With Progressive CKD. *Kidney Int Rep*. 2023 May;8(5):1112-1116. **Impact Factor = 6.0**

Kim Y, Li C, Gu C, Fang Y, Tycksen E, Puri A, Pietka TA, Sivapackiam J, **Kidd K**, Park SJ, Johnson BG, Kmoch S, Duffield JS, Bleyer AJ, Jackrel ME, Urano F, Sharma V, Lindahl M, Chen YM. MANF stimulates autophagy and restores mitochondrial homeostasis to treat autosomal dominant tubulointerstitial kidney disease in mice. *Nat Commun.* 2023 Oct 14;14(1):6493. **Impact Factor = 16.0**

Kmochová T, **Kidd KO**, Orr A, Hnízda A, Hartmannová H, Hodaňová K, Vyleťal P, Naušová K, Brinsa V, Trešlová H, Sovová J, Barešová V, Svojšová K, Vrbacká A, Stránecký V, Robins VC, Taylor A, Martin L, Rivas-Chavez A, Payne R, Bleyer HA, Williams A, Rennke HG, Weins A, Short PJ, Agrawal V, Storsley LJ, Waikar SS, McPhail ED, Dasari S, Leung N, Hewlett T, Yorke J, Gaston D, Geldenhuys L, Samuels M, Levine AP, West M, Hůlková H, Pompach P, Novák P, Weinberg RB, Bedard K, Živná M, Sikora J, Bleyer AJ Sr, Kmoch S. Autosomal dominant ApoA4 mutations present as tubulointerstitial kidney disease with medullary amyloidosis. *Kidney Int.* 2023 Dec 12. **Impact Factor = 18.9**

5.2 Awards

- 2019 **Howard Hughes Medical Institute Scholarship** awarded to attend 60th Annual Short Course in Human and Mammalian Genetics and Genomics, The Jackson Laboratory, Bar Harbor, Maine, USA, July 15-26, 2019.
- 2019 **National Institute of Health Scholarship** awarded to attend 60th Annual Short Course in Human and Mammalian Genetics and Genomics, The Jackson Laboratory, Bar Harbor, Maine, USA, July 15-26, 2019.

5.3 Grants (PI)

None.

5.4 Presentations

Kidd K., Bleyer AJ. Wake Forest MUC1 Registry and Progress. Oral Presentation. MUC1 Kidney Disease Collaborator Spring Retreat, The Broad Institute of Harvard and MIT, Cambridge, Massachusetts, USA. May 7-9, 2019.

Kidd K., Vyleťal P., Živná M., Kmoch S., Bleyer AJ. Association of rs4293393 and rs4072037 Variants in Autosomal Dominant Tubulo-Interstitial Kidney Disease due to UMOD and MUC1 mutations, Poster Presentation. 60th Annual Short Course in Human and Mammalian Genetics and Genomics, The Jackson Laboratory, Bar Harbor, Maine, USA, July 15-26, 2019.

Kidd K., Bleyer AJ. Wake Forest ADTKD Registry and Progress. Oral Presentation. MUC1

Kidney Disease Collaborator Fall Retreat, The Broad Institute of Harvard and MIT, Cambridge, Massachusetts, USA. November 2-3, 2019.

Kidd K. REDCap for ADTKD Registry Creation. Oral Presentation. 1st Annual International ADTKD Summit. Virtual, September 24-25, 2020.

Kidd K., Williams AH., Robins V., Taylor A., Martin L., Kim A., Živná M., Langefeld CD., Knoch S., Bleyer AJ. A Prospective Observational Study of Patients with Autosomal Dominant Tubulointerstitial Kidney Disease (ADTKD). Poster Presentation. American Society of Nephrology Kidney Week, Virtual/San Diego, CA, USA, November 4-7, 2021.

Kidd K., Bleyer AJ. ADTKD Gene Curation and Wake Forest ADTKD Registry Update. Oral Presentation. MUC1 Kidney Disease Collaborator Spring Retreat, The Broad Institute of Harvard and MIT, Cambridge, Massachusetts, USA. March 31, 2022.

Kidd K. Genetic Testing and an Overview of the Diagnostic Process. Oral Presentation. 3rd Annual International ADTKD Summit. Virtual, October 7-8, 2022.

Kidd K., Williams AH., Robins V., Taylor A., Martin L., Kim A., Živná M., Langefeld CD., Knoch S., Bleyer AJ. A Prospective Natural History Study of Patients with Autosomal Dominant Tubulointerstitial Kidney Disease (ADTKD). Poster Presentation. American Society of Nephrology Kidney Week, Orland, FL, USA, November 3-6, 2022.

Kidd K., Williams AH., Taylor A., Kim A., Martin L., Robins V., Rivas-Chavez A.P., Sayer J.A., Olinger E., Mabillard H.R., Papagregoriou G., Deltas C., Stavrou C., Conlon P.J., Hogan R.E., Elhassan E., Vylet'al P., Hodaňová K., Živná M., Knoch S., Bleyer AJ. Poster Presentation. Increased COVID-19 Infection and 9-fold Increased Mortality in Autosomal Dominant Tubulointerstitial Kidney Disease due to *MUC1* Frameshift Variants: An Observational Study. Poster Presentation. American Society of Nephrology Kidney Week, Orland, FL, USA, November 3-6, 2022.

Kidd K. Identification and Characterization of Inherited Kidney Disease. Oral Presentation. 1st Faculty of Medicine, Charles University Lecture Series in Genetics. Prague, Czech Republic February 6, 2023.

Kidd K. Genetic Testing and ADTKD Diagnosis. Oral Presentation. 1st Annual ADTKD Family Day, Wake Forest University School of Medicine, Winston-Salem, USA. September 30, 2023.